Anthropogenically-Intensified Erosion in Incising River Systems

A DISSERTATION
SUBMITTED TO THE FACULTY OF THE GRADUATE SCHOOL
OF THE UNIVERSITY OF MINNESOTA
BY

Stephanie S. Day

IN PARTIAL FULFILLMENT OF THE REQUIREMENTS
FOR THE DEGREE OF
DOCTOR OF PHILOSOPHY

Karen Gran, Chris Paola

July, 2012

Acknowledgements

I would first like to thank my advisers Karen Gran and Chris Paola, without their patience it is difficult for me to imagine this document complete. Thank you for your unwavering enthusiasm and encouragement. I would also like to thank my committee, Calvin Alexander and Vaughan Voller for providing useful feedback throughout this process. There are many people who have provided valuable assistance to me who are not represented here including Patrick Belmont, Carrie Jennings, Tim Wawrzniec, Jed Frechette, Chuck Regan, Karen Campbell and many others. Finally I would like to thank my family and friends who provided unending support; especially my lab and field partner Ryan.

I would also like to thank the groups who funded this research including the Minnesota Pollution Control Agency, the National Center for Earth-surface Dynamics, and the Geological Society of America Student Research Grant Program.

Dedication

This dissertation is dedicated to the teachers I had throughout my life who taught me, encouraged me, and gave me confidence to reach for my dreams, specifically Jollyn Nolan and Tom Higgins.

Abstract

Anthropogenic alterations to landscapes, such as agriculture, can lead to accelerated erosion in incising (or incised) rivers threatening infrastructure and property, and causing unnaturally high sediment loads, which threaten ecosystems. Steep bluffs and ravines are characteristic landforms in incising river systems, and by understanding erosion on these landforms we can begin to mitigate the impacts of the altered landscape. The Le Sueur River watershed, in southern Minnesota, provides an ideal location for studying the impacts of agricultural land-use on erosion in an incising river. Agriculture in this watershed is made possible through the use of tile drains, which remove water from the uplands and route it directly into ravines or the river, reducing the water that pools on the landscape and increasing flows in the river. Using terrestrial laser scanning (TLS) and aerial photographs, bluff erosion rates in the Le Sueur River were measured and used to develop a watershed scale sediment budget. In the Le Sueur River bluffs account for 56 ± 12% of the 2000-2010 average measured total suspended solids load. These data were also used to interpret how changes in land-use and climate have accelerated bluff retreat in this watershed. The data collected paired with field observations show that over-steepening at the bluff toe drives bluff retreat, yet weakening due to groundwater seeps and freeze-thaw also contributes to erosion. The increases in flow rates and volumes brought on by tile drainage in this watershed have resulted in increased bluff erosion. To study ravine response to changing overland flow hydrology, brought on by tile drainage, small physical experiments were used to measure how changing the delivery rate of a fixed volume of water impacts erosion. The results of these experiments showed that regardless of flow rate the volume of sediment removed remained the same, suggesting that the tile drains installed in the Le Sueur River watershed may have decreased ravine growth. Results of each of these projects independently improves our understanding of bluff erosion and ravine growth processes, yet combined they provide insight into how changing hydrology impacts erosion throughout an incising watershed. While agricultural landscape alterations, especially tile drains, have decreased ravine growth they have resulted in increased bluff erosion. Because bluffs in the Le Sueur River watershed account for more than half of the total sediment load, there is a net increase in sediment loads as a result of anthropogenic landscape alterations.

Table of Contents

List of Tables

List of Figures

Introduction:

Erosion is a natural process in rivers throughout the world, yet anthropogenic alterations in many watersheds have led to accelerated erosion and un-naturally high turbidity (e.g. Murgatroyd and Ternan, 1983; Valentin et al., 2005; Shields et al., 2008). Not only does increasing erosion in rivers impact local ecosystems, there also may be a threat to nearby infrastructure and property. This threat is especially common in incising (or incised) rivers where tall bluffs and steep ravines are characteristic landforms.

Incising rivers are typically responding to a drop in local base level. While shallow incision can result from anthropogenic alterations, this research focuses on deeply (10s of meters) incised river systems responding to natural base level changes. Knickpoints form on these rivers and propagate upstream carving the river valley. The knickpoint slope that forms is dependent on the relative shear strength of local stratigraphy (Gardner 1983; Frankel et al., 2011). Steep knickpoints develop when either all or the top units of sediment being incised through have a shear strength near the shear stress being imposed by the flow, while more gentle knickpoints form in more easily eroded material. On steep knickpoints, plunge pools can form at the base and the turbulent flow can cause undercutting and subsequent failure. Gentle knickpoints are expressed more as a zone of steeper gradients rather than a discrete discontinuity. These knickpoints propagate upstream as shear stress is increased locally as a result of steeper slopes (Whipple and Tucker 1999). Along the full continuum of knickpoint slopes one or both of these processes may cause knickpoints to migrate upstream.

As knickpoints move upstream, the newly incised valley is lined with steep bluffs, and overland flow forms steep ravines. Ravines and bluffs continue to erode and evolve even after the knickpoint has passed and is no longer having a direct impact in the area. These steep features are sensitive to landscape alterations or climate changes that alter hydrology. Understanding bluff and ravine erosion and growth will improve our understanding of landscape evolution in incising watersheds. Moreover this is essential to understanding how to slow these processes in areas where they threaten infrastructure and property, and mitigate the anthropogenic effects that have led to accelerated erosion in many places.

The broad goal of this research is to improve our understanding of erosion in incising river systems and how changing hydrology due to land use changes and climate impact erosion. The specific research question addressed in this thesis is: How do changes to hydrology impact bluff and ravine erosion, and are the responses different for these different features? Additional lines of research include how erosion can be measured at a variety of temporal and spatial scales

and later extrapolated, how traditional channel geometry and sediment transport equations can be used to describe ravines, and how Terrestrial Laser Scanning can be used to for geomorphic change detection in a temperate watershed.

While this research applies to rivers throughout the world, the Le Sueur River, a tributary in the Minnesota River, in southern Minnesota provides an ideal location to address these questions. The Le Sueur is an actively incising river with bluffs over 60 meters tall and steep ravines formed out of easily eroded till. Both bluffs and ravines in this channel connect the flat uplands with the river, yet they are distinct features because water is concentrated and funneled through ravines. Changes in this watershed are occurring quickly, allowing even annual change to be measured.

Study Area:

The modern Minnesota River flows through the deeply incised glacial River Warren valley. Incision of glacial River Warren began 11,500 radiocarbon years before present (rcbp) (13,400 calendar years before present) in response to a series of outburst floods from glacial Lake Agassiz (Clayton and Moran 1982; Matsch 1993). Glacial River Warren incised as much as 70 meters in the central Minnesota River basin, spawning knickpoints on all major tributaries (Thorleifson, 1996; Lowell et al., 2005). These tributaries are all still in the process of incising to meet the local base level set by River Warren resulting in high turbidity and sediment loads in the modern and historic Minnesota River.

Just downstream of where the Minnesota River meets the Mississippi River lies Lake Pepin, a naturally dammed lake that acts as a stilling basin for the Mississippi River, capturing most of the fine sediment delivered to it (Fig. 1.1). Cores taken from Lake Pepin provide the story of deposition over time on the Minnesota and upper Mississippi Rivers (Engstrom et al., 2009). These cores show that while sediment loads from the Minnesota River have always been high relative to the upper Mississippi River (Kelley and Nater, 2000), loads increased starting in 1830s and continuing up to the present (Engstrom et al., 2009) (Fig. 1.2). Historical evidence shows that this increase in sediment load corresponds to European settlement and initial land use changes throughout the Minnesota River watershed, and the continued rise in sediment loads

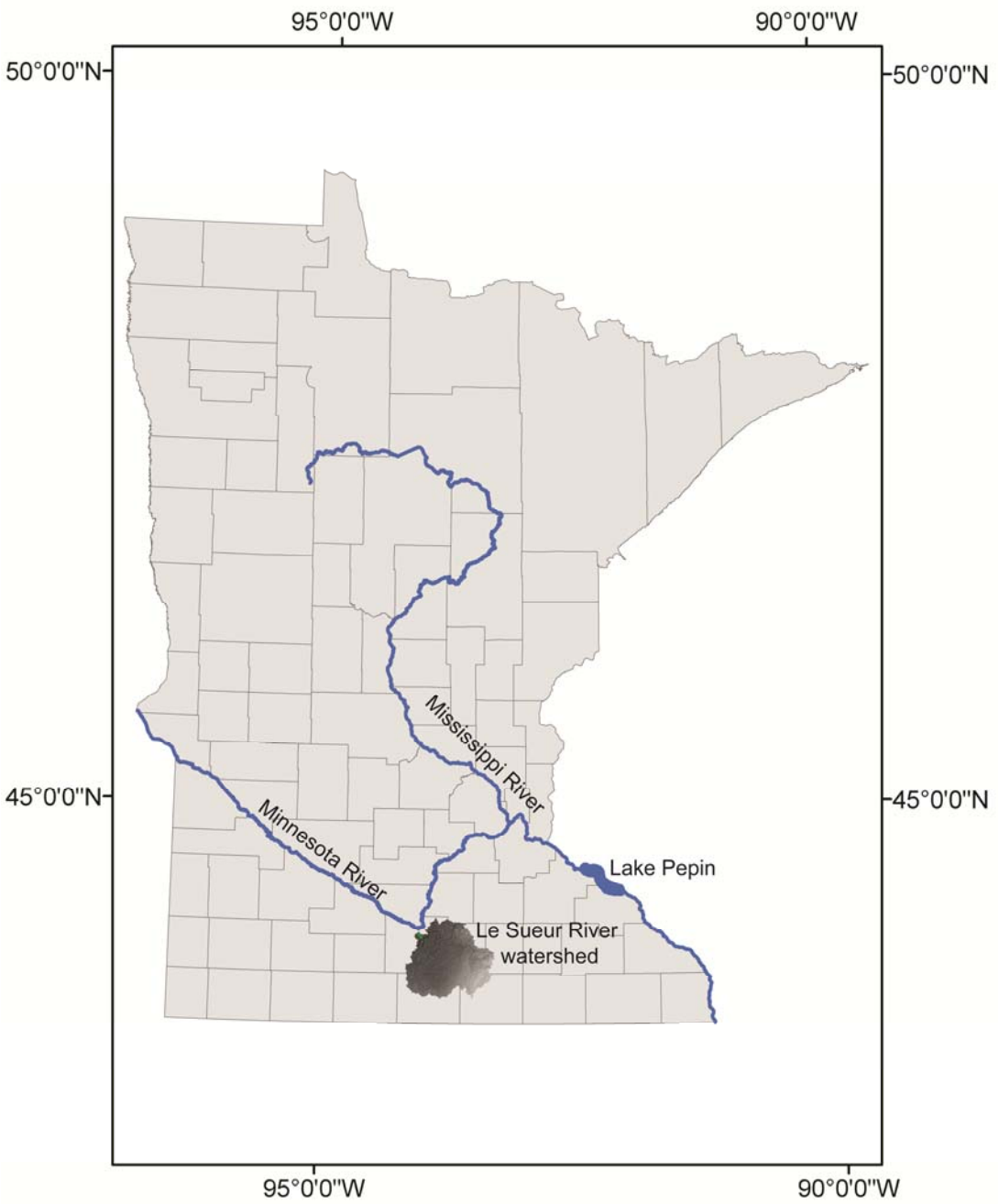

Figure 1.1: This map of Minnesota shows the relationship between Lake Pepin, on the Mississippi River and the Minnesota River. The Le Sueur River watershed is shown as a grey scale DEM.

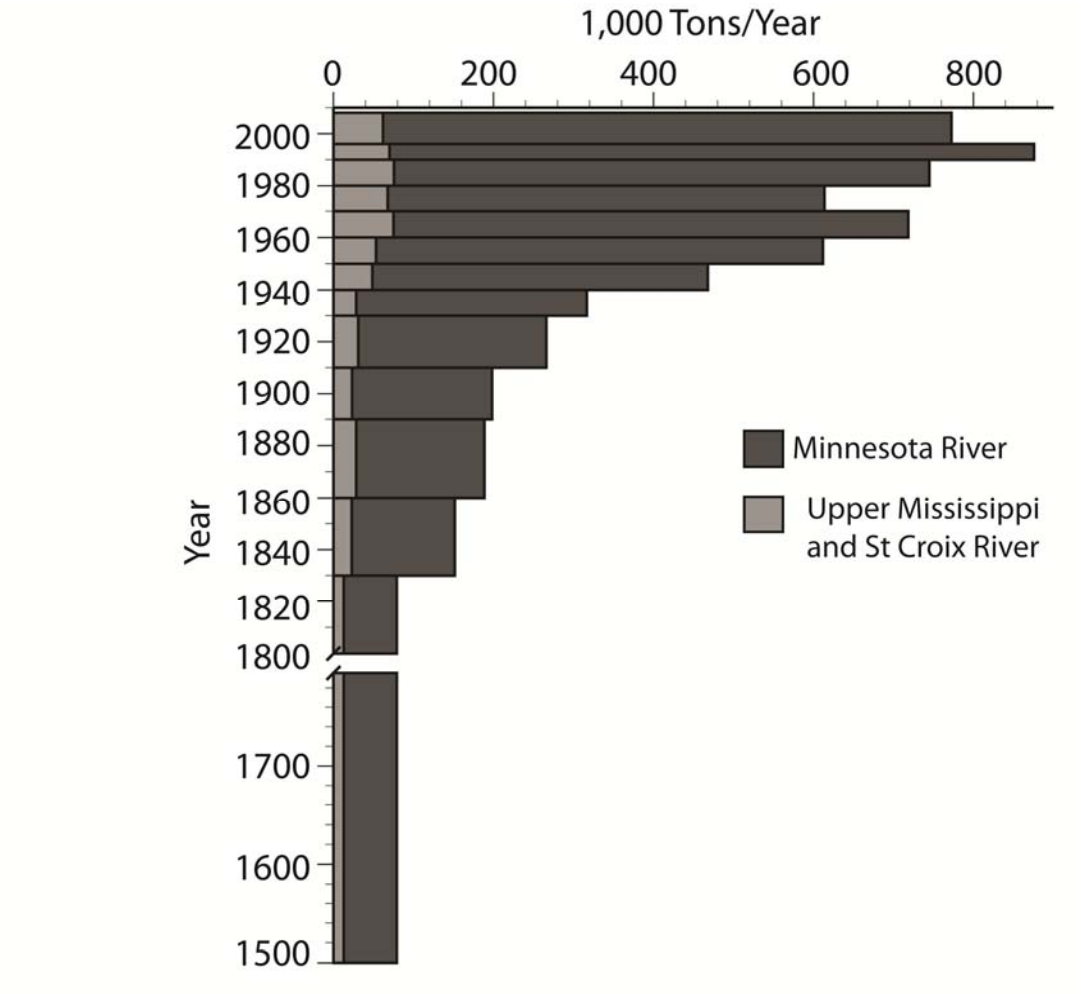

Figure 1.2 This Lake Pepin sediment accumulation curve from Engstrom et al. (2009) and updated by Blumentritt et al. (in prep.) shows the significant increase in sediment load to Lake Pepin beginning in the 1830s. Sediment loads have since stabilized at rates 8-10 times higher than the natural background rates.

correspond with the continued draining of the watershed initially through ditching and later through tile drains (Mulla and Sekely, 2009). Sediment deposition stabilized after 1960 at rates approximately 8-10 times higher than pre-settlement (Engstrom et al., 2009). While deposition rates stabilized, the dominant sediment source shifted from upland agriculturally-derived sediment to predominantly near-channel sources in the mid-1990s. This was due to a combination of the success of BMPs (Best Management Practices) implemented to reduce field erosion coupled with continuing alterations to hydrology (Belmont et al., 2011). In addition to anthropogenic alterations, climate change has resulted in increased precipitation, which may also result in increased erosion (Kelley et al., 2006). While the integrated effects of these changes to hydrology can be documented through the Lake Pepin core samples, identifying the specific sources of increased sediment load requires looking upstream at the Minnesota River and its tributaries.

The Le Sueur River is one such incising tributary that flows into the Blue Earth River and into the Minnesota River (Fig. 1.1), and contributes a disproportionate amount of the total sediment load to the Minnesota River (MPCA et al., 2007; Gran et al., 2009). The Le Sueur River is the site of on-going research to quantify and better understand major sediment sources to the Minnesota River, and ultimately Lake Pepin (Gran et al., 2011; Belmont et al., 2011). While this river may not provide insight into sediment transport through the main stem Minnesota River, it can provide necessary information regarding upstream sediment sources, and how hydrology alterations are affecting the erosional portion of the basin. Major sources of sediment in the Le Sueur River include bluffs, ravines, banks, and low-gradient agricultural uplands (Fig. 1.3).

Bluffs that reach as high as sixty meters are a significant source of sediment (Sekely et al., 2002; Thoma et al., 2005; Gran et al., 2009; Gran et al., 2011; Belmont et al., 2011). There are approximately 31 km of bluffs lining the Le Sueur River and 46 km lining the two main tributaries (the Maple and Big Cobb Rivers). There is strong regional interest in reducing sediment loads to improve water quality and aquatic habitat in the Le Sueur River as well as downstream in the Minnesota River and upper Mississippi River. In order to develop a mitigation plan for these rivers, it is important to understand both the amount of sediment contributed to the river from bluffs as well as the dominant processes by which these bluffs erode.

Glaciolacustrine sediment forms a thin cap overlying much of the Le Sueur River basin. Below this glacial lake sediment lie a series of stacked glacial tills (Jennings, 2010). These tills are composed of predominantly fine-grained, loamy-textured sediment with varying degrees of

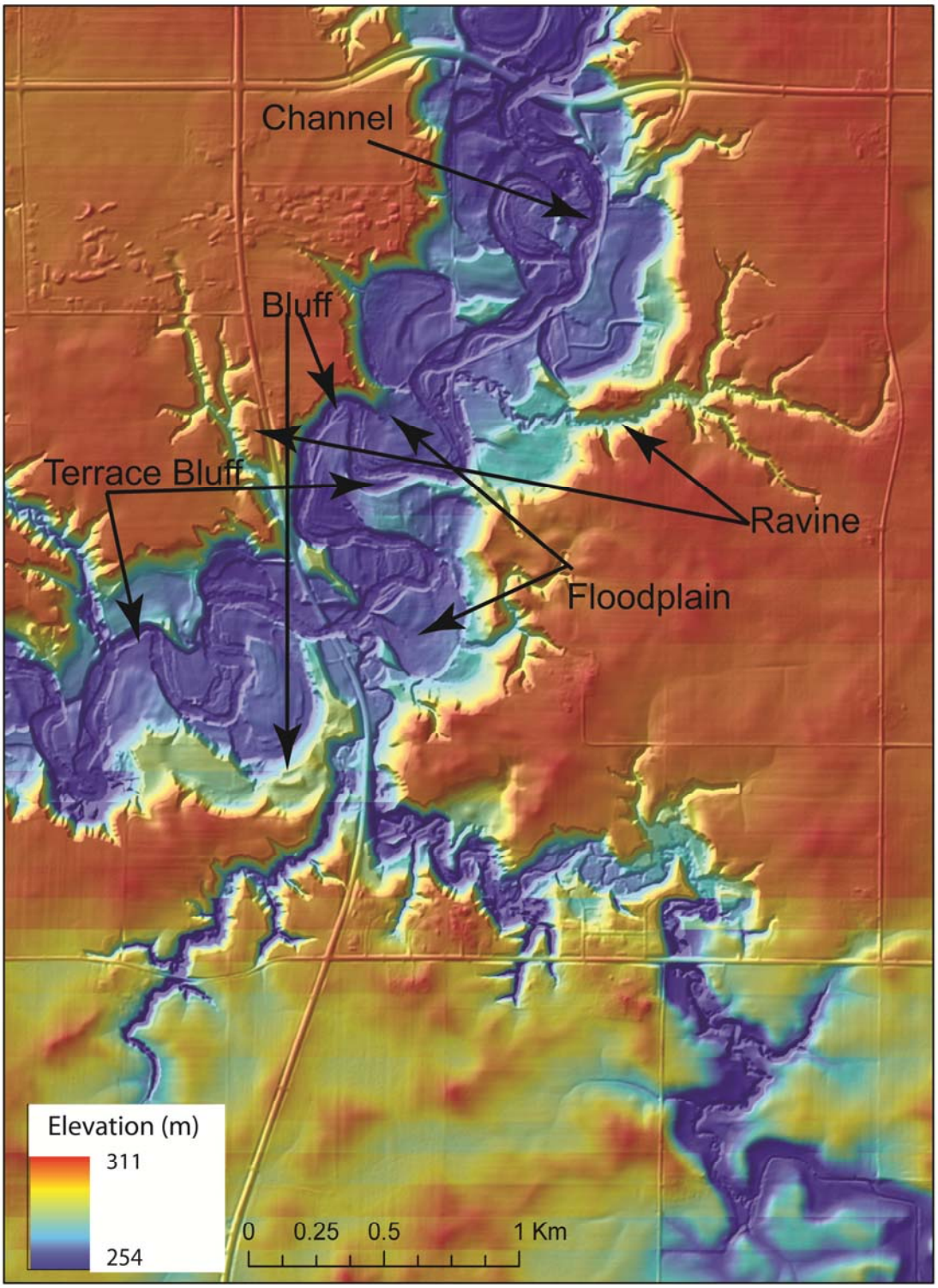

Figure 1.3: This DEM highlights features in the Le Sueur River watershed. Notice the size and depth of the ravines.

consolidation throughout the basin. While most tills are normally-consolidated, some are over-consolidated as indicated by the presence of vertical joints. Over-consolidation is likely a result of glaciers advancing over these tills, compacting and dewatering the sediment (Boulton, 1976; Kirkaldie and Talbot, 1992; Allred, 1999). The bluffs composed of over-consolidated tills often form very steep slopes that cannot easily support vegetation. Bluffs composed of normally-consolidated tills have a wider range of slopes, and many support vegetation ranging from grasses to trees. Within the river valley there are also strath terraces that formed as the river incised and abandoned a previously active floodplain or river channel. In these areas the upper units of till have been eroded and are covered by an alluvial cap. This alluvium is typically around two meters thick with the upper half being fine-grained alluvium and the lower half coarse-grained alluvium overlying a thin gravel unit. These alluvium-capped bluffs are referred to as terrace bluffs.

Steep ravines are also prominent features on the landscape. These features connect the uplands with the incised river up to 60 meters below and funnel both water and sediment off to the channel main stem. They range in length up to 3340 meters with steep head cuts at the tips of the upstream ends. The ravine slope varies throughout the Le Sueur watershed, and results in a range of morphologies ranging from step-pool morphology to meandering channels. These features contribute far less sediment than bluffs, yet there is interest in understanding how changes to hydrology are impacting the growth and evolution of these features (Belmont et al., 2011; Gran et al., 2011). Moreover ravines threaten infrastructure and property, and understanding the erosion of these features is an important aspect in slowing their growth.

Bluff Erosion Processes:

Bluffs are steep features that line incising or incised rivers. These features are differentiated from river banks by height. River banks are part of the active channel and are capped by active floodplain, while bluffs are any vertical feature that is not overtopped in a flood event. Because bluffs are not capped by active floodplains they are strictly sediment sources rather than depositional sinks and do not provide any long-term storage to eroded sediment.

Differences in height, stratigraphy, and geotechnical properties of bluffs affect the processes and rates of erosion. Undercutting or over-steepening is commonly cited as being the most significant erosion process along river bluffs and banks (e.g., Turnbull et al., 1966; Brunsden and Kesel, 1973; Harden et al., 2009). Undercutting occurs when the shear stress of the flow exceeds critical at the bluff toe, leading to toe erosion and subsequent failure as the bluff

slope becomes over-steepened, ultimately forming a new toe. How long deposits at the toe remain depends on the size of the deposits as well as the magnitude and duration of flows in the channel. The critical shear strength of the bluff toe is controlled by grain size, compaction and cohesion. Bluff strength can be reduced by freeze-thaw cycles, making the bluff more susceptible to undercutting by high flows in early spring and subsequent failure (Terzaghi 1962; Kirkby, 1965). Groundwater flow or sapping can also reduce the strength of the sediment by increasing pore pressure. Sapping occurs primarily in units with relatively higher permeability compared with surrounding units and can result in headward migration in the high permeability units as well as erosion of underlying sediment if the flow is great enough to overcome the critical shear strength of the sediment (Brunsden and Kesel, 1973; Thorne and Tovey, 1981; Fox *et al.,* 2007; Chu-Agor *et al.,* 2008; Lindow et al., 2009). Similarly, as water levels recede after large storm event, pore pressures in the bank are relatively high compared to atmospheric pressure, which may cause failure in the recently exposed bluff face (Simon et al., 2000). Pore pressure in bluffs can also increase during snowmelt or long-duration rain events and may contribute to failure.

External factors like aspect can influence the rate of bluff retreat. Aspect affects pore water temperature and thus the number and depth of freeze-thaw cycles (Wynn and Mostaghimi, 2006; Hall, 2007; Bold *et al.,* 2010). West and south-facing bluffs experience warmer afternoon temperatures leading to a greater number of freeze-thaw cycles (Hall, 2007; Bold *et al.,* 2010). Sediment strength is temporarily weakened after each freeze-thaw cycle, in part due to frost heaving, and greater numbers of freeze-thaw cycles may lead to greater erosion rates (Wynn and Mostaghimi, 2006; Thomas *et al.,* 2009; Van Klaveren and McCool, 2010).

The effects of vegetation on bluff erosion are different than may be expected. While vegetation has been shown to be an important stabilizing force on low river banks the same is not true for tall bluffs (Sidle and Ochiai, 2006; Ghahramani *et al.,* 2011). On river bluffs, where bluff erosion is driven primarily by undercutting; even vegetation with extensive root networks can be undercut leading to failure (Docker and Hubble, 2008; Cancienne *et al.,* 2008). Because bluffs are tens of meters tall, roots from vegetation on the bluff crest cannot cross the failure plane, resulting in no additional bluff stability. During low flow, smaller vegetation may be able to become established on the bluff toe, and temporarily slow the process of over-steepening, but large floods, which can destroy this vegetation, will cause the process of over-steepening to resume. If flow is diverted away from the bluff toe, vegetation that develops on the bluff face will not be undercut and will ultimately provide a stabilizing force.

Ravine Growth Processes:

Ravines, commonly referred to as permanent gullies, are deeply-incised first-order with channels depths greater than 0.5 meters (Poesen et al., 2003). In the Le Sueur River basin, ravines can be several km long and tens of meters deep (Fig. 1.3). Some ravines have running water year round, but most are ephemeral. They grow as overland flow or sapping causes steep head cuts to propagate upstream (Higgins, 1982; Bennett and Casalí, 2001).

Ravine head cuts are a type of knickpoint, and while their growth is primarily due to overland flow, the processes by which they erode and expand are similar to those that cause knickpoints to propagate upstream in rivers. As described above, knickpoint slope and propagation rate are dependent on the relative shear strength of the local stratigraphy. Ravine initiation is controlled by the ability of the concentrated flow to remove sediment (Knapen and Poesen 2010). In incised river valleys, ravines may be initiated at crenulations in steep bluffs or banks, where steep slopes result in high shear stress imposed on the surface by the concentrated flow.

Ravines that grow primarily due to sapping can sometimes be identified by "amphitheater" shaped head cuts (Hinds, 1925; Lamb et al., 2006). These ravines are initiated by a concentration of groundwater where sediment above is weakened and underlying sediment is eroded due to the shear stress imposed on the sediment by the concentrated flow.

As with bluffs, ravine head cuts in incising rivers are often too steep or tall to be stabilized by vegetation after they are initiated. Where vegetation may alter ravine growth is through a reduction in overland flow or sapping through locally increased evapotranspiration and surface roughness (Einstein and Barbarossa 1951; Farres, 1978; Römkens and Wang, 1987; Abrahams and Parsons, 1991; Istanbulluoglu et al., 2005; Pierson et al., 2007; Eitel et al., 2011).

Approach:

There are many unanswered questions regarding the primary factors controlling erosion and sediment yield in incising rivers and how changes in hydrology impact erosional processes. Through the use of field, remote sensing and laboratory techniques, this thesis sheds light on the factors that contribute to bluff and ravine erosion. Moreover the techniques developed through this work advance the science of geomorphic change detection.

Measuring bluff erosion rates accurately is not an insignificant task. Traditional methods rely on spatially sparse measurements like surveying or erosion pins, or temporally sparse measurements from aerial photographs. Because bluff erosion is highly episodic both in space

and time these methods provide little insight on how the bluff is truly eroding and may result in incorrect estimation of erosion rates (Resop and Hession, 2010). Terrestrial Laser Scanning (TLS), a new surveying technique, overcomes issues of both spatial and temporal resolution. Unlike traditional surveying TLS collects cm-scale data across entire bluff surfaces, yet like traditional survey methods, TLS is portable and data can be collected and processed quickly allowing for measurements with high temporal resolution (Wawrzyniec et al., 2007; Heritage and Hetherington, 2007). Traditionally TLS has been used for creating models of small simple landforms devoid of vegetation. The techniques developed in this thesis allow TLS data to be used for change detection on vegetated landforms. In addition, a detailed error analysis was performed to document the level of change that can be accurately detected using this technique.

Sites representing a range of bluffs in the Le Sueur watershed were surveyed using TLS over four years. These data were compared to annual flow data over the same period of time in order to make comparisons between precipitation and erosion rates.

In addition to TLS annual erosion rates, decadal bluff retreat rates were measured on aerial photographs. Bluff retreat rates were extrapolated from both the TLS and the aerial photograph data sets using multiple techniques. Detailed error analyses were developed and each extrapolation technique was compared. The final results were compared to the sediment loads measured on the Le Sueur River and analyzed resulting in a deeper understanding of bluff erosion in the watershed. Moreover, these results were paired with independent measurements of additional sediment sources and sinks in the Le Sueur River watershed to develop a sediment budget.

The same techniques used to understand bluff erosion in the field are not useful to measure ravine change. Dense vegetation makes both TLS and aerial photograph analyses impossible. Small scale laboratory-based physical experiments were used to test how varying overland flow on a uniform substrate impacted ravine growth. Data were collected using high resolution topographic scans making it possible to measure how channel geometry changes in response to varied flow rates. Moreover these data were used to demonstrate how basic sediment transport equations might apply to ravine erosion. These experiments improve our understanding of how changes to hydrology impact ravine erosion, allowing us to make interpretations regarding the effects of specific land use changes.

Chapter Layout:

The first chapter entitled "Terrestrial laser scanning methods for change detection" goes into detail on the TLS methods developed to measure bluff change. There is also a detailed error analysis for the techniques presented. The second chapter entitled "Comparing aerial photographs and terrestrial laser scanning to create a watershed scale sediment budget" compares TLS and aerial photograph analyses for determining bluff erosion rates in a large watershed, with a focus on the Le Sueur River watershed. This chapter has a detailed analysis of extrapolation techniques and the associated errors. Both chapters one and two are in review for publication with the journal of *Earth Surface Processes and Landforms*. The third chapter entitled "Ravine growth experiments to understand effects of changing hydrology" discusses the ravine experiments and how changing land use is likely impacting ravine growth. Finally a conclusion summarizes the work presented.

Works Cited:

Abrahams AD, Parsons AJ. 1991. Resistance to overland flow on desert pavement and its implications for sediment transport modeling. Water Resources Research **27**: 1827-1836.

Allred BJ. 1999. Survey of fractured glacial till geotechnical characteristics: hydraulic conductivity, consolidation, and shear strength. Ohio Journal of Science **100**: 63-72.

Belmont P, Gran K, Schottler S, Wilcock P, Day S, Jennings C, Lauer J, Viparelli E, Willenbring J, Engstrom D, Parker G. 2011, Large shift in source of fine sediment in the Upper Mississippi River. Environmental Science and Technology. **45**: 8804–8810. dx.doi.org/10.1021/es2019109

Bennett SJ, Casalí J. 2001. Effect of initial step height on headcut development in upland concentrated flows. Water Resources Research **37**: 1475-1484.

Bold KC, Wood F, Edwards PJ, Williard KWJ, Schoonover JE, 2010. Using photographic image analysis to assess ground cover: a case study of forest road cutbanks. Environmental Monitor Assessment **163**: 685-698.

Boulton GS. 1976. The development of geotechnical properties in glacial tills. Legget RF(ed).Glacial Till. Ottawa: The Royal Society of Canada. Special Publication NO. 12; 292-303.

Brunsden D, Kesel RH, 1973. Slope development on a Mississippi River bluff in historic time. The Journal of Geology **81**: 576-598

Cancienne RM, Fox GA, Simon A. 2008. Influence of seepage undercutting on the stability of root-reinforced streambanks. Earth Surface Processes and Landforms **33**: 1769-1786.

Chu-Agor ML, Fox GA, Cancienne RM, 2008. Seepage caused tension failures and erosion undercutting hillslopes. Journal of Hydrology **359**: 247-259.

Clayton L, Moran SR. 1982. Chronology of late-Wisconsinan glaciations in middle North America. Quaternary Science Reviews **1**: 55-82

Docker BB, Hubble TCT. 2008. Quanitfying root-reiforcement of river bank soils by four Australian tree species. Geomorphology **100**: 401-418.

Einstein HA, Barbarossa NL. 1951. River channel roughness. Transactions of the American Society of Civil Engineers **117**: 1121-1132.

Eitel JUH, Williams CJ, Vierling LA, Al-Hamdan OZ, Pierson FB. 2011. Suitability of terrestrial laser scanning for studying surface roughness effects on concentrated flow erosion processes in rangelands. Catena **87**:398-407.

Engstrom DR, Almendinger JE, Wolin JA, 2009. Historical changes in sediment and phosphorus loading to the upper Mississippi River: mass-balance reconstructions from the sediments of Lake Pepin. Journal of Paleolimnology **41**: 563–588.

Farres PJ. 1978. The role of time and aggregate size in the crusting process. Earth Surface Processes **3**: 243-254

Fox GA, Wilson GV, Simon A, Langendoen EJ, Akay O, Fuchs JW.2007. Measuring streambank erosion due to ground water seepage: correlation to bank pore water pressure, precipitation and stream stage. Earth Surface Processes and Landforms**32**, 1558-1573.

Frankel KL, Pazzaglia FJ, Vaughn JD. 2007. Knickpoints evolution in a vertically bedded substrate, upstream-dipping terraces, and Atlantic slope bedrock channels. Geological Society of America Bulletin **119**: 476-486.

Gardner TW. 1983. Experimental study of knickpoint and longitudinal profile evolution in cohesive homogenous material. Geological Society of America Bulletin **94**: 664-476.

Ghahramani A, Ishikawa Y, Gomi T, Shiraki K, Miyata S, 2011. Effect of ground cover on splash and sheetwash erosion over a steep forested hillslope; a plot-scale study. Catena **85**: 34-47.

Gran KB, Belmont P, Day SS, Jennings C, Johnson A, Perg L, Wilcock PR.2009.Geomorphic evolution of the Le Sueur River, Minnesota, USA, and implications for current sediment loading. James LA, Rathburn SL, Whittecar GR, (eds.). Management and Restoration of Fluvial Systems with Broad Historical Changes and Human Impacts: Geological Society of America Special Paper 451.

Gran KB, Belmont P, Day S, Jennings C, Lauer JW, Viparelli E, Wilcock P, Parker G. 2011, An integrated sediment budget for the Le Sueur River basin. Final report Presented to the Minnesota Pollution Control Agency.

Hall K, 2007. Evidence for freeze-thaw events and their implications for rock weathering in northern Canada: II. The temperature at which water freezes in rock. Earth Surface Processes and Landforms **32**: 249-259.

Harden CP, Foster W, Morris C, Chartrand KJ, Hennry E, 2009. Rates and processes of streambank erosion in tributaries of the Little River, Tennessee. Physical Geography **30**: 1-16.

Heritage G, Hetherington D. 2007. Towards a protocol for laser scanning in fluvial geomorphology. Earth Surface Processes and Landforms **32**: 66-74.

Higgins CG. 1982. Drainage systems developed by sapping on Earth and Mars. Geology **10**: 147-152.

Hinds NEA. 1925 Amphitheater valley heads. Journal of Geology **33**: 816-818.

Istanbulluoglu E, Bras RL, Flores-Cervantes H, Tucker GE. 2005. Implications of bank failures and fluvial erosion for gully development: Field observations and modeling. Journal of Geophysical research **110**: F01014.

Jennings CE. 2010. Draft digital reconnaissance surficial geology and geomorphology of the Le Sueur River watershed (Blue Earth, Waseca, Fairbault, and Freeborn counties in south-central MN). Open File Report 10-03 Minnesota Geological Survey, map, report and digital files. ftp://mgssun6.mngs.umn.edu/pub4/ofr10_03/.

Kelley DW, Nater EA, 2000. Historical sediment flux from three watersheds into Lake Pepin, Minnesota, USA. Journal of Environmental Quality **29**: 561-568.

Kelley DW, Brachfeld SA, Nater EA, Wright HE. 2006. Sources of sediment in Lake Pepin on the upper Mississippi River in response to Holocene climatic changes. Journal of Paleolimnology **35**: 193-206.

Kirkaldie L, Talbot JR. 1992.The effects of soil joints on soil mass properties. Bulletin for the Association of Engineering Geology**25**:415-420.

Kirkby MJ, 1965. Measurements of soil creep. Annals of the Association of American Geographers **55**: 626

Knapen A, Poesen J. 2010. Soil erosion resistance effects on rill and gully initiation points and dimensions. Earth Surface Processes and Landforms **35**: 217-228

Lamb MP, Howard AD, Johnson J, Whipple KX, Dietrich WE, Perron J. 2006. Can springs cun canyons into rock?. Journal of Geophysical Research **111**: E07002.

Lindow N, Fox GA, Evans RO. 2009. Seepage erosion in layered stream bank material. Earth Surface Processes and Landforms **34**:1693-1701.

Lowell TV, Fisher TG, Comer GC. 2005. Testing the Lake Agassiz meltwater trigger for the Younger Dryan: Eos (Transactions, American Geophysical Union) **83**: 365-373

Matsch CL. 1983. River Warren, the southern outlet of Lake Agassiz. Teller JT, Clayton L, (eds). Glacial Lake Agassiz: Geological Association of Canada Special paper **26**: 232-244.

Minnesota Pollution Control Agency (MPCA). Minnesota Department of Agriculture, Minnesota State University, Mankato water Resources Center and Metropolitan Council Environmental Services. 2007. State of the Minnesota River: Summary of Surface Water Quality Monitoring 2000-2005: St. Paul, 20p.

Mulla DJ, Sekely AC. 2009. Historical trends affecting accumulation of sediment and phosphorus in Lake Pepin, upper Mississippi River, USA. Journal of Paleolimnology **41**: 589-602.

Murgatroyd AL, Ternan JL. 1983. The impact of afforestation on stream bank erosion and channel form. Earth Surface Processes and Landforms **8**: 357-369.

Pierson FB, Bates JD, Svejcar TJ, Hardegree SP. 2007. Runoff and erosion after cutting western Juniper. Rangeland Ecology and Management **60**: 285-292.

Poesen J, Nachtergaele J, Verstaeten G, Valentin C. 2003. Gully erosion and environmental change: importance and research needs. Catena **50**: 91-133.

Resop JP, Hession WC. 2010. Terrestrial laser scanning for monitoring streambank retreat: comparison with traditional surveying techniques. Journal of Hydraulic Engineering **136**: 794-798.

Römkens MJM, Wang JY. 1987. Soil roughness changes from rainfall. Transactions of the American Society of Civil Engineers **31**: 408-413.

Sekely AC, Mulla DJ, Bauer DW. 2002. Stream bank slumping and its contributions to the phosphorus and suspended sediment loads of the Blue Earth River, Minnesota. Journal of Soil and Water Conservation57: 243-250.

Shields FD, Pezeshki SR, Wilson GV, Wu MN, Dabney SM. Rehabilitation of an incised stream using plant materials: The dominance of geomorphic processes. Ecology and Society **13**: 54.

Sidle RC, Ochiai H, 2006. Landslides: processes, prediction, and land use. Water Resources Monograph **18**: 312p.

Simon A, Curini A, Darby SE, Langendoen EJ.2000. Bank and near-bank processes in an incised channel. Geomorphology**35**: 193-217.

Terzaghi K, 1962. Stability of steep slopes on hard unweathered rock. Geotechnique **12**: 251-270.

Thoma DP, Gupta SC, Bauer ME, Kirchoff CE. 2005. Airborne laser scanning for riverbank erosion assessment: Remote Sensing of Environment**95**:493-501.

Thomas JT, Iverson NR, Burkart MR, 2009. Bank-collapse processes in a valley-bottom gully, western Iowa. Earth Surface Processes and Landforms **34**: 109-122.

Thorleifson LH. 1996. Review of Lake Agassiz history, Teller JT, Thorleifson LH, Matile G,

Brisbin WC. Sedimentology, Geomorphology and History of the Central lake Agassiz Basin: Geological Association of Canada/Mineralogical Association of Canada Annual Meeting, Winnipeg, Manitoba, field Trip Guidebook **B2**: 55-84

Thorne CR, Tovey NK, 1981. Stability of composite banks. Earth Surface Processes and Landforms **6**: 469-484.

Turnbull WJ, Krinitzsky EL, Weaver FJ, 1966. Bank erosion in soils of the lower Mississippi Valley. Proceedings of the American Society of Civil Engineers **92**: 121-136

Valentin C, Poesen J, Yong L. 2005. Gully erosion: Impacts, factors and control. Catena **63**: 132-153.

Van Klaveren RW, McCool DK, 2010. Free-thaw and water tension effects on soil detachment. Soil Society of America Journal **74**: 1327-1338.

Wawrzyniec TF, McFadden LD, Ellwein A, Meyer G, Scuderi L, McAuliffe J, Fawcett P. 2007. Chronotopographic analysis directly from point-cloud data: A method for detecting small seasonal hillslope change in Black Mesa Escarpment, NE Arizona. Geosphere **3**: 550-567.

Whipple KX, Tucker GE. 1999. Dynamics of the stream-power river incision model: Implications for height limits of mountain ranges, landscape response timescales, and research needs. Journal of Geophysical Research **104**: 17661-17674.

Wynn TM, Mostaghimi S, 2006. Effects of riparian vegetation on stream bank subaerial processes in southwestern Virginia, USA. Earth Surface Processes and Landforms **31**: 399-413.

Chapter 1:
Terrestrial laser scanning methods for change detection

Human activities influence watershed sediment dynamics in profound ways, often resulting in excessive loading of suspended sediment to rivers. One of the primary factors limiting our ability to effectively manage sediment at the watershed scale has been our inability to adequately measure relatively small erosion rates (on the order of mm to cm per year) over annual and sub-annual time scales on spatially-extensive landforms, such as river banks and bluffs. Terrestrial Laser Scanning (TLS) can be employed to address this need. TLS collects high-resolution data allowing for more accurate monitoring of erosion rates and processes, and provides a new opportunity to make precise measurements of geomorphic change on vertical landforms like banks and bluffs, but challenges remain. This research highlights challenges and limitations of using TLS for change detection on river banks and bluffs including the presence of vegetation, natural surface crenulations, and difficulties with creating benchmarks, and provides solutions developed to overcome these limitations. Results indicate that data processing algorithms for change detection can have a dramatic impact on the calculated erosion rates, with different methods producing results that can vary by over 100%. The most accurate change detection technique compares a point cloud to a TIN along a set of vectors that accommodates bluff curvature. This paper outlines a variety of methods used to measure bluff change via TLS and explains the accompanying error analysis that supports these methods.

Introduction:

Throughout the world, changes in land use have caused increased erosion and sediment loading within river basins creating concern among property owners and land and water resource managers. Accelerated erosion of vertical features such as banks and bluffs may threaten infrastructure and often has a negative impact on water quality and aquatic habitat (Shields et al., 1995; Soulsby et al., 2001; Kent and Stelzer, 2008). Slowing erosion of these features and reducing the resultant high sediment loads requires a detailed understanding of both erosion rates and processes. Terrestrial Laser Scanning (TLS) is one new tool that can be employed for that purpose. TLS can be used to generate high-resolution (sub-cm grid resolution) topographic models over large areas (10^2 m^2 to several km^2) in a relatively short time (hours to several days; Wawrzyniec et al., 2007; Heritage and Hetherington, 2007). The technology is rapidly evolving to be extremely useful for measuring and monitoring natural systems at a variety of scales (Gulyaev and Buckeridge, 2004; Rosser et al., 2005; Wawrzyniec et al., 2007; Milan et al., 2007; Alho et al., 2009; Heritage and Milan., 2009; Hodge et al., 2009; Lim et al., 2010; Resop and Hession, 2010; O'Neal and Pizzuto, 2011). Monitoring is important as most bluff erosion processes are episodic, and thus are not spatially uniform.

Using TLS to generate models of natural systems is not devoid of difficulties. Many challenges are site-specific, while others are generalizable. Some challenges are environmental. For example, eye-safe lasers used with most TLS models are highly sensitive to scatter and absorption. Therefore, the laser beam may be interrupted by water vapor, dust and strong variations in air density (e.g., wind) (Wawrzyniec et al., 2007; Heritage and Hetherington, 2007). Vegetation can obscure the erosional surface of interest and must be removed in processing to generate a model of bare earth topography. In addition, vegetation and irregular surfaces can lead to data shadows. Many of these difficulties can be overcome through careful data acquisition and processing. Other challenges are technical. For example, multiple procedures can be used for aligning scans collected at different times, and numerous techniques can be employed for quantifying change and associated uncertainty. Methods used at each step can affect accuracy and precision of TLS. This paper explores the methods of using TLS, including data processing and analysis to examine erosion of bluffs in a river system within a mid-continent temperate climate. The considerations and methods discussed herein are readily portable to measurement of bank erosion.

Terrestrial Laser Scanning:

Unlike the more familiar airborne terrestrial laser mapping (ATLM) approach, terrestrial laser scanning (TLS), also referred to as 'ground-based' or 'terrestrial' lidar is a portable tripod-based light detection and ranging system that can be used to generate digital topography models at very high resolution (sub-cm scale). Because it is set on a tripod, TLS can be easily set up to collect data on surfaces often missed by ATLM, such as nearly vertical surfaces like stream banks and bluffs. ATLM surveys require multiple flight line orientations and spacing to capture steep or sub-vertical surfaces (James et al., 2007). In addition, because TLS does not require motion compensation correction, the resulting data have precision and accuracy at the mm- to cm-scale level, which ATLM simply cannot achieve with existing technology.

In this study, an Optech ILRIS-3_6D, ER (Enhanced Range) lidar system from the Lidar Lab at Western State College of Colorado was deployed to collect 3D imagery to evaluate bluff erosion rates. The Optech scanner creates a 3D image using the 'time of flight' of a series of laser pulses that are reflected off the target. The Optech system has a range gate that can be programmed to collect either the first or second pulse in the return signal (Optech, 2011). The first pulse represents beam reflection off a near-field or primary target. If the laser spot strikes the edge of a primary target, some of the energy may be reflected from a secondary or far field target producing a secondary pulse within the same range gate. Typically, either the first or the last return is recorded. Vegetation growing above the surface of interest may reflect the first return. By collecting the last return, the scanner may be able to collect points through vegetation.

Other techniques that have been used to study bank and bluff erosion include repeat aerial photographs, erosion pins, traditional survey methods with a total station or engineer's level, and photogrammetry. Each of these methods involves logistical problems that make them difficult to use in places where surfaces are steep or inaccessible, and none of them provide the high data resolution available using TLS. Aerial photographs can provide a long record of bluff retreat, but they can only be used to provide information on the crest of the bluff and in some cases the toe of the bluff where it is not blurred by vegetation or shadow effects (Day et al., this issue). They provide little information on the face of the bluff or the processes by which the bluff erodes. In addition, to measure change using aerial photographs the magnitude of change must be greater than the resolution of the photographs and error introduced by the photo orthorectification and alignment algorithms (typically 5 - 10 m for photographs at 1:20,000 scale and scanned at 600 DPI resolution) (Day et al., this issue). Erosion pins are also commonly used to measure bank and bluff erosion. These can provide high resolution data (0.5 mm) about the area immediately

surrounding the pins at low cost (Couper et al., 2002). Unfortunately erosion pins can only be used in areas that are accessible, excluding steep or tall bluffs. Installation of erosion pins may modify surficial and/or internal structure of the target surface and may cause localized scour, both of which can increase local erosion, biasing the data. If a pin is lost, there is no record of the amount of erosion (or deposition) that took place in that spot (Haigh, 1977; Lawler 1978; Thorne, 1981; Couper et al., 2002). Traditional survey methods have many of the same difficulties as erosion pins. All spots measured must be accessible, and while the data are precise at the exact points measured, surveys provide little information about areas between measured points. Photogrammetry uses photograph stereo pairs to create a three-dimensional image of a surface. This technique overcomes accessibility problems on steep bluffs and can provide information about a complete bluff surface rather than a series of measured points. Limitations associated with this technique are primarily due to lens distortions and lighting which may produce shadows on the surface (Rosser et al., 2005; Matthews, 2008).

TLS overcomes many of the difficulties associated with these other techniques. Banks and bluffs can be scanned in their entirety at high resolution regardless of accessibility to the features themselves as long as the tripod can be set up with a direct line of site. TLS does not disrupt the surface or alter the structure of the landform being scanned, as erosion pins may. Because TLS uses an active light source (laser), lighting is never a concern and there are no lens or lighting distortions, as there may be using photographic techniques.

TLS also presents a number of challenges and limitations. Roughness from vegetation or crenulations in the feature being surveyed can create data voids, referred to as shadows (Buckley et al., 2008). In some cases, these shadows can be resolved by scanning the feature from multiple angles (Buckley et al., 2008). However, in places where vegetation is dense, other techniques (e.g. a traditional survey) may be more effective because no bare-earth pulses can be returned to the instrument. Data processing can also be a challenge. The datasets are very large (e.g., as high as 500 Mb per 100 m^2 scanned in this study), sometimes requiring specialized visualization software not easily handled by standard 32-bit desktop configurations. There are a variety of different software packages available (e.g. Polyworks, RiScan Pro, Cyclone) and an absence of format standards. Each point cloud processing tool has benefits and limitations, and data are not easily transferred between software packages.

While TLS is new technology it has been used successfully in a number of environments. The first environmental research applications were primarily for vegetation studies (Lovell et al., 2003; Van der Zande, et al., 2006; Strahler, et al., 2008). Since this time, many more Earth

science applications have been explored (e.g. Williams et al., 2011; Lim et al., 2010; Resop and Hession, 2010; Alho et al., 2009; Hodge et al., 2009; Wawrzyniec et al., 2007; Milan et al., 2007; Gulyaev and Buckeridge, 2004). TLS is especially useful for surveying features that are not accurately measured using aerial lidar, such as cliffs (Rosser et al., 2005), and surveying features in greater detail than can be achieved with either aerial lidar or traditional survey methods (Heritage and Hetherington, 2007).

Several recent studies have used TLS for change detection in natural systems, typically in locations that lack significant vegetation. These include semi-arid environments such as Arizona (Wawrzyniec et al., 2007), highly erosive sea cliffs (Lim et al., 2010; Rosser et al., 2005; Gulyaev and Buckeridge, 2004), proglacial environments in Switzerland (Milan et al., 2007). In each of these environments the time scale over which change is being measured is dependent on how active the features are. The time between scans for each of these studies ranges from years (Rosser et al., 2005; Gulyaev and Buckeridge, 2004) to months (Wawrzyniec et al., 2007) to days (Milan et al., 2007), depending on the rate of change on the surface of the features scanned.

Use of TLS in fluvial environments is only beginning to be explored. The biggest disadvantage to using this technology in fluvial systems is that it cannot survey through water, and has difficulty scanning very wet surfaces. TLS has been used successfully to measure grain size and surface roughness of exposed point bars (Alho et al., 2009; Heritage and Milan, 2009; Hodge et al., 2009). It has also been used successfully to measure erosion on streambanks to track erosion over annual timescales (O'Neal and Pizzuto, 2011 and Resop and Hession, 2010).

Methods:

Data Collection:

Annual bluff TLS surveys were conducted from 2007-2010 to determine the rate and location of bluff erosion. Point cloud survey data were collected using an Optech ILRIS-3_6D ER Terrestrial Laser Scanner. The technical specifications of this equipment are discussed in Wawrzyniec et al. (2007). The scanner was sited in locations with minimal obstructions, which typically required placement on low banks or gravel bars lacking large vegetation. If the bluff surface had significant topographic roughness or trees (Fig. 2.1), more than one scanning station was used to get a full unobstructed instrument view of the bluff. Rebar posts were driven into the ground to mark the scanner location, and the scanner was placed in the same location each year, unless changes in seasonal vegetation or water levels prohibited this. Benchmarks (stable features including infrastructure, trees, large boulders, or installed flagged stakes) in the target

Figure 2.1: This bluff has roughness due to vegetation as well as surface topography. When the scanner is set in only one location a significant portion area is in a shadow. In order to get a complete picture of the bluff the scanner is set in multiple locations and aligned when the data are processed.

scene were used to align the scans between annual scanning campaigns. Ideally at least three benchmarks dispersed evenly across the bluff were scanned at each site. After setting up the scanner, data were collected from the entire surface, though returns were typically not received from saturated or wet surfaces because these areas tend to be less reflective and absorb much of the laser signal. Data were collected with a spatial resolution of 81,600 – 1,190 points/ m^2, with coarser resolution for large bluffs to reduce the total scan time and extend the daily life-cycle of the batteries. Manufacturer error for the Optech ILRIS-3_6D ER includes a raw range accuracy of 7 mm at 100 m a raw angular accuracy of 8 mm at 100 m and a beam diameter of 22 mm at 100 m Optech, 2012). This scanner has a fully-automated 40˚ look-angle in the vertical and horizontal direction and can either be turned manually to continue to survey in other areas of the site or can be set to turn automatically to the next area of interest (Fig. 2.2). When done automatically there is a 5% overlap between each individual scan. When done manually care must be taken to ensure that there is at least an equivalent overlap.

Data Processing:

After the data were collected, they were converted into PTX files using a parser distributed by Optech and processed using Polyworks metrology software (InnovMetric, Quebec City, Canada). Polyworks is specifically designed to measure change, either between two TLS scans or between a TLS scan and a drawn image. Polyworks is comprised of seven modules, of which we used IMAlign, IMMerge, IMEdit, and IMInspect. The basic functionalities of these modules are briefly described below.

Aligning the Scans:

Each individual scan enters Polyworks unaligned in space regardless of if the scanner turned automatically or if manual repositioning was used. Therefore, IMAlign was used to mesh all of the individual scans from a given bluff together into a single image or composite scan. This process is done manually by matching similar features in the overlapping area. Alignment can be improved using Polyworks' automatic alignment algorithm. The software offers a variety of methods to verify the alignment including an RMS value and a histogram, yet visual inspection of the alignment also provides good assurance that the alignment was accurate. A well-aligned scan will be displayed as an even mesh of points in the overlapping area, with uniform representation from both scans.

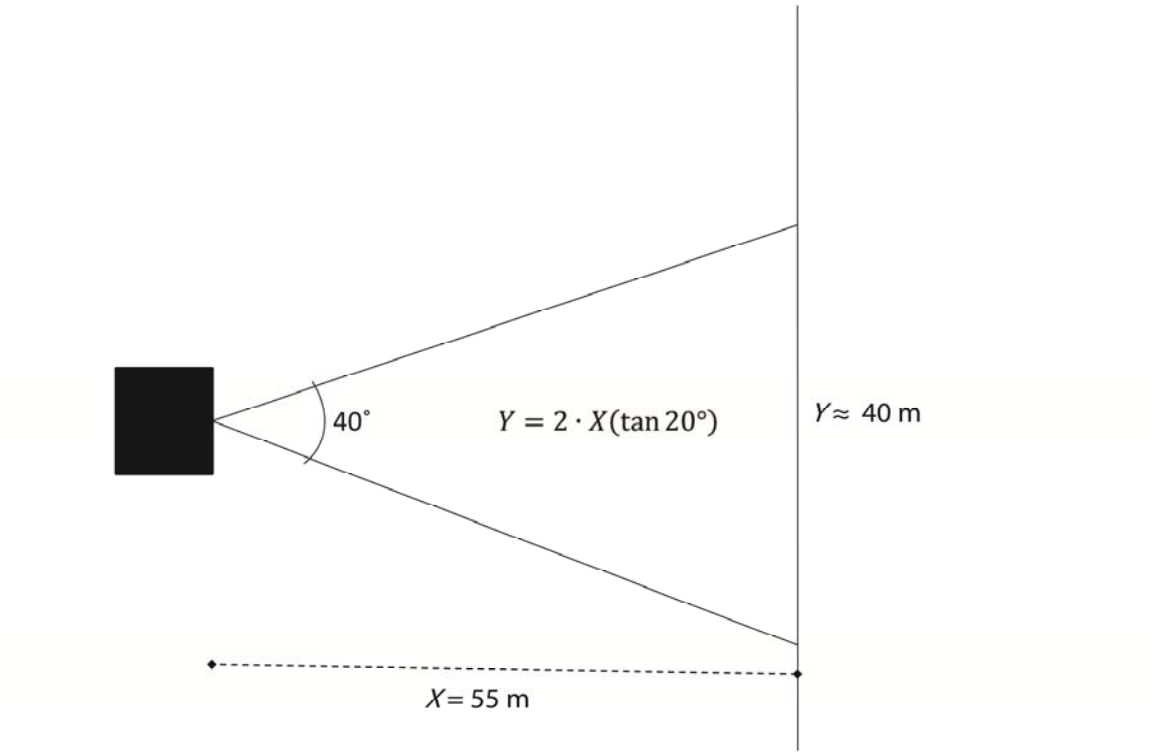

Figure 2.2: The Optech ILRIS-3_6D ER Terrestrial Laser Scanner scans a 40˚ swath at a single facing. The size of the area being scanned is dictated by the distance the scanner is from the surface of interest. The scanner can be fitted with a rotating base that rotate to the next facing with a 5% overlap. Each facing makes an individual scan that must be aligned to create a complete composite scan.

After all scans that comprise a given surface were aligned for each year, the composite scans from different years were aligned to a single coordinate system using the stable features in the scan (mean error = 0.03m) (Buckley et al., 2008; Wawrzyniec et al., 2007). It was important here that the bluffs were aligned based only on the known benchmarks. Polyworks has an automatic alignment algorithm that can be used to align scans based on all points, but this was not used because the bluff face was not a stable surface. By selecting all points that are not known to be stable (i.e. the bluff) and excluding them from the alignment, we used Polyworks' automatic alignment algorithm to align the composite scans based on only the stable features and specifically the benchmarks. Alignment is achieved by minimizing the average alignment error or the 3D distance between a point and a 3D surface. Once the composite scans of individual campaigns were aligned using these stable features, ideal alignment of the benchmarks was visually confirmed within Polyworks. As when aligning individual scans, well-aligned benchmarks will be displayed as an even mesh of points, with equal representation from both scans.

Creating a TIN:

After the composite scans were aligned between years, one scan was used to create a reference TIN (triangulated irregular network). The reference TIN provides a modeled surface against which the point cloud data from other years can be compared. Because the locations of individual points do not exactly align from year to year, the reference TIN allows the points to be compared in the direction of likely change rather than to the nearest point in the second composite scan. While a raster-based digital elevation model (DEM) could be used to achieve a similar goal, a TIN retains the 3D nature of the data rather than reducing it to 2D. This allows natural bluff features such as overhanging blocks and natural surface crenulations to be retained in the data.

The reference TIN was generated from the composite scan at a given site that covered the largest area and had the least vegetation. The reference TIN was then imported into IMEdit to fill in holes and remove vegetation (vegetation removal technique is the same as described later in this paper for point clouds). Holes exist in the TIN where data were not collected because macro-scale roughness elements (e.g. vegetation, boulders, and bluff surface roughness) generated shadows that were inaccessible to the scanning device, or wet areas of the bluff that did not reflect the laser signal. Typically in our scans, within the measured perimeter of the bluff, 0.2-9% of the bluff was missing due to shadowing or saturation. When considering the bluff edges,

which are often obscured by vegetation, the area missing was 6-21%. Holes can be filled automatically based on size or manually by selecting holes that should be filled. These holes were filled using the flat-filling method whereby the surface was connected using a flat plane to connect the points surrounding the hole. All but the largest holes (>10 m long at the longest length for this study) were filled in, so that the maximum number of points could be compared. Where holes were left unfilled, change was not measured in that area. Further discussion of the impact of holes in the data is in the discussion section of this paper.

Deleting Erroneous Data Points:

Once the reference TIN was complete, it was imported into IMInspect along with all the remaining point clouds for that site. IMInspect was used to clean up the data to account for points that lie off of the bare-earth bluff surface. Most of these irrelevant or "erroneous" data in this study were caused by vegetation, but some erroneous points were likely also caused by animals or water vapor. This step of removing these points is essential in calculating an appropriate erosion rate. Erroneous data can bias erosion measurements far more than holes in the data. Generally if an area was covered by vegetation, the points were removed, even if this resulted in an absence of data in the area. Without a regular, smooth surface, most automated algorithms are difficult to implement. In addition, changes in vegetation, or the presence of other erroneous data can cause localized erosion or deposition estimates to be incorrect by many meters. Erroneous data were manually removed by visually rotating the data such that the bluff was perpendicular to the view of the workstation display, allowing the operator to select and delete all points that were positioned above the line of the bluff. (e.g., Resop et al., 2012; Resop, 2010; Roberts, 2009).

Measuring change:

After all erroneous points were removed; scans were compared to find the change in volume between the reference TIN and a second scan. Many different techniques can be employed to compare two data sets; these are discussed further in the error analysis section of this paper. For this study we measured change along a vector normal to the surface of the bluff, or the plane of best fit, for the 3D point cloud (Fig. 2.3). Along curved bluffs, using a single best-fit plane may bias erosion estimates, particularly along the edges of the bluff, so curved bluffs were separated into multiple (2-4) subsections where the points in each subsection are reasonably approximated by a flat plane. The number of subsections was determined by the bluff shape (Fig. 2.4), with a

Figure 2.3: A) If only one vector is used to compare a curved bluff the change on the edges will be overestimated. B) When the bluff is broken into nearly planar areas, comparisons can be made more accurately. Three best fit planes are created for the curved sections of the bluff and vectors used for comparison are normal to these planes.

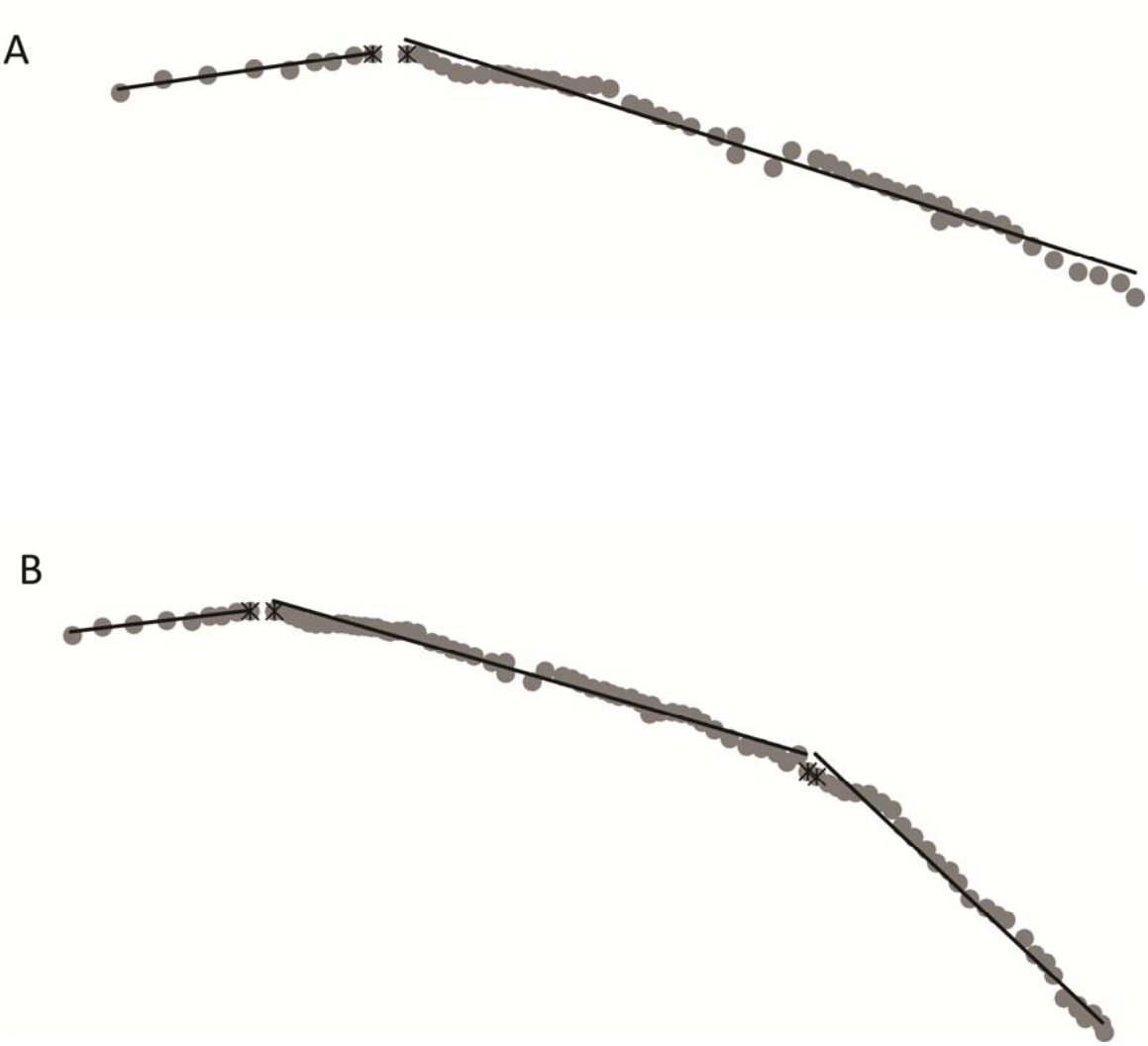

Figure 2.4: Each line of gray points shows a single slice of a bluff. The black lines represent individual planes that would be used to represent that portion of the bluff. The stars show where the bluff is divided (the beginning and end of each plane). Vectors are formed normal to the plane as the direction change is measured along. A) A bluff divided into two sections. B) A bluff with greater curvature than A divided into three sections.

goal of minimizing the number of subsections necessary to capture the curvature of the bluff. Additional planes will minimize error, yet may complicate the details of how the bluff is eroding.

A plane was fitted to the average bluff surface for each section of the point cloud. This plane was not used to determine the amount of change, but rather the direction of change. In all cases, the vector normal to the plane that defines the average bluff surface was used as the change direction vector. The point cloud data were compared to the TIN along the vector direction (Fig. 2.5), and the magnitude and direction (+ or -) of change were measured between each point and the reference TIN.

From the change data, we calculated the amount of erosion and/or deposition at every point on each bluff, and summed them to compute the total volume of sediment removed (or deposited), as well as the average rate of change across the entire surface. These calculations were performed in MatLab. Total change in volume was calculated by summing the length of change at each point and multiplying this by the average cell size or the average area represented by each point (eq. 2.1):

$$V = \sum\left(\sqrt{\Delta x^2 + \Delta y^2 + \Delta z^2}\right)(cell)(dir); \quad (2.1)$$

Where V= total volume of change (m^3); Δx = change in x direction (m); Δy = change in y direction (m); Δz = change in z direction (m); *cell* = cell size (m^2); and *dir* = direction of change (+1 or -1). The cell size at each point is calculated as the nearest neighbor distance squared. For the data sets used here the cell size ranges from $<1x10^{-12}$ to 12.39 m^2 and an average size of $2.09x10^{-4}$ m^2 with the largest cell size at the scan edges (Table 2.1).

Area was calculated based on average cell size and the total number of points compared in the scans. The rate of change (R) was calculated by incorporating the time between scans (T) (eq. 2.2):

$$R = \frac{V/A}{T}; \quad (2.2)$$

where A = area (m^2).

Validating retreat rates

Uncertainties associated with TLS include mechanical error documented for this equipment as 10-15 mm at ranges under 50-100 m (Wawrzyniec et al., 2007), error in aligning individual scans that comprise a given bluff for a given year, error in aligning annual composite scans from year to year, error from creating the TIN, error in removing erroneous points, and error in calculating the volume of sediment lost between the sets of annual composite scans. To

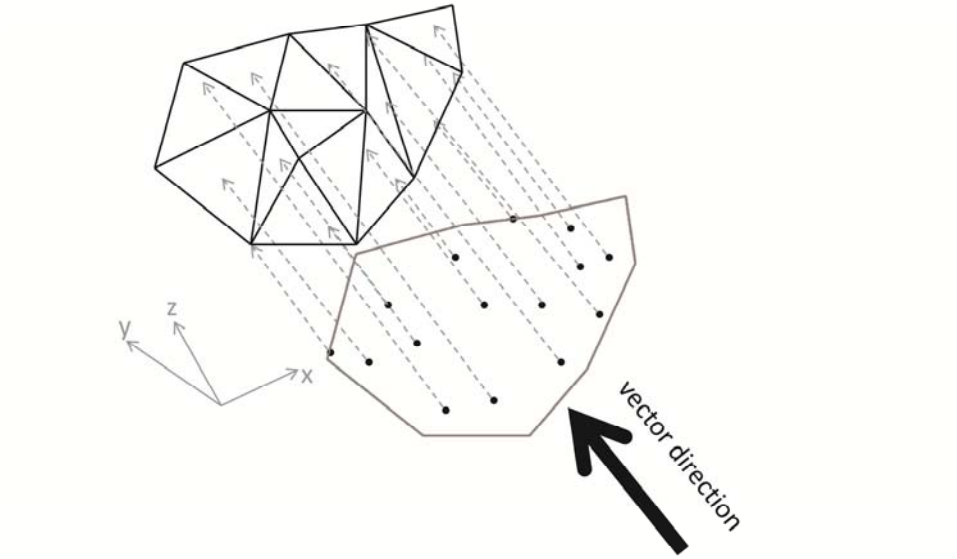

Figure 2.5: Change is measured along the predetermined vector direction. The distance between each point and the TIN is measured in the direction of the vector. This measurement is multiplied by the area represented by each point to determine the total volume of change.

Table 2.1: Cell size statistics (m^2)

Site	5th Percentile	Median	95th Percentile	Maximum	Average
OCTB1	$1.37x10^{-5}$	$2.28x10^{-4}$	$6.45x10^{-4}$	0.735	$2.28x10^{-4}$
TrB1	$2.30x10^{-5}$	$2.22x10^{-4}$	$7.34x10^{-4}$	12.4	$2.40x10^{-4}$
NCTB1	$6.76x10^{-6}$	$1.80x10^{-4}$	$9.86x10^{-4}$	1.17	$2.25x10^{-4}$
NCTB2	$3.25x10^{-5}$	$1.35x10^{-4}$	$2.89x10^{-4}$	1.53	$1.42x10^{-4}$

quantify net uncertainty, particularly the error associated with the change detection analysis methods, we performed two separate experiments.

Same-day validation analysis was used to quantify error created by data processing and analysis steps described above in cases where we were certain that no (or negligible) change had actually occurred. Two sets of scans were generated, one immediately after the completion of the other, at each of four different bluffs. Between each set of scans the scanner was removed from the tripod, the tripod was removed and then replaced, and the scanner was reassembled. These scans were processed and compared according to the same procedure outlined above. Only the known stable points were used to align the two sets of scans and the bluff area was excluded from the alignment algorithm as was done for the annual scans. The primary benefit of this validation method is that it provides the range of error associated with the range of circumstances present at each bluff, including vegetation and other erroneous data points.

Although the same-day validation analysis gives a measure of error due to instrumentation, alignment, TIN creation, and erroneous points, it does not incorporate error associated with the method used to measure bluff change. To examine the possible range of error introduced by using different change detection methods, we analyzed six different configurations that include change measurements along (a) a single vector; (b) multiple vectors; (c) the shortest distance from each point, and; (d) along the axial direction (X,Y,Z) that is primarily normal to the bluff. The single and multiple vector analyses measure change along a vector that is normal to either the entire bluff surface or a subsection of the bluff. The shortest distance method measures change from a given point to the nearest point in any direction. The last method tested uses an existing axial direction that is the most normal to the bluff surface (for many scanners this will be the Z direction). Each configuration was evaluated using the same-day validation test sites. Change detection results should be zero for these two experiments.

Results:

Results of the error tests described above showed that when data are appropriately processed total error in our application of this technology is very small, generally at least an order of magnitude less than recorded retreat rates for our study sites. Results for each of the error analyses and bluff retreat results from our study site are presented in corresponding sections below.

Error Analysis Results:

Using the methods described above including alignment using natural benchmarks, manually removing vegetation, and comparing the bluff in multiple subsections, the same day-validation analysis compares two scans taken such that there is no physical change to the surface being measured between scans. Results of the same-day validation analysis demonstrate that total root mean square error (RMSE) integrated across the entire bluff surface is between 0.023 and 0.086 for the bluffs surveyed (Table 2.2). The greatest error at an individual point is 1-4 meters for the bluffs measured, yet typically on 99% of the bluff there is less than 0.25 m error. This analysis sums the various error sources associated with using TLS in the way we present here including, error associated with the irregular bluff surface, the presence of erroneous points, alignment error, and mechanical error.

While the same day validation analysis resulted in a low amount of error, the change detection method test demonstrated that the way that change is measured may result in significant error (Table 2.3). Dividing the bluff into multiple subsections typically results in the lowest error measurements (RMSE: 0.023-0.086). The largest errors were derived when using the shortest distance change detection method (RMS: 0.19-0.86). This method uses an algorithm built into Polyworks that matches up each point with the closest point on the reference TIN.

Bluff Erosion Results:

The TLS methods presented here were tested in the Le Sueur River watershed in southern Minnesota. This is an actively evolving watershed with bluffs composed of fine-grained (65% mud) till ranging in height from 2 to 60 meters (Gran et al., 2009; Gran et al., 2011; Jennings, 2010; Day et al., this issue). There are three types of bluffs in the watershed: normally-consolidated bluffs (NCTB), over-consolidated bluffs (OCTB), and terrace bluffs (TrB). Normally-consolidated till bluffs form a wide range of slopes and support vegetation ranging from grasses to trees. Over-consolidated tills form as a result of glaciers re-advancing over the till, compacting and dewatering the sediment (Boulton, 1976; Kirkaldie and Talbot, 1992; Allred, 1999). The bluffs composed of over-consolidated tills often form very steep slopes that cannot easily support vegetation, and can be characterized by the presence of vertical joints. Terrace bluffs are strath terraces formed as the river incised and abandoned a previously active floodplain or river channel. On these bluffs the upper units of till have been eroded and are covered by an alluvial cap. This alluvium is typically around two to three meters thick with the upper half being fine-grained alluvium and the lower half coarse-grained alluvium overlying a thin gravel

Table 2.2: Same-Day Validation Analysis Results

Site name	**Volume lost (m^3)$^+$**	**Area compared (m^2)**	**Volume lost per area (m^3/m^2)***
OCTB	9.43	729.64	0.044
TrB	64.81	539.77	0.083
NCTB2	1.4107	229.54	0.023
NCTB1	52.73	1170.70	0.087

$^+$ If there was no error in these measurements the volume lost would be 0 m^3.

Table 2.3: Same-Day Vector Comparison Results[+]

Site Name	OCTB1*	TrB1*	NCTB1*	NCTB2*
Bluff divided into sections using multiple vectors	0.044 (3 vectors)	0.083 (2 vectors)	0.023 (2 vectors)	0.087 (2 vectors)
One vector generated along best fit plane	0.046	0.061	0.024	0.099
Shortest distance method	0.19	0.28	0.86	0.54
Along axial direction into bluff	0.065	0.065	0.036	0.25

***** All values reported as RMSE.

[+] If there was no error in these measurements the RMSE would be 0.

unit. Of the 480 bluffs in the Le Sueur watershed, 15 representative bluffs were scanned annually using TLS.

Annual change rates measured on the bluffs throughout the Le Sueur watershed ranged from 0.23 m/yr of deposition to 0.95 m/yr of erosion with an average net change of 0.20 m/yr of erosion (Table 2.4). At all sites, change was spatially and temporally variable (Fig. 2.6, Table 2.4). Colorized change maps provide a visual representation of spatial variability and can be used to interpret bluff erosion processes throughout the watershed (Fig. 2.7).

Discussion:

Results from the error analyses presented in this paper demonstrate that the methods used for this study can be successful at measuring bluff change with a low amount of error, an order of magnitude less than the rate of bluff erosion in this location. These error analyses demonstrate that annual scans can be aligned successfully using natural benchmarks such as bridges and trees. Results for the same-day validation analysis show that even when the tripod is repositioned, total error is an order of magnitude less than the calculated erosion rate (Table 2.2; Table 2.4).

The experiment testing different change detection methods indicates that the largest source of potential error depends on the analysis method used. The shortest distance change detection method often resulted in the greatest error. The shortest distance method creates a different vector direction for each point based on the direction of the nearest point in the TIN. Higher erosion rates were erroneously computed as a result of holes in the TIN, because points overlying those holes measured distances to the edge of the hole, which could be several meters in places with large gaps in the data due to surface roughness or dense vegetation. When using the shortest distance change detection method, holes resulted in areas where the erosion estimates were extremely high, which increased the overall average erosion rate for the entire bluff. The shortest distance change detection method could also obscure study of erosional processes. Without having a clear understanding of the direction along which change is being measured it may be difficult to identify the type of failure that occurred. High errors were also generated when change was simply measured along an axial direction primarily normal to the bluff. By measuring change along in a direction normal to the average bluff surface, errors are reduced substantially. While a single vector is acceptable for small bluffs with low curvature, dividing curved bluffs into multiple subsections greatly minimizes error. This technique is a simple method of accommodating bluff curvature, and reduces the occurrence of erroneously high retreat rates at bluff edges. The number of subsections the bluff should be divided into depends on the

Table 2.4: Bluff retreat results from the Le Sueur River

	0 to 1 year between scans			1 to 2 years between scans			2 to 3 years between scans		
Site	**Average Volume Lost (m^3)**	**Average Area Measured (m^2)**	**Average Retreat Rate (m/yr)**	**Average Volume Lost (m^3)**	**Average Area Measured (m^2)**	**Average Retreat Rate (m/yr)**	**Average Volume Lost (m^3)**	**Average Area Measured (m^2)**	**Average Retreat Rate (m/yr)**
NCTB1	18.77	300.73	0.07	19.43	224.46	0.07	35.67	198.14	0.07
NCTB2	583.44	2777.00	0.22	203.55	2145.90	0.07	422.76	1837	0.08
NCTB3	2655.55	6996.80	0.44	2125.70	7892.45	0.26	2593	2901.35	0.38
NCTB4	39.87	353.86	0.14	-64.73	341.91	-0.16			
NCTB5	17.25	147.04	0.17	55.70	138.19	0.28	84.82	106.54	0.29
NCTB6	8.37	210.17	0.05	43.86	105.40	0.22	21.86	25.78	0.26
NCTB7	-42.41	960.89	-0.06	1419.55	1092.34	0.84			
OCTB1	59.14	742.19	0.10	318.23	705.60	0.32	554.01	618.90	0.27
OCTB2				177.65	591.42	0.25	571.45	550.85	0.43
OCTB3	0.72	189.04	0.005	1.02	182.79	0.06			
OCTB4	253.82	423.56	0.72	81.53	506.83	0.11	171.90	558.68	0.12
TrB1	73.75	624.67	0.14	211.11	687.59	0.20	433.87	576.11	0.23
TrB2	1.34	29.47	0.05	8.03	71.75	0.07			
TrB3				54.15	160.73	0.26	133.43	165.99	0.33
TrB4	27.49	151.68	0.18						

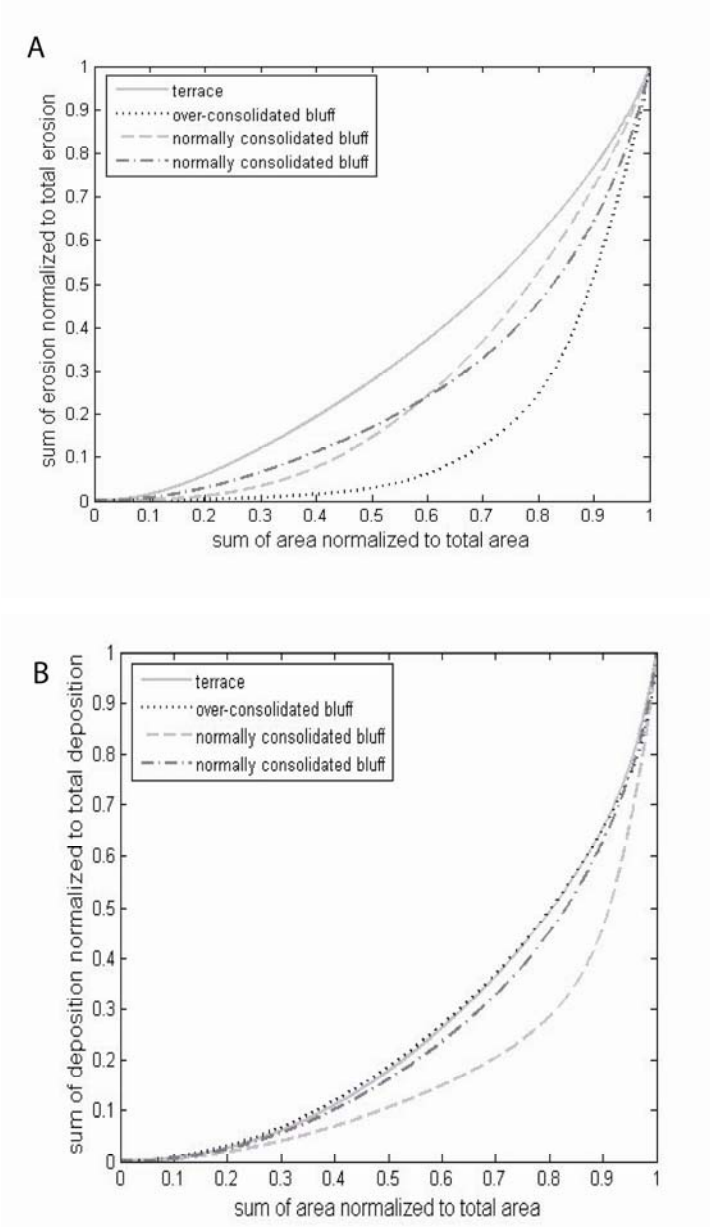

Figure 2.6: A) The cumulative erosion at each of the four bluffs normalized to the total erosion. B) The cumulative deposition normalized to the total deposition. In both cases area is normalized to total area. A 1:1 line would indicate that erosion or deposition is evenly distributed across the entire surface of the bluff. Erosion is most localized on OCTB and most evenly distributed on TrB. Deposition is most localized on NCTB1 where sediment collected at the toe of the bluff.

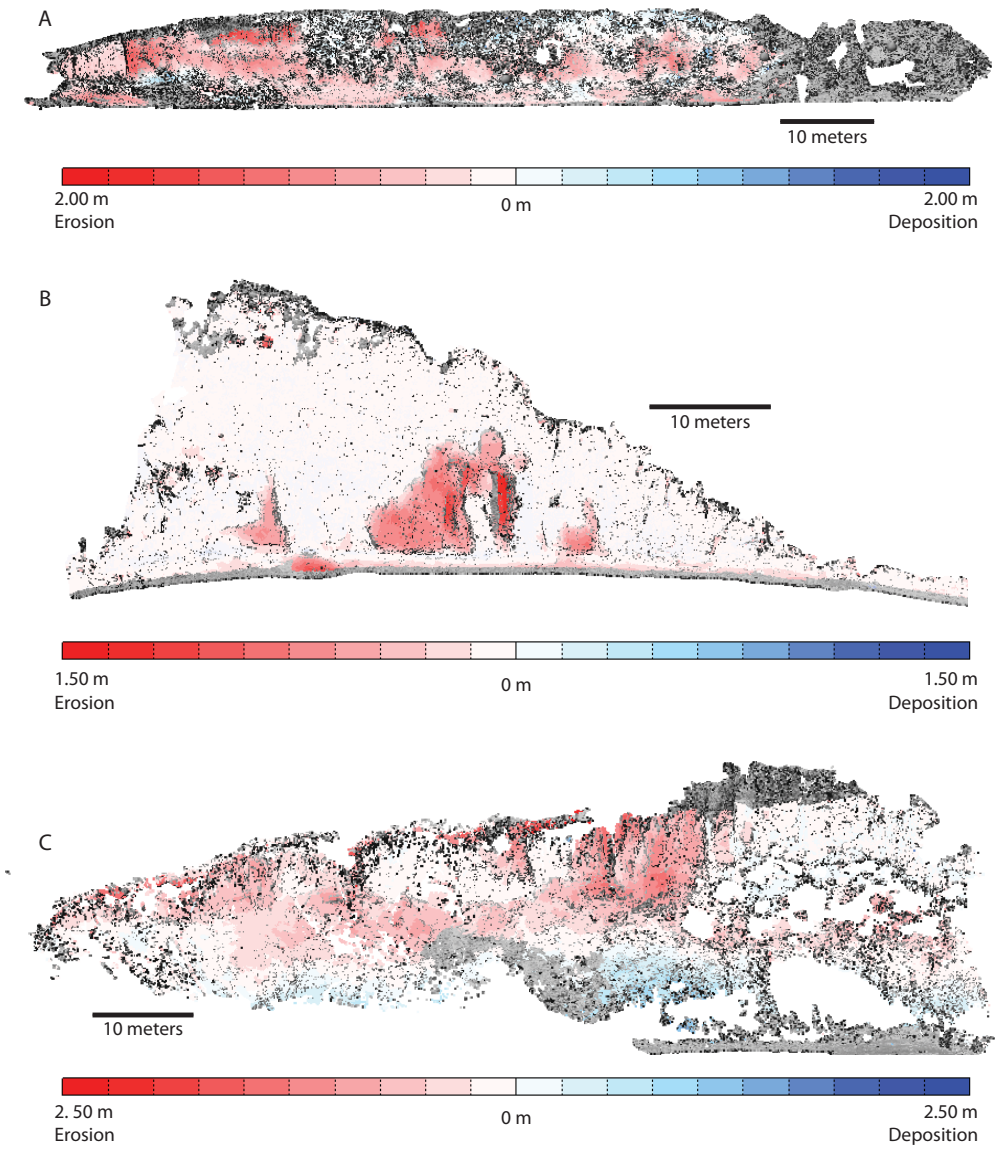

Figure 2.7: Color maps show change on individual bluffs. A) A terrace bluff, TrB, where the upper portion of the bluff is composed of alluvium. A thin gravel unit separates the upper alluvium from the lower tills, and is a source of seeps in this type of bluff. Change from 2007-2008 shows a 2 meter rotational failure in the alluvium at this site. B) An over-consolidated till bluff, OCTB, with vertical jointing that is indicative of this type of bluff. Change from 2008-2009 shows that erosion occurred primarily along the joints. C) A normally-consolidated till bluff. Change from 2007-2009 shows erosion at the top of the bluff and deposition at the toe. Typically toe deposition is removed quickly and these scans capture a moment when this hasn't yet occurred.

bluff curvature. It is important that a plane can be used to represent most points in each subsection of the bluff. This process of dividing the bluff into subsections can be done simply by visual inspection. In figure 2.4, for example, a single plane can be fitted to a subsection with this low curvature without resulting in exceptionally high error values.

Using the methods proposed in this paper, the presence of holes in the data sets due to surface roughness or areas of vegetation that must be removed are not a concern. While data holes can result in high errors when using the shortest distance change detection method as discussed above, we recommend that this change detection method is not used. Holes can be thought of as the areas between data points that occur when using coarse resolution data sets like bank pins or traditional surveys. Depending on the specific research questions being addressed, and the nature of the surface being measured, it is possible to interpolate across these data holes or simply leave the holes empty and focus only on known areas. Because TLS generates very high resolution data sets there are fewer holes to be concerned with, and the size of these holes can be highly variable across the bluff surface. We found error to be reduced when we interpolated between small holes (less than 10 m measured along the longest axis for this study), while leaving large holes in the TIN unfilled. Filling small holes in the TIN maximizes the area of the bluff surface that can be compared from year to year. Leaving all holes unfilled would have reduced the compared area in most scans by approximately 30% (Fig. 2.8). For our study the larger holes were of little concern, as these areas were simply excluded from our consideration. Moreover, because many of the holes were in areas where vegetation was removed from the bluff surface, it is likely that these areas underwent less change over the annual time scales we measured (Day et al., this issue).

Vegetation continues to be a concern for the use of TLS in natural environments. Manually removing vegetation can be tedious and potentially subjective, but we had little success applying automated algorithms to this process. Natural surface variations of bluff features make it impossible to assume a smooth surface that represents the bluff. Techniques that have been successfully applied to aerial lidar data processing cannot be used with the same success for TLS data. For example, in processing aerial lidar the assumption is often made that the last return represents the ground surface. This assumption is less effective using TLS (Sharma et al., 2010). In some cases automated techniques or last returns can provide a good first pass at removing vegetation and other erroneous points, but manual removal makes it possible to remove any remaining vegetation points. We suggest being aggressive with vegetation removal to ensure these erroneous points are removed. While this may result in a greater number of data holes, error

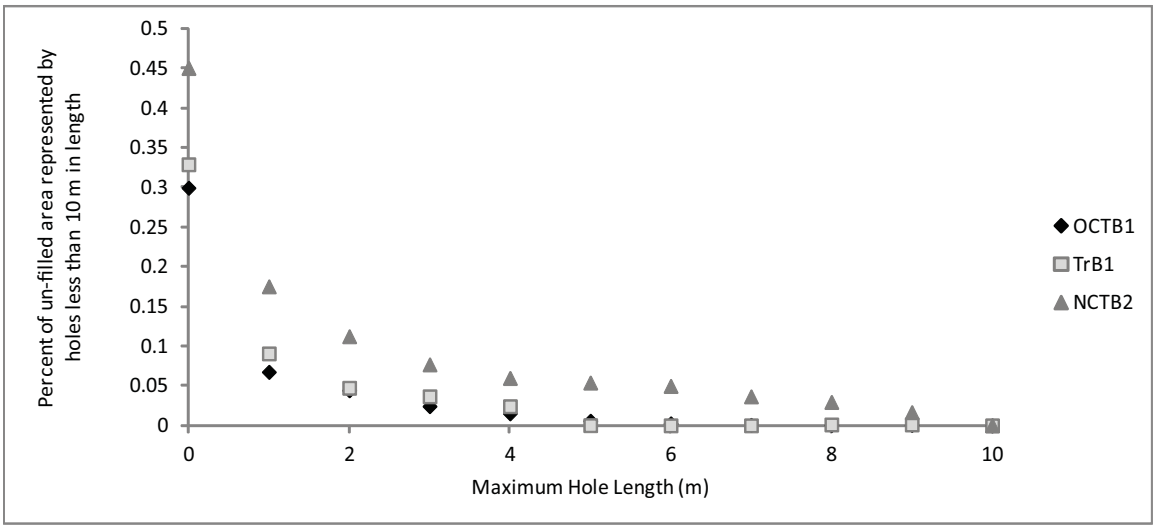

Figure 2.8: In this study we filled holes where the maximum length of the hole was less than 10 meters. Not filling these holes would have reduced the measurable bluff area by approximately 35%. This chart shows the percent area filled at each hole size for a maximum of a hole that is less than 10 meters long.

produced by vegetation changes is greater than the error produced from holes for the reasons discussed above. Care should also be taken by collecting data at the appropriate time of year to minimize vegetative cover. In many areas this may mean scanning in the late fall or early spring during leaf off, or in the winter if snow cover is not an issue.

On average, total error is only 30% of the retreat rates measured at our study site on the Le Sueur River. In addition to measuring retreat rates over the complete bluff surface we were able to use the data generated to identify bluff erosion processes and measure the spatial variability of bluff erosion. On the sites we studied, over 50% of the erosion or deposition occurred on only 10-30% of the bluff surface (Fig. 2.6). Most other traditional change detection techniques would likely have missed much of this detail causing change estimates to be overestimated or underestimated (Resop and Hession, 2010). Given the spatially variable nature of bluff erosion, if the selected points measured using traditional surveying or erosion pins were in an area of high erosion, resulting estimates for bluff erosion volume or rate could be erroneously high. In places where we observed very high erosion rates, the depth of material removed (>1 meter) would likely have resulted in loss of the bank pins in those locations.

The distribution of erosion can be observed in detail using colorized change maps (Fig. 2.7). These maps can be used to interpret the dominant bluff erosion mechanisms at each bluff site. The location and shape of the failure at each of the sites shown in figure 2.6 demonstrate a different erosion process important to the Le Sueur watershed including, over-steepening at the bluff toe, failure due to moisture-saturation associated with seeps, and failure due to weakening by freeze-thaw. The relative importance of the different bluff erosion processes is impacted by bluff material properties.

Conclusion

Accurate bank and bluff erosion estimates are essential for improving our understanding of near-channel sediment dynamics. Conventional tools for measuring bank and bluff change, such as banks pins or total station surveys provide very coarse resolution and potentially biased data (Resop and Hession, 2010). Further, these techniques are limited to locations where the surface of interest is directly accessible. TLS overcomes these difficulties by relying on a time of flight system that collects data at mm - cm scale resolution. The methods outlined in this paper demonstrate one method that can be used to overcome some of the difficulties inherent with using this technology in a riverine environment including the presence of vegetation, natural surface crenulations, difficulties with re-establishing the same spot annually, and difficulties with

creating benchmarks on inaccessible surfaces. We have evaluated techniques for processing and interpreting change detection data using Polyworks metrology software, which is a publicly-available software capable of processing large point cloud data sets that can be used to compare scans collected at different points in time.

Error analyses presented here demonstrate the low possible error that can be achieved using TLS for change detection. Potential sources of error inherent with this technology include error associated with the irregular surface of the bluff, the presence of erroneous points, alignment error, mechanical error, and the error associated with the change detection method used. While vegetation introduces challenges for using TLS in natural settings, removing it from the scan during data processing can significantly reduce the associated error. In some cases removing the vegetation from the scans can result in data holes. As noted in the discussion these holes are similar to areas with no data that occur when using bank pins or total station surveys. It is possible to interpolate between holes or to simply not measure change in the holes. In this paper we interpolated between the smallest holes, while we ignored the largest holes and left them out of the change measurements. This method maximized the data without relying on significant interpolation, which otherwise would have increased error.

These methods for measuring change using TLS can be applied to river bluffs and banks throughout the world. The level of detail achieved using TLS allows us to not only measure retreat rates, but can also help us gain insight into the processes and drivers of erosion. While additional research is needed to ensure that the highest data quality is being generated each time we use TLS, the benefits of the technology are clear. The ability to rapidly collect high resolution data across an entire bluff surface is not achieved in any other way, and while there is a steep learning curve associated with using the technology and processing the data, the equipment and software is rapidly becoming more user friendly.

Works Cited:

Alho P, Kukko A, Hyyppä H, Kaartinen H, Hyyppä J, Jaakkola A. 2009. Application of boat-based laser scanning for river survey. Earth Surface Processes and Landforms**34**:1831-1838.

Allred BJ. 1999. Survey of fractured glacial till geotechnical characteristics: hydraulic conductivity, consolidation, and shear strength. Ohio Journal of Science**100**: 63-72.

Boulton GS. 1976. The development of geotechnical properties in glacial tills. Legget RF(ed).Glacial Till. Ottawa: The Royal Society of Canada. Special Publication NO. 12; 292-303.

Buckley SA, Howell JA, Enge HD, Kurz TH. 2008. Terrestrial laser scanning in geology: data acquisition, processing, and accuracy considerations. Journal of the Geological Society of London**165**:625-638.

Couper P, Scott T, Maddock I. 2002. Insights into river bank erosion processes derived from analysis of negative erosion pin recordings: observations from three recent UK studies. Earth Surface Processes and Landforms**27**:59-79.

Day S, Gran K, Belmont P, Wawrzyniec T. this issue. Measuring bluff erosion part 2:Pairing aerial photographs and terrestrial laser scanning to create a watershed scale sediment budget. Earth Surface Processes and Landforms.

Gran KB, Belmont P, Day SS, Jennings C, Johnson A, Perg L, Wilcock PR.2009.Geomorphic evolution of the Le Sueur River, Minnesota, USA, and implications for current sediment loading. James LA, Rathburn SL, Whittecar GR, (eds.). Management and Restoration of Fluvial Systems with Broad Historical Changes and Human Impacts: Geological Society of America Special Paper 451.

Gran KB, Belmont P, Day S, Jennings C, Lauer JW, Viparelli E, Wilcock P, Parker G. 2011, An integrated sediment budget for the Le Sueur River basin. Final report Presented to the Minnesota Pollution Control Agency.

Gulyaev SA, Buckeridge JS.2004, Terrestrial methods for monitoring cliff erosion in an urban environment. Journal of Costal Research**20**, 871-878.

Haigh MJ. 1977. The use of erosion pins in the study of slope evolution. Shorter Technical Methods (II), Finlayson BL (ed). British Geomorphological Research Group Technical Bulletin Group **18**: 31–49.

Heritage G, Hetherington D. 2007.Towards a protocol for laser scanning in fluvial geomorphology. Earth Surface Processes and Landforms**32**:66-74.

Heritage GL, Milan DJ. 2009. Terrestrial laser scanning of grain roughness in a gravel bed river. Geomorphology **113**: 4-11.

Hodge R, Brasington J, Richards K. 2009. Analysing laser-scanned digital terrain models of gravel bed surfaces: linking morphology to sediment transport processes and hydraulics. Sedimentology **56**: 2024-2043.

James LA, Watson DG, Hansen WF. 2007. Using Lidar data to map gullies and headwater streams under forest canopy: South Carolina, USA. Catena **71**: 132-144.

Jennings CE. 2010. Draft digital reconnaissance surficial geology and geomorphology of the Le Sueur River watershed (Blue Earth, Waseca, Fairbault, and Freeborn counties in south-central MN). Open File Report 10-03 Minnesota Geological Survey, map, report and digital files. ftp://mgssun6.mngs.umn.edu/pub4/ofr10_03/.

Kent TR, Stelzer RS. 2008. Effects of fine sediment on life history traits of Physa integra snails. Hydrobiologia **596**: 329-340.

Kirkaldie L, Talbot JR. 1992.The effects of soil joints on soil mass properties. Bulletin for the Association of Engineering Geology**25**:415-420.

Lawler DM. 1978. The use of erosion pins in river banks. Swansea Geographer**16**:9–18.

Lim M, Rosser NJ, Allison RJ, Petley DN.2010. Erosional processes in the hard rock coastal cliffs at Staithes, North Yorkshire. Geomorphology**114**:12-21.

Lovell JL, Jupp DLB, Culvenor DS, Coops NC. 2003. Using airborne and ground-based ranging lidar to measure canopy structure in Australian forests. Canadian Journal of Remote Sensing **29**:607-622.

Matthews N. 2008, Aerial and Close-Range Photogrammetric Technology: Providing Resource Documentation, Interpretation, and Preservation. by Neffra A. Matthews Technical Note 428 Bureau of Land Management

Milan DJ, Heritage GL, Hetherington D. 2007.Application of 3D laser scanner in the assessment of erosion and deposition volumes and channel change in a proglacial river. Earth Surface Processes and Landforms**32**:1657-1674.

.

Optech, 2011. http://www.optech.ca/aboutlaser.htm. website accessed July 19, 2011.

Optech, 2012. http://optech.ca/pdf/ILRIS_SpecSheet_110309_Web.pdf. pdf accessed April 19, 2012

Resop JP, 2010. Terrestrial laser scanning for quantifying uncertainty in fluvial applications.Doctor of Philosophy Thesis from Virginia Polytechnic Institute and State University.128 pages.

Resop JP, Hession WC. 2010. Terrestrial laser scanning for monitoring streambank retreat: comparison with traditional surveying techniques. Journal of Hydraulic Engineering**136**: 794-798.

Resop JP, Kozarek JL, Hession WC. 2012. Terrestrial laser scanning for delineating in-stream boulders and quantifying habitat complexity measures. Photogrammetric Engineering and Remote Sensing **78**: 363 - 371

Roberts L. 2009. Biogeomorphology and soil geomorphology of small semiarid basins, Northeastern Arizona: influences of topoclimate and climate variations. Master of Science Thesis from the University of New Mexico.80 pages.

Rosser NJ, Petley DN, Lim M, Dunning SA, Allison RJ. 2005. Terrestrial laser scanning for monitoring the process of hard rock costal cliff erosion. Quarterly Journal of Engineering Geology and Hydrogeology**38**: 363-375.

Sharma M, Paige GB, Miller SN. 2010. DEM development from ground-based LiDAR data: A method to remove non-surface objects. Remote Sensing **2**: 2629-2642

Shields FD, Knight SS, Cooper CM. 1995. Use of index biotic integrity to assess physical habitat degradation inwarmwater streams. Hydrobiologia **312**: 191-208

Soulsby C, Youngson AF, Moir HJ, Malcolm IA. 2001. Fine sediment influence on salmonid spawning habitat in a lowland agricultural stream: a preliminary assessment. Science of the Total Environment **265**: 295:307.

Strahler AH, Jupp DLB, Woodcock CE, Schaaf CB, Yao T, Zhao F, Yang X, Lovell J, Culvenor D, Newnham G, Ni-Miester W, Boykin-Morris W. 2008. Retrieval of forest structural parameters using a ground based lidar instrument. Canadian Journal of Remote Sensing**34**:426-440.

Thorne CR. 1981. Field measurements of rates of bank erosion and bank material strength.Erosion and Sediment Transport Measurement (Proceedings of the Florence Symposium, June 1981). IAHS Publication 133, International Association of HydrologicalSciences: Wallingford. 503–512.

Van der Zande D, Hoet W, Jonckheere L, van Aardt J, Coppin P. 2006. Influence of measurement set-up of ground based Lidar for derivation of tree structure. Agricultural and Forest Meteorology **141**:147-160.

Wawrzyniec TF, McFadden LD, Ellwein A, Meyer G, Scuderi L, McAuliffe J, Fawcett P. 2007. Chronotopographic analysis directly from point-cloud data: A method for detecting small seasonal hillslope change in Black Mesa Escarpment, NE Arizona. Geosphere**3**:550-567.

Williams RD, Brasington J, Vericat D, Hicks D, Labrosse F, Neal MN. 2011. Monitoring braided river change using terrestrial laser scanning and optical bathymetric mapping. In Smith M, Paron P, and Griffiths J. 2011. Geomorphological Mapping. Elsevier.

Chapter 2:

Comparing aerial photographs and terrestrial laser scanning to create a watershed scale sediment budget

Effectively managing and reducing high suspended sediment loads in rivers requires an understanding of the magnitude of major sediment sources as well as erosion and transport processes that deliver excess fine sediments to the channel network. Tall bluffs were identified as a source of fine sediment on the 2880 km^2 Le Sueur watershed, Minnesota, USA. To better understand erosion rates on these near-vertical features, we coupled analyses of seven decades of aerial photographs with four years of repeat terrestrial laser scanning (TLS). Together, these datasets provide decadal-scale retreat rates throughout the entire watershed and high-resolution geomorphic change detection on a subset of bluffs to better constrain erosion rates and document bluff erosion mechanisms. Here we discuss methods used to measure erosion rates from aerial photographs and TLS and extrapolate those measurements to obtain estimates of sediment loading from these features throughout the watershed. The utility of each approach is discussed as well as how these data were used in an integrated sediment budget to assist with management of high sediment loads in the Le Sueur watershed. We used aerial photographs and TLS to extrapolate from 243 and 15 measured bluffs, respectively, to all 480 bluffs in the Le Sueur River watershed. Despite different spatial and temporal measurement scales, the aerial photograph and TLS estimates yielded similar results for bluff retreat rate and total mass of sediment derived from bluffs. Bluffs in the Le Sueur watershed yield 135,000 ± 39,000 Mg/yr of fine sediment, which comprises 57±16% of the 2000-2010 average measured total suspended solids load.

Introduction:

Anthropogenic disturbances can have a negative impact on watershed ecosystems (e.g., Harding *et al.,* 1998; Bernhardt and Palmer, 2007; Maloney and Weller, 2011). Often these disturbances result in increased erosion leading to high suspended sediment loads (e.g., Dotterweich, 2008). Because excess sediment loading comes from widely dispersed nonpoint sources, management of high sediment loads is ideally done at the watershed level. Detailed sediment budgeting is one tool for watershed assessment wherein all sediment sources and sinks are quantified, evaluated, and compared to gauge records throughout the basin for a specified period of time. The sediment budget can then help direct conservation efforts in the watershed and focus restoration efforts on the dominant erosional processes and the areas of greatest concern.

Rivers in agricultural landscapes are commonly cited as having unnaturally high sediment loads (Montgomery, 2007; Wilkenson and McElroy, 2007). Anthropogenic changes in these landscapes are not limited to the changes in vegetation. Fields are commonly tilled and left unvegetated for some portion of the year, leaving them susceptible to erosion from runoff and wind (Lobb *et al.,* 1995). Hydrology is often altered through irrigation and/or artificial surface and subsurface drainage, an effect that may lead to high erosion on fields and nearby channels (e.g. Blann et al., 2009; Hirt *et al.,* 2011; Belmont *et al.,* 2011). Determining whether the dominant sources of sediment in agricultural landscapes are upland erosion or near-channel erosion remains a significant challenge (De Vente *et al.,* 2007; Smith et al., 2011). This is primarily due to difficulties associated with adequately constraining sediment transport and storage dynamics within the landscape and channel floodplain network.

Watershed erosion and sediment transport processes are complex, and linking landscape erosion with river sediment loads is not a straightforward problem. Trimble (1999) demonstrated that sediment yield from Coon Creek, in southwestern Wisconsin, remained relatively constant over the past two centuries, despite extraordinary changes in upland erosion, because much of the eroded sediment remained stored in the landscape and channel-floodplain system. Similarly, Walter and Merritts (2008) demonstrated that modern sediment loads of many streams throughout the mid-Atlantic United States are primarily controlled by historic erosion of the landscape and storage of sediment in milldams, both anthropogenic effects. In both of these cases detailed measurements of near-channel erosion would provide critical information for making predictions about sediment yield in the river.

Belmont *et al.* (2011) synthesized multiple independent measurements of sources and sinks into an integrated sediment budget for the Le Sueur River, south-central Minnesota, USA. Sediment sources included agricultural uplands, ravines, bluffs, and streambanks. The dominant source of sediment was tall bluffs that line the incised, lower 40 km of the Le Sueur River and its two main tributaries the Maple and Big Cobb / Little Cobb Rivers (referred to jointly as the Cobb River). This is consistent with results found on nearby rivers with a similar evolution and geology (Sekely et al., 2002; Thoma et al., 2005). These bluffs, and the methods used to constrain the sediment loads derived from them, are the focus of this paper.

Constraining bluff erosion requires measurements of bluff extent and retreat rates through time. In this study, bluff erosion was measured over annual to semi-annual time scales using terrestrial laser scanning (TLS) (Day *et al.,* this issue) and over decadal scales using historic aerial photography. This paper focuses on the methods used both for measuring bluff retreat rates and for extrapolating these rates to all bluffs throughout the entire Le Sueur River watershed to determine the role of bluffs on the total sediment budget. Results show the estimated range of sediment loads derived from bluffs using multiple extrapolation techniques and how these sediment loads compare to the total sediment load measured at gauging stations throughout the watershed. Because bluffs contribute the majority of the fine sediment load in the Le Sueur River, making an accurate estimate of bluff erosion is critical both for compiling a sediment budget and determining potential effectiveness of various management options to reduce excess sediment loading. The measurement techniques are demonstrated on bluffs in the Le Sueur River watershed yet they could easily be used for similar features, including river banks.

Study Area:

The Le Sueur River is a 2880 km^2 watershed in south-central Minnesota (Fig. 3.1), that contributes a disproportionate amount of fine-grained (silt and clay) sediment to the turbidity-impaired Minnesota and Upper Mississippi Rivers. Sediment loads in the Le Sueur River are naturally high because it is a young, actively incising river (Gran *et al.,* 2009; Gran *et al.,* 2011). The Le Sueur River watershed is evolving in response to rapid incision by glacial River Warren beginning 11,500 radiocarbon years before present (rcbp; 13,400 calendar years before present) in response to outburst floods from glacial Lake Agassiz (Clayton and Moran 1982; Matsch 1983; Gran et al., 2009; Belmont, 2011). A series of floods punctuated by periods of quiescence incised glacial River Warren as much as 70 meters (Thorleifson, 1996; Lowell *et al.,* 2005), spawning knickpoints on all major tributaries. The modern Minnesota River Valley now

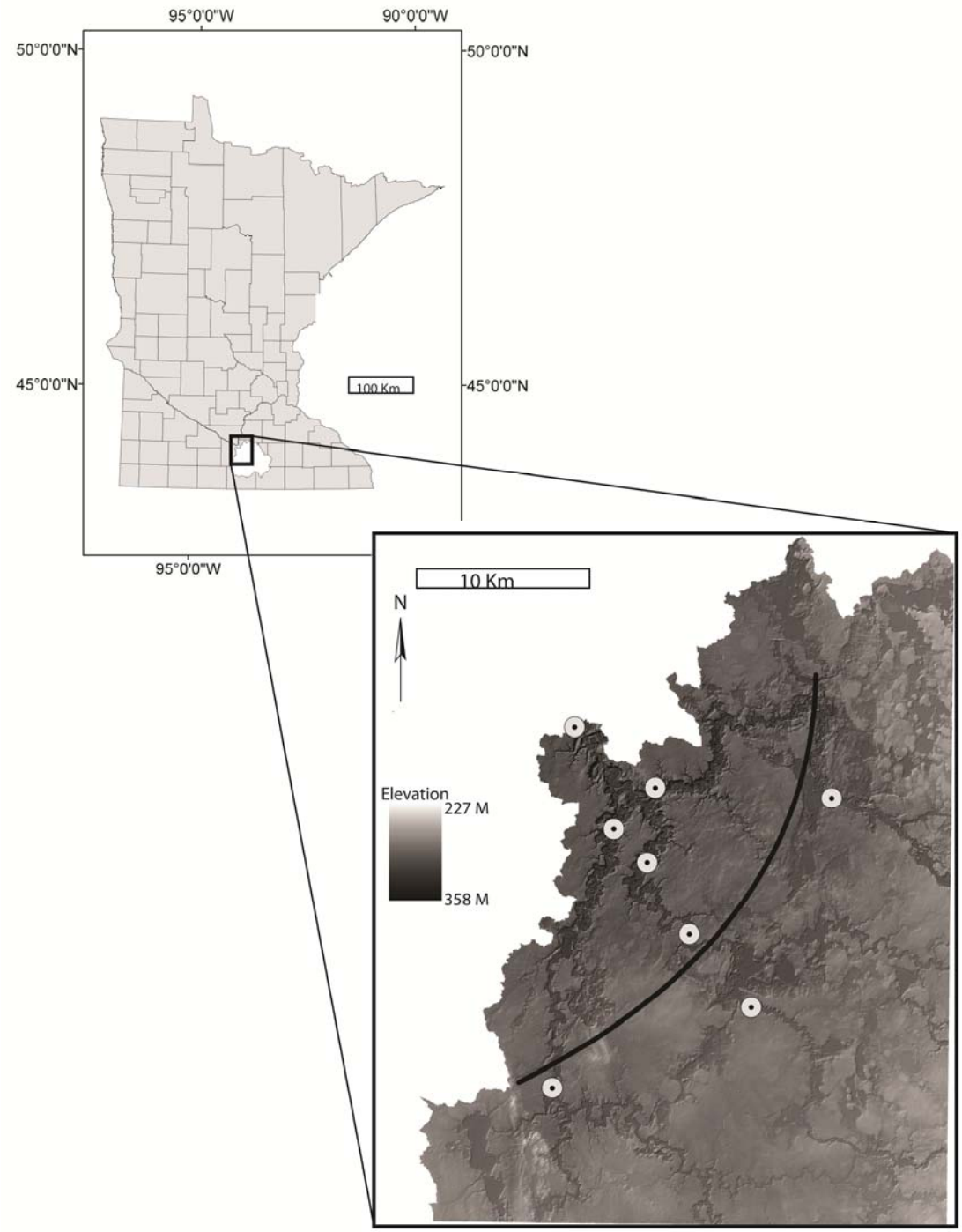

Figure 3.1: Inset shows the portion of the Le Sueur River watershed that is within Blue Earth County Minnesota, including the entire knick zone, the upper extent of which is indicated by the black solid line. White circles show locations of water and sediment gauging stations.

occupies the channel carved by glacial River Warren. The Minnesota River is listed as impaired for turbidity under the US Clean Water Act due in part to the still actively-evolving tributaries (including the Le Sueur River) within its watershed.

The Le Sueur River is incising through a series of stacked fine-grained tills, deposited over several glacial cycles, interbedded with glaciofluvial sands and gravels. Throughout most of the basin tills are capped by glaciolacustrine silts and clays. Tills in the watershed are generally fine-grained (< 1% gravel and boulders) and range in their degree of consolidation from normally-consolidated to over-consolidated (Fig. 3.2) (Jennings, 2010; Belmont et al., 2011). Because the Le Sueur River is carving through mechanically weak glacial sediments, the knickpoint has not maintained steep face, but instead has laid back forming a diffuse knick zone (Gardner, 1983; Belmont, 2011). The top of the knick zone, which we will refer to as the knickpoint is located approximately 40 km upstream on the Le Sueur, Cobb and Maple river networks (Fig. 3.1) (Gran *et al.,* 2009). The knickpoint is migrating upstream at a rate of 3.0-3.5 m/yr and incising at a rate of 2.6 mm/yr resulting in the formation of tall bluffs and steep ravines in the valley downstream (Finnegan et al., 2010).

The Le Sueur River was selected for a detailed study because it contributes ~24-30% of the total sediment load to the Minnesota River yet only makes up 7% of the watershed area (Minnesota Pollution Control Agency [MPCA] *et al.,* 2007). The Le Sueur River watershed has the added benefits of having high-resolution aerial lidar data available throughout the incised portion of the watershed and an extensive network of gauging stations.

The Le Sueur River and its two main tributaries, the Maple and Cobb Rivers, are all gauged, with a total of 8 water and sediment gauges, each monitored for three to eleven years (Water Resources Center [WRC] and MPCA, 2009). Gauge data available over the past decade indicates that sediment yields increase significantly within the knick zone. On each of the three main branches of the Le Sueur River there are at least two gauges bracketing the knick zone (Fig. 3.1). Analysis of annual TSS load at the mouth of the Le Sueur over the period of 2000-2010 shows that an average of 225,000 Mg/yr reaches the mouth, with 60% derived within the knick zone, an area covering less than 30% of the watershed, and much of this sediment is derived from near-channel sources that make up less than 1% of the watershed area (Gran et al., 2011). In 2006, for example, TSS yield on the Maple Rivers increased from 9.9 to 25.4 Mg/km^2 as the river flowed through the knick zone, while yields on the Cobb River increased from 11.8 to 45.4 Mg/km^2 (Gran *et al.,* 2009). The vast majority of ravines and bluffs exist below the upper gauges on each branch within the knick zone. Above this point, the river has not incised significantly,

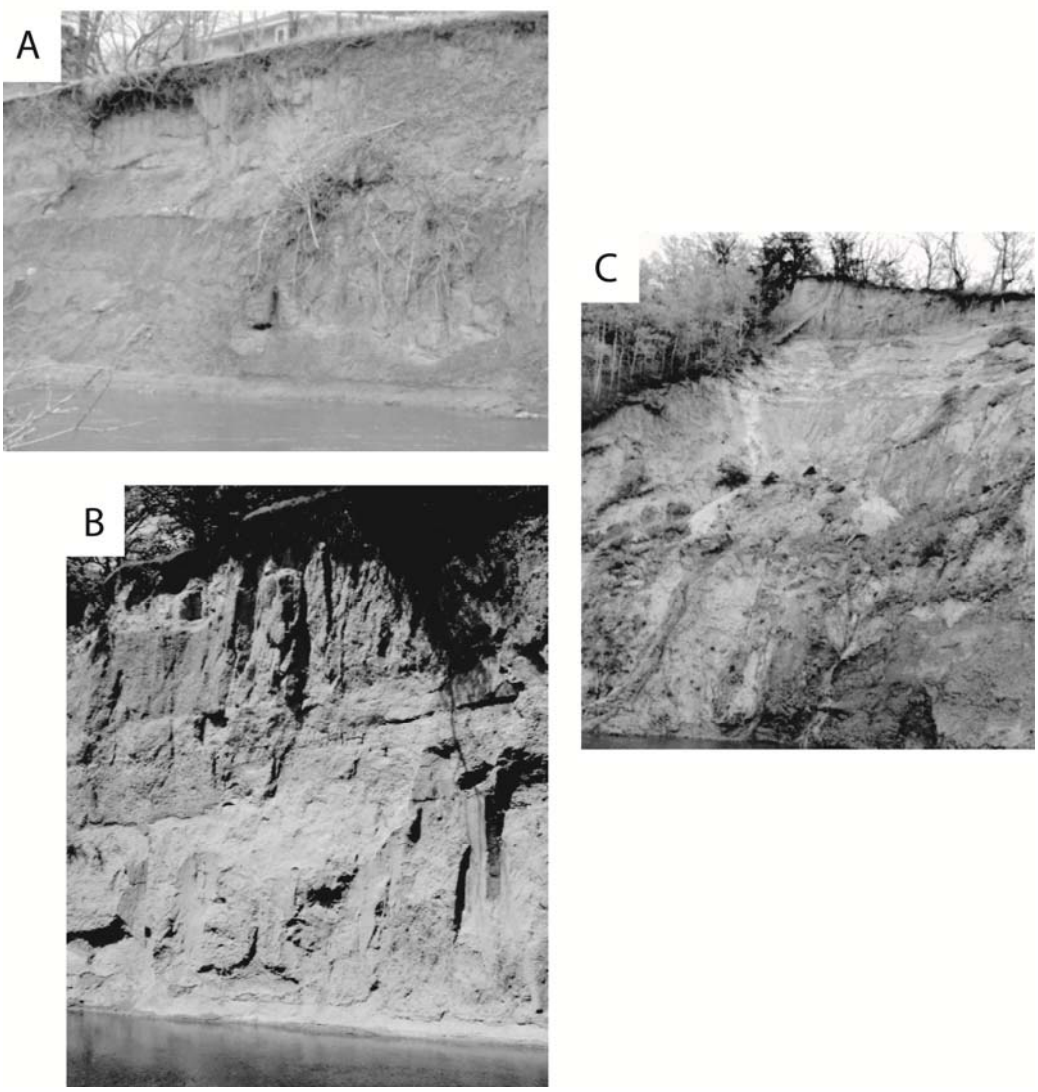

Figure 3.2: Only bluffs in direct contact with the river were considered for this analysis. Pictures show a selection of bluffs in the watershed that demonstrate different bluff types discussed throughout the paper. A) Terrace bluffs have a 2 meter thick unit of alluvium overlying in situ till. A coarse gravel unit forms the base of the alluvium. B) Over consolidated till bluffs appear jointed, rarely support vegetation and can form vertical faces and overhanging blocks of sediment. C) Normally consolidated till bluffs have a massive appearance, can support vegetation on their face and are often lower angle.

and ravines and bluffs have not been formed except in a few locations where the river has meandered into higher-standing topography.

Primary Bluff erosion processes in the Le Sueur:

Near-channel sediment sources include stream banks, bluffs, and ravines. Bluffs are tall features, reaching as high as 70 m in the deeply-incised lower part of the Le Sueur River valley. Bluffs are distinguished from stream banks because they are composed of parent material (primarily glacially-derived till) and also because they exceed the height of the floodplain and are thus hydraulically-disconnected from the modern channel. Many bluffs are also valley walls, extending as much as 70 m from the elevation of the modern river all the way up to the flat upland surface above. Other bluffs within the incised valley are strath terraces and are composed of till capped by alluvium.

The three main processes that drive bluff erosion in the Le Sueur River watershed are undercutting (or over-steepening), sapping, and freeze-thaw. The type of erosion is often dictated by bluff stratigraphy and consolidation state. At most sites, undercutting is a significant contributing factor to erosion, as commonly seen in other field locales (e.g., Turnbull et al., 1966; Brunsden and Kesel, 1973; Harden *et al.,* 2009). Undercutting occurs when the shear stress of the flow exceeds critical at the bluff toe, leading to toe erosion and subsequent failure as the bluff slope becomes over-steepened. The critical shear strength of the bluff toe is controlled by grain size and cohesion. Bluff strength can be reduced by freeze-thaw cycles, making the bluff more susceptible to undercutting by high flows in early spring (Terzaghi 1962; Kirkby, 1965). Groundwater flow or sapping can also reduce the strength of the sediment by increasing pore pressure. Sapping occurs primarily in units with relatively higher permeability compared with surrounding units and can result in failure of sediment where sapping is located as well as erosion of underlying sediment if the flow is great enough to overcome the critical shear strength of the sediment (Thorne and Tovey,1981; Fox *et al.,* 2007; Chu-Agor *et al.,* 2008; Lindow et al.,2009).

External factors that influence the rate of bluff retreat include aspect and vegetation. Aspect affects pore water temperature and thus the number and depth of freeze-thaw cycles (Hall, 2007; Wynn and Mostaghimi, 2006; Bold *et al.,* 2010). West and south-facing bluffs experience warmer afternoon temperatures leading to a greater number of freeze-thaw cycles (Hall, 2007; Bold *et al.,* 2010). Sediment strength is temporarily weakened after each freeze-thaw cycle, in part due to frost heaving, and greater numbers of freeze-thaw cycles may lead to greater erosion rates (Wynn and Mostaghimi, 2006; Thomas *et al.,* 2009; Van Klaveren and McCool, 2010).

Vegetation stabilizes sediment where the roots pass through the potential failure plane. On hillslopes, vegetation has been shown to allow steeper slope formation and protect against shallow landslides (Montgomery *et al.,* 2000). Areas with no vegetation are also more susceptible to erosion from overland flow and seepage (Sidle and Ochiai, 2006; Ghahramani *et al.,* 2011). On river bluffs, vegetation has not shown to be a significant long-term stabilizing factor, especially in areas where bluff erosion is driven primarily by undercutting; even vegetation with extensive root networks can be undercut leading to failure (Docker and Hubble, 2008; Cancienne *et al.,* 2008). The influence of vegetation and aspect on bluff retreat rates are discussed below.

Methods:

This paper describes methods used to evaluate bluff retreat using aerial photographs and TLS. In addition, we detail the methods used to evaluate error associated with using aerial photographs to measure change. The methods section of this paper is divided into individual subsections highlighting the techniques used for each of these analyses.

Aerial photograph methods and extrapolation:

Aerial photographs are available on a decadal basis for the Le Sueur basin beginning in 1938. Photographs from 1938 and 1971 with a scale of 1:20,000 were scanned at 600 dpi to be analyzed digitally. The scanned images have a ground pixel size of 95 cm and were aligned to photographs from 2005 using the ArcGIS georeferencing tool. The 2005 photographs were taken with a ground pixel size of 15 cm and orthorectified by Optimal Geomatics in Huntsville, Alabama. The ArcGIS Georeferencing Tool aligns the photographs using user-selected control points, present in both sets of photographs, such as roads, houses, or stable fence lines. A minimum of eight control points were used to align each photograph, followed by a first-order polynomial transformation. Because the river is the feature of interest we selected photographs where the river was near the center and used control points at road intersections and bridge crossings near the river wherever possible. These techniques were used to minimize georefrencing error (Hughes *et al.,* 2006).

Bluffs were mapped from a 3m-resolution digital elevation model (DEM) derived from airborne lidar topographic data (15cm vertical RMS error and 1m horizontal RMS error) collected in 2005. Bluffs were identified automatically using an algorithm that selected any feature with greater than three meters of relief in an 81 m^2 window. The three meter threshold was determined

from field observations, which suggested that features shorter than this are inundated by the river during high flow events, making these shorter features floodplains, by definition. This algorithm was used to select all bluffs in the watershed, including bluffs that are immediately adjacent to the river as well as bluffs that are separated from the river by a floodplain or terrace. Bluffs that are separated from the river were excluded from erosion analysis because field observations indicate that these features are relatively stable and it is unlikely that any sediment eroded from these features is transported to the river, across intervening floodplains and terraces.

To track bluff retreat and estimate multi-decadal sediment contributions from these features, each bluff crest was traced in both 1938 and 2005 photographs based on changes in vegetation and shadows from the flat upland surface to the steep bluff face. Characteristics used to distinguish the transition between the bluff face and upland surface were field checked at various sites throughout the watershed. Using the aerial lidar DEM, the exact location of the bluff crest in 2005 could be verified (at 10 bluffs the 2005 crest lines were compared with the DEM and it was found that on average the lines were within 0.44m of each other), yet to be consistent with the 1938 delineation, the 2005 bluff crests were mapped using the aerial photographs. To calculate average bluff retreat distance, the area between crests in 1938 and 2005 was divided by the river length along the bluff. The area was calculated by adding together areas of positive retreat (the 2005 crest line is further from the river than the 1938 crest line) and negative retreat (the 1938 line is further from the river than the 2005 crest line) (Fig. 3.3). In reality, there are no physical processes that cause negative retreat at bluff crests, which indicates that perceived negative retreat is a byproduct of error from the photograph alignment and/or manual tracing of the bluff crest. Assuming that both sources of error are non-systematic/ non-directional, summing the areas of positive and negative retreat minimized the effect of these errors. Retreat distance was divided by the time between the photographs (67 years) to determine an average annual bluff crest retreat rate.

To calculate the volume of sediment removed, V, the 3m DEM was used to calculate bluff height as the difference between average bluff crest elevation and average river elevation along the bluff. It was initially assumed that bluff retreat was parallel (Fig. 3.4), thus

$$V = H \cdot R \cdot L \tag{3.1}$$

where R is the bluff retreat rate, H is the bluff height and L is the river length along the bluff. Over long time scales the assumption of parallel retreat is reasonable, as evidenced by the consistently steep faces of bluffs of all ages distributed throughout the knick zone. However, over

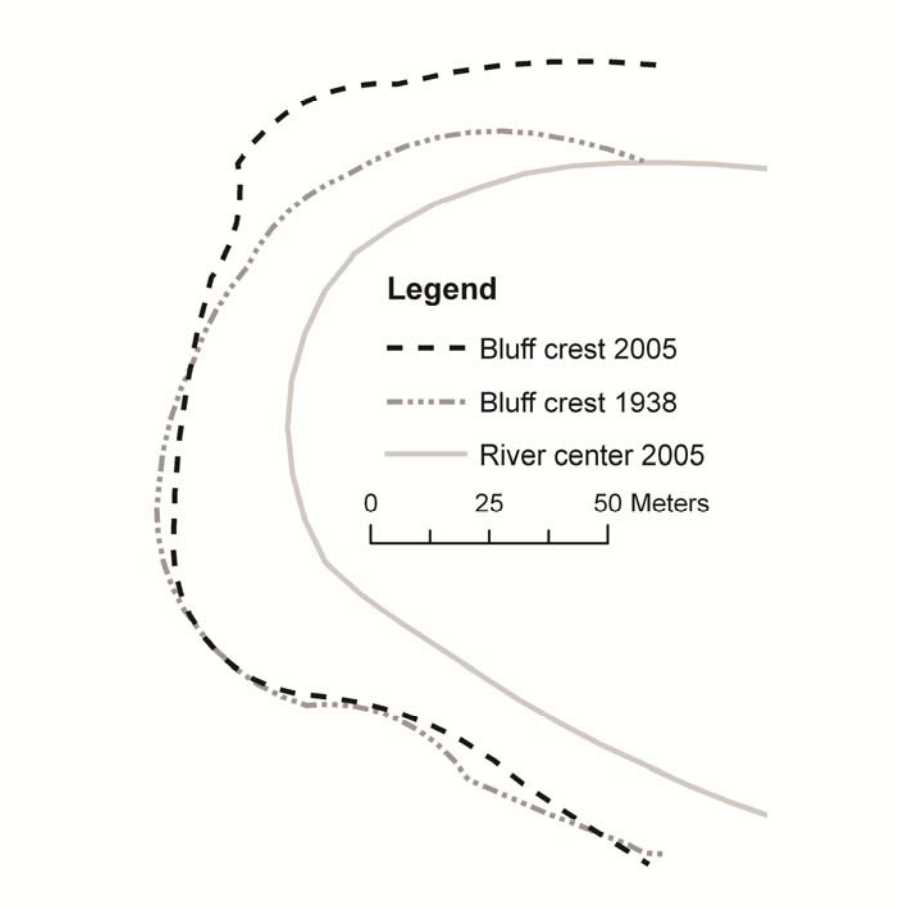

Figure 3.3: Variations in bluff shape can influence the measured length of the bluff crest; therefore the length of the river in direct contact with the bluff is used as the bluff length. Because there is no physical reason that the bluff crest should move toward the river, areas of negative bluff retreat are subtracted from areas of positive retreat to reduce error associated with tracing the bluff crest and georeferencing the photographs.

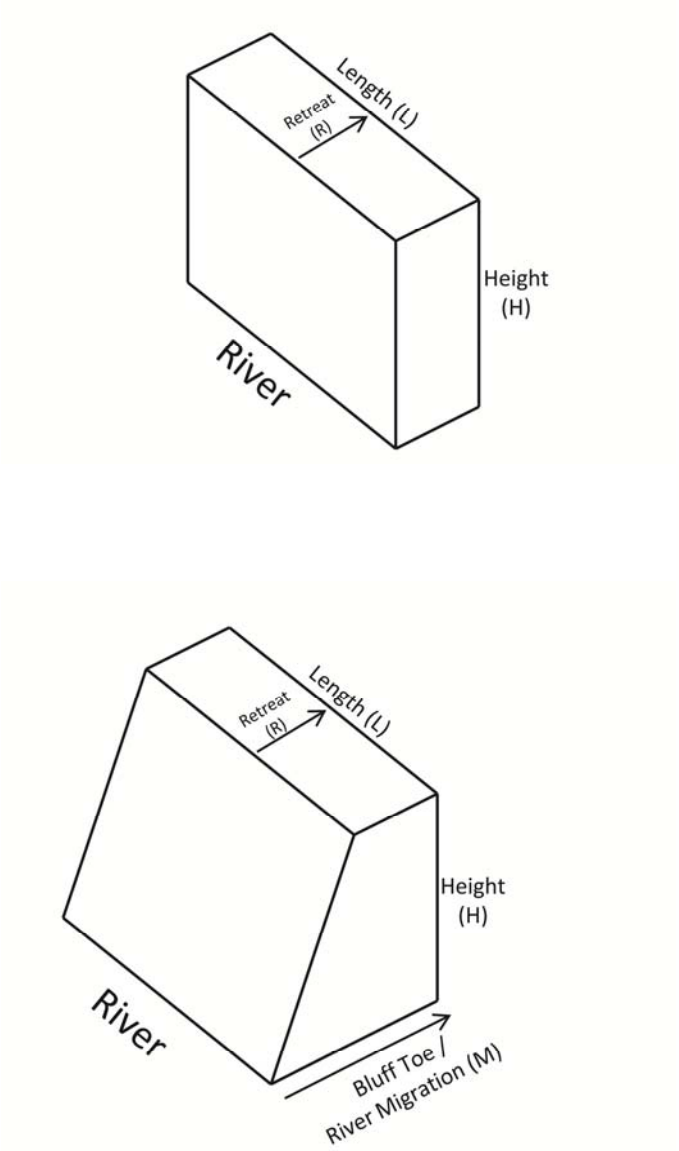

Figure 3.4: A) Parallel bluff retreat, where the bluff retreat rate is assumed to be equal at all points on the bluff surface. B) Retreat of the bluff toe is computed using the river meander migration rate, rather than assuming equal retreat at all points on the bluff surface.

decadal timescales bluff crest and toe may not always retreat at the same rate. Equation 3.1 was thus refined to account for the difference between the bluff crest retreat rate and the average river migration rate along each bluff toe. River migration rates were calculated using the Planform Statistics Tool developed by Lauer and Parker (2008) and available online as part of the National Center for Earth-surface Dynamics Stream Restoration Toolbox (http://www.nced.umn.edu/content/tools-and-data). This ArcGIS-based tool interpolates a channel centerline from manually digitized bank lines and calculates river migration rates as the difference in river center lines between two points in time. To perform this calculation we discretized the channel centerlines every 10 m.

The river migration rate provides an estimate of the average retreat rate at the base of the bluff (Fig. 3.4). By combining the river migration rate with the bluff crest retreat rate we can determine if individual bluffs are laying back (i.e., crest is retreating faster than the toe) or becoming steeper (i.e., toe is retreating faster than the crest). Where the river is migrating away from the bluff we assume zero migration of the bluff's toe. Field observations suggest that typically any colluvial deposition at the base of the bluff is quickly removed by the river. Also, migration away from the bluff may be artificial due to higher water levels when the 2005 photographs were taken. Where one edge of the river is lined by a bluff, the higher water level in the 2005 aerial photograph causes the river's center line to appear closer to the opposite bank. The final calculation for finding the volume of sediment removed from each bluff (V) is :

$$V = \left[R + {}^{1}/_{2}\,(M - R)\right] \cdot H \cdot L \qquad (3.2)$$

where M is the river migration rate.

Both equations 3.1 and 3.2 compute the total volume of sediment eroded over a given time. The primary concern in this watershed is fine sediment, so the volumes calculated are modified to reflect the fine sediment load alone using a bulk density of 1.8 Mg/m^3 (Thoma *et al.,* 2005) and an average grain size distribution for the tills of 65% silt and clay (Gran *et al.,* 2009).

In many places vegetation or poor photograph quality obscures the bluff crest. All bluff crests visible in both 1938 and 2005 were traced on the Maple and Le Sueur Rivers; of the 354 bluffs mapped from the 3m DEM, 183 were traced. To calculate the bluff sediment loading from the entire watershed, it was necessary to extrapolate from all traced bluffs to the remaining 171 bluffs. Because the height (H), length of the river along the bluff (L), and the meander migration rate (M) were all measured independently, the only unknown variable for the non-traced bluffs

was the crest retreat rate. To extrapolate the retreat rate for the non-traced bluffs, bluffs were binned based on aspect and vegetation cover attributes, as these may affect bluff erosion rates.

To extrapolate the measured retreat rate to each of the non-traced bluffs using aspect, bluffs were binned into eight groups, each representing 45˚ (Table 3.1). Average retreat rate was calculated for each bin, and this rate was the applied to all non-traced bluffs in that aspect bin. A second technique extrapolated retreat rates based on vegetation and location. Bluffs were separated into six groups based on vegetated/ un-vegetated surfaces and location with respect to the gauging network (which also delineates the knick zone) (Table 3.2). Average retreat rate was determined for each of the six groups, and applied to all non-traced bluffs in that group.

Terrestrial laser scanning methods and extrapolation:

Terrestrial laser scanning (TLS), also referred to as ground-based or tripod-based lidar, is a laser-based topographic measuring system. Like aerial lidar, TLS relies on time-of-flight laser pulse returns to measure topography, but because TLS is tripod-based it can be used to measure vertical features like bluffs. For this project we used an Optech ILRIS 3_6D lidar system rented from the Lidar Lab now at Western State College of Colorado. This equipment has centimeter-scale resolution with an accuracy of 7mm in the direction parallel to the laser (Gulyaev and Buckeridge, 2004; Rosser *et al.,* 2005; Wawrzyniec, 2007; Milan *et al.,* 2007; Resop and Hession, 2010; Lim *et al.,* 2010; Optech, 2011; Day *et al.,* this issue). While this technique provides high resolution data on the surveyed bluffs, significant data collection and processing time (approximately 2 days per site per year) make it impossible to collect data at all 482 bluffs in the watershed.

TLS data were collected annually for four years (2007-2010) at fifteen sites and processed based on the procedures outlined in Day et al. (this issue). The scans were aligned using stable features and vegetation was removed from the scan data. Sites were selected to represent a range of stratigraphies and locations. Eight sites were scanned on the Le Sueur River, six within the knick zone and two upstream. On the Maple and Cobb Rivers, two and three sites, respectively, were scanned within the knick zone and zero and one, respectively, upstream of the knickpoint (Fig. 3.1). Data from these fifteen sites were used to estimate bluff erosion throughout the basin.

Two different extrapolation analyses were performed to determine sediment loads from bluffs between 2007-2010. For both extrapolation analyses, the height and length measurements of the bluffs were the same as those used for the aerial photograph analysis. For each

Table 3.1: Bluff data for groups based on aspect

	Le Sueur River			**Maple River**			**Cobb River**		
	Total # bluffs	# Traced Bluffs	Measured retreat rate (m/yr)	Total # bluffs	# Traced Bluffs	Measured retreat rate (m/yr)	Total # bluffs	# Traced Bluffs	Measured retreat rate (m/yr)
0˚-45˚	33	14	0.18	8	5	0.04	16	11	0.23
45˚-90˚	28	12	0.10	13	7	0.09	6	4	0.22
90˚-135˚	29	9	0.05	19	15	0.03	25	12	0.24
135˚-180˚	36	16	0.09	17	11	0.07	20	8	0.11
180˚-225˚	33	18	0.14	14	10	0.19	20	9	0.04
225˚-270˚	30	9	0.18	18	10	0.21	9	3	0
270˚-315˚	19	10	0.16	23	15	0.20	7	1	0
315˚-360˚	25	15	0.24	9	7	0.09	23	12	0.13

Table 3.2: Bluff data for groups based on vegetation

		Le Sueur River			Maple River			Cobb River		
		Total # Bluffs	# Traced Bluffs	Measured retreat Rate (m/yr)	Total # Bluffs	# Traced Bluffs	Measured Retreat Rates (m/yr)	Total # Bluffs	# Traced Bluffs	Measured Retreat Rates (m/yr)
Vegetated	Above Gauges	22	5	0.10	24	14	0.12	33	12	0.08
	Between Gauges	96	32	0.09	60	40	0.18	26	9	0.13
	Below Gauges	56	22	0.15	14	6	0.14	1	1	0.22
Unvegetated	Above Gauges	16	6	0.05	3	3	0.24	1	1	0.25
	Between Gauges	85	60	0.20	42	34	0.20	79	35	0.24
	Below Gauges	34	23	0.17	6	5	0.21	5	1	0.15

extrapolation analysis we used the erosion rate calculated over the longest time span measured. In most cases this was approximately three years (9 bluff sites), but some sites were not measured either the first or last year, so the time span is shorter. The first extrapolation technique simply averaged the rates measured at all sites and applied that rate to all the bluffs in the basin. This method gives equal weight to all bluffs regardless of their characteristics. The second method extrapolated rates based on an empirical relationship between mass erosion rate (Mg/yr) and the surface area (m^2), similar to Sekely et al., (2002). A linear regression was plotted through these points and forced through the origin. The slope of this line is the bluff retreat rate in $Mg/m^2 \cdot y$. Because the TLS data preferentially measure the unvegetated portions of the bluffs, rates were applied exclusively to the unvegetated bluff length measured from the 2005 aerial photographs. For comparison, the same analysis was done using the entire bluff area. In both cases, bluffs that displayed no retreat during the 67 year aerial photograph record were assumed stationary and were not included in the extrapolation analysis.

Validation and Error Analysis:

There are many possible sources of error in using aerial photographs for change detection. While methods are not standardized, many aspects of how these analyses should be done and what range of errors can be expected have been evaluated by other authors (Hughes *et al.,* 2006; Walter and Tullos, 2010). To evaluate the specific range of error associated with the methods presented here, some of these tests were repeated and some were expanded. The aspects of this analysis that were tested include tracing error, georeferencing error, and extrapolation error.

Tracing Error:

One significant source of error in the aerial photograph analysis comes from manually tracing bluff crests. In some cases the bluff crest is easily defined, yet in other places vegetation obscures the bluff crest, making it necessary to rely on shadows. Photograph quality can also vary greatly, affecting one's ability to locate bluff crests. To quantify error associated with tracing bluff crests, ten bluffs were traced ten times each in both the 1938 and 2005 photographs. Selected bluffs represent the range of bluff types and photograph quality observed throughout the basin. To reduce bias, traces were not done consecutively, but instead several hours or days passed between each of the ten traces. Retreat rate was calculated for each bluff trace using the methods outlined above and the volume lost was calculated using equation 1. The consistency of

the volume measurements was evaluated at each individual site. This test determines the tracing error at a single bluff.

Georeferencing Error and Intermediate Photograph Test:

Georeferencing aerial photographs can introduce a range of errors based on the type of control points and the specific polynomial transformation used. For first-order polynomial transformations, Hughes et al. (2006) found the georeferencing error to be approximately 5m for photographs of the same scale, scanned and processed in the same way, as the photographs used here. A similar analysis for our study indicated error between 3 to 6 meters on each photograph. A georeferencing error of 5 meters corresponds to a retreat rate error of ±0.07 m/yr for our study comparing photographs from 1938 and 2005. For a first order polynomial transformation, it is likely that the error is not random but shifts the picture in one direction. Because a single photograph contains many bluffs, shifting the image in one direction would increase rate estimates for some bluffs, while decreasing rate estimates for others. For this reason, the actual error in average crest retreat rates is likely much lower than ±0.07 m/yr, and the overall retreat rates used are more robust than retreat rates measured at individual bluffs.

We tested the combined georeferencing and tracing error using an intermediate set of photographs to determine how significantly these errors impact the total average volume eroded from bluffs. The intermediate photograph test was performed on the Maple River bluffs using photographs from 1971, which are at the same resolution and were aligned in the same way as the 1938 photograph set. The same bluff crest tracing analysis described above was performed on these photographs. If the georeferencing and tracing errors are low, essentially becoming random noise when using a large data set, then the sum of the area between the crest lines from 1938-1971 and the area between the 1971-2005 lines should equal the area between the crest lines from 1938-2005. From this data set we can also evaluate if retreat rates changed between these two time intervals.

Extrapolation Error:

In the Le Sueur basin it was impossible to trace every bluff crest as some of them were heavily vegetated or the image quality was poor. To evaluate how many bluffs are needed to achieve a desired level of accuracy in estimating the total volume of sediment contributed to the river by bluffs, we performed a jackknife analysis (Miller, 1974). For the Le Sueur, Maple, and Cobb Rivers, traced bluffs were compiled and the total volume of sediment lost from those bluffs

was calculated using measured retreat rates for each bluff. Using a random number generator, bluffs were then selected and the corresponding retreat rate data removed, one at a time. The average retreat rate for the remaining bluffs was calculated and assigned to all removed bluffs. A new volume was then calculated and compared to the original volume measured. We recorded how many bluffs could be removed from the original dataset before the error was greater than 10, 15 and 20%. This calculation was performed 100 times for each river. In addition, we recorded the percent error generated from removing one bluff to identify the potential importance of individual bluffs. The rate from each bluff was removed one at a time and replaced by the average of the remaining bluff rates. The new volume was calculated and compared to the original measured volume.

Summation of Error:

All of the errors discussed above must be combined to determine the total uncertainty in retreat rate of a single bluff and the uncertainty associated with calculation of the final volume of sediment eroded from bluffs in the watershed. Due to the non-systematic nature of the georeferencing and tracing errors, we would expect that the uncertainty will be much larger for a single bluff than for the total volume calculation. However, while georeferencing and tracing errors are minimized as additional bluffs are considered, the final bluff calculation relies on extrapolation to non-traced bluffs resulting in an additional source of error.

A conservative approach to determining the total uncertainty would be to simply add each source of error. This approach assumes that each source of error is completely independent of the other errors. In this study the errors are nested such that the test used to determine the magnitude of one error relies on the assumption that there are no other sources of error. For example, when considering a single bluff, the test used to measure the tracing error assumes accurate georeferencing. As tracing error becomes very large, the accuracy of the georeferencing becomes less important. The percent total uncertainty at a single bluff ($U_{tot\text{-}single}$) is summed as

$$U_{tot\text{-}single} = E_{T\text{-}single} + \left(1 - E_{T\text{-}single}\right)E_{G\text{-}single} \qquad (3.3)$$

Where $E_{G\text{-}single}$ is the percent georeferencing error at a single bluff and $E_{T\text{-}single}$ is the percent tracing error at a single bluff less than 100%. Where $E_{T\text{-}single}$ is greater than 100% the error is dominated by that component.

For the total volume calculation we use the results of the intermediate photograph test, which pairs the georeferencing and tracing errors. Again we have a nested error scenario where

the extrapolation error assumes the accuracy of the georeferencing and tracing. The percent total uncertainty for the complete volume calculation ($U_{tot\text{-}volume}$) is summed as

$$U_{tot-volume} = E_{E-volume} + (1 - E_{E-volume}) E_{GT-volume} \quad (3.4)$$

Where $E_{GT\text{-}volume}$ is the combined percent tracing and georeferencing error of the final volume calculation and $E_{E\text{-}volume}$ is the percent extrapolation error of the final volume calculation less than 100%. Where $E_{E\text{-}volume}$ is greater than 100% the error is dominated by that component.

Benefit of Additional Data:

Ideally extrapolating would be minimized and the actual crest retreat rate and river migration rate of each bluff could be measured using the methods described above. However, in the Cobb River, many of the 1938 photographs are unavailable, making it impossible to perform the analysis as it was done for the Le Sueur and Maple Rivers. Therefore we used the Cobb River to measure how additional data improves the estimated sediment load. Using the aerial lidar, bluffs were identified using the same algorithm as was used on the Maple and Le Sueur Rivers. The length, height, and aspect of each bluff were also measured using the lidar.

We performed four tests progressively adding data beginning with only the aerial lidar data. The first test assumed no aerial photographs were available along the Cobb River. For this test we used the retreat rates measured from the Maple River and applied them to the Cobb River based on aspect alone, because this characteristic could be measured without aerial photographs. For this analysis we assumed parallel retreat (equation 1). The second test used all available photographs. We measured the crest retreat rate on 48% of the bluffs and extrapolated using both vegetation and aspect. For this test we again used parallel retreat to calculate the mass of sediment lost. The third test included migration rate data from the Maple River. On both the Maple and the Le Sueur Rivers the river is migrating toward 50% of the bluffs at an average rate of 0.18 m/yr. We applied this average migration rate to 50% of the bluffs on the Cobb River and assumed zero migration for the other 50% because, as stated above, river migration away from the bluff may be a result of higher water levels in the 2005 photographs, rather than deposition at the toe. The total load was calculated using equation 2. The final test used migration rates measured on the portions of the river where the 1938 aerial photographs were available. At 72% of the bluffs we were able to measure the migration rate and we applied the average migration rate on the Cobb to half of the remaining bluffs and zero migration to the other half.

Results:

The results presented here show the effects of time between measurements, how the methods of extrapolation impact results, and how the extrapolated rates compare with measured TSS loads in the Le Sueur River watershed. These results also demonstrate the value of aerial photographs for measuring retreat over a large area and TLS for measuring bluff erosion in detail at individual sites.

Overview:

Regardless of the method of measurement and extrapolation used, bluff erosion rates in the Le Sueur River watershed are high and account for a large percentage of the total fine sediment load in the rivers. Based on the analyses described above, an average of approximately 135,000 ± 39,000 Mg/yr of bluff-derived fine sediment passes the Le Sueur River mouth gauge, which is 57±16% of the average total measured TSS load at that gauge between 2000 and 2010. An additional 17,100±14,000 Mg/yr enters downstream of the mouth gauge from a single bluff Pairing aerial photographs and TLS demonstrates the effect of different time-averaging intervals on estimated retreat rates. Averaging time-intervals is an important consideration in estimating rates of stochastic processes (Ganti *et al.,* 2011) because measurements must be of sufficient duration to average out variability. In our case, the four-year TLS study and 67-year aerial photograph measurements converge on similar rates, suggesting that the four years we performed TLS scans, and the range of flows the river experienced, were sufficient to average out much of the variability in this watershed.

Bluff retreat results:

The episodic nature of bluff retreat makes it essential to measure bluff erosion over multiple time scales (Day *et al.,* this issue). When only one year of change was measured using TLS, erosion rates ranged from -0.17 m/yr (deposition occurring at the toe) to 1.01 m/yr with an average rate of 0.19 m/yr. Retreat rate depends on the bluff type and magnitude of the flow throughout that year. Data integrated over two years from 2007-2009 had a more narrow range of retreat rates, from -0.17 m/yr to 0.21 m/yr with an average rate of 0.08 m/yr. Key pieces of information can be obtained at both timescales. While the longer timescale provides a more accurate constraint on average bluff erosion rates throughout the watershed, the annual and sub-annual measurements provide insight regarding erosional mechanisms and responses to specific environmental conditions.

Average annual retreat rates measured from TLS data correspond well with the magnitude of the peak flows. Flow rates in 2009 were very low compared to the multi-decadal average, while in 2010 a rapid snow melt paired with significant spring rainfall, resulted in a record peak discharge. The average bluff retreat measured at the fifteen sites between spring 2009 and spring 2010 was 0.43 m/yr. The three-year average erosion rate from 2007 – 2010 was 0.20 m/yr. When longer time periods between scans were considered, the effect of a single event was reduced and retreat rates approached the 67 year average measured using aerial photographs (Fig. 3.5). This three-year average is more similar to the multi-decadal retreat rate measured from aerial photographs of 0.14 m/yr. The longer aerial photograph record averages over wet and dry years, reducing the impacts of an individual large storm event.

Retreat rates measured from aerial photographs for individual bluffs range from 0 to 0.96 m/yr, averaged over 67 years. For extrapolation, bluffs were grouped in two different ways, based on aspect and vegetation/location as described above. Retreat rates averaged within each group were used to extrapolate to the non-traced bluffs within each group (Tables 3.1, 3.2). The total mass of sediment derived from bluff retreat in the watershed when aspect and vegetation/location were used for extrapolation is 158,000±33,000 Mg/yr and 182,000±38,000 Mg/yr, respectively.

Results from the fifteen TLS sites were also used with two different extrapolation methods to estimate total sediment mass derived from bluffs. The two extrapolation analyses performed using the TLS data resulted in total fine sediment mass estimates ranging from 105,000±53,000 to 129,000±64,000 Mg/yr when only the unvegetated bluffs were measured and 255,000±128,000 to 315,000±157,000 Mg/yr when the entire bluff area was used (Table 3.3). Using a simple average from the 15 sites measured with TLS, the mean erosion rate is 0.20 m/yr, or 0.23 $Mg/m^2 \cdot yr$ (using a bulk density of 1.8 Mg/m^3 and percent of silt and clay of 65%), which yields the lower mass estimates given above. Average bluff erosion rate measured using linear regression between the bluff surface area and mass erosion rate is 0.25 m/yr, or 0.29 $Mg/m^2 \cdot yr$ (Fig. 3.6).

Both TLS and aerial photograph data show a weakly increasing trend in the downstream direction, in mass of sediment removed from each bluff, as indicated by the increasing slope of the cumulative mass curves (Fig. 3.7). On the Maple River this increase is most pronounced. After passing the upper gauge and entering the knick zone (40 km from the mouth) only 1 of the 45 eroding bluffs contributes < 10 Mg/yr of fine sediment, and all the bluffs that contribute >1000 Mg/yr of fine sediment are downstream of this point. On the Le Sueur River, bluffs with low

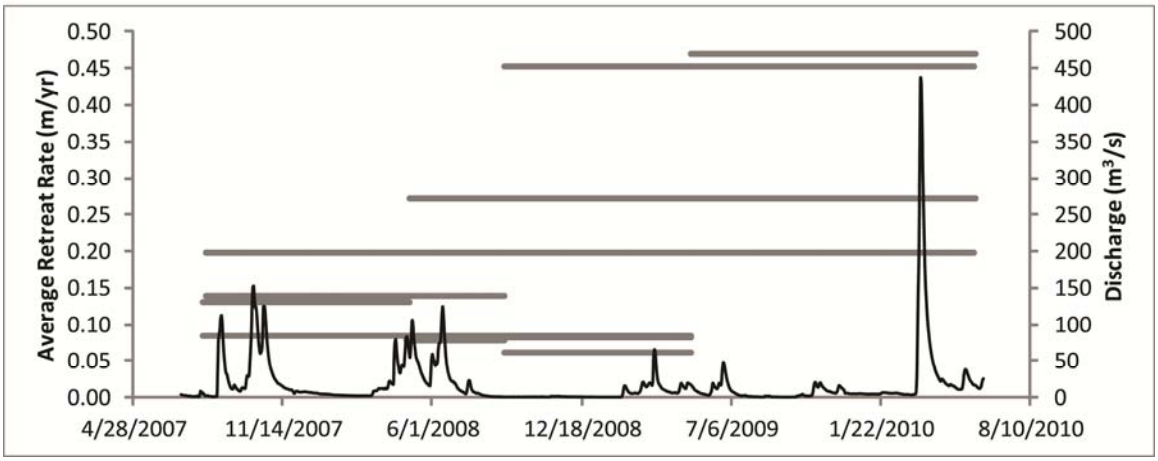

Figure 3.5: Higher peak discharge results in a higher retreat rate while time averaging reduces the importance of an individual flow event. The hydrograph shows flow over the entire study period. Horizontal lines indicate the average retreat rate measured on the fifteen bluffs scanned using TLS over the interval they cover on the x axis. Bluff retreat over short (annual) time intervals respond strongly to the flows during that period. Retreat rates over longer intervals begin to approach the four year average (0.20m/yr).

Table 3.3: Results from TLS up-scaling

	Linear Regression All bluffs (Mg/yr)	Linear Regression Un-vegetated bluffs (Mg/yr)	Average All bluffs (Mg/yr)	Average Un-vegetated bluffs (Mg/yr)
Maple				
Below Gauges	22,000	7,000	18,000	5,800
Between Gauges	47,000	23,000	38,000	18,000
Above Gauges	8,000	1,700	6,500	1,400
Total	77,000	32,000	62,000	26,000
Le Sueur				
Below Gauges	21,000	2,800	17,000	2,300
Red Jacket to Hwy 8	64,000	22,000	52,000	18,000
Hwy 8 to St Claire	54,000	24,000	44,000	20,000
Above Gauges	12,000	4,200	9,500	3,400
Total	150,000	53,000	122,000	43,000
Cobb				
Below Gauges	27,000	21,000	22,000	17,000
Between Gauges	60,000	23,000	49,000	19,000
Above Gauges	760	110	620	90
Total	87,000	44,000	71,000	36,000
Total from all	315,000	129,000	255,000	105,000
Total at mouth gauge	294,000	126,000	238,000	103,000

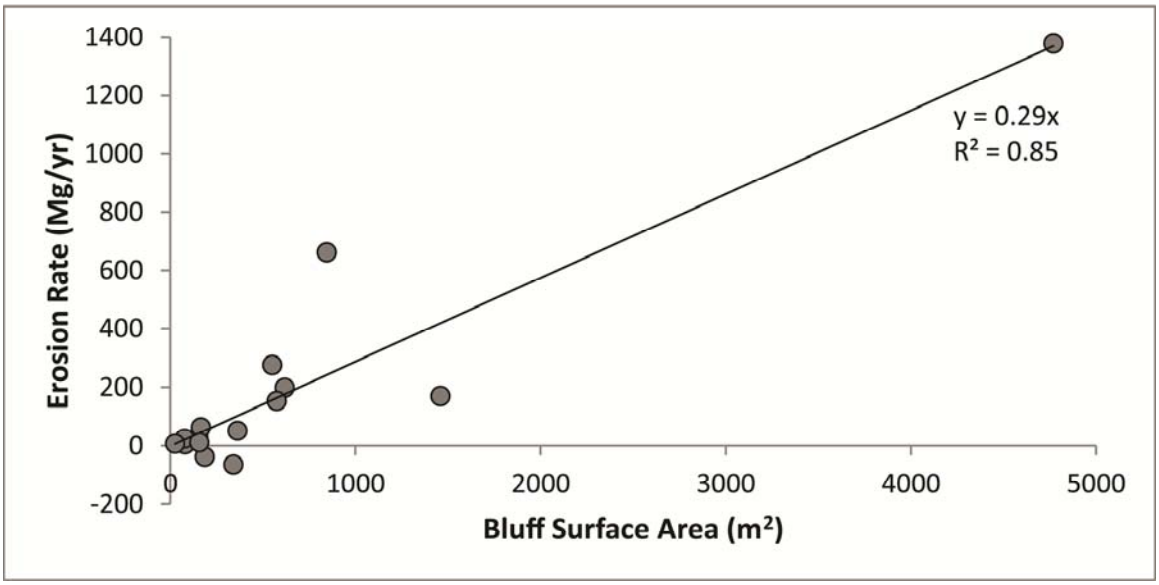

Figure 3.6: The relationship between the average annual mass lost and the surface area for the fifteen sites measured with TLS. The slope of the line is the average retreat rate in $Mg/m^2 \cdot yr$ and is used to scale to all bluffs in the watershed.

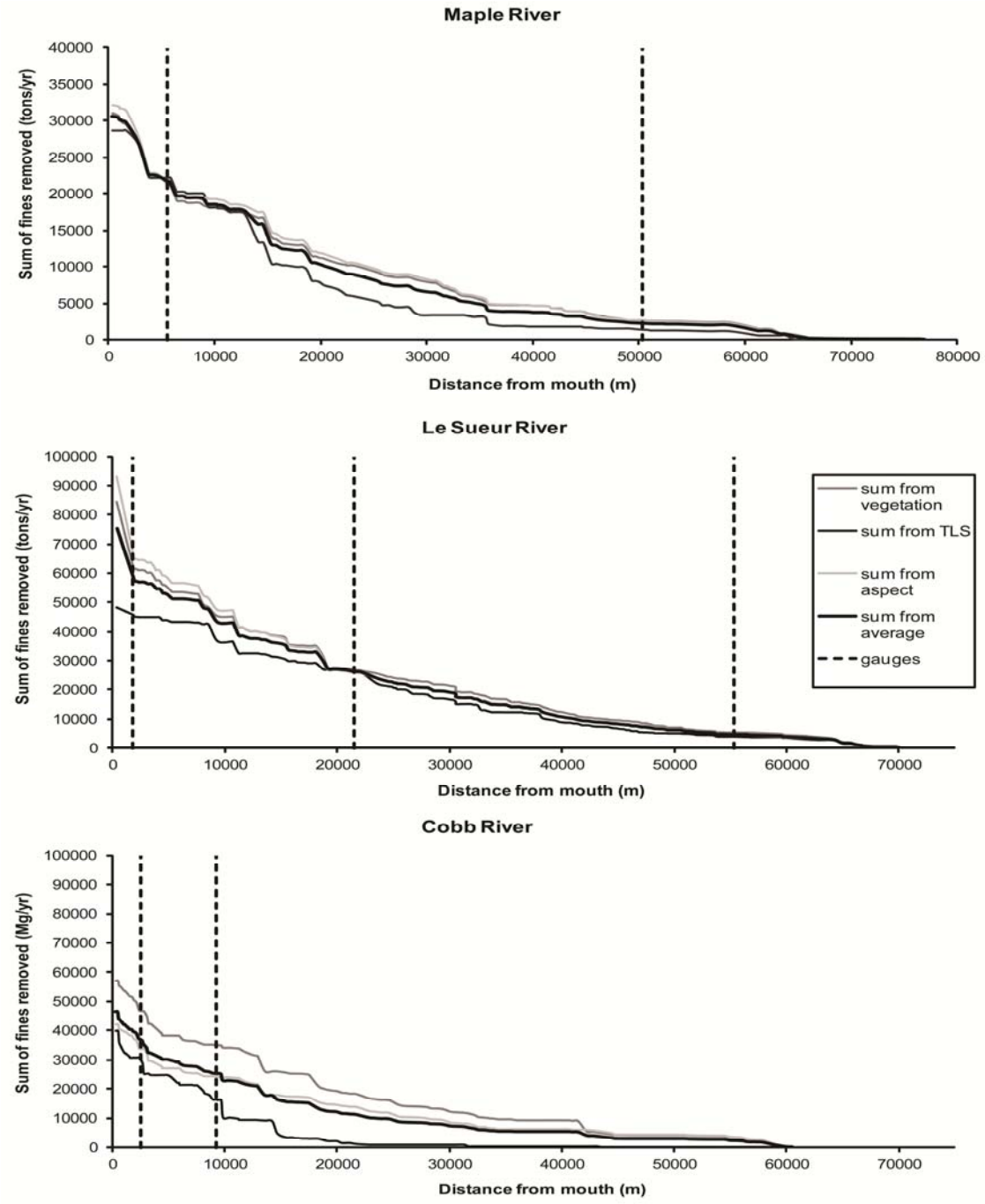

Figure 3.7: Cumulative Distribution of the mass of sediment contributed from bluffs to the Maple (top), Le Sueur (middle), and Cobb (bottom) Rivers. Slope of the mass curves increases in the downstream direction, indicating that the larger bluffs found in the lower parts of the channel network contribute disproportionately more sediment. Gauges are delineated with vertical dashed lines.

erosion volumes exist along the entire length of the river, yet those bluffs with the highest erosion volumes (> 1500 Mg/yr) are all concentrated at the furthest downstream portions of the river in the lower portion of the knick zone and where the knickpoint has already passed (< 25 km from the mouth). This is consistent with higher erosion rates measured in the downstream reaches of the river below the gauges (Table 3.4) as well as larger bluffs being present downstream where the relief is greater. This result occurs regardless of the extrapolation method used.

Error Evaluation:

The sources of error using aerial photographs to measure bluff retreat include tracing error, georeferencing error, and extrapolating error. Each of these was evaluated through a series of tests. These errors were evaluated for individual bluffs, in which case extrapolation error is not applicable, but georeferencing and tracing errors are maximized, as well as for multiple bluff sites where the non-systematic errors like georeferencing and tracing are minimized, but extrapolation error must be considered.

At a single bluff, error averages 86% when both georeferencing and tracing errors are considered and combined using equation 3. This average error will vary for each bluff based on the actual georeferencing error for the photograph, the bluff's specific retreat rate, and visibility of the bluff crest. As discussed in the methods section, georeferencing error at a single bluff is ±0.07m/yr or 50% of the average bluff retreat rate, 0.14 m/yr. At a given site the tracing error may also be quite high. The signal-to-noise ratio (SNR) at a single site ranges from 20- 140%, where the average SNR is 72%. The greatest tracing error (averaging 97%) is associated with bluffs where the bluff crest is heavily vegetated or the photograph quality is poor. This error is much greater than the average 55% error at non-vegetated bluffs.

Despite this high georeferencing and tracing errors at individual bluffs the errors are significantly reduced as more bluffs are considered. The combined georeferencing and tracing error of the total volume calculation was found using the intermediate photograph test. In addition to the 1938 and 2005 photographs that were used to trace bluffs throughout the watershed, 1971 photographs were used on the Maple River. Results show that the sum of the area between the crest lines from 1938-1971 and 1971-2005 is within 3% of the area between the crest lines encompassing the entire period (1938-2005), indicating that georeferencing and tracing error are quite low when considering all traced bluffs together.

Table 3.4: Mass of sediment (Mg/yr) calculated from bluffs assuming three scaling methods

	Vegetation	Aspect	TLS*
Maple			
Below Gauges	10,400	9,520	6,500
Between Gauges	18,900	18,800	21,000
Above Gauges	2,710	2,700	1,600
Total	32,100±3,800	31,000±3,600	28,600±14,300
Le Sueur			
Below Gauges	26,600	22,300	2,500
Red Jacket to Hwy 8	40,700	35,400	20,000
Hwy 8 to St Claire	20,800	21,300	22,000
Above Gauges	4,960	5,520	3,800
Total	93,100±18,000	84,500±17,300	48,100±24,100
Cobb			
Below Gauges	20,000	16,000	19,000
Between Gauges	37,000	25,000	21,000
Above Gauges	320	410	100
Total	57,000±12,000	42,000±7,000	39,800±19,900
Total from all	182,000±38,000	158,000±33,000	117,000±58,000
Total at Mouth Gauge	156,000±33,000	135,000±28,000	113,000±56,000

*TLS numbers for unvegetated bluff area only

A jackknife analysis was used to calculate the total extrapolation error and determine if there are ever individual bluffs that have characteristics that make them more important to measure accurately compared to the others. The jackknife analysis indicated that only 30-40% of bluffs must be traced to keep extrapolation error below 20%. If 65-70% of bluffs are traced, the error is reduced to 10%. This analysis also showed that some bluffs are more important than others. Very large bluffs can contribute a disproportionately large amount of sediment and should be traced if at all possible. For example, replacing the measured retreat rate with the average retreat rate on a highly active 380 meter long bluff on the Maple River resulted in a 10% difference in total mass of sediment.

At the watershed scale, error associated with tracing and georeferencing is 3%, and the remaining error is due to extrapolation and is dependent on the number of bluffs traced on each river. Along each river, 44-66% of bluffs were traced, which results in an extrapolation error of 9-18% based on a linear trend between the error and the number of bluffs traced (Fig. 3.8). Using equation 3.4, we find 11 - 20% error in the total volume of sediment calculated from aerial photographs.

Total error in the sediment mass estimate derived from TLS data is 50%. TLS measurement error is 30% (Day et al., this issue). An important factor in the large total error associated with the TLS estimates is a result of extrapolation, which is much higher (28%) relative to extrapolation error associated with aerial photograph analysis because only a small proportion of bluffs in the watershed were scanned. TLS error was summed using equation 4 where the measurement error is used as $E_{GT\text{-}volume}$.

Benefit of additional data:

The Cobb River was used to evaluate the benefit of additional data. Using all available data, the total fine sediment load ranges from 40,000-57,000 Mg/yr based on extrapolating the crest retreat using aspect and vegetation/location, respectively (Table 3.5). These are the target numbers we compare to as data are removed and extrapolated from other sources. The data available included 48% of bluff crest retreat rates and river migration rates at 72% of bluffs. When parallel retreat using the crest retreat rate measured on the Cobb River bluffs was used for calculating bluff volume lost, the total fine sediment loads for extrapolation using aspect and vegetation/location were 58,000 and 67,000 Mg/yr respectively. When migration rates from the Maple River were applied, estimated loads dropped considerably to 45,000 and 56,000Mg/yr. Based on results of the error analyses described above, the total uncertainty associated with

Table 3.5: Results from "value of additional data" test using the Cobb River

	Aspect for up-scaling Total fine sediment (Mg/yr)	Vegetation for up-scaling Total fine sediment (Mg/yr)
Parallel retreat* All values from Maple River	41,000	
Parallel Retreat Crest retreat measured on Cobb River	58,000	67,000
With Migration Crest retreat measured on Cobb River Migration values from Maple River	45,000	56,000
With Migration Crest retreat measured on Cobb River Migration measured on Cobb River	40,000	57,000

*The first test assumes no aerial photographs are available and all values are extrapolated from the Maple River. With no aerial photographs vegetated bluffs cannot be identified and therefore there is no value for the total load using vegetation fro up-scaling where all values are assumed from the Maple River retreat rates.

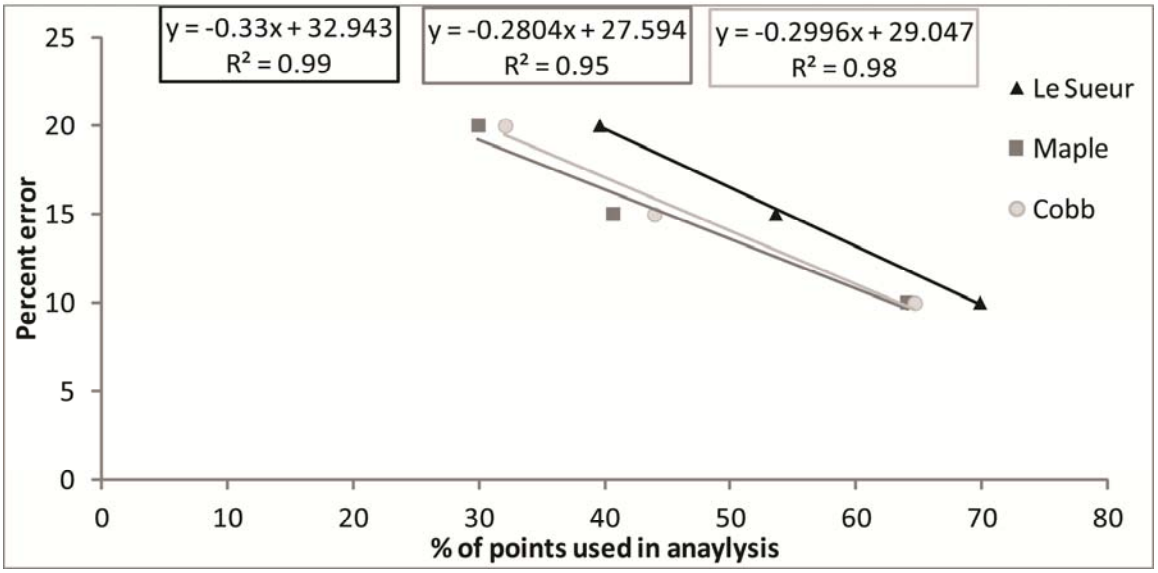

Figure 3.8: A linear regression is used to determine the error due to extrapolation for each of the rivers based on the percentage of bluffs traced.

tracing bluffs, georeferencing photographs, and extrapolating rates in the Cobb River is 18%. When applying this uncertainty to bluff load calculated measured using all available data only the value calculated using the crest retreat rates measured on the Cob bluffs as parallel retreat rates and using aspect to extrapolate were outside the uncertainty bounds. The retreat rates on the Cobb were not much greater than the rates on the Maple, yet they were distributed differently resulting in a large increase in total measured sediment load when these data were used. When river migration information was included in the calculation, the total mass of sediment was much lower, regardless of whether the migration rate used was the average rate measured on the Maple River or the actual migration rate measured along Cobb River bluffs. The average migration rate toward bluffs on the Cobb was 0.16 m/yr which is approximately 89% of the average migration rate on the Maple. In addition, as observed on the Maple and Le Sueur Rivers, 50% of Cobb River bluffs displayed river migration toward the bluff rather than away.

Role of bluffs in sediment budget:

Calculated sediment loads from bluffs were compared to gauging records at multiple locations throughout the watershed (Fig.3.2). Gauging records are available beginning in 2000 at the mouth gauge and 2006 or 2007 for all other locations (WRC and MPCA, 2009). To develop an average load from 2000-2010 annual loads at each gauge were interpolated using mouth gauge data. At the upper gauges, bluffs account for 12±3%, 7±2%, and 4±1% of the average measured TSS load on the Maple, Le Sueur, and Cobb Rivers respectively (Table 3.6). At the mouth of the Le Sueur, average bluff loads from the three extrapolation methods accounts for 57±16% of the average TSS load measured from 2000 – 2010, which equals 238,000 Mg/yr (Table 3.6). When all additional sediment sources are considered (i.e. ravines, upland fields, and streambanks), bluffs account for 46-54% of the total estimated decadal load (Belmont *et al.,* 2011; Gran *et al.*, 2011).

Gauge data from 2007-2010 are compared directly to the TLS results (Table 3.7). The results of this comparison are similar to the decadal comparison made using the bluff loads from all extrapolation techniques. Using the TLS results and the 2007-2010 gauge data bluffs account for 52±11% at the mouth of the Le Sueur (Table 3.7).

Discussion:

Bluffs line 32% of the river and can be up to 60 m tall in the Le Sueur watershed. They are exclusively sediment sources with only temporary storage of sediment at the bluff toe, in

Table 3.6: 2000-2010 gauge data

Gauge	Average TSS load 2000-2010 (Mg/yr)*	Average Bluff Erosion Volume (Mg/yr)+	Percent decadal TSS due to bluff erosion
Upper Maple	18,884	2,340	12%
Lower Maple	68,607	21,900	32%
Upper Cobb	7,460	280	4%
Lower Cobb	32,003	27,900	87%
Upper Le Sueur	67,715	4,760	7%
Lower Le Sueur	88,168	26,100	30%
Le Sueur Mouth	238,329	135,000	57%

*2000-2010 average based on available gauge data and scaling from Le Sueur River mouth gauge for missing data (Belmont et al., 2011; Gran et al., 2011)

+ Bluff erosion volume calculated as average of results from aerial photograph analysis and TLS.

Table 3.7: 2007-2010 Gauge Data

Gauge	TSS Load				Average TSS load 2007-2010 (Mg/yr)	Average Bluff Erosion volume measured from TLS 2007-2010 (Mg/yr)	Percent TSS due to Bluff erosion using TLS results (2007-2010)
	2007	2008	2009	2010			
Upper Maple*	18,001	6,215	8,217	23,397	13,958	1,600	11%
Lower Maple*	51,366	22,898	11,702	212,352	74,580	22,200	30%
Upper Cobb*	5,982	3,139	3,723	9,667	5,628	100	2%
Lower Cobb*	29,578	15,007	15,025	53,044	28,164	21,100	75%
Upper Le Sueur*	57,200	22,974	10,209	50,474	35,214	3,800	11%
Lower Le Sueur*	101,144	43,882	31,906	142,782	79,928	26,000	33%
Le Sueur Mouth	184,874	88,495	62,610	533,168	217,287	114,000	52%

*TSS Loads only measured seasonally. Values reported here are scaled to annual load using data from mouth gauge.

contrast to river banks, which serve as both sources and sinks for sediment. Based on their size and abundance alone it is not surprising that this study shows that bluffs contribute a significant portion of the total sediment load in the Le Sueur River watershed. Using the methods presented in this paper we found that bluffs account for 57±16% of the TSS load measured at the mouth of the Le Sueur River. Sediment yield from each bluff generally increases in the downstream direction because taller bluffs occur in the downstream reaches of the river where the knickpoint has already passed.

While aerial photographs and TLS measure bluff erosion over very different spatial and temporal scales, the total annual mass of sediment estimated from each technique are within 36% of each other. This suggests that the TLS data collected annually from 2007-2010 do a good job at representing the multi-decadal average measured using aerial photographs from 1938 and 2005. It is only through collecting data over multiple years, representing the wide range of flows experienced by this river, that we approached the average decadal sediment yield. Low to average flows from 2007-2009 resulted in lower than average retreat rates, yet high flows in the early spring of 2010 led to rapid erosion. Similar ranges of yields measured from TLS and aerial photographs also suggest that the TLS data were collected from a range of bluff types that accurately reflect bluffs throughout the watershed. This study benefited from careful site selection, where bluffs were selected to represent those that appeared to be rapidly eroding and those that appeared to be relatively stable. In addition, bluffs were selected to be distributed throughout the watershed and along each of the three main rivers.

Extrapolating TLS data using only the unvegetated portion of the bluffs is the preferred method of extrapolation. The terrestrial laser scanning system collects data from the first surface it comes in contact with. To ensure that we are not measuring change in vegetation, all points that are believed to represent vegetation are removed (Day *et al.,* this issue). While some erosion may occur on vegetated areas of the bluff it is likely a relatively insignificant amount of erosion when compared to the unvegetated portion of the bluff. The stability of these vegetation patches from year to year suggests that vegetation is important for stabilizing bluffs over short time intervals.

Even though vegetation is an indicator of short-term stability, aerial photographs show that multi-decadal erosion rates are not well correlated with vegetation cover. Crest retreat rates measured on aerial photographs from vegetated and unvegetated bluffs (in 2005) were similar on all rivers. This counter intuitive results prompted an air photo study of intermediate years between 1938 and 2005 (1950,1958,1964,1971) found that no bluff connected to the channel was

vegetated over the entire 67 years of record, and also that bluffs likely eroded when they were unvegetated. This apparent contradiction on the importance of vegetation cover demonstrates the importance of time scale; over decadal time scales vegetation cannot stabilize the bluffs, but the presence of vegetation does demonstrate short-term stability. This highlights a fundamental difference between bluffs and shorter streambanks where roots can pass through the failure plane; vegetation on bluffs can be undercut and thus cannot stabilize the slope long-term (Docker and Hubble, 2008; Cancienne *et al.,* 2008).

While vegetation didn't play a significant role in bluff retreat rates, aspect does correlate well with bluff erosion. Higher retreat rates on west facing bluffs in the Le Sueur and Maple Rivers suggest that the increased number of freeze-thaw cycles contribute to higher erosion rates (Fig. 3.9). In Minnesota, west facing bluffs typically experience a greater number of thawing events in winter than do east-facing bluffs (Miller and Buell, 1956). Freeze-thaw and frost heave can disrupt the structure of the till fabric and therefore make it more easily erodible. In contrast, however, our results from the Cobb River bluffs indicate that east-facing bluffs have the highest retreat rates. This finding suggests that while these processes clearly contribute to bluff erosion in the Le Sueur watershed, they are not the primary drivers. It should be noted that we have very few data for west-facing bluffs (aspect 225˚-315˚) on which to base this finding and additional data are needed to support or refute this suggestion. Nevertheless, it is potentially an important insight for predicting how bluff erosion rates may respond to future climate change.

TLS data paired with field observations suggest that undercutting and toe erosion drive bluff retreat (Day *et al.,* this issue). Bluffs maintain steep faces and do not lie back over time suggesting that the river quickly removes any material deposited at the toe of the bluff. A positive relationship between peak flows and average erosion rates measured using the TLS data provide further evidence that bluff retreat is driven by erosion at the bluff toe. High spring flows in 2010 resulted in high erosion rates measured between 2009 and 2010. Relatively low flows in 2007 and 2009 caused the retreat rate in those years to be much lower (Fig. 3.5).

To put the contribution of sediment derived from bluffs into the context of the total sediment load in the Le Sueur watershed, it is essential that we understand the error associated with both the data processing and extrapolation. Aerial photograph error is derived from tracing bluff crests, georeferencing photographs, and extrapolating rates.

Validation tests show that total error due to georeferencing and tracing a single bluff using aerial photographs to measure retreat rate is ~86%, but errors decrease for watershed-average retreat rates and total volumes of sediment contributed to each river. Georeferencing

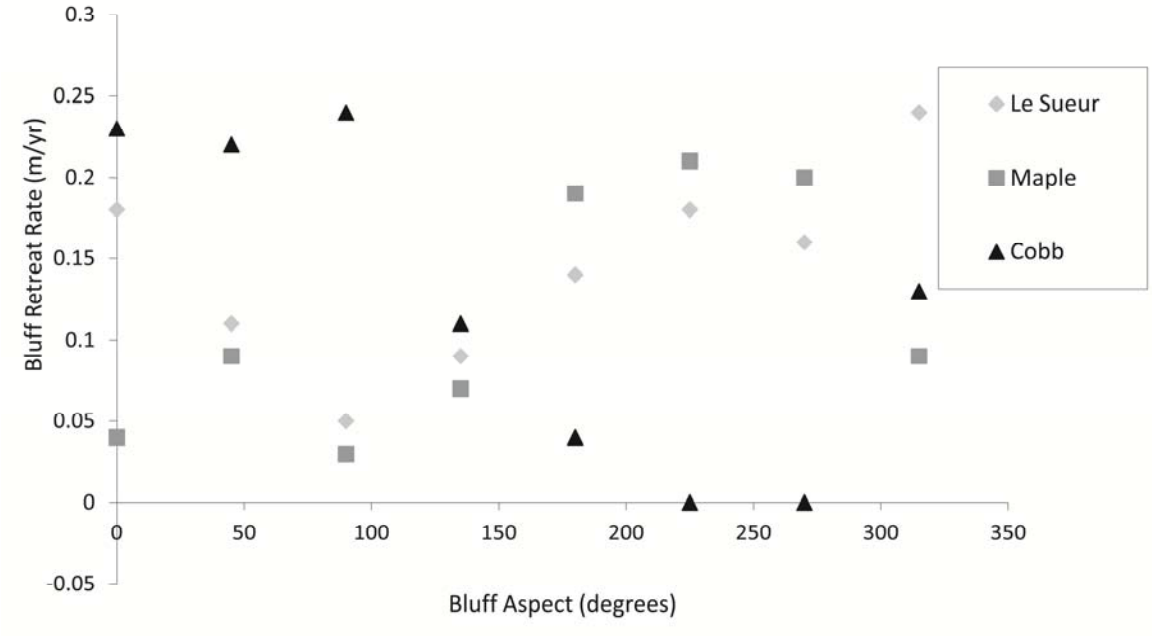

Figure 3.9: Retreat rate appears to be strongly correlated with aspect. In both the Maple and the Le Sueur Rivers west facing bluffs have the greatest retreat rates, while the retreat rates measured from the Cobb River are completely out of phase, reaching a maximum on east facing slopes. The results from the Cobb River are likely due to the small number of west facing bluffs measured on that river.

could shift an individual bluff such that average georeferencing error for that bluff is 50%, yet because bluffs are randomly distributed on both sides of the river in each photograph, the error is off-set for the group as a whole. The intermediate aerial photographs from 1971 strongly support this argument. The sum of the area between crest lines from measured bluffs between the time period 1938-1971 plus the area between crest lines from 1971-2005 is within 3% of the sum of the area between the crest lines from 1938-2005. This result demonstrates that because the orientation of the bluffs is non-systematic, as more retreat rates are measured, the georeferencing error is reduced. With a greater number of bluffs traced this error may be reduced further, but to be conservative, we use 3% of the total load as the error due to georeferencing and tracing in this paper.

Error from the TLS data is different from the aerial photograph error in that the TLS extrapolation error is much greater as a result of extrapolating from the 15 bluffs scanned using TLS to all 480 bluffs in the watershed. Error associated with TLS data processing is thoroughly covered in Day et al. (this issue), which concludes that TLS measurement and processing error combined is 30% for this study.

Results on the Cobb River demonstrate the value of additional data. While the additional data presumably improves our estimate, most calculated volumes are within the error associated with measuring the Cobb River bluffs. This suggests that while additional data can be beneficial, reasonable values from nearby rivers can allow us to get within the range of the error estimates if necessary.

Evaluation of TLS vs. aerial photography as a change detection tool:

Based on the results of this study, the best method for measuring bluff erosion is highly dependent on the type of information required. For many stream restoration projects it may be important to not only understand the total sediment loads but also erosion processes; in these cases TLS provides valuable information that can direct restoration efforts. Aerial photographs capture bluffs at oblique angles and over decadal time scales, making it difficult or impossible to infer the processes that drive erosion. Using three-dimensional TLS data, specific bluff erosion processes can be interpreted even in a small area (Day et al., this issue). When only retreat rates are required, aerial photographs can provide the necessary data set at a much lower cost. Aerial photographs also provide greater spatial coverage, making it possible to make measurements throughout a watershed rather than in a few select areas.

Time is also an important consideration in many restoration projects. TLS requires the ability to conduct repeat scans at a time interval determined by the typical rates of change for the area of interest. In addition, measurements should be made multiple times in order to capture the episodic nature of the change. Thus, the time interval needed to obtain useful TLS data may range from days to decades. Because the Le Sueur River watershed is a rapidly evolving system, annual time scales sufficed, yet in many areas change rates are much lower and will therefore require longer intervals. In river systems it may also be important to capture change over a variety of flow conditions, as the processes of erosion may be different in high or low flows as compared with average flows. Aerial photographs record integrated change over many years making it difficult to identify when the change took place, but reducing the necessary time investment for the study.

Conclusion:

Pairing aerial photographs with TLS provides the watershed context that is necessary to create a sediment budget with the feature-scale detail that enables us to understand the processes that cause bluff erosion (Belmont et al., 2011; Day et al., this issue). With four years of TLS data, retreat rates measured using both methods approached a common mean, providing validity to the measurements and indicating that the four years of TLS data, over a range of high and low flow events, were adequate to average over the episodic nature of bluff erosion at these sites.

We have highlighted how both methods can be used to measure bluff retreat, and presented an analysis of error associated with each. The sources of error associated with using aerial photographs to measure bluff retreat include error from tracing bluff crests, georeferencing photographs, and extrapolation of rates. Each of these errors is reduced by measuring a larger number of bluffs and by focusing on the most clearly visible bluffs in the watershed.

These techniques are not exclusive to this watershed and could be applied to measure change on other features, including banks and ravines. As the number of turbidity-impaired watersheds continues to grow and the number of stabilization projects increases it is necessary to have tools that can be applied to create robust sediment budgets. Aerial photographs provide a useful tool to measure watershed-scale decadal changes of a variety of features. Watershed managers and researchers who are interested in modern changes over a large scale can use aerial photographs to quantify change, yet must be aware of the errors outlined in this paper. TLS data provide significant insights to understanding the details of erosion, including the rates and

processes among a few select features. TLS also provides a more accurate assessment of erosion on an individual bluff.

High bluff erosion rates are only part of the story in the Le Sueur basin. A significant amount of additional research and an extensive gauge network has allowed us to create a complete sediment budget (Belmont *et al.,* 2011; Gran *et al.,* 2011; Gran *et al.,* 2009). The total sediment budget shows that bluff erosion accounts for approximately 46 - 54% of the total sediment load in the watershed. Rapid bluff erosion is not unexpected in this young actively evolving watershed, yet these rates have likely been intensified as a result of anthropogenic changes to the vegetation and hydrology.

Pairing aerial photographs and TLS further informs the sediment budget by showing that the erosion rates measured on bluffs today are consistent with the 70-year average. The combination of these data sets show that although vegetation may indicate short-term bluff stability, over decadal time scales even fully vegetated bluffs eventually fail.

Works Cited:

Belmont P, Gran K, Schottler S, Wilcock P, Day S, Jennings C, Lauer J, Viparelli E, Willenbring J, Engstrom D, Parker G. 2011, Large shift in source of fine sediment in the Upper Mississippi River. Environmental Science and Technology. **45**: 8804–8810. dx.doi.org/10.1021/es2019109

Bernhardt ES, Palmer MA, 2007. Restoring streams in an urbanizing world. Freshwater Biology **52**: 738-751.

Blann KL, Anderson JL, Sands GR, Vondracek B. 2009. Effects of agricultural drainage on aquatic ecosystems: a review. Critical Reviews in Environmental Science and Technology **39**: 909-1001

Bold KC, Wood F, Edwards PJ, Williard KWJ, Schoonover JE, 2010. Using photographic image analysis to assess ground cover: a case study of forest road cutbanks. Environmental Monitor Assessment **163**: 685-698.

Brunsden D, Kesel RH, 1973. Slope development on a Mississippi River bluff in historic time. The Journal of Geology **81**: 576-598

Cancienne RM, Fox GA, Simon A. 2008. Influence of seepage undercutting on the stability of root-reinforced streambanks. Earth Surface Processes and Landforms **33**: 1769-1786.

Chu-Agor ML, Fox GA, Cancienne RM, 2008. Seepage caused tension failures and erosion undercutting hillslopes. Journal of Hydrology **359**: 247-259.

Clayton L, Moran SR. 1982. Chronology of late-Wisconsinan glaciations in middle North America. Quaternary Science Reviews **1**: 55-82

Day SS, Gran KB, Belmont P, Wawrzyniec T, this issue. Measuring bluff erosion part 1: Terrestrial laser scanning methods for change detection and determining bluff erosion processes. Earth Surface Processes and Landforms.

De Vente J, Poesen J, Arabkhedri M, Verstraeten G. 2007. The sediment delivery problem revisited. Progress in Physical Geography **31**: 155-178. DOI 10.1177/0309133307076485.

Docker BB, Hubble TCT. 2008. Quanitfying root-reiforcement of river bank soils by four Australian tree species. Geomorphology **100**: 401-418.

Dotterweich M, 2008. The history of soil erosion and fluvial deposits in small catchments of central Europe: Deciphering the long-term interaction between humans and the environment – A review. Geomorphology **101**: 192-208.

Finnegan NJ, Gran K, Johnson A, Belmont P, Wilcock P, Dietrich WE, 2010. The importance of downstream bed surface coarsening in predicting the wave of incision in response to a sudden base level drop at the mouth of a river: the Holocene Le Sueur River, Minnesota, USA, Abstract EP52A-01 presented at the 2010 Fall Meeting, AGU, San Francisco, California, 13-17 Dec.

Fox GA, Wilson GV, Simon A, Langendoen EJ, Akay O, Fuchs JW. 2007. Measuring streambank erosion due to ground water seepage: correlation to bank pore water pressure, precipitation and stream stage. Earth Surface Processes and Landforms **32**, 1558-1573.

Ganti V, Straub KM, Foufoula-Georgiou E, Paola C, 2011. Space-time dynamics of depositional systems: Experimental evidence and theoretical modeling of heavy-tailed statistics. Journal of Geophysical Research **116**: F02011.

Gardner TW. 1983. Experimental study of knickpoint and longitudinal profile evolution in cohesive, homogeneous material. Geological Society of America Bulletin **94**: 664-672.

Ghahramani A, Ishikawa Y, Gomi T, Shiraki K, Miyata S, 2011. Effect of ground cover on splash and sheetwash erosion over a steep forested hillslope; a plot-scale study. Catena **85**: 34-47.

Gran KB, Belmont P, Day SS, Jennings C, Johnson A, Perg L, Wilcock PR. 2009. Geomorphic evolution of the Le Sueur River, Minnesota, USA, and implications for current sediment loading. James LA, Rathburn SL, Whittecar GR, (eds). Management and Restoration of Fluvial Systems with Broad Historical Changes and Human Impacts: Geological Society of America Special Paper **451**.

Gran KB, Belmont P, Day S, Jennings C, Lauer JW, Viparelli E, Wilcock P, Parker G. 2011, An integrated sediment budget for the Le Sueur River basin. Final report Presented to the Minnesota Pollution Control Agency.

Gulyaev SA, Buckeridge JS. 2004, Terrestrial methods for monitoring cliff erosion in an urban environment. Journal of Costal Research **20**, 871-878.

Hall K, 2007. Evidence for freeze-thaw events and their implications for rock weathering in northern Canada: II. The temperature at which water freezes in rock. Earth Surface Processes and Landforms **32**: 249-259.

Harden CP, Foster W, Morris C, Chartrand KJ, Hennry E, 2009. Rates and processes of streambank erosion in tributaries of the Little River, Tennessee. Physical Geography **30**: 1-16.

Harding JS, Benfield EF, Bolstad PV, Helfman GS, Jones EBD, 1998. Stream biodiversity: the ghost of landuse past. Proceedings of the National Academy of Sciences **95**: 14843-14847

Hirt U Wetzig A Amatya MD Matranga M, 2011. Impact of seasonality on artificial drainage discharge under temperate climate conditions. International Review of Hydrobiology **96**: 561-577.

Hughes ML, McDowell PF, Marcus WA, 2006. Accuracy assessment of georectified aerial photographs; implications for measuring lateral channel movement in a GIS. Geomorphology **74**: 1-16.

Jennings CE, 2010. Draft digital reconnaissance surficial geology and geomorphology of the Le Sueur River watershed (Blue Earth, Waseca, Fairbault, and Freeborn counties in south-central Minnesota). Map, scale 1:100,000, report, digital files.

Kirkby MJ, 1965. Measurements of soil creep. Annals of the Association of American Geographers **55**: 626

Lauer JW, Parker G, 2008. Net local removal of floodplain sediment by river meander migration. Geomorphology **96**: 123-149.

Lim M, Rosser NJ, Allison RJ, Petley DN. 2010. Erosional processes in the hard rock coastal cliffs at Staithes, North Yorkshire. Geomorphology **114**: 12-21.

Lindow N, Fox GA, Evans RO. 2009. Seepage erosion in layered stream bank material. Earth Surface Processes and Landforms **34**: 1693-1701.

Lobb DA, Kachanoski RG, Miller MH. 1995. Tillage translocation and tillage erosion on shoulder slope landscape positions measured using ^{137}Cs as a tracer. Canadian Journal of Soil Science **75**: 211-218.

Lowell TV, Fisher TG, Comer GC. 2005. Testing the Lake Agassiz meltwater trigger for the Younger Dryan: Eos (Transactions, American Geophysical Union) **83**: 365-373

Maloney KL, Weller DE, 2011. Anthropogenic disturbance and streams: land use and land-use change affect stream ecosystems via multiple pathways. Freshwater Biology **56**: 611-626.

Matsch CL. 1983. River Warren, the southern outlet of Lake Agassiz. Teller JT, Clayton L, (eds). Glacial Lake Agassiz: Geological Association of Canada Special paper **26**: 232-244.

Milan DJ, Heritage GL, Hetherington D. 2007. Application of 3D laster scanner in the assessment of erosion and deposition volumes and channel change in a proglacial river. Earth Surface Processes and Landforms **32**: 1657-1674.

Miller HC, Buell MF. 1956. Life form spectra of contrasting slopes in Itasca Park, Minnesota. Botanical Gazette **117**: 259-263.

Miller RG. 1974. The jackknife – a review. Biometrika **61**: 1-15.

Minnesota Pollution Control Agency (MPCA). Minnesota Department of Agriculture, Minnesota State University, Mankato water Resources Center and Metropolitan Council Environmental Services. 2007. State of the Minnesota River: Summary of Surface Water Quality Monitoring 2000-2005: St. Paul, 20p.

Montgomery D. 2007. Soil erosion and agriculture sustainability. PNAS **104**: 13268-132772.

Montgomery DR, Schmidt KM, Greenberg HM, Dietrich WE, 2000 Forest clearing and regional landsliding. Geology **28**: 311-314.

Optech, 2011. http://www.optech.ca/pdf/Brochures/ILRIS-DS-LR.pdf. website accessed July 24, 2011.

Resop JP, Hession WC. 2010. Terrestrial laser scanning for monitoring streambank retreat: comparison with traditional surveying techniques. Journal of Hydraulic Engineering **136**: 794-798.

Rosser NJ, Petley DN, Lim M, Dunning SA, Allison RJ. 2005. Terrestrial laser scanning for monitoring the process of hard rock costal cliff erosion. Quarterly Journal of Engineering Geology and Hydrogeology **38**: 363-375.

Sekely AC, Mulla DJ, Bauer DW. 2002. Stream bank slumping and its contributions to the phosphorus and suspended sediment loads of the Blue Earth River, Minnesota. Journal of Soil and Water Conservation **57**: 243-250.

Sidle RC, Ochiai H, 2006. Landslides: processes, prediction, and land use. Water Resources Monograph **18**: 312p.

Smith SMC, Belmont P, Wilcock PR. 2011. Closing the gap between watershed modeling, sediment budgeting, and stream restoration. Stream Restoration in Dynamic Fluvial Systems: Scientific Approaches, Analysis and Tools Geophysical Monograph Series **194**: 293-317.

Terzaghi K, 1962. Stability of steep slopes on hard unweathered rock. Geotechnique **12**: 251-270.

Thoma DP, Gupta SC, Bauer ME, Kirchoff CE. 2005. Airborne laser scanning for riverbank erosion assessment: Remote Sensing of Environment **95**: 493-501.

Thomas JT, Iverson NR, Burkart MR, 2009. Bank-collapse processes in a valley-bottom gully, western Iowa. Earth Surface Processes and Landforms **34**: 109-122.

Thorleifson LH. 1996. Review of Lake Agassiz history, Teller JT, Thorleifson LH, Matile G, Brisbin WC. Sedimentology, Geomorphology and History of the Central lake Agassiz Basin: Geological Association of Canada/Mineralogical Association of Canada Annual Meeting, Winnipeg, Manitoba, field Trip Guidebook **B2**: 55-84

Thorne CR, Tovey NK, 1981. Stability of composite banks. Earth Surface Processes and Landforms **6**: 469-484.

Trimble SW. 1999. Decreased rates of alluvium sediment storage in the Coon Creek Basin, Wisconsin, 1975-93. Science 285: 1244-1246. DOI:10.1126/science.285.5431.1244

Turnbull WJ, Krinitzsky EL, Weaver FJ, 1966. Bank erosion in soils of the lower Mississippi Valley. Proceedings of the American Society of Civil Engineers **92**: 121-136

Van Klaveren RW, McCool DK, 2010. Free-thaw and water tension effects on soil detachment. Soil Society of America Journal **74**: 1327-1338.

Walter RC, Merritts DJ. 2008. Natural streams and the legacy of water-powered mills. Science 319: 299-304. DOI: 101126/science.1151716.

Walter C, Tullos DD, 2010.Downstream channel changes after a small dam removal; using aerial photos and measurement error for context; Calapooia River, Oregon. River Research and Applications **26**: 1220-1245

Water Resources Center (WRC), Minnesota State University, Mankato, and Minnesota Pollution Control Agency (MPCA). 2009. State of the Minnesota River: Summary of surface water quality monitoring 2000–2008: 42 p.

Wawrzyniec TF, McFadded LD, Ellwein A, Meyer G, Scuderi L, McAuliffe J, Fawcett P. 2007. Chronotopographic analysis directly from point-cloud data: A method for detecting small seasonal hillslope change in Black Mesa Escarpment, NE Arizona. Geosphere **3**: 550-567.

Wilkinson BH, McElroy BJ. 2007. The impact of human on continental erosion and sedimentation. Geological Society of America Bulletin **119**: 140-156. DOI 10.1130/B25899.1

Wynn TM, Mostaghimi S, 2006. Effects of riparian vegetation on stream bank subaerial processes in southwestern Virginia, USA. Earth Surface Processes and Landforms **31**: 399-413

Chapter 3:

Ravine growth experiments to understand effects of changing hydrology

Ravines grow as the head cut propagates upstream in response to overland flow. Altered hydrology can impact the rate at which ravines grow. Using a set of small physical experiments we tested how changing overland flow rates for a fixed volume of water alters the total volume of erosion and the ravine morphology. We tested ravines in both detachment-limited and transport-limited systems, and found that in both cases the total volume of erosion was independent of the flow rate. The dominant hydrologic alteration that accelerates ravine growth is the volume of water entering the ravine, where a greater water volume results in greater erosion. This response is not typical when compared to pre-existing channels where higher flow rates result in greater erosion. Ravines do not respond like pre-existing channels because channel morphology including channel slope can adjust more quickly in these systems in response to changing flows.

Introduction:

Ravines (or permanent gullies) are 1st order deeply incised ephemeral streams with steep head cuts. Ravines evolve as the head cut propagates upstream due to overland flow or sapping. In studies of ravines worldwide, ravines have been found to account for 10-94% of the total sediment yield in a watershed (Poesen et al., 2003). Ravine head-cuts can propagate quickly (as fast as 10 m/ yr) depending on sediment type, climate, and land-use (Poesen et al., 2003; Sidorchuk 2006). For this reason, in many parts of the world ravines pose a risk to agricultural production or infrastructure, and may pose a hazard to people who live nearby or use the area for recreation (Verstraeten and Poesen, 1999; Boardman, 2001; Poesen et al., 2003). Like all aspects of fluvial systems, ravine growth is affected by changes to hydrology resulting from development of agricultural or urban areas as well as climate change (Poesen et al., 2003Istanbulluoglu et al., 2005).

Hydrology is altered through changes to the volume and/or rate at which water enters river networks as overland flow, groundwater flow, or pipe flow (commonly pipe flow is anthropogenically derived, but caves or lava tubes may be considered as natural pipe flow). Agricultural development often requires direct modification of hydrology either in the form of irrigation in dry climates and sandy soils or drainage in highly impermeable soils. Irrigation has little direct impact on overland flow as much of the water is transpired (Haddeland et al., 2005). However agricultural drainage can have a strong impact on overland flow. Tile drains (and ditches) are designed to accelerate the rate at which water leaves fields. Tile drains are perforated pipes that are buried approximately 1 meter beneath the surface. When water enters the pipe it is quickly routed into a nearby river, ravine, or ditch, thereby allowing for continuous infiltration. By increasing the infiltration capacity of the sediment, tile drains decrease the volume of overland flow entering ravines by 29 to 65% depending on specific soil, topography, climate and vegetation (Bengtson et al., 1984; Schwab et al., 1985; Kladivko et al., 2001). In addition to decreasing runoff volumes, if overland flow is generated in these areas the peak overland flow rates are reduced by 15-30% (Schwab et al., 1985; Kladivko et al., 2001).

Another indirect hydrologic modification takes place on most fields when crops are harvested and fields are left bare for a portion of the year (1-6 months). This leads to a significant drop in evapotranspiration, which can lead to increased volume of overland flow particularly if the ground is frozen and infiltration cannot occur (Pierson et al., 2007). In addition, the removal of roughness elements when fields are bare can lead to increased rates of overland flow entering

ravines (Einstein and Barbarossa 1951; Farres, 1978; Römkens and Wang, 1987; Abrahams and Parsons, 1991; Eitel et al., 2011).

Here, the focus is on ravine growth due to overland flow and the effects of agricultural hydrology alterations. Using a small experimental basin we measured how changing overland flow rate affects erosion volumes in ravines. Two different experimental substrates were used, which allowed us to measure the effects of changing flow rates on both detachment-limited and transport-limited erosion in ravines. These two types of erosion represent a continuum, where the volume of sediment carried out of the system is controlled by the ability of the flow to dislodge sediment from the substrate vs. the ability of the flow to carry easily eroded sediment. Commonly "detachment limited" is used to describe bedrock rivers, while "transport limited" is used to describe alluvial rivers.

Experiments, like the one we discuss here, offer a setting where most variables can be controlled and time scales for channel evolution are greatly reduced. Moreover, using experiments allows us to make measurements at a high spatial and temporal density to ensure that much of the variability in the system is captured. Such experiments are not intended as scale models; rather, they are small systems in which scale-independent processes can be studied under controlled conditions (Paola et al., 2010). Here we focus on a single basic question: how does changing the rate of delivery of a fixed quantity of water change the total volume of sediment removed and the form of the resulting ravine?

Methods:

The experiments were performed at the St. Anthony Falls Laboratory at the University of Minnesota, in Minneapolis, Minnesota. The primary goal of these experiments is to test how different overland flow rates affect erosion and ravine growth. To ensure that a range of natural ravines were represented, we used two different substrates. The main variable between the two substrate materials was cohesion. The more cohesive material was 12 μm ceramic spheres (i.e. mud), and the non-cohesive material was 96 μm quartz sand. The experimental basin size varied for each material type; the basin used with the mud substrate was 1x1m, while the basin filled with the sand substrate was 2x4m. For both substrates, the water flowed out through a 76 mm wide notch at the downstream end of the basin (Fig. 4.1). To initiate each run, the notch was dropped to 0.14 m below the surface of the substrate, thus creating a single abrupt base level drop. During each run a knickpoint developed at this notch and propagated upstream, carving a deep ravine in the substrate.

The substrate material was mixed with water and smoothed into the basin to create a flat bed. Experiments began with a saturated bed to ensure that water flowed over the surface rather than infiltrated into it. We determined that the bed was at saturation and no longer over-saturated when there was no longer water on the surface of the sediment and water was no longer flowing out the downstream outlet. Determining when the bed was at saturation was done by visual inspection rather than waiting a standard length of time because changes to humidity and temperature affected evaporation rates. Beginning with a saturated substrate allowed us to make the assumption that the net flow was relatively constant in the cross channel direction and no water was lost to saturate the sediment.

For each experimental run, water flowed over the uniform substrate as overland flow. An even sheet flow was generated by allowing water to flow over a broad crested weir as water was added to an upstream settling basin (Fig. 4.1). The flow rate of the water entering the settling basin was controlled by a constant head tank, which received water from a tank with a predetermined volume of water (190 or 380 liters). The flow rate was held constant through the entire run when only 190 liters of water were used. When 380 liters of water were used, the flow rate was held constant for the first 190 liters, then increased and held constant for the second 190 liters. Flow rates varied from 4 to 311 ml/sec in the mud substrate and 55 to 262 ml/sec in the sand (Table 4.1; Fig. 4.2).

Topographic data were collected before, during, and after each experimental run using a fully automated topographic scanner at 2 x 2.5 cm point spacing and approximately 0.5 mm vertical resolution. For each experiment 2-5 topographic scans per 190 liters of water were collected.

Topographic data were gridded to form a Digital Elevation Model (DEM). To determine the total volume of sediment removed during each experimental run the DEM of the last scan was subtracted from the DEM created from the initial scan over the flat initial surface. At each cell the length of change was multiplied by the area of the cell. The total volume of change was

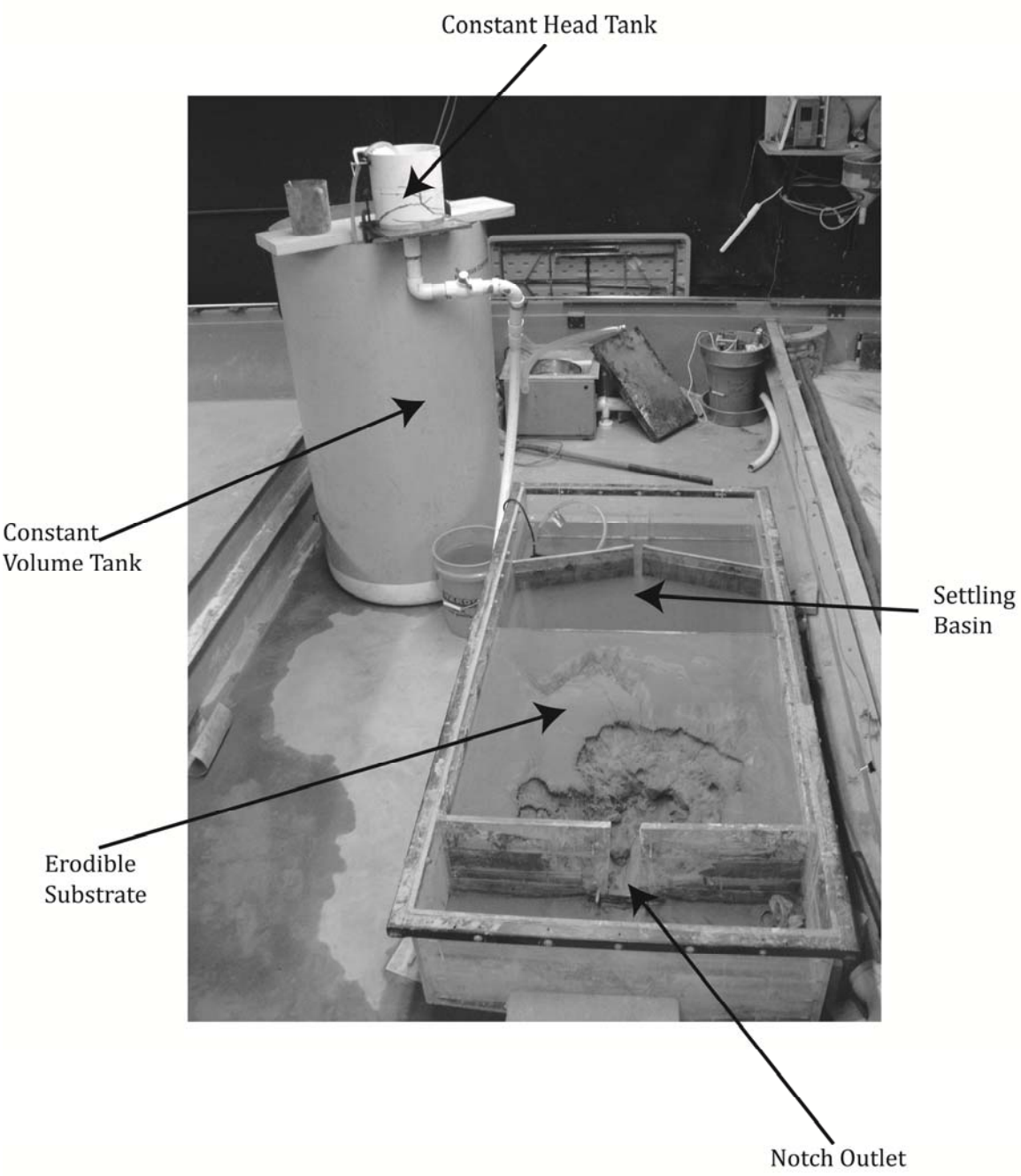

Figure 4.1: The experimental set up shown here allows water to flow from a settling basin over an erodible substrate and out through a 7.6 x 14 cm notch. The flow rates entering the basin range from 4 to 311 cm^3/s and are controlled by a constant head tank. For each run a constant volume of water either 190 or 380 liters is run over the erodible substrate. This figure shows the set up for the mud substrate, but the sand substrate set up was similar yet the erodible substrate was larger.

Table 4.1: Experimental Run Parameters

Run	Substrate	Water Volume (gallons)	Time (min)	Flow 1st 190 liters (cm^3/s)	Flow 2nd 190 liters (cm^3/s)
1	Mud	190	60	52.58	
2	Mud	190	32	98.58	
3	Mud	190	16	197.16	
4	Mud	190	21.25	148.45	
5	Mud	190	11	286.77	
6	Mud	190	872	3.62	
7	Mud	190	10.13	311.40	
8	Mud	190	21.5	146.72	
9	Mud	190	15.5	203.52	
10	Mud	380	91.5	71.69	66.41
11	Mud	380	65	73.36	143.39
12	Mud	380	54.5	76.94	233.67
13	Sand	190	25.25	124.93	
14	Sand	190	56.5	55.83	
15	Sand	190	13.5	233.67	
16	Sand	190	12	262.88	
17	Sand	190	20.25	155.78	
18	Sand	380	56	80.88	185.56
19	Sand	380	71.5	55.34	217.55
20	Sand	380	89	42.06	225.32

A)

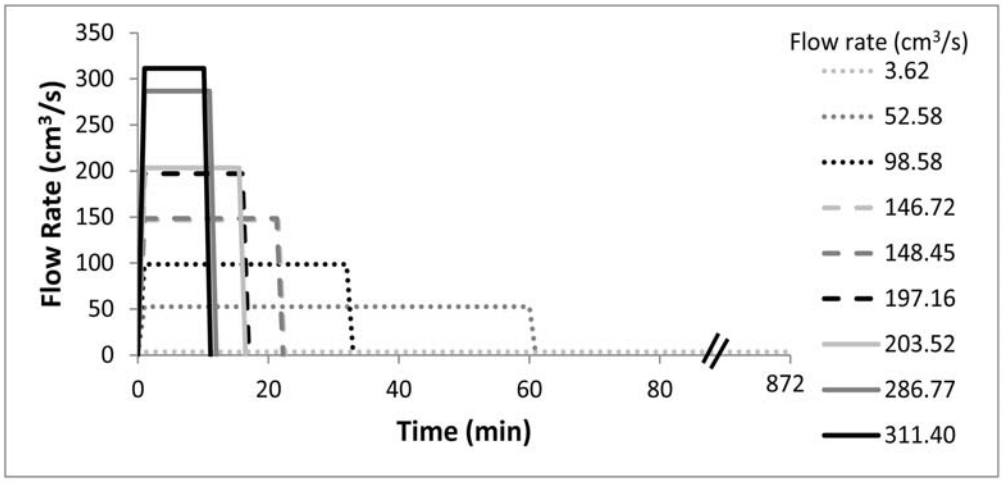
Flow Rate (cm³/s)
350
300
250
200
150
100
50
0
0
20
40
60
80
872
Time (min)
Flow rate (cm³/s)
3.62
52.58
98.58
146.72
148.45
197.16
203.52
286.77
311.40

B)

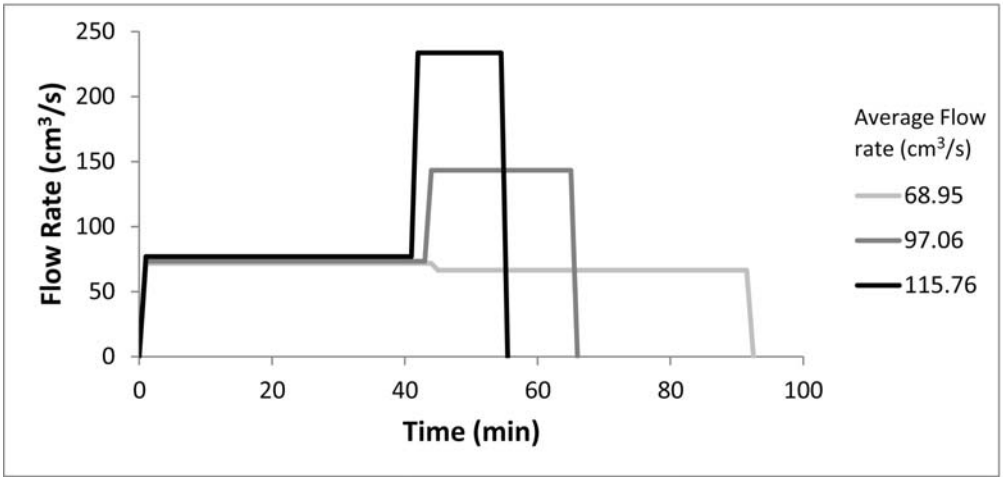
Flow Rate (cm³/s)
250
200
150
100
50
0
0
20
40
60
80
100
Time (min)
Average Flow rate (cm³/s)
68.95
97.06
115.76

C)

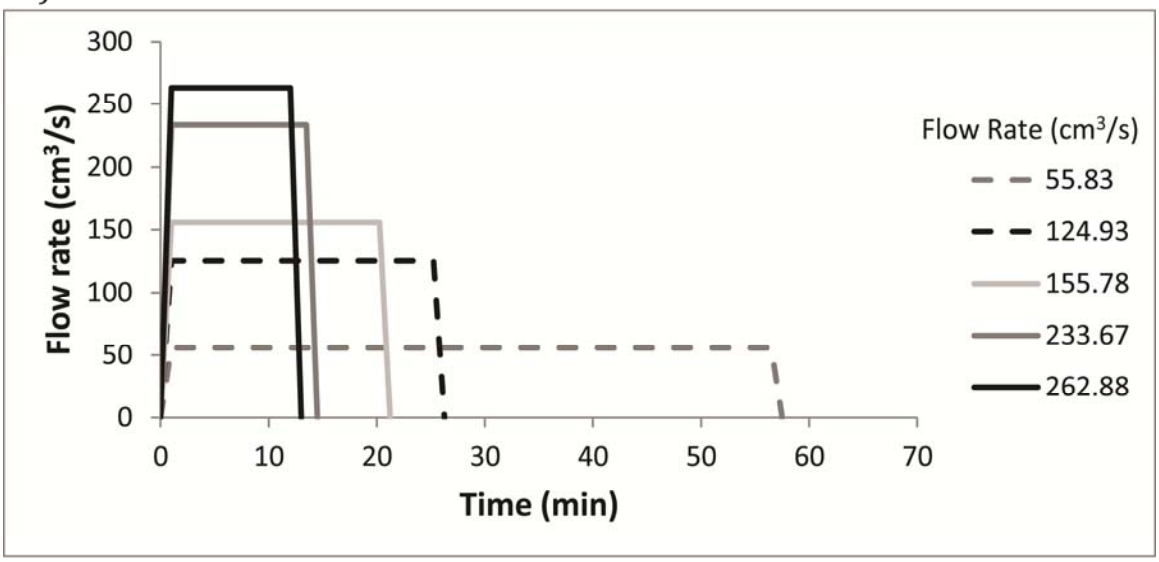

D)

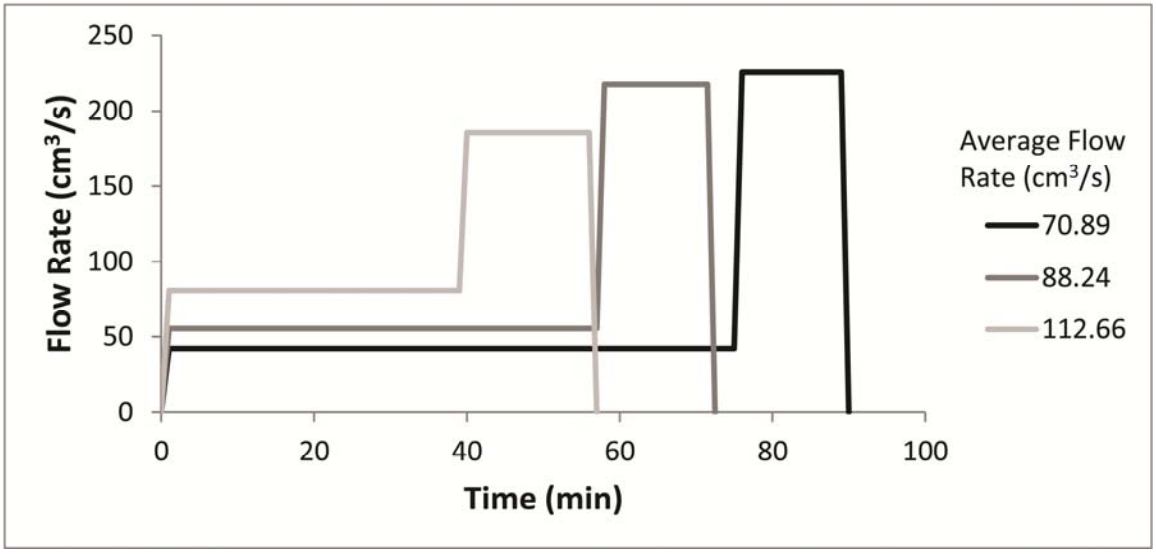

Figure 4.2: These hydrographs show the range of flow rates tested. Each set of curves is for a separate set of experimental runs. A) 190 liters of water over the mud substrate. B) 380 liters of water over the mud substrate. C) 190 liters of water over the sand substrate. D) 380 liters of water over the sand substrate.

summed for each experimental run. The volume of sediment eroded was also calculated at intermediate scans to measure sediment flux over time. Because these data only provide coarse measurements of sediment flux, for experimental run 11 samples were also taken every minute to measure sediment flux at higher resolution.

The DEMs were also imported into ArcGIS to measure channel characteristics such as width and slope. Both channel width and slope were measured using the profile tool in the 3D analyst toolbox. Channel width was measured as the distance between the channel banks on a cross section. In the mud substrate channel width was roughly equal to the valley width along the full channel length. In the sand substrate, channels meandered so channel width was measured in the most upstream portion of the channel where migration had not yet occurred, and the valley width was equal to the channel width. Slope was measured along the channel profile. In the mud substrate channel slope was measured three ways: along the bed, along the knickpoint, and the average channel slope along the complete channel. Where there was more than one knickpoint, the bed slope and knickpoint slope were measured for each section and averaged. Average channel slope is a function of channel length as elevation change for each channel is essentially the same. Only one slope measurement was made on channels formed in the sand substrate. The average channel slope was the only measurement, because the knickpoint and bed slope could not be distinguished. The channel length was also measured and used to approximate the knickpoint retreat rate. In both substrates the channel length was measured from the outlet to the break in slope at the flat upland surface.

Results and Analysis:

The most important outcome of the experiments is that the total eroded volume shows no consistent trend with rate of delivery of the water. For all 190 liter experimental runs the volume of sediment removed ranges from 8 – 25 cm^3 with no clear trend (Fig. 4.3). This result was the same for both the sand and the mud substrate. Similarly there is no trend in the volume of sediment removed in the 380 liter runs, yet the volume of sediment is greater (28-40 cm^3) than for the 190 liter runs (Fig. 4.3). Put another way, the sediment discharge is linearly related to water discharge. For a natural system this implies that in a given storm event the amount of sediment removed is proportional to the amount of precipitation rather than the storm intensity.

A)

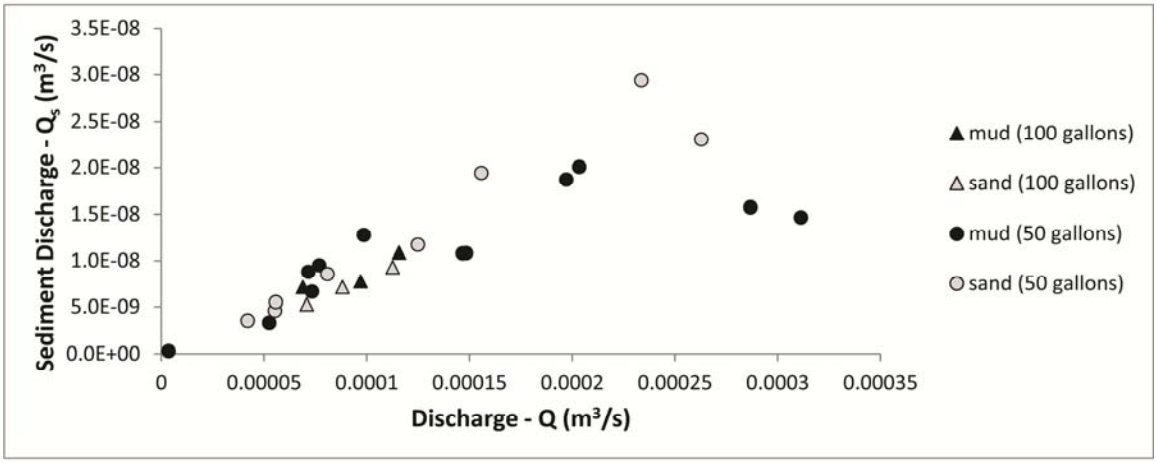

B)

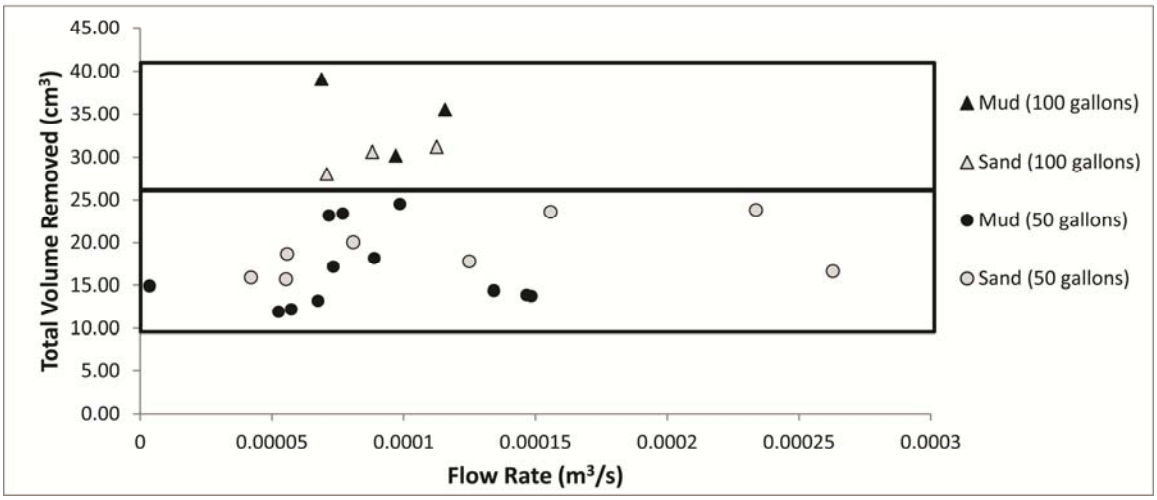

Figure 4.3: The results from these experiments show that the total volume of sediment removed is not dependant of flow rate (A) or that sediment discharge is linearly related to water discharge (B). These charts also show that while sediment discharge is the same for the 380 liter runs as it is for the 190 liter runs at a given discharge, the total volume of sediment removed is greater in the 380 liters runs.

Channel morphology:

While the volumes of sediment removed are roughly the same in the mud and sand channels, there are differences in how they erode. Channels in the mud substrate erode primarily via head cut propagation. In contrast channels in the sand substrate erode due to head cut propagation as well as lateral channel migration. In addition to demonstrating the importance the total volume of flow has on erosion volumes, the 390 liter runs reveal how increasing flow rates affect channel geometry. In the cohesive mud substrate higher flows in the second half of the experiment formed a wider channel upstream of the already eroded ravine, yet the pre-existing channel was not altered (Fig. 4.4). Channel widths before the increased flow ranged from 0.16 to 0.38 m for a flow rate of 73-77 ml/sec and increased to 0.28 to 0.61 m for flow rates ranging from 143 to 234 ml/sec. The channel formed in the sand substrate responded differently; these channels widened along the entire channel length when flow was increased (Fig. 4.4). In the sand channels widths varied from 0.14 to 0.19 m for initial flows which varied from 42 to 81 ml/sec and the full channel width increased to 0.24 to 0.43 m for the higher flows ranging from 88 to 113 ml/sec (Table 4.2). There was also a trend relating channel width and discharge in the 190 liter experiments ($R^2 = 0.40$ in mud substrate and 0.86 in sand substrate). Generally higher flows resulted in wider channels, which were also shorter to maintain a constant erosion volume (Table 4.2).

As mentioned above, channel slope in the mud run was measured along the bed, along the knickpoint, and as the average channel slope along the complete channel. The average channel slope is the only slope measurement that shows a trend with discharge. As suggested by the width variations, higher discharge results in shorter channels with a greater average slope (Table 4.2). Both the knickpoint and bed slopes appear to be unrelated to discharge (Fig. 4.5). In the sand channels the slope is poorly correlated with discharge (Fig. 4.5).

Using the topographic data collected during the intermediate scans the change in sediment flux can also be measured. During the 190 liter runs there is no distinct trend that all runs follow, yet generally there appears to be a sediment flux peak followed by a reduction in sediment flux (Fig. 4.6). This is trend is further supported by sample data taken every minute during the first 190 liters of Run 6 (Fig. 4.7). During the 390 liter runs there was an increase in erosion as the flow rate was increased. Similar to the 190 liter runs, after this second peak, in most cases the sediment flux dropped (Fig. 4.8).

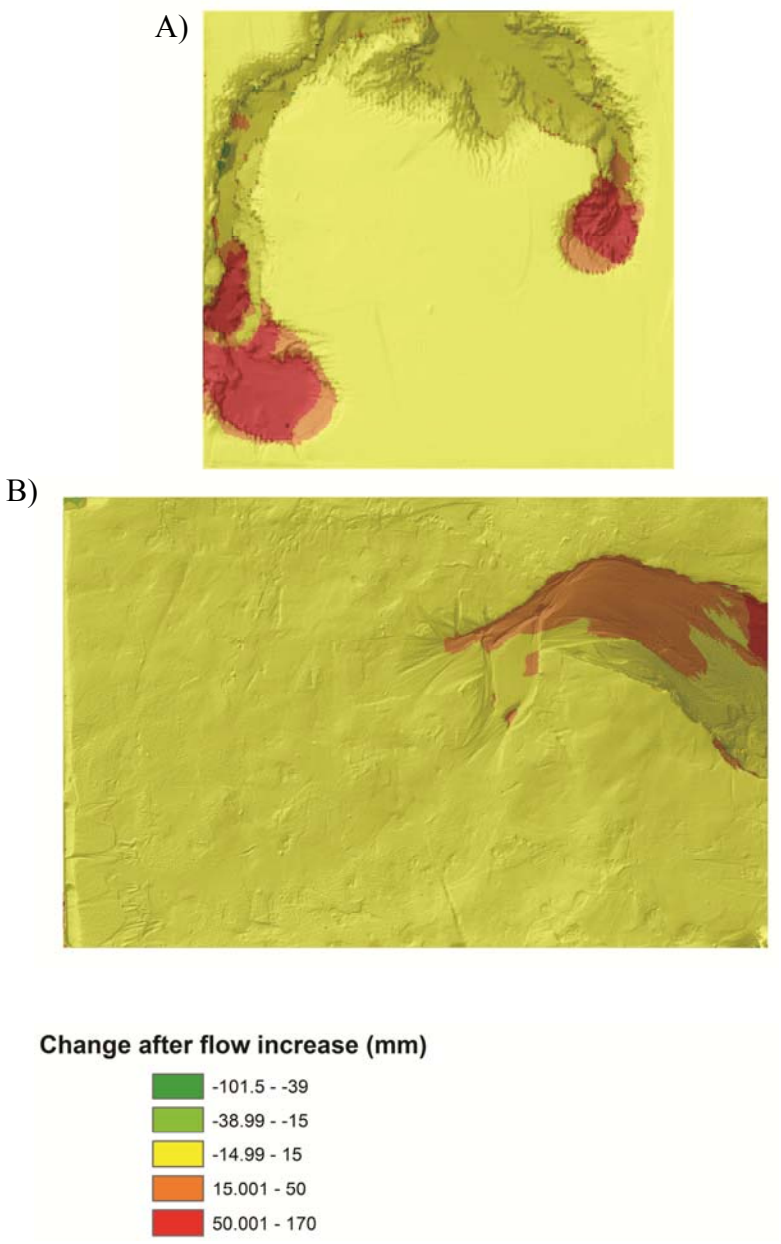

Figure 4.4: These DEMs show how changes in flow impact channel width. In the mud runs (A) the width changed only in the newly formed channel, while in the sand runs (B) the channel width was altered along the entire channel length.

Table 4.2: Experimental Results

Run*	Volume Sediment Removed (cm^3)	Average Slope	Bed Slope	Knickpoint Slope	Width 1st 190 liters (cm)	Width 2nd 380 liters (cm)
M-1	11.92	0.17	0.06	1.19	22	
M-2	24.51	0.20	0.04	0.60	48	
M-3	17.94	0.21	0.04	0.36	24	
M-4	13.78	0.27	0.03	0.62	43	
M-5	10.38	0.29	0.04	1.22	26	
M-6	14.90	0.12	0.10	0.27	13	
M-7	8.91	0.42	0.11	0.71	38	
M-8	13.91	0.37	0.06	0.67	43	
M-9	18.65	0.22	0.07	0.58	52	
M-10	39.05	0.15	0.05	0.81	40	49
M-11	30.16	0.14	0.05	0.56	16	28
M-12	35.53	0.16	0.03	0.29	38	61
S-13	17.76	0.06			20	
S-14	18.65	0.07			13	
S-15	23.80	0.06			28	
S-16	16.59	0.06			27	
S-17	23.57	0.06			29	
S-18	31.17	0.07			19	39
S-19	30.59	0.06			14	43
S-20	28.03	0.06			15	24

** M indicates run in the mud substrate, and S indicates run in the sand substrate.*

A)

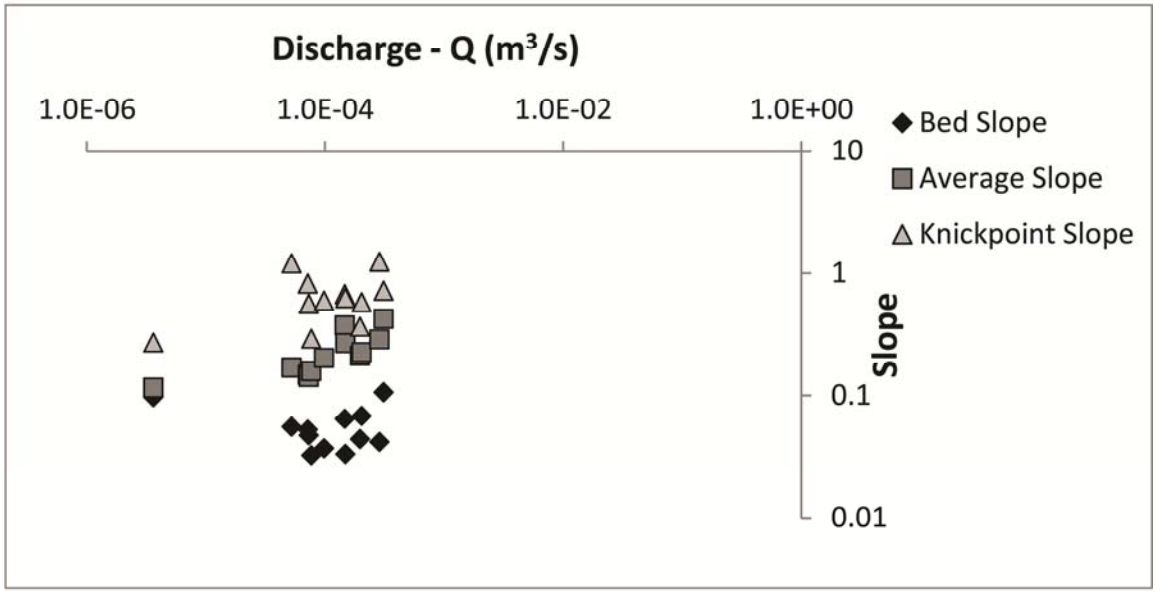

B)

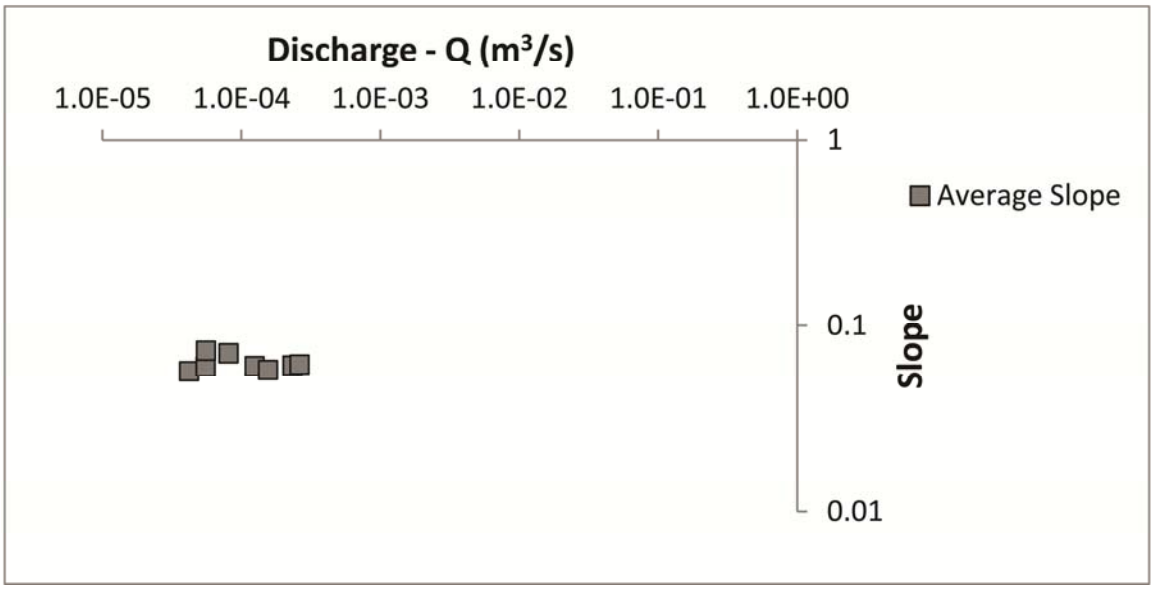

Figure 4.5: Channel slope between each run is not well related to discharge for either the mud (A) or the sand (B) runs.

A)

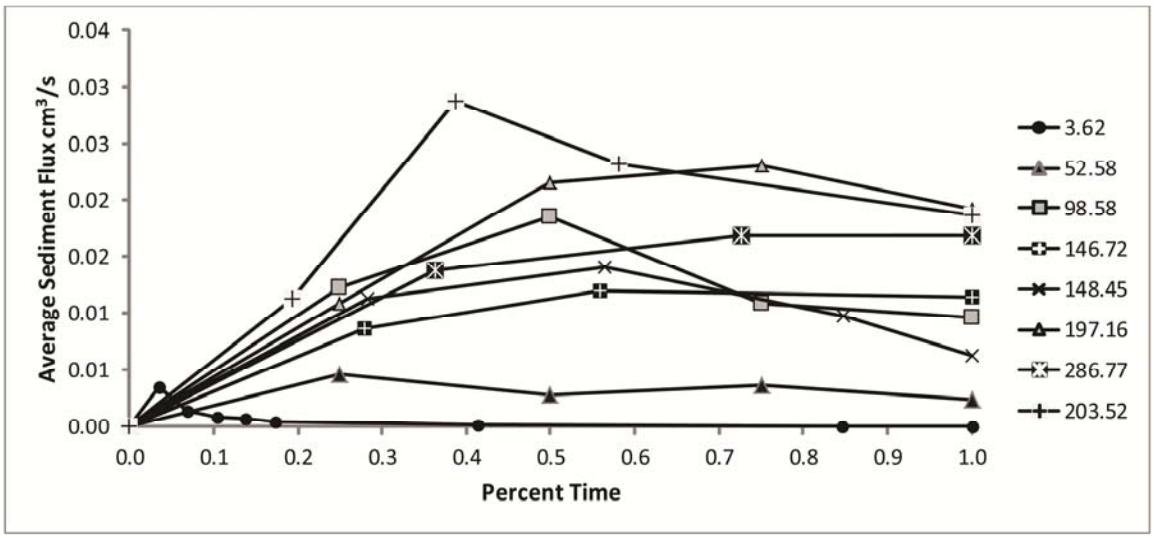

B)

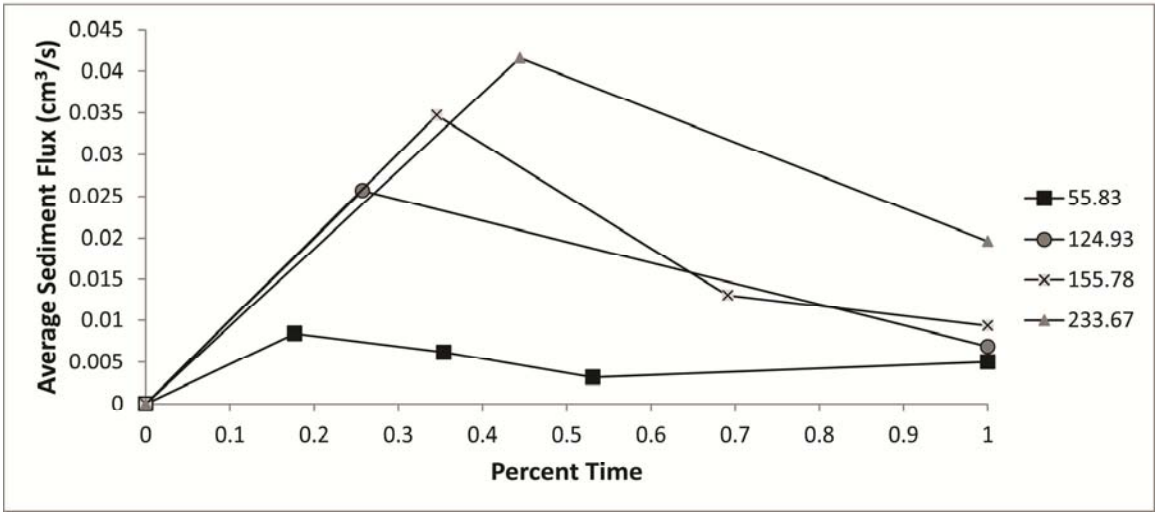

Figure 4.6: The sediment flux over time in the 190 liter runs appears to peak than later decrease for both the mud (A) and the sand (B) runs.

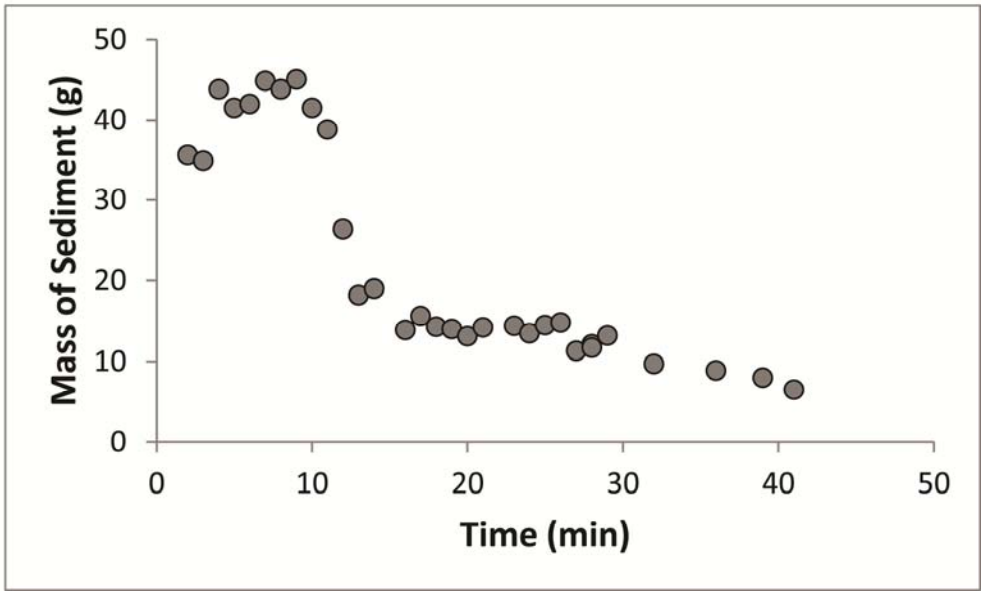

Figure 4.7: Samples collected every minute during the first 190 liters of run 11 show a decrease in sediment load with time after an initial peak.

A)

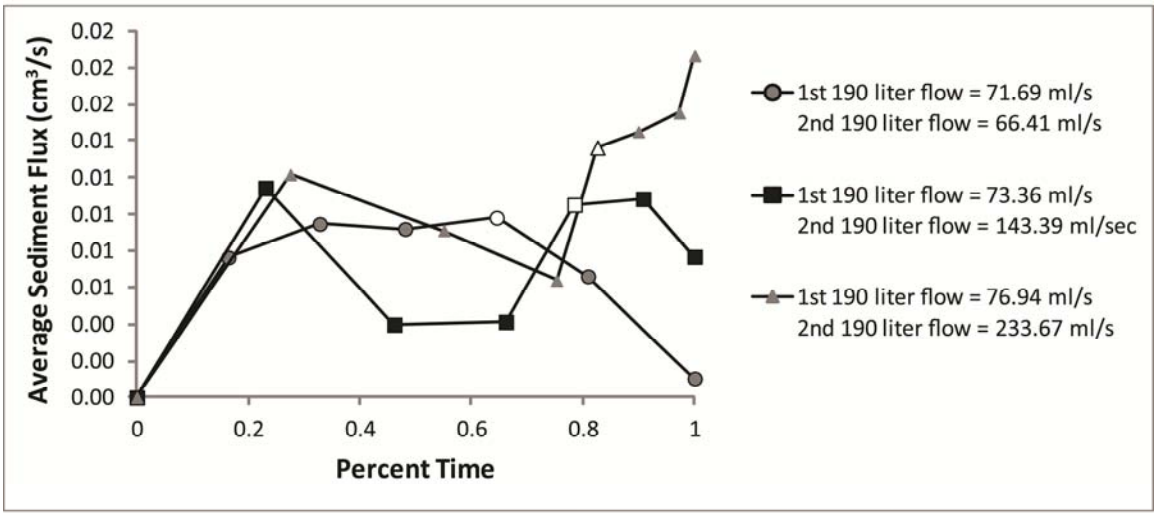

B)

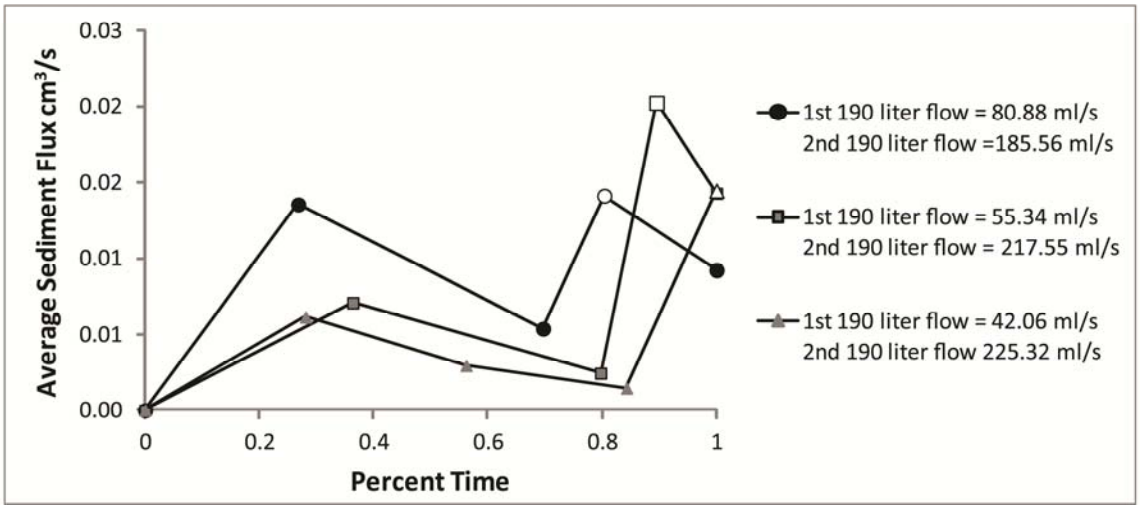

Figure 4.8: In the 380 liter runs sediment flux initially peaked for the first 190 liters and then underwent a second peak when flow was increased for the second 190 liters. This trend can be seen in both the mud (A) and the sand (B) runs, where the increase in discharge is indicated with a hollow marker.

As stated above, both slope and width changed in response to discharge. Hydraulic geometry equations are commonly used to describe how channel width (W), depth (h) and velocity (v) vary with discharge (Q) (Leopold and Maddock, 1953).

$$W = aQ^b \quad (4.1)$$

$$h = cQ^f \quad (4.2)$$

$$v = kQ^m \quad (4.3)$$

where a, b, c, f, k, and m are constants. In these experiments we did not measure channel depth or flow velocity so we will focus on how channel width and discharge are related.

For each of these hydraulic geometry relationships a range of empirically-derived exponents has been measured. For equation 4.1 the range of values reported for b is between 0.3 and 0.5 derived from field measurements of both bedrock and alluvial streams (Leopold and Maddock, 1953; Knighton, 1998; Montgomery and Gran, 2001; Whipple, 2004).

To test how well these field-measured values describe our experimental channels we calculated width using the reported values for b and iterated to find the best fit for a. In addition we also iterated to determine what b value most accurately describes the trend in our experimental data. The root mean square error (RMSE) was calculated for each data set between the known and modeled values and is reported as a percentage of the average measured value.

Using the field-derived exponents ranging from 0.3-0.5 the RMSE is 32-39% of the average measured width in the mud substrate. The best fit for the experimental data results in a b value of 0.18 and an RMSE of 31% (Fig. 4.9). In the sand substrate the best fit for the data falls within the range of field-derived exponents. The error is minimized when b is 0.40 resulting in a percent RMSE of 11% (Fig. 4.9).

Role of Cohesion:

The use of two different substrate materials allowed us to test how sediment with different cohesion responded to different flow rates. Cohesion is an important factor in the distinction between detachment-limited and transport-limited systems in nature. Currently there are no measured topographic distinctions between transport-limited and detachment-limited erosional systems and therefore distinguishing between the two systems is done by comparing

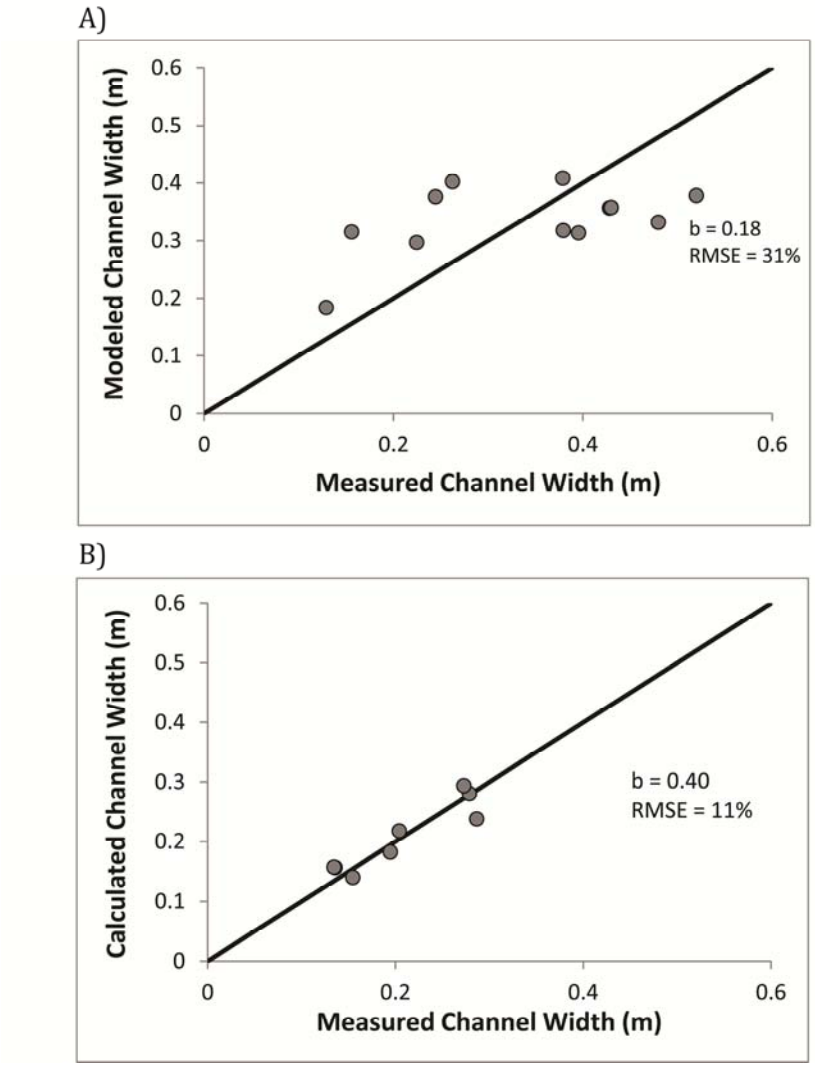

Figure 4.9: Channel width can be modeled using the hydraulic geometry relationship. In both plots the solid black line is a 1:1 line A) The relationship measured in the channels formed in the mud substrate has a constant *b* value that is less than the values commonly observed in nature. B) The relationship measured in the channels formed in the sand substrate has a constant *b* value of 0.4, which in the intermediate range of the commonly proposed constants.

calculated and actual sediment loads (Pelletier, 2011). To test if the cohesion of the mud substrate was strong enough to distinguish it from the sand and form a detachment-limited system we compared the expected sediment transport calculated using the Engelund and Hansen (1967) formula with the actual measured sediment transport (equations 4.4-4.7).

$$q_s = \frac{0.05}{C_f}\tau_*^{5/2} \tag{4.4}$$

$$\tau_* = \frac{\tau}{(\rho_s - \rho) g D_{50}} \tag{4.5}$$

$$C_f = \left[\frac{1}{0.4}\left(LN\left(\frac{h}{D_{50}/_{30}}\right) - 1\right)\right]^{-2} \tag{4.6}$$

$$q_s = q_s\sqrt{\left(\frac{\rho_s}{\rho} - 1\right) g D_{50}^{\ 3}} \tag{4.7}$$

where τ is shear stress, D_{50} is the median grain size, h is the flow depth, q_s is the volumetric unit sediment flux, and ρ_s and ρ are sediment and water density. Because the exact water depth was not measured a range of possible water depths between 0.5 and 3 cm was used based on observations during the experiments.

The results of this analysis show that the expected q_s is at least one order of magnitude greater than the measured sediment flux for the mud when the knickpoint slope or the average channel slope is used, and *qs* is still greater than the measured sediment flux when the lowest measured slope, the bed slope, is used at the lowest water depth considered (Fig. 4.10). The results of equations 4.4-4.7 in the sand substrate were within the range of measured values and indicate that this is indeed a transport-limited system (Fig. 4.10).

Modeled Sediment Transport:

While the absence of a relationship between sediment yield and discharge appears to conflict with standard sediment transport relationships, even very simple sediment transport or erosion equations relate sediment flux to both discharge and slope.

Commonly erosion in detachment-limited systems is modeled by the stream power incision model (Howard and Kerby, 1983):

$$\frac{dz}{dt} = kQ^{m_d}S_k^{n_d} \tag{4.8}$$

Where *k, m_d* and n_d are constants, *dz/dt* is vertical erosion rate, and S_k is the knickpoint slope. In the detachment-limited mud substrate, all erosion took place at the knickpoint and therefore we

A)

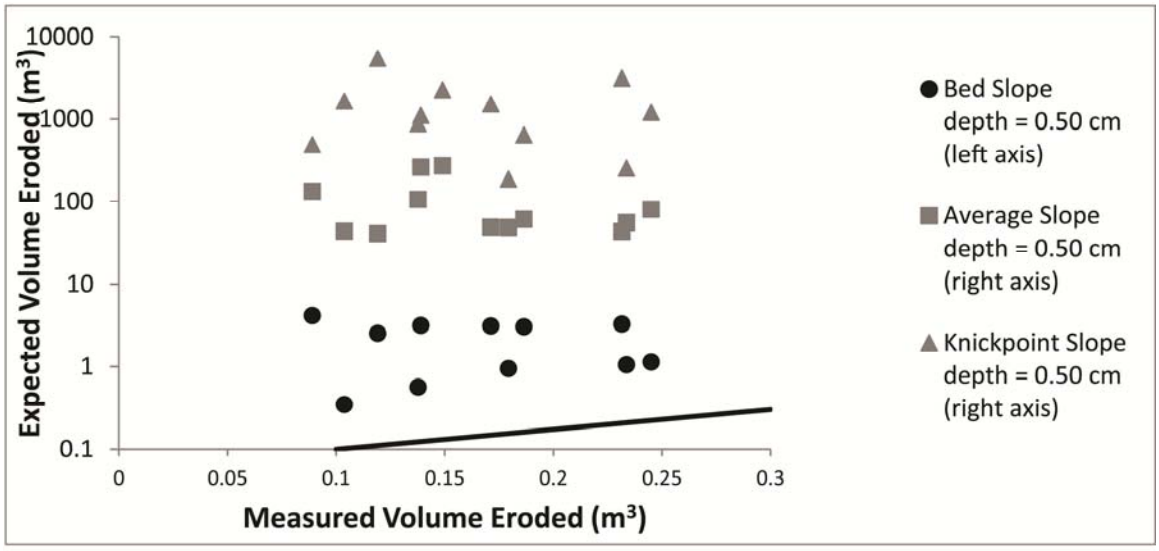

B)

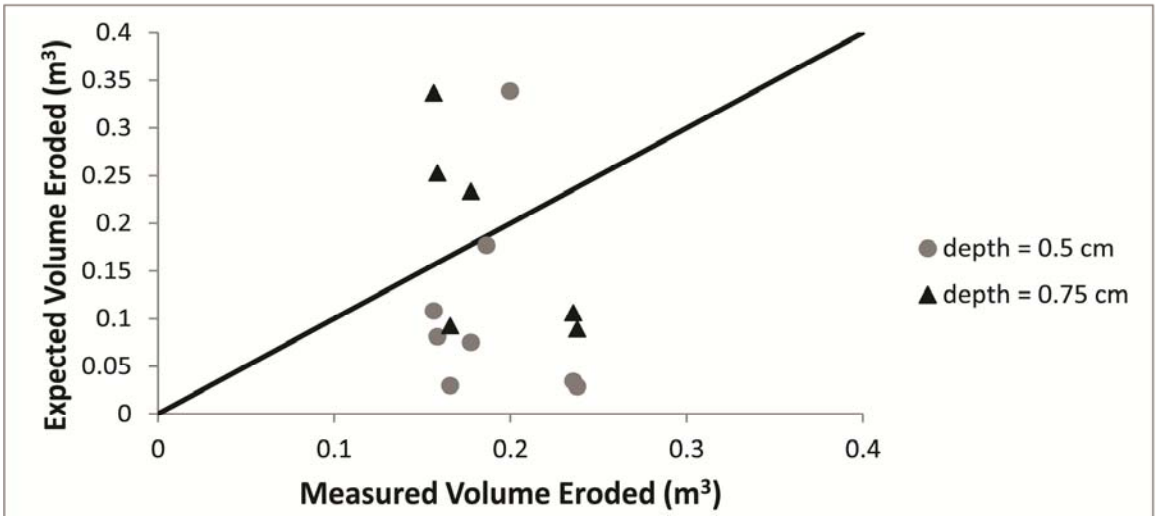

Figure 4.10: Using common sediment transport equations we can define the mud and sand substrates as detachment or transport limited. In both plots the solid black line is a 1:1 line A) The results of this analysis from the mud substrate even at a low water depth (0.5 cm) demonstrate that the channels are detachment limited. Note results are plotted on a semi-log plot. B) The channels formed in the sand substrate are transport limited. A water depth between 0.5 and 0.75 cm accurately predicts the range of eroded sediment volumes.

consider only knickpoint retreat rate. Because this rate is a horizontal rather than vertical retreat rate we must convert equation (4.8) appropriately:

$$U \cdot S_k = \frac{dz}{dt} \tag{4.9}$$

$$U = kQ^{m_d} S_k^{n_d - 1} \tag{4.10}$$

where U is the knickpoint retreat rate. The exponents m_d and n_d have been derived for a variety of natural environments. Typically the m/n ratio is approximately 0.35-0.6 (Whipple and Tucker, 1999; Baldwin et al., 2003). The exponent n_d ranges between 2/3 and 5/3 depending on the erodability of the substrate where more easily eroded sediment has a lower value for the exponent n_d (Foley 1980; Howard and Kirby 1983; Whipple et al., 2000). The exponents m_d and n_d for uniform detachment limited landscapes (ie. badlands) reported by Howard and Kerby (1983) are 4/9 and 2/3 respectively. While the m/n ratio (concavity index) is slightly higher than reported elsewhere, we used these values to model erosion in our experiments because, like the badlands, our experimental set-up was spatially homogeneous and easily eroded. RMSE was measured between the calculated U and the measured U and minimized by modifying the coefficient k. The RMSE was 22% of the measured average knickpoint retreat rate (Fig. 4.11).

Sediment loads from the sand substrate were modeled with the transport limited equation (Pelletier, 2011):

$$q_s = kQ^{m_t} S^{n_t} \tag{4.11}$$

Where k, m_t and n_t are constants and q_s is the volumetric unit sediment flux. This equation can be derived from the Engelund and Hansen (1967) equation where both m_t and n_t equal 5/3. Engelund and Hansen (1967) is the ideal equation to use because it does not have an incipient motion threshold as many other sediment transport equations do. Here again the RMSE was measured between the measured and calculated q_s and minimized using the coefficient k. The RMSE was 34% of the average volumetric unit sediment discharge (Fig. 4.12).

Both equations (4.10) and (4.11) were applied to both the sand and the mud substrates. This provided a secondary test to check that the mud substrate is detachment limited and the sand substrate is transport limited. The detachment-limited relationship clearly fit the mud substrate

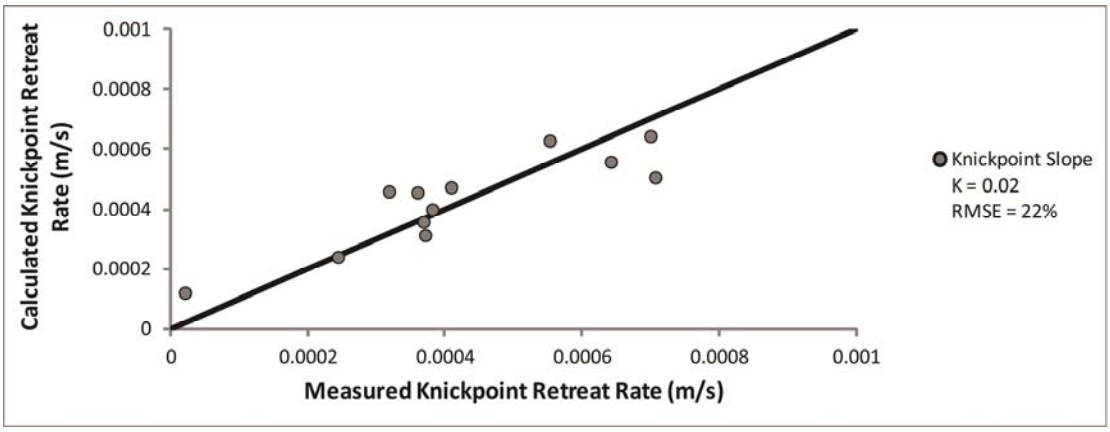

Figure 4.11: Modeling the channels in the mud substrate as detachment limited can accurately predict the measured erosion rate (knickpoint retreat rate). The solid black line is a 1:1 line.

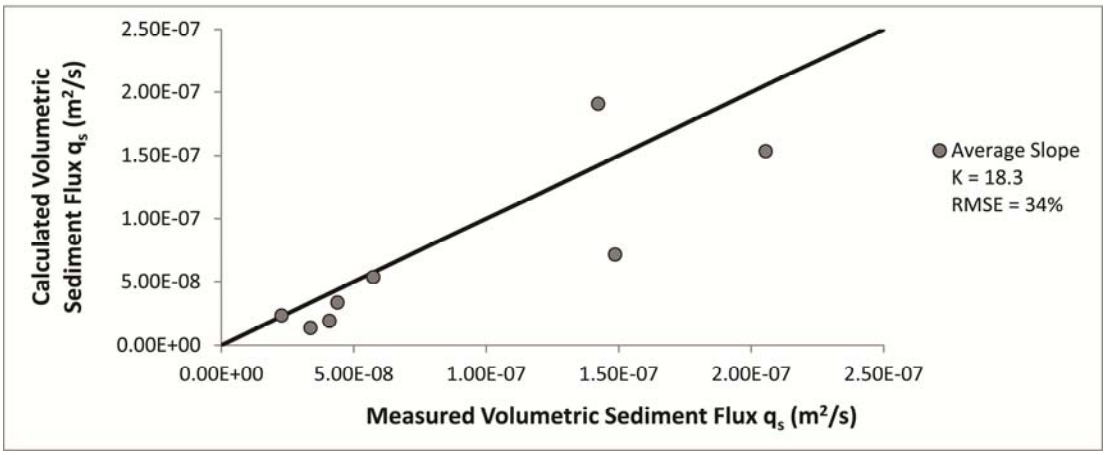

Figure 4.12: Modeling the channels formed in the sand substrate using the transport limited sediment flux equation with constants derived from Engelund and Hansen (1967) accurately predicts the sediment flux measured. The solid black line is a 1:1 line.

data better than the transport-limited relationship, as was predicted. In the sand substrate both relationships fit the data well, yet the RMSE was lower for the transport-limited relationship.

Discussion:

These experiments demonstrate that, over a range of experimental conditions, the sediment volume eroded during ravine growth under application of a fixed volume of water is independent of the rate at which the water is supplied. Thus sediment discharge is linearly related to water discharge in both detachment limited and transport limited systems, which is surprising because erosion in each of these systems is thought to occur differently. These results are also unexpected compared to results for many pre-existing streams where changing flow intensity has resulted in increased erosion volume (ie. Ma et al., 2010; Naik and Jay, 2011; Boateng et al., 2012).

The documented response that pre-existing streams show a non-linear increase in sediment discharge with increased water discharge may not be directly applicable to ravines, because ravines are undergoing active head-ward erosion in response to overland flow. We hypothesize that because ravines are actively evolving to a given hydrology, the channel morphology that develops reflects that hydrology with erosion balanced by altering channel slope and width. This is supported by sediment transport equations (4.10) and (4.11), which when applied to the mud and sand substrate, respectively, are able to predict the measured sediment discharges. In pre-existing channels where channel slope may take tens of thousands of years to adjust to changing flows, both of these equations would predict a non-linear increase in sediment discharge with increasing water discharge. Ravine slopes evolve more rapidly in response to the imposed discharge and can balance erosion by altering channel slope.

Moreover our findings suggest that anthropogenic changes to discharge regime could affect channel morphology, without changing sediment input derived from ravines. It is also important to note that there was an increased sediment discharge when discharge was increased in the 390 liter runs, but the channel quickly evolved to the new discharge. In natural pre-existing streams channels adjustments in response to changes in discharge occur over long time intervals.

The effects of changing hydrology on newly evolved channels are difficult to study in nature, but numerical models can be used to examine long-term channel evolution under a range of conditions. In one numerical study, Istanbulluoglu et al. (2005) tested the effect of changing rain intensity while storm volume was held constant. The modeled results of this study showed an increase in the volume of sediment eroded as intensity increased. This result is in direct

conflict with our results, yet there are many distinctions between the two studies that may explain this discrepancy. The Istanbulluoglu et al. (2005) model assumed gully erosion due to slab failure in a detachment-limited system. While the mud substrate in our physical experiments was also detachment limited, erosion occurred grain by grain rather than as large blocks. Once these grains were detached, the flow was easily able to carry them through the channel and there was no measurable deposition in any of the experimental runs. In contrast, erosion in the slab failure model occurred in response to pore pressure build up in tension cracks resulting in large failures. This model does not require that the flow be able to carry the detached sediment and often resulted in deposition at the toe of the knickpoint, which increases resistance to future failure.

It is likely that both slab failure and grain by grain knickpoint propagation occur in ravines throughout the world. The relative importance of each process is dependent on sediment type and the knickpoint slope. Tension cracks develop behind steep slopes where shrinkage occurs due to desiccation and horizontal tensile stresses generated in large part by gravity are greater than the tensile strength of the sediment (Darby and Thorne, 1994). Cracks like this are likely to form on the landscape above steep ravine head cuts in cohesive sediment, between storm events. If we had modeled individual storm events rather than a constant overland flow it is likely we would have also developed tension cracks in the cohesive mud substrate. Because this was outside of the scope of these experiments it is difficult to form accurate conclusions on how the development of tension cracks and the subsequent failure events would have altered our results, but an analogous study that encouraged erosion by slab failure would be a useful follow-on to our work.

The results of these experiments follow the hydraulic geometry relationship for width in equation (1) although with lower exponents than usually measured in field studies. While this relationship is typically applied to describing width or discharge changes in a single channel, it works here for these separate channels because each comparable channel is carving through the same substrate. In the mud substrate the empirical exponent b for these data is much lower than has been derived for natural channels. This may be a result of the steep channel walls developed in these experiments; in natural ravines where near vertical channel walls are less common, we expect that this exponent would be closer to the reported values. In the sand substrate where steep channel walls could not develop the empirical exponent b is 0.40 which is only slightly lower than the range typically considered for alluvial channels (Rodriquez-Iturbe and Rinaldo, 1997).

Based on the results of this study and the comparison with pervious ravine studies it is important to consider a wide range of variables when mitigating ravine erosion. The results from these experiments suggest that increasing overland flow rates will not result in increased sediment yield, if the volumes of water delivered are not changed. Moreover, while sediment loads are not affected by changing flow rates, channel morphology is. Another important variable to consider is the mode of head cut retreat. The experimental results apply in environments with steep slopes where erosion is grain-by-grain. In places where tension cracks develop, the slab failure mechanism highlighted by Istanbulluoglu et al. (2005) might apply. If this failure mechanism is the dominant process of head cut retreat, flow rates and storm intensity may become more important than in this study.

The results presented here can be applied to reducing ravine growth to protect property and infrastructure or reduce sediment loads. The primary goal should be to reduce total annual overland flow volume entering ravines. In many areas this can be done most effectively by increasing evapotranspiration. A reduction in overland flow can also be achieved through tile drainage, yet the downstream effects of this should also be considered. River banks and bluffs are often eroded due to over-steepening as the river removes sediment from the base of these features (Brunsden and Kessel, 1973; Turnbull et al., 1996; Harden et al., 2009; Day et al., in review). The increased channel flow rates and volumes brought on by tile draining can lead to accelerated over-steepening and increased river bank and bluff erosion. Where river bank and bluff erosion are a concern in addition to ravine tip growth it is essential that we consider the cumulative effect of increasing infiltration capacity through tile draining.

Conclusion:

Ravine erosion is a concern in throughout the world where propagating head cuts threaten infrastructure and property. In many places land-use changes have altered hydrology which may contribute to erosion. The experiments we report on here suggest that water volume, rather than discharge, controls the volume of erosion. Moreover, this result holds true for both transport and detachment limited systems.

While flow rate does not appear to contribute significantly to the volume of erosion, it does affect channel geometry. In both substrates, variations in channel width were described by the well-known hydraulic geometry relationship proposed by Leopold (1953), and wider channels formed in response to higher discharge. To balance the removed sediment volume wider channels were also typically shorter.

The sediment transport in both the sand and mud substrates was well described by the transport limited sediment flux equation and the detachment-limited stream power equation, respectively. It appears that indirect effects of changing discharge on channel morphology (width and slope) compensate for the direct effects of discharge on erosion rate to result in a constant volume of erosion.

The effects of changing flow measured in these experiments can be applied to understanding ravine evolution and growth. It is unlikely that these results directly translate to pre-existing channels undergoing changes in discharge, because they lack the free parameter in slope that headcuts can adjust quickly.

Works Cited:

Abrahams AD, Parsons AJ. 1991. Resistance to overland flow on desert pavement and its implications for sediment transport modeling. Water Resources Research **27**: 1827-1836.

Baldwin JA, Whipple KX, Tucker GE. 2003. Implications of the shear stress river incision model for the timescale of postorogenic decay of topography. Journal of Geophysical Research **108**: 2158.

Belmont P, Gran K, Schottler S, Wilcock P, Day S, Jennings C, Lauer J, Viparelli E, Willenbring J, Engstrom D, Parker G. 2011, Large shift in source of fine sediment in the Upper Mississippi River. Environmental Science and Technology. **45**: 8804–8810. dx.doi.org/10.1021/es2019109.

Bengtson RL, Carter CE, McDaniel V, Halverson BE. 1984. Corn silage response to subsurface drainage in alluvial soil. Transactions of the American Society of Civil Engineers **27**: 1391.

Boardman J. 2001. Storms, floods and soil erosion on the South Downs, East Sussex, Autumn and Winter 2000-01. Geomorphology **86**: 346-355.

Brunsden D, Kesel RH, 1973. Slope development on a Mississippi River bluff in historic time. The Journal of Geology **81**: 576-598.

Einstein HA, Barbarossa NL. 1951. River channel roughness. Transactions of the American Society of Civil Engineers **117**: 1121-1132.

Eitel JUH, Williams CJ, Vierling LA, Al-Hamdan OZ, Pierson FB. 2011. Suitability of terrestrial laser scanning for studying surface roughness effects on concentrated flow erosion processes in rangelands. Catena **87**:398-407.

Farres PJ. 1978. The role of time and aggregate size in the crusting process. Earth Surface Processes **3**: 243-254

Finnegan NJ, Roe G, Montgomery DR, Hallet B. 2005. Controls on the channel width of rivers: Implications for modeling fluvial incision of bedrock. Geology **33**: 229-232.

Foley MG. 1980. Bed-rock incision by streams. Geological Society of America Bulletin **91**: 2189-2213.

Gran KB, Belmont P, Day S, Jennings C, Lauer JW, Viparelli E, Wilcock P, Parker G. 2011, An integrated sediment budget for the Le Sueur River basin. Final report Presented to the Minnesota Pollution Control Agency.

Haddeland I, Lettenmaier DP, Skaugen T. 2005. Effects of irrigation on the water and energy balances of the Colorado and Mekong river basins. Journal of Hydrology. **324**:210-223.
Howard AD, Kirby G. 1983. Channel changes in badlands. Geological Society of Bulletin **94**: 739-752.

Harden CP, Foster W, Morris C, Chartrand KJ, Hennry E, 2009. Rates and processes of streambank erosion in tributaries of the Little River, Tennessee. Physical Geography **30**: 1-16.

Istanbulluoglu E, Bras RL, Flores-Cervantes H, Tucker GE. 2005. Implications of bank failures and fluvial erosion for gully development: Field observations and modeling. Journal of Geophysical research **110**: F01014.

Kladivko EJ, Brown LC, Baker JL. 2001. Pesticide transport to subsurface tile drains in humid regions of North America. Critical Reviews in Environmental Science and Technology **31**:1-62.
Montgomery DR, Gran KB. Downstream variations in the width of bedrock channels. Water Resources Research **37**: 1841-1846.

Montgomery DR, Gran KB. 2001. Downstream variations in the width of bedrock channels. Water Resources Research **37**: 1841-1846.

Pierson FB, Bates JD, Svejcar TJ, Hardegree SP. 2007. Runoff and erosion after cutting western Juniper. Rangeland Ecology and Management **60**: 285-292.

Poesen JW, Vandaele K, Van Wesemael B. 1996. Contribution of gully erosion to sediment production on cultivated lands and rangelands. IAHS Publications **236**: 251-266.

Poesen J, Nachtergaele J, Verstaeten G, Valentin C. 2003. Gully erosion and environmental change: importance and research needs. Catena **50**: 91-133.

Rodriquez-Iturbe I, Rinaldo A. 1997. Fractal River Basins: Chance and Self-Organization, 547 pp., Cambridge Univ. Press, New York.

Römkens MJM, Wang JY. 1987. Soil roughness changes from rainfall. Transactions of the American Society of Civil Engineers **31**: 408-413.

Schwab GO, Fausey NR, Desmond ED, Holman JR. 1985. Tile and surface drainage of clay soils. IV. Hydrologic performance with field crops (1973-80); V. Corn, oats, and soybean yields (1973-80); VI. Water quality; VII. Cross moling over tile drains. Resources Bulletin **116**, OARDC, Wooster, OH 29p.

Sidorchuk A. 2006. Stages in gully evolution and self-organized criticality. Earth Surface Processes and Landforms **31**: 1329-1344.

Turnbull WJ, Krinitzsky EL, Weaver FJ, 1966. Bank erosion in soils of the lower Mississippi Valley. Proceedings of the American Society of Civil Engineers **92**: 121-136

Verstraeten G, Poesen J. 1999. The nature of small-scale flooding, muddy floods and retention pond sedimentation in central Belgium. Geomorphology **29**: 275-292.

Whipple KX, Tucker GE. 1999. Dynamics of the stream-power river incision model: Implications for height limits of mountain ranges, landscape response timescales, and research needs. Journal of Geophysical Research **104**: 17661-17674.

Whipple KX, Hancock GS, Anderson RS. 2000. River incision into bedrock: Mechanics and relative efficacy of plucking, abrasion, and cavitation. GSA Bulletin **112**: 490-503.

Synthesis

Thesis Results:

The findings reported in this thesis advance our understanding of erosion in incising/incised rivers. The focus on bluffs and ravines targets features that are common in incised rivers and also features that raise concern from land owners and managers. Both bluff erosion and ravine growth have been reported to threaten property and infrastructure throughout the world. The Le Sueur River watershed in southern Minnesota provides an ideal location for studying these features.

High bluff erosion rates in the Le Sueur River watershed make annual change measurements possible. Traditionally change is measured with coarse spatial resolution that cannot accurately measure the episodic change bluffs undergo. The high point density Terrestrial Laser Scanning (TLS) provides makes it possible to capture even highly localized change. Unfortunately due to the nature of the technology, TLS has traditionally been used in places with sparse vegetation and typically change is measured only on small features. The techniques developed through this work extend the benefits of TLS to regions with large features and vegetated areas. In addition the error analyses performed address the total error for the technique rather than the point by point error which is more commonly cited. These techniques were tested and utilized to examine bluff change in the Le Sueur River basin.

By pairing 4 years of TLS data on 15 bluffs with 67 years of aerial photograph data on 243 of 480 mapped bluffs in the Le Sueur River basin, bluff retreat was measured over contrasting temporal and spatial scales. The measured rates were then extrapolated to calculate the total volume of suspended sediment derived from bluffs in the watershed. Remarkably the volumes calculated from both the aerial photograph and the TLS data sets were approximately the same. In total, bluffs account for approximately half the total suspended sediment load measured in the Le Sueur watershed and retreat at an average rate of 14-20 cm/yr. These data emphasize how important it is to understand bluff erosion in incising rivers. Not only do high rates of retreat threaten infrastructure and property, the high sediment loads threaten riverine ecosystems.

The results of the bluff retreat analysis have also increased our understanding of the impacts of hydrology on bluff erosion. The four years of TLS data were compared to corresponding gauge and precipitation data to reveal that large erosion events commonly occur in years where large precipitation events resulted in high flows. Moreover the TLS data showed that over long time scales individual events are less significant and retreat rates converge on the

average. Interpretations of the TLS data also reveal important information on bluff erosion processes. Additional future research may be able to demonstrate specific timing of bluff failure, including seasonal response and the response to individual storm events.

Extending this line of analysis, using TLS and aerial photographs, to ravines in the Le Sueur watershed proved to be impossible. To advance our understanding of ravines, small scale physical experiments were used to examine how changing flow rates impact erosion. The results of this work show that erosion volume in ravines is not related to overland flow rate, but rather overland flow volume. Moreover channel width in both detachment-limited and transport-limited substrates was described by common channel geometry relationships. The total sediment load measured from both substrates was also described using sediment transport equations where sediment discharge is a function of both flow and channel slope. These findings could be used to mitigate ravine growth in anthropogenically-altered landscapes. Based on these results a reduction in overland flow volume could result in decreased ravine erosion. Additional research is needed to understand downstream effects where overland flow is reduced through increased drainage and direct routing of water into the river.

Discussion:

The individual results of each study outlined in this thesis advances our understanding of bluff and ravine erosion, yet the combined results help advance our understanding of how changes to hydrology alter erosion system wide. In the Le Sueur River basin tile drains have been used to increase the infiltration capacity of the sediment, and reduce standing water on the upland surface. As infiltration capacity is increased, both overland flow and evapotranspiration are reduced. As shown in chapter three the reduction in overland flow likely slows ravine growth. The downstream effects of reducing overland flow and evapotranspiration include greater peak flows and greater flow volumes. The effect of these flow alterations on bluff erosion must also be considered. Results highlighted in chapter one and two emphasize the importance of over-steepening on bluff retreat rates, which is driven by erosion at the bluff toe. Additional results from chapter two show a positive relationship between river stage and bluff retreat rate. While these data are not available from before drainage was pervasive on the landscape, it is likely that increased peak flows and flow volumes, brought on by tile drains, are accelerating the rate of bluff retreat.

Results from the pre-settlement and modern sediment budgets support the hypothesis that bluff retreat has accelerated in the past 150 years by showing that modern bluff erosion volumes exceed pre-settlement average annual total loads (Gran et al., 2011). Anticipating that the

sediment flux had not been consistent throughout the entire Holocene, Johnson (2012) used data collected through optically stimulated luminescence and carbon dating to inform a river evolution and channel migration model. Results from this model showed that sediment flux peaked shortly after incision began and decreased to a near steady-state (Gran et al., 2011; Finnegan et al., 2011). This model further suggests that the observed increase in sediment load between pre- and post-settlement is not a natural trend, and sediment loads would have remained at steady-state had the landscape not been dramatically altered.

Results found by Gran et al., (2011) follow a similar sediment flux trend to that reported in chapter three. This trend, where sediment flux peaks shortly after a sudden base level fall and then decreases reaching a steady-state, was also measured by Parker (1977). In each of these cases incision was occurring in response to a single sudden base level fall. This has important implications to river managers and in the case of the Le Sueur River (and other rivers responding to a single base level drop) suggests that a recent increase in sediment is not natural.

Future research:

The research presented in this thesis has contributed to the research on TLS, bluff erosion, ravine growth, and the effects of anthropogenic land use, yet there is additional research that should be pursued. In each chapter there are many lines of research that will advance our understanding of the specific goals of reported in the introduction. Three of these potential lines of research are highlighted below.

In chapter one, the TLS methods presented can be used in field settings to improve change detection in both erosional and depositional environments. To use these techniques in temperate climates it is essential that vegetation is removed. Here we suggest manually removing vegetation by angling the bluff surface so that points measured on vegetation can easily be selected and deleted. There is certainly room for improvement on this technique. Ideally vegetation would not simply be removed yet rather could be registered as a point of vegetation rather than a rock point. This would allow multiple scientists interested in either the sediment or the vegetation to utilize a single data set. By using color and intensity data available on many new TLS scanners this process may be automated, and made to be more user-friendly.

In chapter two, bluff erosion rates were measured in the Le Sueur watershed using TLS and aerial photographs. This research should be expanded into other watersheds to improve our understanding of specific bluff erosion processes. The measured rates should also be compared with geotechnical data of the different till types. By adding these additional data it may be possible to determine what characteristics cause some bluffs to erode more rapidly than others.

These results paired with event scale change research can be used to better understand bluff erosion processes including toe erosion, freeze-thaw, and sapping. Ultimately these data could be combined to develop a predictive model of bluff erosion, which could inform hazard mapping to protect property.

Finally the experiments used in chapter three to understand ravine growth and the effects of changing flow rates should be expanded to improve our understanding of erosion in pre-existing channels. By understanding if channel bluff and bank erosion is predominantly driven by the magnitude of flows or the flow volume, land managers may be able to better direct efforts to reduce erosion.

Works Cited:

Finnegan NJ, Gran K, Johnson A, Belmont P, Wilcock P, Dietrich WE. 2010. The importance of downstream bed surface coarsening in predicting the wave of incision in response to a sudden base level drop at the mouth of a river: the Holocene Le Sueur River, Minnesota, USA, Abstract EP52A-01 presented at the Fall Meeting, AGU, San Francisco, California, 13-17 DEC.

Gran KB, Belmont P, Day SS, Finnegan N, Jennings C, Lauer JW, Wilcock PR. 2011. Landscape evolution in south-central Minnesota and the role of geomorphic history on modern erosional processes. GSA Today **21**: 7-9.

Johnson A. 2012. Timing and pattern of valley excavation, Le Sueur River, south-central Minnesota, USA, Master's Thesis from University of Minnesota. 54 pages.

Parker RS. 1977. Experimental study of drainage basin evolution and its hydrologic implications. Doctor of Philosophy Thesis from Colorado State University. 64 pages.

Bibliography:

Abrahams AD, Parsons AJ. 1991. Resistance to overland flow on desert pavement and its implications for sediment transport modeling. Water Resources Research **27**: 1827-1836.

Alho P, Kukko A, Hyyppä H, Kaartinen H, Hyyppä J, Jaakkola A. 2009. Application of boat-based laser scanning for river survey. Earth Surface Processes and Landforms**34**:1831-1838.

Allred BJ. 1999. Survey of fractured glacial till geotechnical characteristics: hydraulic conductivity, consolidation, and shear strength. Ohio Journal of Science**100**: 63-72.

Baldwin JA, Whipple KX, Tucker GE. 2003. Implications of the shear stress river incision model for the timescale of postorogenic decay of topography. Journal of Geophysical Research **108**: 2158.

Belmont P, Gran K, Schottler S, Wilcock P, Day S, Jennings C, Lauer J, Viparelli E, Willenbring J, Engstrom D, Parker G. 2011, Large shift in source of fine sediment in the Upper Mississippi River. Environmental Science and Technology. **45**: 8804–8810. dx.doi.org/10.1021/es2019109.

Bengtson RL, Carter CE, McDaniel V, Halverson BE. 1984. Corn silage response to subsurface drainage in alluvial soil. Transactions of the American Society of Civil Engineers **27**: 1391.

Bennett SJ, Casalí J. 2001. Effect of initial step height on headcut development in upland concentrated flows. Water Resources Research **37**: 1475-1484.

Bernhardt ES, Palmer MA, 2007. Restoring streams in an urbanizing world. Freshwater Biology **52**: 738-751.

Blann KL, Anderson JL, Sands GR, Vondracek B. 2009. Effects of agricultural drainage on aquatic ecosystems: a review. Critical Reviews in Environmental Science and Technology **39**: 909-1001

Boardman J. 2001. Storms, floods and soil erosion on the South Downs, East Sussex, Autumn and Winter 2000-01. Geomorphology **86**: 346-355.

Bold KC, Wood F, Edwards PJ, Williard KWJ, Schoonover JE, 2010. Using photographic image analysis to assess ground cover: a case study of forest road cutbanks. Environmental Monitor Assessment **163**: 685-698.

Boulton GS. 1976. The development of geotechnical properties in glacial tills. Legget RF(ed).Glacial Till. Ottawa: The Royal Society of Canada. Special Publication NO. 12; 292-303.

Brunsden D, Kesel RH, 1973. Slope development on a Mississippi River bluff in historic time. The Journal of Geology **81**: 576-598.

Buckley SA, Howell JA, Enge HD, Kurz TH. 2008. Terrestrial laser scanning in geology: data acquisition, processing, and accuracy considerations. Journal of the Geological Society of London**165**:625-638.

Cancienne RM, Fox GA, Simon A. 2008. Influence of seepage undercutting on the stability of root-reinforced streambanks. Earth Surface Processes and Landforms **33**: 1769-1786.

Chu-Agor ML, Fox GA, Cancienne RM, 2008. Seepage caused tension failures and erosion undercutting hillslopes. Journal of Hydrology **359**: 247-259.

Clayton L, Moran SR. 1982. Chronology of late-Wisconsinan glaciations in middle North America. Quaternary Science Reviews **1**: 55-82

Couper P, Scott T, Maddock I. 2002. Insights into river bank erosion processes derived from analysis of negative erosion pin recordings: observations from three recent UK studies. Earth Surface Processes and Landforms**27**:59-79.

Day S, Gran K, Belmont P, Wawrzyniec T. this issue. Measuring bluff erosion part 2:Pairing aerial photographs and terrestrial laser scanning to create a watershed scale sediment budget. Earth Surface Processes and Landforms.

Day SS, Gran KB, Belmont P, Wawrzyniec T, this issue. Measuring bluff erosion part 1: Terrestrial laser scanning methods for change detection and determining bluff erosion processes. Earth Surface Processes and Landforms.

De Vente J, Poesen J, Arabkhedri M, Verstraeten G. 2007. The sediment delivery problem revisited. Progress in Physical Geography **31**: 155-178. DOI 10.1177/0309133307076485.

Docker BB, Hubble TCT. 2008. Quanitfying root-reiforcement of river bank soils by four Australian tree species. Geomorphology **100**: 401-418.

Dotterweich M, 2008. The history of soil erosion and fluvial deposits in small catchments of central Europe: Deciphering the long-term interaction between humans and the environment – A review. Geomorphology **101**: 192-208.

Einstein HA, Barbarossa NL. 1951. River channel roughness. Transactions of the American Society of Civil Engineers **117**: 1121-1132.

Eitel JUH, Williams CJ, Vierling LA, Al-Hamdan OZ, Pierson FB. 2011. Suitability of terrestrial laser scanning for studying surface roughness effects on concentrated flow erosion processes in rangelands. Catena **87**:398-407.

Engstrom DR, Almendinger JE, Wolin JA, 2009. Historical changes in sediment and phosphorus loading to the upper Mississippi River: mass-balance reconstructions from the sediments of Lake Pepin. Journal of Paleolimnology **41**: 563–588.

Farres PJ. 1978. The role of time and aggregate size in the crusting process. Earth Surface Processes **3**: 243-254

Finnegan NJ, Roe G, Montgomery DR, Hallet B. 2005. Controls on the channel width of rivers: Implications for modeling fluvial incision of bedrock. Geology **33**: 229-232.
Foley MG. 1980. Bed-rock incision by streams. Geological Society of America Bulletin **91**: 2189-2213.

Finnegan NJ, Gran K, Johnson A, Belmont P, Wilcock P, Dietrich WE. 2010. The importance of downstream bed surface coarsening in predicting the wave of incision in response to a sudden base level drop at the mouth of a river: the Holocene Le Sueur River, Minnesota, USA, Abstract EP52A-01 presented at the Fall Meeting, AGU, San Francisco, California, 13-17 DEC.

Fox GA, Wilson GV, Simon A, Langendoen EJ, Akay O, Fuchs JW. 2007. Measuring streambank erosion due to ground water seepage: correlation to bank pore water pressure, precipitation and stream stage. Earth Surface Processes and Landforms **32**, 1558-1573.

Frankel KL, Pazzaglia FJ, Vaughn JD. 2007. Knickpoints evolution in a vertically bedded substrate, upstream-dipping terraces, and Atlantic slope bedrock channels. Geological Society of America Bulletin **119**: 476-486.

Ganti V, Straub KM, Foufoula-Georgiou E, Paola C, 2011. Space-time dynamics of depositional systems: Experimental evidence and theoretical modeling of heavy-tailed statistics. Journal of Geophysical Research **116**: F02011.

Gardner TW. 1983. Experimental study of knickpoint and longitudinal profile evolution in cohesive, homogeneous material. Geological Society of America Bulletin **94**: 664-672.

Ghahramani A, Ishikawa Y, Gomi T, Shiraki K, Miyata S, 2011. Effect of ground cover on splash and sheetwash erosion over a steep forested hillslope; a plot-scale study. Catena **85**: 34-47.

Gran KB, Belmont P, Day SS, Jennings C, Johnson A, Perg L, Wilcock PR. 2009. Geomorphic evolution of the Le Sueur River, Minnesota, USA, and implications for current sediment loading. James LA, Rathburn SL, Whittecar GR, (eds). Management and Restoration of Fluvial Systems

with Broad Historical Changes and Human Impacts: Geological Society of America Special Paper **451**.

Gran KB, Belmont P, Day SS, Finnegan N, Jennings C, Lauer JW, Wilcock PR. 2011. Landscape evolution in south-central Minnesota and the role of geomorphic history on modern erosional processes. GSA Today **21**: 7-9.

Gran KB, Belmont P, Day S, Jennings C, Lauer JW, Viparelli E, Wilcock P, Parker G. 2011, An integrated sediment budget for the Le Sueur River basin. Final report Presented to the Minnesota Pollution Control Agency.

Gulyaev SA, Buckeridge JS. 2004, Terrestrial methods for monitoring cliff erosion in an urban environment. Journal of Costal Research **20**, 871-878.

Haddeland I, Lettenmaier DP, Skaugen T. 2005. Effects of irrigation on the water and energy balances of the Colorado and Mekong river basins. Journal of Hydrology. **324**:210-223.
Howard AD, Kirby G. 1983. Channel changes in badlands. Geological Society of Bulletin **94**: 739-752.

Haigh MJ. 1977. The use of erosion pins in the study of slope evolution. Shorter Technical Methods (II), Finlayson BL (ed). British Geomorphological Research Group Technical Bulletin Group **18**: 31–49.

Hodge R, Brasington J, Richards K. 2009. Analysing laser-scanned digital terrain models of gravel bed surfaces: linking morphology to sediment transport processes and hydraulics. Sedimentology **56**: 2024-2043.

Hall K, 2007. Evidence for freeze-thaw events and their implications for rock weathering in northern Canada: II. The temperature at which water freezes in rock. Earth Surface Processes and Landforms **32**: 249-259.

Harden CP, Foster W, Morris C, Chartrand KJ, Hennry E, 2009. Rates and processes of streambank erosion in tributaries of the Little River, Tennessee. Physical Geography **30**: 1-16.

Harding JS, Benfield EF, Bolstad PV, Helfman GS, Jones EBD, 1998. Stream biodiversity: the ghost of landuse past. Proceedings of the National Academy of Sciences **95**: 14843-14847

Hasbargen LE, Paola C, 2000. Landscape instability in an experimental drainage basin. Geology **28**: 1067-1070.

Heritage G, Hetherington D. 2007.Towards a protocol for laser scanning in fluvial geomorphology. Earth Surface Processes and Landforms**32**:66-74.

Heritage GL, Milan DJ. 2009. Terrestrial laser scanning of grain roughness in a gravel bed river. Geomorphology **113**: 4-11.

Hall K, 2007. Evidence for freeze-thaw events and their implications for rock weathering in northern Canada: II. The temperature at which water freezes in rock. Earth Surface Processes and Landforms **32**: 249-259.

Higgins CG. 1982. Drainage systems developed by sapping on Earth and Mars. Geology **10**: 147-152.

Hinds NEA. 1925 Amphitheater valley heads. Journal of Geology **33**: 816-818.

Hirt U Wetzig A Amatya MD Matranga M, 2011. Impact of seasonality on artificial drainage discharge under temperate climate conditions. International Review of Hydrobiology **96**: 561-577.

Hughes ML, McDowell PF, Marcus WA, 2006. Accuracy assessment of georectified aerial photographs; implications for measuring lateral channel movement in a GIS. Geomorphology **74**: 1-16.

Istanbulluoglu E, Bras RL, Flores-Cervantes H, Tucker GE. 2005. Implications of bank failures and fluvial erosion for gully development: Field observations and modeling. Journal of Geophysical research **110**: F01014.

James LA, Watson DG, Hansen WF. 2007. Using Lidar data to map gullies and headwater streams under forest canopy: South Carolina, USA. Catena **71**: 132-144.

Jennings CE, 2010. Draft digital reconnaissance surficial geology and geomorphology of the Le Sueur River watershed (Blue Earth, Waseca, Fairbault, and Freeborn counties in south-central Minnesota). Map, scale 1:100,000, report, digital files.

Johnson A. 2012. Timing and pattern of valley excavation, Le Sueur River, south-central Minnesota, USA, Master's Thesis from University of Minnesota. 54 pages.

Kelley DW, Nater EA, 2000. Historical sediment flux from three watersheds into Lake Pepin, Minnesota, USA. Journal of Environmental Quality **29**: 561-568.

Kelley DW, Brachfeld SA, Nater EA, Wright HE. 2006. Sources of sediment in Lake Pepin on the upper Mississippi River in response to Holocene climatic changes. Journal of Paleolimnology **35**: 193-206.

Knapen A, Poesen J. 2010. Soil erosion resistance effects on rill and gully initiation points and dimensions. Earth Surface Processes and Landforms **35**: 217-228

Kent TR, Stelzer RS. 2008. Effects of fine sediment on life history traits of Physa integra snails. Hydrobiologia **596**: 329-340.

Kirkaldie L, Talbot JR. 1992.The effects of soil joints on soil mass properties. Bulletin for the Association of Engineering Geology**25**:415-420.

Kirkby MJ, 1965. Measurements of soil creep. Annals of the Association of American Geographers **55**: 626.

Kladivko EJ, Brown LC, Baker JL. 2001. Pesticide transport to subsurface tile drains in humid regions of North America. Critical Reviews in Environmental Science and Technology **31**:1-62.

Lamb MP, Howard AD, Johnson J, Whipple KX, Dietrich WE, Perron J. 2006. Can springs cun canyons into rock?. Journal of Geophysical Research **111**: E07002.

Lauer JW, Parker G, 2008. Net local removal of floodplain sediment by river meander migration. Geomorphology **96**: 123-149.

Lawler DM. 1978. The use of erosion pins in river banks. Swansea Geographer**16**:9–18.

Lim M, Rosser NJ, Allison RJ, Petley DN. 2010. Erosional processes in the hard rock coastal cliffs at Staithes, North Yorkshire. Geomorphology **114**: 12-21.

Lindow N, Fox GA, Evans RO. 2009. Seepage erosion in layered stream bank material. Earth Surface Processes and Landforms **34**: 1693-1701.

Lobb DA, Kachanoski RG, Miller MH. 1995. Tillage translocation and tillage erosion on shoulder slope landscape positions measured using ^{137}Cs as a tracer. Canadian Journal of Soil Science **75**: 211-218.

Lovell JL, Jupp DLB, Culvenor DS, Coops NC. 2003. Using airborne and ground-based ranging lidar to measure canopy structure in Australian forests. Canadian Journal of Remote Sensing **29**:607-622.

Lowell TV, Fisher TG, Comer GC. 2005. Testing the Lake Agassiz meltwater trigger for the Younger Dryan: Eos (Transactions, American Geophysical Union) **83**: 365-373

Maloney KL, Weller DE, 2011. Anthropogenic disturbance and streams: land use and land-use change affect stream ecosystems via multiple pathways. Freshwater Biology **56**: 611-626.

Matsch CL. 1983. River Warren, the southern outlet of Lake Agassiz. Teller JT, Clayton L, (eds). Glacial Lake Agassiz: Geological Association of Canada Special paper **26**: 232-244.

Matthews N. 2008, Aerial and Close-Range Photogrammetric Technology: Providing Resource Documentation, Interpretation, and Preservation. by Neffra A. Matthews Technical Note 428 Bureau of Land Management

Milan DJ, Heritage GL, Hetherington D. 2007.Application of 3D laser scanner in the assessment of erosion and deposition volumes and channel change in a proglacial river. Earth Surface Processes and Landforms**32**:1657-1674.

Miller HC, Buell MF. 1956. Life form spectra of contrasting slopes in Itasca Park, Minnesota. Botanical Gazette **117**: 259-263.

Miller RG. 1974. The jackknife – a review. Biometrika **61**: 1-15.

Minnesota Pollution Control Agency (MPCA). Minnesota Department of Agriculture, Minnesota State University, Mankato water Resources Center and Metropolitan Council Environmental Services. 2007. State of the Minnesota River: Summary of Surface Water Quality Monitoring 2000-2005: St. Paul, 20p.

Montgomery D. 2007. Soil erosion and agriculture sustainability. PNAS **104**: 13268-132772.

Montgomery DR, Schmidt KM, Greenberg HM, Dietrich WE, 2000 Forest clearing and regional landsliding. Geology **28**: 311-314.

Mulla DJ, Sekely AC. 2009. Historical trends affecting accumulation of sediment and phosphorus in Lake Pepin, upper Mississippi River, USA. Journal of Paleolimnology **41**: 589-602.

Murgatroyd AL, Ternan JL. 1983. The impact of afforestation on stream bank erosion and channel form. Earth Surface Processes and Landforms **8**: 357-369.

Optech, 2012. http://optech.ca/pdf/ILRIS_SpecSheet_110309_Web.pdf. pdf accessed April 19, 2012

Optech, 2011. http://www.optech.ca/pdf/Brochures/ILRIS-DS-LR.pdf. website accessed July 24, 2011.

Parker RS. 1977. Experimental study of drainage basin evolution and its hydrologic implications. Doctor of Philosophy Thesis from Colorado State University. 64 pages.

Pierson FB, Bates JD, Svejcar TJ, Hardegree SP. 2007. Runoff and erosion after cutting western Juniper. Rangeland Ecology and Management **60**: 285-292.

Poesen JW, Vandaele K, Van Wesemael B. 1996. Contribution of gully erosion to sediment production on cultivated lands and rangelands. IAHS Publications **236**: 251-266.

Poesen J, Nachtergaele J, Verstaeten G, Valentin C. 2003. Gully erosion and environmental change: importance and research needs. Catena **50**: 91-133.

Resop JP, Hession WC. 2010. Terrestrial laser scanning for monitoring streambank retreat: comparison with traditional surveying techniques. Journal of Hydraulic Engineering **136**: 794-798.

Resop JP, 2010. Terrestrial laser scanning for quantifying uncertainty in fluvial applications.Doctor of Philosophy Thesis from Virginia Polytechnic Institute and State University.128 pages.

Resop JP, Kozarek JL, Hession WC. 2012. Terrestrial laser scanning for delineating in-stream boulders and quantifying habitat complexity measures. Photogrammetric Engineering and Remote Sensing **78**: 363 – 371

Roberts L. 2009. Biogeomorphology and soil geomorphology of small semiarid basins, Northeastern Arizona: influences of topoclimate and climate variations. Master of Science Thesis from the University of New Mexico.80 pages.

Rodriquez-Iturbe I, Rinaldo A. 1997. Fractal River Basins: Chance and Self-Organization, 547 pp., Cambridge Univ. Press, New York.

Römkens MJM, Wang JY. 1987. Soil roughness changes from rainfall. Transactions of the American Society of Civil Engineers **31**: 408-413.

Rosser NJ, Petley DN, Lim M, Dunning SA, Allison RJ. 2005. Terrestrial laser scanning for monitoring the process of hard rock costal cliff erosion. Quarterly Journal of Engineering Geology and Hydrogeology **38**: 363-375.

Schwab GO, Fausey NR, Desmond ED, Holman JR. 1985. Tile and surface drainage of clay soils. IV. Hydrologic performance with field crops (1973-80); V. Corn, oats, and soybean yields (1973-80); VI. Water quality; VII. Cross moling over tile drains. Resources Bulletin **116**, OARDC, Wooster, OH 29p.

Sekely AC, Mulla DJ, Bauer DW. 2002. Stream bank slumping and its contributions to the phosphorus and suspended sediment loads of the Blue Earth River, Minnesota. Journal of Soil and Water Conservation **57**: 243-250.

Sharma M, Paige GB, Miller SN. 2010. DEM development from ground-based LiDAR data: A method to remove non-surface objects. Remote Sensing **2**: 2629-2642

Shields FD, Knight SS, Cooper CM. 1995. Use of index biotic integrity to assess physical habitat degradation inwarmwater streams. Hydrobiologia **312**: 191-208

Shields FD, Pezeshki SR, Wilson GV, Wu MN, Dabney SM. Rehabilitation of an incised stream using plant materials: The dominance of geomorphic processes. Ecology and Society **13**: 54.

Sidle RC, Ochiai H, 2006. Landslides: processes, prediction, and land use. Water Resources Monograph **18**: 312p.

Sidorchuk A. 2006. Stages in gully evolution and self-organized criticality. Earth Surface Processes and Landforms **31**: 1329-1344.

Simon A, Curini A, Darby SE, Langendoen EJ.2000. Bank and near-bank processes in an incised channel. Geomorphology**35**: 193-217.

Smith SMC, Belmont P, Wilcock PR. 2011. Closing the gap between watershed modeling, sediment budgeting, and stream restoration. Stream Restoration in Dynamic Fluvial Systems: Scientific Approaches, Analysis and Tools Geophysical Monograph Series **194**: 293-317.

Soulsby C, Youngson AF, Moir HJ, Malcolm IA. 2001. Fine sediment influence on salmonid spawning habitat in a lowland agricultural stream: a preliminary assessment. Science of the Total Environment **265**: 295:307.

Strahler AH, Jupp DLB, Woodcock CE, Schaaf CB, Yao T, Zhao F, Yang X, Lovell J, Culvenor D, Newnham G, Ni-Miester W, Boykin-Morris W. 2008. Retrieval of forest structural parameters using a ground based lidar instrument. Canadian Journal of Remote Sensing**34**:426-440.

Terzaghi K, 1962. Stability of steep slopes on hard unweathered rock. Geotechnique **12**: 251-270.

Thoma DP, Gupta SC, Bauer ME, Kirchoff CE. 2005. Airborne laser scanning for riverbank erosion assessment: Remote Sensing of Environment **95**: 493-501.

Thomas JT, Iverson NR, Burkart MR, 2009. Bank-collapse processes in a valley-bottom gully, western Iowa. Earth Surface Processes and Landforms **34**: 109-122.

Thorleifson LH. 1996. Review of Lake Agassiz history, Teller JT, Thorleifson LH, Matile G, Brisbin WC. Sedimentology, Geomorphology and History of the Central lake Agassiz Basin: Geological Association of Canada/Mineralogical Association of Canada Annual Meeting, Winnipeg, Manitoba, field Trip Guidebook **B2**: 55-84

Thorne CR. 1981. Field measurements of rates of bank erosion and bank material strength.Erosion and Sediment Transport Measurement (Proceedings of the Florence Symposium, June 1981). IAHS Publication 133, International Association of HydrologicalSciences: Wallingford. 503–512.

Thorne CR, Tovey NK, 1981. Stability of composite banks. Earth Surface Processes and Landforms **6**: 469-484.

Trimble SW. 1999. Decreased rates of alluvium sediment storage in the Coon Creek Basin, Wisconsin, 1975-93. Science 285: 1244-1246. DOI:10.1126/science.285.5431.1244

Turnbull WJ, Krinitzsky EL, Weaver FJ, 1966. Bank erosion in soils of the lower Mississippi Valley. Proceedings of the American Society of Civil Engineers **92**: 121-136

Valentin C, Poesen J, Yong L. 2005. Gully erosion: Impacts, factors and control. Catena **63**: 132-153.

Van der Zande D, Hoet W, Jonckheere L, van Aardt J, Coppin P. 2006. Influence of measurement set-up of ground based Lidar for derivation of tree structure. Agricultural and Forest Meteorology **141**:147-160.

Van Klaveren RW, McCool DK, 2010. Free-thaw and water tension effects on soil detachment. Soil Society of America Journal **74**: 1327-1338.

Verstraeten G, Poesen J. 1999. The nature of small-scale flooding, muddy floods and retention pond sedimentation in central Belgium. Geomorphology **29**: 275-292.

Walter RC, Merritts DJ. 2008. Natural streams and the legacy of water-powered mills. Science 319: 299-304. DOI: 101126/science.1151716.

Walter C, Tullos DD, 2010.Downstream channel changes after a small dam removal; using aerial photos and measurement error for context; Calapooia River, Oregon. River Research and Applications **26**: 1220-1245

Water Resources Center (WRC), Minnesota State University, Mankato, and Minnesota Pollution Control Agency (MPCA). 2009. State of the Minnesota River: Summary of surface water quality monitoring 2000–2008: 42 p.

Wawrzyniec TF, McFadded LD, Ellwein A, Meyer G, Scuderi L, McAuliffe J, Fawcett P. 2007. Chronotopographic analysis directly from point-cloud data: A method for detecting small seasonal hillslope change in Black Mesa Escarpment, NE Arizona. Geosphere **3**: 550-567.

Whipple KX, Tucker GE. 1999. Dynamics of the stream-power river incision model: Implications for height limits of mountain ranges, landscape response timescales, and research needs. Journal of Geophysical Research **104**: 17661-17674.

Whipple KX, Hancock GS, Anderson RS. 2000. River incision into bedrock: Mechanics and relative efficacy of plucking, abrasion, and cavitation. GSA Bulletin **112**: 490-503.

Wilkinson BH, McElroy BJ. 2007. The impact of human on continental erosion and sedimentation. Geological Society of America Bulletin **119**: 140-156. DOI 10.1130/B25899.1

Williams RD, Brasington J, Vericat D, Hicks D, Labrosse F, Neal MN. 2011. Monitoring braided river change using terrestrial laser scanning and optical bathymetric mapping. In Smith M, Paron P, and Griffiths J. 2011. Geomorphological Mapping. Elsevier.

Wynn TM, Mostaghimi S, 2006. Effects of riparian vegetation on stream bank subaerial processes in southwestern Virginia, USA. Earth Surface Processes and Landforms **31**: 399-41

Appendix A: List of Variables

A	area
a	constant
b	constant
c	constant
cell	cell size
D_{50}	median grain size
dir	direction of change (+1 or -1)
$E_{E\text{-}volume}$	extrapolation error for the final volume calculation
$E_{G\text{-}single}$	georeferencing error at a single bluff
$E_{GT\text{-}volume}$	tracing and georefencing error for the final volume calculation
$E_{T\text{-}single}$	tracing error at a single bluff
f	constant
H	bluff height
h	channel depth
k	constant
L	bluff length
M	meander migration rate
m	constant
m_d	constant
m_t	constant
n_d	constant
n_t	constant
Q	discharge
q_s	volumetric sediment flux
R	rate of change
R	bluff retreat rate
S_k	knickpoint slope
T	time between scans
U	knickpoint retreat rate
$U_{tot\text{-}single}$	total uncertainty at a single bluff
$U_{tot\text{-}volume}$	uncertainty for complete volume calculation
V	total volume of change
V	volume of sediment removed
v	channel velocity
W	channel width
ρ	water density
ρ_s	sediment density
τ	shear stress
Δx	change in x direction
Δy	change in y direction

Δz	change in z direction
dz/dt	vertical erosion rate

Appendix B: Terrestrial Laser Scanning Results

Site	Scan 1 date	Scan 2 Date	days	years	Number of vectors	number of points	Volume Lost (m3)	Area (m2)	Retreat Rate (m/yr)	volume lost (m^3/yr)
H90LS	9/5/2008	5/7/2009	244	0.67	3	2500088	-36.2476	960.8892	-0.05647	-54.26
H90LS	5/7/2009	6/1/2010	390	1.07	3	4197265	1446.3	1338.6	1.01189	1354.516
H90LS	9/5/2008	6/1/2010	634	1.74	3	2178743	980.2803	846.0811	0.667482	564.7435
BOM2	8/17/2007	9/5/2008	385	1.05	3	4170177	41.7774	702.1824	0.056444	39.63427
BOM2	8/17/2007	5/20/2009	642	1.76	3	5196580	84.3593	734.3487	0.065356	47.99413
BOM2	9/5/2008	5/20/2009	257	0.70	3	5537289	47.3857	757.834	0.088865	67.34485
BOM2	8/17/2007	9/5/2008	385	1.05	3	3670132	66.2924	843.6259	0.074549	62.89169
BOM2	8/17/2007	5/20/2009	642	1.76	3	3608126	122.5682	836.1478	0.083397	69.73214
BOM2	9/5/2008	5/20/2009	257	0.70	3	4289999	53.7116	726.5383	0.105067	76.33526
BOM2	5/20/2009	6/2/2010	378	1.03	3	4926486	464.5507	600.4054	0.74763	448.8813
BOM2	9/5/2008	6/2/2010	635	1.74	3	4649531	465.9292	663.8435	0.403711	268.001
BOM2	8/17/2007	6/2/2010	1020	2.79	3	4824733	473.517	618.9038	0.27397	169.5609
JQLS	5/5/2008	5/16/2009	376	1.03	4	6255066	926.4767	9810.3	0.091739	899.9883
JQLS	8/7/2007	5/5/2008	272	0.74	4	2926349	2269.7	6996.8	0.435602	3047.823
JQLS	8/7/2007	6/6/2010	1034	2.83	4	2323363	3334.9	4769.7	0.24698	1178.02
JQLS	5/16/2009	6/7/2010	387	1.06	4	5294116	2707.2	5974.6	0.427652	2555.051
JQLS	5/5/2008	6/8/2010	764	2.09	4	9521629	1098.9	1033	0.508575	525.3576
H83LS	5/6/2008	5/11/2009	370	1.01	2	3715323	65.2963	613.0349	0.105146	64.45804
H83LS	5/6/2008	6/3/2010	758	2.08	2	5195507	488.4222	550.8547	0.427247	235.3512
H83LS	5/11/2009	6/3/2010	388	1.06	2	3409008	238.3704	569.8018	0.39381	224.3938
WWP	7/7/2007	5/14/2009	677	1.85	2	523084	7.2134	78.8282	0.04937	3.89172
WWP	7/7/2007	5/14/2009	677	1.85	2	449038	9.8111	80.592	0.065679	5.293212
WWP	4/30/2008	5/14/2009	379	1.04	3	189698	5.21	63.7811	0.078722	5.020983
WWP	7/7/2007	4/30/2008	298	0.82	2	70992	1.1425	29.4687	0.047519	1.400329
WWP2	7/10/2007	4/30/2008	295	0.81	2	738679	35.0025	186.1629	0.232795	43.33784
WWP2	7/10/2007	4/30/2008	295	0.81	2	745788	11.9881	117.1905	0.126656	14.84289

Site	Scan 1 date	Scan 2 Date	days	years	Number of vectors	number of points	Volume Lost (m3)	Area (m2)	Retreat Rate (m/yr)	volume lost (m^3/yr)
WWP3	9/4/2008	5/14/2009	252	0.69	2	1386115	0.6178	189.0351	0.004737	0.895442
WWP3	7/10/2007	5/14/2009	674	1.85	1	1554749	-59.5831	185.9711	-0.17362	-32.2889
WWP3	7/10/2007	9/4/2008	422	1.16	1	1255990	61.3216	179.6054	0.29551	53.07515
H16BC	8/1/2007	4/28/2008	271	0.74	3	546034	21.4864	106.1752	0.272748	28.95907
H16BC	8/1/2007	9/6/2008	402	1.10	3	572447	21.70202	103.7848	0.18999	19.71807
H16BC	4/28/2008	9/6/2008	131	0.36	3	666082	2.4281	165.6986	0.040857	6.769951
H16BC	4/28/2008	9/6/2008	131	0.36	3	611799	9.4498	202.5063	0.130108	26.34763
H16BC	9/6/2008	5/12/2009	248	0.68	3	809994	16.8005	150.8316	0.164047	24.74348
H16BC	4/28/2008	5/12/2009	379	1.04	3	850274	15.6696	218.9055	0.068985	15.10111
H16BC	8/1/2007	5/12/2009	650	1.78	3	620699	40.9204	119.3218	0.192707	22.99412
H16BC	4/28/2008	5/12/2009	379	1.04	3	999960	30.3853	206.681	0.141682	29.28293
H16BC	5/12/2009	5/22/2010	375	1.03	3	708612	83.5743	147.4988	0.551878	81.40137
H16BC	4/28/2008	5/23/2010	755	2.07	3	709072	84.5522	134.764	0.303525	40.90423
H16BC	9/6/2008	5/23/2010	624	1.71	3	558851	68.8215	107.5715	0.374483	40.28374
H16BC	8/1/2007	5/23/2010	1026	2.81	3	523635	60.4406	78.3217	0.27472	21.5165
BOM	5/1/2008	5/20/2009	384	1.05	1	829232	16.8206	207.3811	0.077149	15.99928
BOM	8/15/2007	5/20/2009	644	1.76	1	513584	21.4622	106.8607	0.11391	12.17247
BOM	5/1/2008	6/2/2010	762	2.09	1	937647	114.0397	165.9898	0.329314	54.66273
BOM	5/20/2009	6/2/2010	378	1.03	1	906331	100.5644	167.9392	0.578616	97.17235
H16BC2	8/2/2007	9/6/2008	401	1.10	4	124004	6.4829	39.6129	0.149066	5.904936
H16BC2	8/2/2007	5/12/2009	649	1.78	4	113053	6.2112	35.0052	0.099859	3.495594
H16BC2	9/6/2008	5/12/2009	248	0.68	4	1202007	14.0798	230.8467	0.089828	20.73648
H16BC2	5/12/2009	5/22/2010	375	1.03	4	1251667	83.7704	204.7055	0.398584	81.59237
H16BC2	9/6/2008	5/22/2010	623	1.71	4	953867	53.4825	142.2884	0.220366	31.35551
H16BC2	9/6/2008	5/12/2009	248	0.68	4	1720258	0.2318	189.4903	0.001802	0.341391
H16BC2	8/2/2007	5/22/2010	1024	2.80	4	64416	18.6857	25.7799	0.258534	6.664992
BOBC	8/14/2007	5/1/2008	261	0.71	1	1431217	216.9394	423.5555	0.716767	303.5905
BOBC	5/1/2008	5/13/2009	377	1.03	1	2471147	19.3292	450.0265	0.041613	18.72676

Site	Scan 1 date	Scan 2 Date	days	years	Number of vectors	number of points	Volume Lost (m3)	Area (m2)	Retreat Rate (m/yr)	volume lost (m^3/yr)
BOBC	5/1/2008	5/27/2010	756	2.07	2	9017784	169.1923	754.0843	0.1084	81.74271
BOBC	5/13/2009	5/27/2010	379	1.04	2	8816324	106.7335	709.8631	0.144903	102.8612
BOBC	8/14/2007	5/13/2009	638	1.75	1	1140336	82.9842	360.5983	0.131747	47.5078
BOBC	8/14/2007	5/27/2010	1017	2.78	2	1175217	124.6489	363.2831	0.123229	44.76697
H22LS	5/2/2008	5/11/2009	374	1.02	2	433351	-55.3215	341.9067	-0.15802	-54.0272
H22LS	9/7/2008	5/11/2009	246	0.67	2	706668	34.0767	353.8604	0.142982	50.59559
LSH8	7/6/2007	5/8/2009	672	1.84	3	4921656	182.186	1638.8	0.060424	99.02297
LSH8	5/4/2008	5/8/2009	369	1.01	3	6350899	60.4743	2541.6	0.023552	59.85972
LSH8	7/6/2007	5/4/2008	303	0.83	3	5664939	501.0302	2779.9	0.217261	603.9646
LSH8	7/6/2007	5/4/2008	303	0.83	2	5659257	496.2978	2774.1	0.215659	598.26
LSH8	7/6/2007	5/23/2010	1052	2.88	3	5041426	417.9575	1460.6	0.099352	145.1131
LSH8	5/4/2008	5/23/2010	749	2.05	3	6153380	304.7156	2213.4	0.067134	148.5946
LSH8	5/8/2009	5/23/2010	380	1.04	3	6555961	279.2546	2257.3	0.11891	268.4151
H16LS	8/3/2007	5/17/2009	653	1.79	4	2145126	189.8821	518.0013	0.205036	106.2089
H16LS	9/3/2008	5/17/2009	256	0.70	4	2093658	63.0321	624.6656	0.143967	89.93154
H16LS	5/17/2009	5/28/2010	376	1.03	4	3976826	170.9941	857.173	0.193783	166.1053
H16LS	8/3/2007	5/28/2010	1029	2.82	4	3430468	370.8329	576.1138	0.228478	131.6295
H16LC	8/2/2007	5/1/2008	273	0.75	2	1076132	16.041	300.7289	0.071365	21.46145
H16LC	5/1/2008	5/13/2009	377	1.03	2	1563823	3.1887	243.0096	0.012713	3.089317
H16LC	8/2/2007	5/13/2009	650	1.78	2	935994	18.2652	255.0888	0.040236	10.26364
H16LC	5/1/2008	5/13/2009	377	1.03	2	1217509	11.0892	207.1987	0.051852	10.74358
H16LC	8/2/2007	5/21/2010	1023	2.80	2	855494	28.7816	156.7314	0.065565	10.27613
H16LC	5/1/2008	5/21/2010	750	2.05	2	1155501	32.1866	239.5437	0.065436	15.67487
H16LC	5/13/2009	5/21/2010	373	1.02	2	1056563	24.4077	193.2008	0.123708	23.90057

Appendix C: Bluff data from aerial photographs

River	ID	Bank	Distance From Mouth	River Length along Bluff	Vegetated Length	Height	Average Aspect	Migration Rate (m/yr) negative #s indicate deposition	1938-2005 top area lost (m^2) Total	1938-2005 top area gained (m^2) Total	1938-2005 top area (m^2)	Traced rate (m/yr) Vegetated	Traced rate (m/yr) Un-Vegetated	Traced rate (m/yr)
Le Sueur	30	L	400	1030	890	69.39	105	0.48	NA	NA	NA	NA	NA	NA
Le Sueur	180	R	1880	210	140	34.10	224	0.00	NA	NA	NA	NA	NA	NA
Le Sueur	57	L	1930	50	50	4.28	42	-0.17	NA	NA	NA	NA	NA	NA
Le Sueur	59	L	1980	80	80	4.46	37	-0.17	NA	NA	NA	NA	NA	NA
Le Sueur	60	L	2060	40	0	3.57	38	-0.16	NA	NA	NA	NA	NA	NA
Le Sueur	181	R	2150	100	100	34.50	241	-0.21	NA	NA	NA	NA	NA	NA
Le Sueur	65	R	2320	130	60	4.76	298	-0.34	NA	NA	NA	NA	NA	NA
Le Sueur	66	L	2330	280	280	11.55	94	0.23	391	475	-84	0.00	0.00	0.00
Le Sueur	182	R	2820	300	300	23.38	173	0.20	543	176	366	0.02	NA	0.02
Le Sueur	69	R	3150	50	50	4.06	260	-0.33	NA	NA	NA	NA	NA	NA
Le Sueur	183	L	3470	260	260	38.70	85	0.25	2579	373	2206	0.13	NA	0.13
Le Sueur	184	R	3850	140	140	22.37	215	-0.04	1904	130	1774	0.19	NA	0.19
Le Sueur	83b	L	3850	30	30	3.32	55	0.08	NA	NA	NA	NA	NA	NA
Le Sueur	83	L	3930	100	60	2.54	55	0.11	896	0	896	0.05	0.27	0.13
Le Sueur	185	L	4210	250	110	26.93	81	0.28	NA	NA	NA	NA	NA	NA
Le Sueur	91	L	4470	30	30	4.37	47	0.13	NA	NA	NA	NA	NA	NA
Le Sueur	187	R	4620	110	110	39.33	213	-0.16	NA	NA	NA	NA	NA	NA
Le Sueur	186	R	4740	100	100	26.34	228	-0.31	NA	NA	NA	NA	NA	NA
Le Sueur	94	L	4860	380	250	18.34	77	0.34	NA	NA	NA	NA	NA	NA
Le Sueur	102	L	5300	30	30	4.61	340	0.86	NA	NA	NA	NA	NA	NA
Le Sueur	98	L	5440	60	60	4.45	324	-0.04	NA	NA	NA	NA	NA	NA
Le Sueur	107	L	6320	110	110	6.30	196	-0.10	1429	0	1429	0.19	NA	0.19
Le Sueur	109	L	6510	180	180	6.16	202	-0.05	2984	0	2984	0.25	NA	0.25
Le Sueur	108	L	6800	260	150	7.64	151	0.13	3246	335	2911	0.12	0.23	0.17
Le Sueur	115	L	7390	80	80	3.81	46	0.00	0	1246	-1246	0.00	0.00	0.00
Le Sueur	117	L	7480	80	80	3.50	66	0.00	0.00	0.00	0.00	NA	NA	0.00
Le Sueur	127	L	7590	20	20	4.93	55	0.33	NA	NA	NA	NA	NA	NA

River	ID	Bank	Distance From Mouth	River Length along Bluff	Vegetated Length	Height	Average Aspect	Migration Rate (m/yr) negative #s indicate deposition	1938-2005 top area lost (m^2) Total	1938-2005 top area gained (m^2) Total	1938-2005 top area (m^2)	Traced rate (m/yr) Vegetated	Traced rate (m/yr) Un-Vegetated	Traced rate (m/yr)
Le Sueur	129	L	7620	40	40	7.50	57	0.37	NA	NA	NA	NA	NA	NA
Le Sueur	188	L	7660	30	30	16.30	44	0.41	NA	NA	NA	NA	NA	NA
Le Sueur	133	L	7700	360	290	29.55	44	0.32	NA	NA	NA	NA	NA	NA
Le Sueur	138	L	8060	140	140	14.37	337	0.18	2260	0	2260	0.24	NA	0.24
Le Sueur	137	L	8200	130	130	9.94	333	0.58	2755	0	2755	0.32	NA	0.32
Le Sueur	224	R	8570	640	260	59.40	191	-0.05	7750	1868	5882	0.00	0.24	0.14
Le Sueur	135	L	9380	80	0	3.61	110	0.44	192	19	173	NA	0.03	0.03
Le Sueur	157	L	10670	40	40	1.97	150	0.04	5.96	17.44	-11.47	0.00	0.00	0.00
Le Sueur	152	L	10730	510	260	61.46	110	0.14	NA	NA	NA	NA	NA	NA
Le Sueur	164	L	11240	140	60	3.15	359	0.00	NA	NA	NA	NA	NA	NA
Le Sueur	161	R	11560	140	140	10.07	149	1.53	NA	NA	NA	NA	NA	NA
Le Sueur	162	R	12240	250	250	7.50	221	-0.18	318	1695	-1377	0.00	0.00	0.00
Le Sueur	166	L	12670	180	150	3.53	63	-0.01	4841	0	4841	0.43	0.25	0.40
Le Sueur	165	L	13010	80	0	3.01	332	0.31	3029	0	3029	NA	0.57	0.57
Le Sueur	190	L	13090	190	140	14.17	273	-0.03	1719	143	1576	0.20	0.00	0.12
Le Sueur	163	L	13290	50	0	3.59	220	0.14	193	0	193	NA	0.06	0.06
Le Sueur	154	R	13590	450	330	17.18	130	0.16	1692	1376	317	0.00	0.18	0.01
Le Sueur	189	R	14050	70	20	23.46	138	-0.20	NA	NA	NA	NA	NA	NA
Le Sueur	158	L	14220	80	0	5.80	38	0.49	1666	0	1666	NA	0.31	0.31
Le Sueur	145	R	14640	120	50	39.03	117	0.15	NA	NA	NA	NA	NA	NA
Le Sueur	191	L	15370	150	40	23.78	336	0.16	9630	0	9630	0.68	1.06	0.96
Le Sueur	141	R	15660	270	270	21.26	141	-0.13	NA	NA	NA	NA	NA	NA
Le Sueur	227	L	16090	120	120	3.10	318	0.27	2578	0	2578	0.32	NA	0.32
Le Sueur	139	R	16200	70	70	5.90	117	-0.44	NA	NA	NA	NA	NA	NA
Le Sueur	192	R	16290	140	0	11.74	92	-0.21	NA	NA	NA	NA	NA	NA
Le Sueur	126	R	16480	30	0	5.90	120	-0.18	NA	NA	NA	NA	NA	NA
Le Sueur	125	R	16520	20	20	5.16	156	-0.12	NA	NA	NA	NA	NA	NA
Le Sueur	119	R	16540	80	0	4.13	147	0.01	405	0	405	NA	0.08	0.08

River	ID	Bank	Distance From Mouth	River Length along Bluff	Vegetated Length	Height	Average Aspect	Migration Rate (m/yr) negative #s indicate deposition	1938-2005 top area lost (m^2) Total	1938-2005 top area gained (m^2) Total	1938-2005 top area (m^2)	Traced rate (m/yr) Vegetated	Traced rate (m/yr) Un-Vegetated	Traced rate (m/yr)
Le Sueur	118b	R	17100	90	90	9.05	154	0.03	NA	NA	NA	NA	NA	NA
Le Sueur	118	R	17190	110	0	6.06	154	0.06	245	57	188	NA	0.03	0.03
Le Sueur	120	R	17340	40	0	3.34	214	-0.09	572	0	572	NA	0.21	0.21
Le Sueur	123	R	17380	10	0	4.06	226	-0.01	NA	NA	NA	NA	NA	NA
Le Sueur	194	L	17790	150	150	8.28	44	0.17	25	364	-339	0.00	0.00	0.00
Le Sueur	193	R	18150	520	360	51.40	199	0.10	NA	NA	NA	NA	NA	NA
Le Sueur	195	L	18790	400	400	41.34	44	0.28	4395	1262	3132	0.12	NA	0.12
Le Sueur	144	L	19190	40	40	6.56	243	-0.47	NA	NA	NA	NA	NA	NA
Le Sueur	225	R	19710	60	60	9.65	108	0.11	NA	NA	NA	NA	NA	NA
Le Sueur	121	R	19790	200	200	11.97	183	-0.12	344	478	-134	0.00	0.00	0.00
Le Sueur	134	L	20100	180	0	3.91	51	0.29	892	0	892	NA	0.07	0.07
Le Sueur	140	L	20330	90	0	2.86	22	0.42	455	0	455	NA	0.08	0.08
Le Sueur	131	L	20660	50	10	5.05	249	0.76	NA	NA	NA	NA	NA	NA
Le Sueur	114	R	20870	150	0	11.29	97	0.21	NA	NA	NA	NA	NA	NA
Le Sueur	122	L	21330	120	0	3.94	25	0.38	1626	0	1626	NA	0.20	0.20
Le Sueur	122b	L	21450	30	30	9.62	44	0.27	NA	NA	NA	NA	NA	NA
Le Sueur	112	R	22040	270	0	9.98	202	0.09	2304	293	2012	NA	0.11	0.11
Le Sueur	89	R	22370	770	320	28.95	125	0.05	3282	2656	625	0.00	0.04	0.01
Le Sueur	106	L	23590	270	30	12.54	315	0.19	6593	0	6593	0.36	0.36	0.36
Le Sueur	196	R	24470	110	70	15.07	164	-0.15	NA	NA	NA	NA	NA	NA
Le Sueur	95	L	24630	100	0	2.68	324	0.21	1735	0	1735	NA	0.26	0.26
Le Sueur	90	L	24870	230	0	6.13	305	0.12	4084	0	4084	NA	0.27	0.27
Le Sueur	88	R	25060	70	0	4.13	115	-0.93	NA	NA	NA	NA	NA	NA
Le Sueur	86	L	25190	70	0	2.55	291	0.10	1186	0	1186	NA	0.25	0.25
Le Sueur	84b	L	25270	100	0	15.29	230	-0.10	NA	NA	NA	NA	NA	NA
Le Sueur	84	L	25370	190	190	6.41	230	-0.02	67	580	-513	0.00	0.00	0.00
Le Sueur	85	R	25630	80	0	1.98	39	0.58	2707	0	2707	NA	0.51	0.51
Le Sueur	79	L	25860	120	90	7.60	109	0.15	NA	NA	NA	NA	NA	NA

River	ID	Bank	Distance From Mouth	River Length along Bluff	Vegetated Length	Height	Average Aspect	Migration Rate (m/yr) negative #s indicate deposition	1938-2005 top area lost (m^2) Total	1938-2005 top area gained (m^2) Total	1938-2005 top area (m^2)	Traced rate (m/yr) Vegetated	Traced rate (m/yr) Un-Vegetated	Traced rate (m/yr)
Le Sueur	197	L	26110	150	0	9.11	316	0.34	1007	146	861	NA	0.09	0.09
Le Sueur	198	L	26320	230	90	28.74	250	0.00	1460	742	718	0.02	0.07	0.05
Le Sueur	70	R	26720	40	0	2.41	71	0.37	NA	NA	NA	NA	NA	NA
Le Sueur	63	L	27080	100	0	3.01	300	0.15	850	0	850	NA	0.13	0.13
Le Sueur	61	R	27190	20	20	4.13	277	-0.09	NA	NA	NA	NA	NA	NA
Le Sueur	199	L	27210	100	100	18.11	247	-0.12	NA	NA	NA	NA	NA	NA
Le Sueur	52	R	27550	80	80	5.62	113	-0.14	NA	NA	NA	NA	NA	NA
Le Sueur	51	R	27740	50	0	3.20	124	-0.05	NA	NA	NA	NA	NA	NA
Le Sueur	48	L	27780	140	0	2.44	301	-0.02	373	0	373	NA	0.04	0.04
Le Sueur	44	L	27990	40	10	6.30	247	-0.05	NA	NA	NA	NA	NA	NA
Le Sueur	31b	R	28100	110	0	14.74	44	-0.15	NA	NA	NA	NA	NA	NA
Le Sueur	31	R	28210	290	0	7.61	44	0.26	3165	0	3165	NA	0.16	0.16
Le Sueur	200	R	28500	60	0	13.49	170	0.30	NA	NA	NA	NA	NA	NA
Le Sueur	32	R	28560	80	0	4.71	201	0.20	560	0	560	NA	0.10	0.10
Le Sueur	38	L	28890	40	40	3.95	33	0.28	NA	NA	NA	NA	NA	NA
Le Sueur	27	R	29360	300	250	9.74	127	0.02	NA	NA	NA	NA	NA	NA
Le Sueur	24	R	29700	290	70	6.20	209	0.15	4735	62	4673	0.03	0.31	0.24
Le Sueur	34	L	30210	40	0	3.15	75	0.09	345	0	345	NA	0.13	0.13
Le Sueur	201	R	30370	150	30	20.54	270	0.06	NA	NA	NA	NA	NA	NA
Le Sueur	42	L	30580	320	230	33.91	44	0.01	NA	NA	NA	NA	NA	NA
Le Sueur	47	L	30580	290	290	14.71	51	0.10	NA	NA	NA	NA	NA	NA
Le Sueur	39	R	31110	450	450	9.78	166	-0.04	1358	1473	-115	0.00	0.00	0.00
Le Sueur	49b	L	31950	210	110	9.62	315	0.14	NA	NA	NA	NA	NA	NA
Le Sueur	49	L	32170	110	30	5.73	315	0.10	2771	0	2771	0.19	0.45	0.38
Le Sueur	35	R	32500	280	110	31.79	104	-0.03	1357	266	1091	0.01	0.09	0.06
Le Sueur	202	L	32770	180	30	6.15	15	0.08	1864	24	1840	0.00	0.18	0.15
Le Sueur	37	R	32980	110	110	8.41	182	0.03	NA	NA	NA	NA	NA	NA
Le Sueur	40	L	33150	160	60	26.66	31	0.18	2339	53	2286	0.20	0.22	0.21

River	ID	Bank	Distance From Mouth	River Length along Bluff	Vegetated Length	Height	Average Aspect	Migration Rate (m/yr) negative #s indicate deposition	1938-2005 top area lost (m^2) Total	1938-2005 top area gained (m^2) Total	1938-2005 top area (m^2)	Traced rate (m/yr) Vegetated	Traced rate (m/yr) Un-Vegetated	Traced rate (m/yr)
Le Sueur	226	L	33750	20	0	1.90	336	0.08	290	0	290	NA	0.22	0.22
Le Sueur	203	R	33920	90	90	15.62	159	0.12	NA	NA	NA	NA	NA	NA
Le Sueur	28	R	34530	30	0	4.11	139	0.23	391	0	391	NA	0.19	0.19
Le Sueur	205	L	35070	160	160	27.78	74	0.13	NA	NA	NA	NA	NA	NA
Le Sueur	204	R	35310	40	40	5.87	150	-0.02	NA	NA	NA	NA	NA	NA
Le Sueur	206	L	35390	130	130	21.79	44	0.08	NA	NA	NA	NA	NA	NA
Le Sueur	45	L	35510	90	90	16.78	327	0.01	186	215	-29	0.00	0.00	0.00
Le Sueur	207	R	36250	80	80	19.77	171	0.23	NA	NA	NA	NA	NA	NA
Le Sueur	208	L	36490	80	0	10.69	21	-0.04	572	0	572	NA	0.11	0.11
Le Sueur	25	R	36670	70	70	6.89	158	0.32	596	0	596	0.13	NA	0.13
Le Sueur	209	L	36900	70	0	6.34	340	0.05	749	40	709	NA	0.15	0.15
Le Sueur	22	R	37070	60	60	11.14	150	0.48	NA	NA	NA	NA	NA	NA
Le Sueur	21	R	37180	90	90	10.37	175	0.18	77	214	-137	0.00	0.00	0.00
Le Sueur	210	L	37380	70	0	14.41	37	0.19	1342	0	1342	NA	0.29	0.29
Le Sueur	12	L	37990	330	60	20.02	283	-0.17	NA	NA	NA	NA	NA	NA
Le Sueur	10	R	38320	270	130	21.04	44	0.23	NA	NA	NA	NA	NA	NA
Le Sueur	211	R	39440	60	0	5.58	94	0.18	334	0	334	NA	0.08	0.08
Le Sueur	3	R	39510	160	120	16.75	167	-0.06	NA	NA	NA	NA	NA	NA
Le Sueur	11	L	39610	170	40	6.73	326	-0.03	525	42	483	0.01	0.05	0.04
Le Sueur	5	L	39800	70	20	7.30	284	-0.10	NA	NA	NA	NA	NA	NA
Le Sueur	0	R	39950	260	200	9.78	118	0.14	1547	213	1334	0.08	0.06	0.08
Le Sueur	2	L	40330	250	250	9.03	44	0.11	NA	NA	NA	NA	NA	NA
Le Sueur	1	R	40740	140	0	6.84	158	0.07	1098	0	1098	NA	0.12	0.12
Le Sueur	4	R	41020	40	0	4.08	242	0.26	1017	0	1017	NA	0.38	0.38
Le Sueur	6	R	41090	50	50	5.20	285	-0.14	NA	NA	NA	NA	NA	NA
Le Sueur	8b	L	41140	270	260	19.61	44	-0.13	NA	NA	NA	NA	NA	NA
Le Sueur	8	L	41410	190	60	13.78	44	0.06	1481	197	1284	0.01	0.14	0.10
Le Sueur	9	R	41780	100	60	5.44	105	0.15	NA	NA	NA	NA	NA	NA

River	ID	Bank	Distance From Mouth	River Length along Bluff	Vegetated Length	Height	Average Aspect	Migration Rate (m/yr) negative #s indicate deposition	1938-2005 top area lost (m^2) Total	1938-2005 top area gained (m^2) Total	1938-2005 top area (m^2)	Traced rate (m/yr) Vegetated	Traced rate (m/yr) Un-Vegetated	Traced rate (m/yr)
Le Sueur	7	R	41880	120	110	3.91	180	0.18	2258	0	2258	0.06	2.75	0.28
Le Sueur	13	R	42350	40	0	3.65	259	0.03	444	0	444	NA	0.17	0.17
Le Sueur	212	L	42440	110	50	11.22	60	-0.05	1055	0	1055	0.22	0.08	0.14
Le Sueur	14	R	42620	110	0	5.79	201	0.05	1831	0	1831	NA	0.25	0.25
Le Sueur	15	L	42820	110	110	9.64	110	0.08	NA	NA	NA	NA	NA	NA
Le Sueur	18	L	42950	70	0	4.82	48	0.08	438	38	400	NA	0.09	0.09
Le Sueur	17	R	43080	30	30	3.94	147	0.09	NA	NA	NA	NA	NA	NA
Le Sueur	16	R	43300	50	0	2.85	240	0.24	1664	0	1664	NA	0.50	0.50
Le Sueur	19	R	43400	30	30	4.90	331	0.01	NA	NA	NA	NA	NA	NA
Le Sueur	20	L	43510	50	50	4.42	132	0.08	NA	NA	NA	NA	NA	NA
Le Sueur	26	R	43590	30	30	3.39	318	-0.01	NA	NA	NA	NA	NA	NA
Le Sueur	23	L	43620	120	100	7.79	142	0.02	NA	NA	NA	NA	NA	NA
Le Sueur	29	R	43780	90	90	5.95	257	0.07	NA	NA	NA	NA	NA	NA
Le Sueur	36	L	44020	70	30	5.62	26	0.01	NA	NA	NA	NA	NA	NA
Le Sueur	33b	R	44140	140	110	8.57	248	-0.04	NA	NA	NA	NA	NA	NA
Le Sueur	33	R	44220	160	0	6.57	246	-0.02	875	34	841	NA	0.08	0.08
Le Sueur	41	L	44450	60	60	5.04	147	0.03	NA	NA	NA	NA	NA	NA
Le Sueur	43	L	44530	90	50	7.56	142	-0.01	NA	NA	NA	NA	NA	NA
Le Sueur	46	R	44670	60	60	6.47	258	0.01	NA	NA	NA	NA	NA	NA
Le Sueur	50	L	44830	170	40	7.87	126	0.01	NA	NA	NA	NA	NA	NA
Le Sueur	53	R	45210	110	110	5.47	240	0.15	NA	NA	NA	NA	NA	NA
Le Sueur	54	R	45340	70	40	4.77	207	-0.05	NA	NA	NA	NA	NA	NA
Le Sueur	58	L	45480	100	0	5.34	324	-0.05	502	13	490	NA	0.07	0.07
Le Sueur	55	L	45630	120	0	6.07	217	-0.03	543	0	543	NA	0.07	0.07
Le Sueur	214	L	45760	70	70	9.26	136	-0.25	426	2629	-2203	0.00	0.00	0.00
Le Sueur	213	R	45970	230	80	9.18	283	0.00	3358	480	2878	0.49	0.02	0.19
Le Sueur	64	L	46230	70	70	5.16	147	0.13	NA	NA	NA	NA	NA	NA
Le Sueur	68	L	46560	50	0	3.00	338	0.23	1857	0	1857	NA	0.55	0.55

River	ID	Bank	Distance From Mouth	River Length along Bluff	Vegetated Length	Height	Average Aspect	Migration Rate (m/yr) negative #s indicate deposition	1938-2005 top area lost (m^2) Total	1938-2005 top area gained (m^2) Total	1938-2005 top area (m^2)	Traced rate (m/yr) Vegetated	Traced rate (m/yr) Un-Vegetated	Traced rate (m/yr)
Le Sueur	62	R	46720	100	10	14.33	200	-0.10	224	0	224	0.10	0.03	0.03
Le Sueur	67	R	46860	230	230	15.21	253	-0.01	NA	NA	NA	NA	NA	NA
Le Sueur	72b	R	47090	30	30	7.76	309	0.07	NA	NA	NA	NA	NA	NA
Le Sueur	72	R	47120	50	0	5.55	309	0.00	371	0	371	NA	0.11	0.11
Le Sueur	71	L	47240	170	170	6.96	148	-0.11	376	1189	-813	0.00	0.00	0.00
Le Sueur	74b	R	47550	80	80	16.11	250	0.09	NA	NA	NA	NA	NA	NA
Le Sueur	74	R	47590	50	0	6.79	250	0.18	707	6	700	NA	0.21	0.21
Le Sueur	77	R	47850	250	250	17.29	296	-0.08	NA	NA	NA	NA	NA	NA
Le Sueur	82	R	48130	80	0	6.17	32	0.15	1214	0	1214	NA	0.23	0.23
Le Sueur	82b	R	48210	30	10	11.13	44	0.15	NA	NA	NA	NA	NA	NA
Le Sueur	78	L	48460	50	50	3.88	244	-0.08	NA	NA	NA	NA	NA	NA
Le Sueur	76	L	48560	30	0	3.94	231	0.10	NA	NA	NA	NA	NA	NA
Le Sueur	73	L	48620	140	140	9.44	185	0.09	300	97	203	0.02	NA	0.02
Le Sueur	75	L	49090	260	260	19.52	147	0.06	NA	NA	NA	NA	NA	NA
Le Sueur	80	R	49370	50	0	3.85	223	0.29	NA	NA	NA	NA	NA	NA
Le Sueur	81	R	49420	20	20	5.21	256	0.07	NA	NA	NA	NA	NA	NA
Le Sueur	92	L	50230	70	70	10.29	92	0.28	63	167	-104	0.00	0.00	0.00
Le Sueur	93b	R	50640	140	110	12.35	224	0.04	NA	NA	NA	NA	NA	NA
Le Sueur	93	R	50710	290	290	9.76	231	0.02	4235	0	4235	0.22	NA	0.22
Le Sueur	97	R	51070	30	30	4.28	315	0.04	NA	NA	NA	NA	NA	NA
Le Sueur	96	L	51140	70	40	3.93	134	0.11	907	0	907	0.17	0.22	0.19
Le Sueur	96b	L	51210	20	20	4.12	134	-0.04	NA	NA	NA	NA	NA	NA
Le Sueur	100	R	51310	30	0	3.69	328	0.03	NA	NA	NA	NA	NA	NA
Le Sueur	99	L	51410	230	110	5.11	67	0.08	1570	320	1250	-0.04	0.19	0.08
Le Sueur	101	R	51780	140	0	4.58	173	0.14	2808	0	2808	NA	0.30	0.30
Le Sueur	103	R	51930	40	40	4.08	266	-0.08	NA	NA	NA	NA	NA	NA
Le Sueur	104	R	51970	30	30	3.66	277	-0.18	NA	NA	NA	NA	NA	NA
Le Sueur	105	L	52010	30	0	4.38	114	0.13	NA	NA	NA	NA	NA	NA

River	ID	Bank	Distance From Mouth	River Length along Bluff	Vegetated Length	Height	Average Aspect	Migration Rate (m/yr) negative #s indicate deposition	1938-2005 top area lost (m^2) Total	1938-2005 top area gained (m^2) Total	1938-2005 top area (m^2)	Traced rate (m/yr) Vegetated	Traced rate (m/yr) Un-Vegetated	Traced rate (m/yr)
Le Sueur	111	L	52170	40	40	4.97	33	0.00	NA	NA	NA	NA	NA	NA
Le Sueur	110	R	52330	40	10	4.94	210	0.58	NA	NA	NA	NA	NA	NA
Le Sueur	113	R	52590	70	70	5.40	294	-0.09	NA	NA	NA	NA	NA	NA
Le Sueur	215b	R	52830	40	40	10.30	288	-0.05	NA	NA	NA	NA	NA	NA
Le Sueur	215	R	52860	60	30	3.87	288	-0.08	677	0	677	0.14	0.19	0.17
Le Sueur	116	R	53290	120	70	14.45	155	0.05	NA	NA	NA	NA	NA	NA
Le Sueur	124	R	53670	140	60	8.18	205	0.01	2950	0	2950	0.21	0.39	0.31
Le Sueur	128 S	R	53670	90	0	8.01	222	-0.03	954	0	954	NA	0.16	0.16
Le Sueur	128 N	R	53920	100	100	8.01	318	-0.09	471	687	-216	0.00	0.00	0.00
Le Sueur	142	R	54250	30	30	4.80	239	-0.23	NA	NA	NA	NA	NA	NA
Le Sueur	143	R	54400	130	130	5.30	230	-0.05	NA	NA	NA	NA	NA	NA
Le Sueur	150	L	54610	50	50	1.92	58	0.00	0	257	-257	0.00	0.00	0.00
Le Sueur	151	L	54720	70	70	5.07	68	-0.01	NA	NA	NA	NA	NA	NA
Le Sueur	156	L	54870	50	0	4.96	59	-0.14	NA	NA	NA	NA	NA	NA
Le Sueur	153	L	56150	60	0	2.93	53	-0.26	36	499	-464	NA	0.01	0.00
Le Sueur	159	L	56150	110	110	9.40	321	-0.17	58	12	46	0.00	0.00	0.01
Le Sueur	216	R	56540	120	70	7.48	53	0.00	NA	NA	NA	NA	NA	NA
Le Sueur	155	L	56850	40	40	2.33	14	0.00	0	128	-128	0.00	0.00	0.00
Le Sueur	217	R	57010	240	240	9.07	219	0.22	NA	NA	NA	NA	NA	NA
Le Sueur	218	R	59610	100	50	18.00	141	0.10	690	16	674	0.14	0.06	0.10
Le Sueur	218b	R	59700	60	60	16.15	169	0.11	NA	NA	NA	NA	NA	NA
Le Sueur	219	R	59910	110	0	16.41	196	0.14	NA	NA	NA	NA	NA	NA
Le Sueur	167	L	61750	160	160	8.88	56	-0.02	NA	NA	NA	NA	NA	NA
Le Sueur	168	L	61910	30	0	8.08	315	-0.03	NA	NA	NA	NA	NA	NA
Le Sueur	169	L	61940	50	30	9.79	315	-0.04	NA	NA	NA	NA	NA	NA
Le Sueur	170	L	62230	140	100	13.46	65	0.16	NA	NA	NA	NA	NA	NA
Le Sueur	220	R	63030	60	60	11.99	192	0.35	NA	NA	NA	NA	NA	NA
Le Sueur	171	L	63660	370	360	11.65	42	-0.01	NA	NA	NA	NA	NA	NA

River	ID	Bank	Distance From Mouth	River Length along Bluff	Vegetated Length	Height	Average Aspect	Migration Rate (m/yr) negative #s indicate deposition	1938-2005 top area lost (m^2) Total	1938-2005 top area gained (m^2) Total	1938-2005 top area (m^2)	Traced rate (m/yr) Vegetated	Traced rate (m/yr) Un-Vegetated	Traced rate (m/yr)
Le Sueur	172	R	64340	340	50	15.79	202	0.19	NA	NA	NA	NA	NA	NA
Le Sueur	221	L	64960	50	30	15.39	116	0.28	NA	NA	NA	NA	NA	NA
Le Sueur	174	L	65720	240	180	15.61	44	0.11	NA	NA	NA	NA	NA	NA
Le Sueur	222	R	66150	90	30	10.37	177	0.10	1590	0	1590	0.32	0.24	0.26
Le Sueur	223	L	66520	90	50	11.71	44	0.13	NA	NA	NA	NA	NA	NA
Le Sueur	173b	R	66740	70	70	14.77	200	0.20	NA	NA	NA	NA	NA	NA
Le Sueur	173	R	66810	80	0	12.71	199	0.15	284	206	79	NA	0.01	0.01
Le Sueur	175	L	67270	160	50	10.38	166	-0.02	NA	NA	NA	NA	NA	NA
Le Sueur	176	R	67990	120	120	9.84	231	-0.03	399	247	151	0.02	NA	0.02
Le Sueur	177	R	69520	40	40	9.07	216	0.00	NA	NA	NA	NA	NA	NA
Le Sueur	178	L	69820	230	230	15.45	54	0.11	NA	NA	NA	NA	NA	NA
Le Sueur	179	L	70050	190	120	16.02	54	0.01	NA	NA	NA	NA	NA	NA
Maple	0	L	346	430	NA	7.048	150.988	0.14	123	2629	-2507	0.00	NA	0.00
Maple	1	R	406	250	250	12.8	310.047	-0.19	NA	NA	NA	NA	NA	NA
Maple	2	R	916	300	300	12.928	274.811	-0.18	NA	NA	NA	NA	NA	NA
Maple	3	L	1046	230	230	17.475	247.474	-0.06	NA	NA	NA	NA	NA	NA
Maple	4	L	1046	230	NA	9.986	103.402	0.15	0	642	-642	0.00	NA	0.00
Maple	5	R	1316	310	310	14.47	88.223	-0.01	NA	NA	NA	NA	NA	NA
Maple	6	L	1656	660	450	35.986	82.000	-0.08	10556	1506	9050	0.33	0.00	0.20
Maple	7	R	2846	490	120	45.477	226.526	-0.03	11160	1737	9423	0.00	0.45	0.29
Maple	8	R	3776	130	100	13.687	290.773	-0.01	942	187	755	0.05	0.20	0.09
Maple	9	R	3926	110	110	14.646	268.908	-0.13	NA	NA	NA	NA	NA	NA
Maple	10	L	4586	630	630	18.353	134.599	-0.36	9023	2212	6811	0.16	NA	0.16
Maple	12	L	5496	60	NA	7.245	56.371	-0.13	34	134	-100	0.00	NA	0.00
Maple	13	R	5586	240	240	11.084	233.084	0.06	NA	NA	NA	NA	NA	NA
Maple	14	R	5826	470	260	35.453	297.109	-0.07	NA	NA	NA	NA	NA	NA
Maple	15	L	6396	130	130	7.782	170.322	0.14	NA	NA	NA	NA	NA	NA
Maple	16	L	6526	340	NA	10.107	83.455	0.09	93	224	-131	NA	NA	0.00

River	ID	Bank	Distance From Mouth	River Length along Bluff	Vegetated Length	Height	Average Aspect	Migration Rate (m/yr) negative #s indicate deposition	1938-2005 top area lost (m^2) Total	1938-2005 top area gained (m^2) Total	1938-2005 top area (m^2)	Traced rate (m/yr) Vegetated	Traced rate (m/yr) Un-Vegetated	Traced rate (m/yr)
Maple	17	L	7096	310	190	7.091	315.000	-0.21	3604	47	3557	0.12	0.25	0.17
Maple	18	R	7386	460	NA	31.544	252.127	0.03	502	1996	-1493	0.00	0.00	0.00
Maple	19	L	7916	150	NA	5.452	114.385	0.36	40	305	-265	0.00	NA	0.00
Maple	20	L	8536	120	70	10.45	179.964	0.46	839	133	707	0.14	0.02	0.09
Maple	21	R	8986	310	0	19.821	252.704	0.01	1112	738	374	NA	0.02	0.02
Maple	22	R	9296	100	0	7.296	332.670	0.01	NA	NA	NA	NA	NA	NA
Maple	23	L	9536	70	NA	5.568	212.507	0.38	0	331	-331	0.00	NA	0.00
Maple	24	L	9726	190	NA	29.863	110.365	0.15	388	640	-252	NA	0.00	0.00
Maple	25	R	10206	40	0	9.388	263.273	0.16	840	0	840	NA	0.31	0.31
Maple	26	R	10246	40	0	6.812	242.200	0.44	NA	NA	NA	NA	NA	NA
Maple	27	R	10856	140	10	13.187	201.127	0.19	2390	0	2390	0.27	0.25	0.25
Maple	28	L	11386	50	50	5.94	138.485	-0.21	NA	NA	NA	NA	NA	NA
Maple	29	R	11686	80	NA	5.885	44.000	0.48	4	206	-202	NA	0.00	0.00
Maple	30	L	11996	180	100	12.9	121.100	-0.08	1736	678	1058	0.24	0.00	0.09
Maple	31	R	12836	490	50	32.914	315.000	-0.04	3069	621	2447	0.00	0.10	0.07
Maple	32	R	14076	70	0	6.947	270.759	-0.15	NA	NA	NA	NA	NA	NA
Maple	33	R	14576	380	0	29.289	242.340	0.02	9643	43	9600	NA	0.38	0.38
Maple	34	R	15346	60	60	11.421	282.336	0.53	NA	NA	NA	NA	NA	NA
Maple	35	R	15796	110	40	12.53	294.310	0.09	4498	0	4498	0.67	0.57	0.61
Maple	36	L	16386	90	90	14.864	144.075	-0.11	NA	NA	NA	NA	NA	NA
Maple	37	L	16716	50	10	20.609	146.552	-0.01	915	0	915	0.29	0.27	0.27
Maple	38	L	17726	360	NA	21.8	104.496	0.14	26	2144	-2118	NA	0.00	0.00
Maple	39	R	18306	170	20	12.12	197.953	0.26	2622	0	2622	0.24	0.23	0.23
Maple	40	R	18706	280	0	19.14	217.566	0.14	4579	1835	2744	NA	0.15	0.15
Maple	41	L	19136	60	0	3.564	144.899	0.29	100	24	76	NA	0.02	0.02
Maple	42	L	19466	80	0	6.906	46.574	0.24	1965	0	1965	NA	0.37	0.37
Maple	43	L	19836	230	0	6.405	85.924	0.05	900	0	900	NA	0.06	0.06
Maple	120	R	20216	150	30	3.908	216.365	0.08	2552	0	2552	0.58	0.17	0.25

River	ID	Bank	Distance From Mouth	River Length along Bluff	Vegetated Length	Height	Average Aspect	Migration Rate (m/yr) negative #s indicate deposition	1938-2005 top area lost (m^2) Total	1938-2005 top area gained (m^2) Total	1938-2005 top area (m^2)	Traced rate (m/yr) Vegetated	Traced rate (m/yr) Un-Vegetated	Traced rate (m/yr)
Maple	121	R	20426	120	20	19.03	309.240	-0.16	3447	0	3447	0.54	0.41	0.43
Maple	44	L	21596	300	130	17.509	187.478	0.00	3136	1657	1478	0.00	0.26	0.07
Maple	45	R	22396	60	60	8.871	289.937	-0.24	NA	NA	NA	NA	NA	NA
Maple	46	R	22456	90	0	6.923	306.878	-0.11	504	156	348	NA	0.06	0.06
Maple	47	R	23126	280	0	10.149	241.488	-0.13	10836	0	10836	NA	0.58	0.58
Maple	48	R	25356	140	0	12.547	288.079	0.09	1942	0	1942	NA	0.21	0.21
Maple	49	R	25766	170	170	16.764	27.645	0.10	328	57	271	0.02	NA	0.02
Maple	50	L	26396	80	0	13.044	181.297	0.03	NA	NA	NA	NA	NA	NA
Maple	51	L	27016	100	NA	5.682	146.877	0.01	18	835	-817	0.00	NA	0.00
Maple	52	L	27726	90	NA	15.702	118.061	-0.03	0	483	-483	0.00	NA	0.00
Maple	53	R	28296	280	0	10.014	216.030	-0.07	2727	0	2727	NA	0.15	0.15
Maple	54	R	28796	100	0	12.75	281.205	-0.04	2123	29	2094	NA	0.31	0.31
Maple	55	L	29416	80	80	13.81	97.660	0.40	NA	NA	NA	NA	NA	NA
Maple	56	R	30466	100	100	11.375	151.133	-0.05	573	58	514	0.08	NA	0.08
Maple	57	R	30886	120	120	18.943	223.153	0.26	1859	0	1859	0.23	NA	0.23
Maple	58	R	31606	180	180	11.741	252.836	-0.03	426	0	426	0.04	NA	0.04
Maple	59	R	31866	230	230	12.806	312.683	-0.06	3019	690	2328	0.15	NA	0.15
Maple	60	L	32236	260	260	10.328	148.889	-0.02	1372	0	1372	0.08	NA	0.08
Maple	61	L	32526	110	110	12.665	120.509	0.07	NA	NA	NA	NA	NA	NA
Maple	62	L	32726	300	300	15.718	101.040	-0.06	3056	15	3041	0.15	NA	0.15
Maple	63	L	33076	140	140	16.66	315.000	-0.26	1149	0	1149	0.12	NA	0.12
Maple	64	L	33496	110	30	7.993	44.000	-0.18	1097	0	1097	0.09	0.17	0.15
Maple	65	R	34056	60	30	11.23	227.928	-0.16	1108	0	1108	0.31	0.24	0.28
Maple	66	R	34396	200	200	16.628	220.390	0.08	NA	NA	NA	NA	NA	NA
Maple	67	L	35446	240	0	12.646	157.961	0.10	NA	NA	NA	NA	NA	NA
Maple	68	L	35686	160	100	15.921	102.307	0.06	720	203	517	0.10	0.00	0.05
Maple	69	L	35846	90	30	14.053	80.720	-0.08	NA	NA	NA	NA	NA	NA
Maple	70	R	37026	280	NA	14.202	282.430	-0.08	166	763	-597	0.00	NA	0.00

River	ID	Bank	Distance From Mouth	River Length along Bluff	Vegetated Length	Height	Average Aspect	Migration Rate (m/yr) negative #s indicate deposition	1938-2005 top area lost (m^2) Total	1938-2005 top area gained (m^2) Total	1938-2005 top area (m^2)	Traced rate (m/yr) Vegetated	Traced rate (m/yr) Un-Vegetated	Traced rate (m/yr)
Maple	71	L	37496	480	NA	12.214	132.583	-0.01	899	1530	-632	0.00	NA	0.00
Maple	72	L	37986	50	50	12.224	42.362	-0.29	NA	NA	NA	NA	NA	NA
Maple	73	R	38846	50	0	6.469	166.898	-0.02	311	90	221	NA	0.07	0.07
Maple	74	R	39596	70	NA	10.609	297.336	-0.44	14	94	-80	0.00	NA	0.00
Maple	75	R	39626	110	110	10.594	315.000	-0.29	NA	NA	NA	NA	NA	NA
Maple	76	L	39976	40	40	8.549	155.557	0.01	NA	NA	NA	NA	NA	NA
Maple	77	L	40016	190	NA	10.566	138.275	-0.01	195	661	-465	0.00	NA	0.00
Maple	78	L	40486	210	NA	11.462	58.210	-0.32	840	1815	-974	NA	0.00	0.00
Maple	79	R	40846	270	270	9.605	205.865	0.01	749	268	482	0.03	NA	0.03
Maple	80	R	41516	60	60	12.965	238.975	-0.02	NA	NA	NA	NA	NA	NA
Maple	81	R	41576	90	90	12.284	277.166	-0.14	1531	0	1531	0.25	NA	0.25
Maple	82	R	41706	130	130	13.624	44.000	-0.15	NA	NA	NA	NA	NA	NA
Maple	83	R	42636	90	90	10.087	300.233	-0.03	NA	NA	NA	NA	NA	NA
Maple	84	R	42776	140	140	12.414	297.168	-0.14	1493	0	1493	0.16	NA	0.16
Maple	85	R	42936	100	100	8.979	311.606	-0.13	NA	NA	NA	NA	NA	NA
Maple	86	L	43186	300	300	11.673	133.307	-0.03	802	574	228	0.01	NA	0.01
Maple	87	L	43796	50	NA	10.97	122.095	-0.09	0	394	-394	NA	0.00	0.00
Maple	88	L	44446	80	80	11.552	90.548	-0.09	345	214	131	0.02	NA	0.02
Maple	89	L	44546	160	110	10.614	74.962	-0.07	NA	NA	NA	NA	NA	NA
Maple	90	L	44836	250	250	6.998	310.842	-0.07	4051	82	3969	0.24	NA	0.24
Maple	91	R	45346	650	600	9.976	158.215	-0.05	4305	520	3785	0.09	0.01	0.09
Maple	92	R	46506	300	300	9.439	204.682	0.03	NA	NA	NA	NA	NA	NA
Maple	93	R	48386	170	170	8.927	299.762	-0.16	2352	0	2352	0.21	NA	0.21
Maple	94	R	49066	70	0	9.564	113.034	-0.09	NA	NA	NA	NA	NA	NA
Maple	95	R	50336	60	60	5.025	247.205	0.14	877	0	877	0.22	NA	0.22
Maple	96	L	50736	80	20	6.188	114.348	-0.12	66	62	4	0.03	0.00	0.00
Maple	97	L	51036	70	NA	6.827	69.984	-0.19	61	188	-128	NA	0.00	0.00
Maple	98	L	51106	50	50	7.549	43.809	-0.23	NA	NA	NA	NA	NA	NA

River	ID	Bank	Distance From Mouth	River Length along Bluff	Vegetated Length	Height	Average Aspect	Migration Rate (m/yr) negative #s indicate deposition	1938-2005 top area lost (m^2) Total	1938-2005 top area gained (m^2) Total	1938-2005 top area (m^2)	Traced rate (m/yr) Vegetated	Traced rate (m/yr) Un-Vegetated	Traced rate (m/yr)
Maple	99	L	51326	70	NA	8.625	27.916	-0.15	84	176	-92	0.00	NA	0.00
Maple	100	R	51706	10	10	5.684	142.899	0.17	NA	NA	NA	NA	NA	NA
Maple	101	L	52326	50	NA	9.68	93.067	-0.12	0	118	-118	0.00	NA	0.00
Maple	102	L	52486	150	150	6.105	315.000	-0.19	776	50	726	0.07	NA	0.07
Maple	103	L	52486		NA	11.93	315.000	-0.06	328	882	-554	0.00	NA	0.00
Maple	104	L	53776	110	50	6.579	275.469	-0.32	2487	0	2487	0.30	0.37	0.34
Maple	105	L	56566	60	60	6.515	29.847	-0.29	237	162	75	0.02	NA	0.02
Maple	106	R	58566	370	70	7.749	196.414	-0.16	13090	0	13090	0.23	0.60	0.53
Maple	107	R	61226	30	30	7.847	247.180	-0.08	NA	NA	NA	NA	NA	NA
Maple	108	R	61286	430	NA	7.642	248.594	-0.20	1533	2628	-1095	0.00	NA	0.00
Maple	109	L	62366	570	570	9.306	61.011	0.10	NA	NA	NA	NA	NA	NA
Maple	110	L	63236	230	230	6.907	315.000	-0.15	1649	235	1415	0.09	NA	0.09
Maple	111	R	63856	550	270	8.097	175.787	-0.11	3684	1561	2123	0.11	0.01	0.06
Maple	112	L	64716	480	480	9.689	315.000	-0.32	3869	286	3583	0.11	NA	0.11
Maple	113	R	65716	180	180	7.337	185.879	-0.24	NA	NA	NA	NA	NA	NA
Maple	114	R	65936	140	140	7.003	278.748	-0.15	490	307	183	0.02	NA	0.02
Maple	115	R	66086	50	50	6.179	244.161	0.45	NA	NA	NA	NA	NA	NA
Maple	116	L	69606	80	80	7.451	89.272	-0.25	NA	NA	NA	NA	NA	NA
Maple	117	R	76536	70	70	5.059	245.670	-0.28	NA	NA	NA	NA	NA	NA
Maple	118	L	76756	60	60	6.655	86.195	-0.02	NA	NA	NA	NA	NA	NA
Maple	119	R	76916	170	170	4.763	124.416	0.01	NA	NA	NA	NA	NA	NA
Big Cobb	1	L	260	60	0	6.62	83.74	-0.11	NA	NA	NA	NA	NA	NA
Big Cobb	2	L	470	220	**0**	54.76	15.00	-0.07	4000	423	3577	NA	0.21	0.21
Big Cobb	2	L	650	70	40	54.76	15.00	0.13	NA	NA	NA	NA	NA	NA
Big Cobb	4	R	1010	350	0	28.33	226.13	-0.10	5051	7698	-2647	NA	0.00	0.00
Big Cobb	5	L	1530	60	0	7.26	149.48	0.28	191	0	191	NA	0.05	0.05
Big Cobb	6	L	1720	140	0	30.37	15.00	-0.11	3941	0	3941	NA	0.42	0.42
Big Cobb	6	L	1860	60	0	30.37	15.00	0.37	NA	NA	NA	NA	NA	NA

River	ID	Bank	Distance From Mouth	River Length along Bluff	Vegetated Length	Height	Average Aspect	Migration Rate (m/yr) negative #s indicate deposition	1938-2005 top area lost (m^2) Total	1938-2005 top area gained (m^2) Total	1938-2005 top area (m^2)	Traced rate (m/yr) Vegetated	Traced rate (m/yr) Un-Vegetated	Traced rate (m/yr)
Big Cobb	7	L	2120	260	260	53.99	15.00	-0.21	6740	1280	5460	0.31	NA	0.31
Big Cobb	8	R	2330	120	120	3.85	209.01	0.62	325	113	212	0.03	NA	0.03
Big Cobb	9	R	2650	70	70	8.65	204.80	-0.07	235	82	153	0.03	NA	0.03
Big Cobb	10	L	2760	100	100	24.94	360.00	0.18	6043	0	6043	0.90	NA	0.90
Big Cobb	11	L	3040	150	0	49.49	15.00	0.15	4171	149	4022	NA	0.42	0.40
Big Cobb	12	R	3390	270	0	50.48	360.00	0.17	4144	2951	1193	NA	0.07	0.07
Big Cobb	13	L	4350	100	100	32.83	134.50	-0.02	2392	101	2291	0.34	NA	0.34
Big Cobb	14	R	4570	50	50	8.28	219.47	-0.23	96	25	71	0.02	NA	0.02
Big Cobb	15	R	4880	110	0	17.33	235.57	0.02	243	2041	-1798	NA	0.00	0.00
Big Cobb	16	R	5200	40	40	4.29	141.72	0.01	NA	NA	NA	NA	NA	NA
Big Cobb	17	R	551	80	80	9.48	332.83	0.06	NA	NA	NA	NA	NA	NA
Big Cobb	18	R	5900	110	110	21.03	207.01	-0.07	NA	NA	NA	NA	NA	NA
Big Cobb	19	L	5970	250	250	45.44	155.65	0.00	3902	917	2986	0.18	NA	0.18
Big Cobb	20	L	6330	160	20	19.94	53.13	-0.08	NA	NA	NA	NA	NA	NA
Big Cobb	21	R	7070	180	0	41.11	253.75	-0.10	0	15734	-15734	NA	0.00	0.00
Big Cobb	21	R	7290	30	50	41.11	253.75	0.03	NA	NA	NA	NA	NA	NA
Big Cobb	22	R	7530	240	0	12.04	15.00	0.32	NA	NA	NA	NA	NA	NA
Big Cobb	23	R	8170	50	50	4.07	217.77	-0.11	604	0	604	0.18	NA	0.18
Big Cobb	24	L	8610	70	70	36.36	151.05	0.07	126	1799	-1673	0.00	NA	0.00
Big Cobb	25	L	8900	60	0	12.91	98.89	0.13	NA	NA	NA	NA	NA	NA
Big Cobb	26	R	9240	110	110	37.47	360.00	0.19	22	1094	-1072	0.00	NA	0.00
Big Cobb	27	R	9660	200	0	35.64	35.00	0.19	0	1175	-1175	NA	0.00	0.00
Big Cobb	28	R	10390	90	0	35.64	340.00	-0.02	713	0	713	NA	0.12	0.12
Big Cobb	29	L	1088	80	0	32.49	118.51	0.40	1565	0	1565	NA	0.29	0.29
Big Cobb	30	L	11220	180	0	30.71	99.79	0.15	NA	NA	NA	NA	NA	NA
Big Cobb	31	L	11840	50	50	31.61	53.76	0.40	832	0	832	0.25	NA	0.25
Big Cobb	32	L	12520	90	0	9.69	360.00	NA	NA	NA	NA	NA	NA	NA
Big Cobb	33	R	12860	80	33	8.64	181.04	NA	NA	NA	NA	NA	NA	NA

River	ID	Bank	Distance From Mouth	River Length along Bluff	Vegetated Length	Height	Average Aspect	Migration Rate (m/yr) negative #s indicate deposition	1938-2005 top area lost (m^2) Total	1938-2005 top area gained (m^2) Total	1938-2005 top area (m^2)	Traced rate (m/yr) Vegetated	Traced rate (m/yr) Un-Vegetated	Traced rate (m/yr)
Big Cobb	34	R	12910	760	0	29.46	360.00	NA	NA	NA	NA	NA	NA	NA
Big Cobb	35	L	14210	50	50	4.48	100.68	NA	NA	NA	NA	NA	NA	NA
Big Cobb	36	L	14670	80	20	26.08	15.00	NA	NA	NA	NA	NA	NA	NA
Big Cobb	37	L	15480	190	80	11.99	296.81	NA	NA	NA	NA	NA	NA	NA
Big Cobb	38	L	15710	50	0	3.97	246.56	NA	NA	NA	NA	NA	NA	NA
Big Cobb	39	L	15980	30	30	3.88	113.05	NA	NA	NA	NA	NA	NA	NA
Big Cobb	40	R	16280	30	30	5.24	116.24	NA	NA	NA	NA	NA	NA	NA
Big Cobb	41	L	16500	70	50	5.95	40.21	NA	NA	NA	NA	NA	NA	NA
Big Cobb	42	R	16910	80	10	9.96	169.95	NA	NA	NA	NA	NA	NA	NA
Big Cobb	43	R	17370	170	130	21.79	187.35	NA	NA	NA	NA	NA	NA	NA
Big Cobb	44	R	17520	720	0	22.38	243.19	NA	NA	NA	NA	NA	NA	NA
Big Cobb	45	L	18330	390	110	17.89	360.00	NA	NA	NA	NA	NA	NA	NA
Big Cobb	46	R	18820	110	110	21.78	221.23	NA	NA	NA	NA	NA	NA	NA
Big Cobb	47	R	19200	170	170	20.64	305.89	NA	NA	NA	NA	NA	NA	NA
Big Cobb	48	L	19560	150	0	4.69	128.59	0.06	3539	0	3539	NA	0.35	0.35
Big Cobb	49	R	19980	170	170	23.39	209.92	0.11	1181	888	293	0.03	NA	0.03
Big Cobb	50	L	20400	80	0	6.64	56.90	-0.23	1990	0	1990	NA	0.37	0.37
Big Cobb	51	L	20820	110	110	11.46	104.82	0.04	2145	0	2145	0.29	NA	0.29
Big Cobb	52	R	21180	60	0	3.82	285.24	0.04	NA	NA	NA	NA	NA	NA
Big Cobb	53	L	21660	550	550	19.53	112.88	0.02	7282	0	7282	0.20	NA	0.20
Big Cobb	54	L	22800	140	0	15.09	15.00	-0.16	1786	0	1786	NA	0.19	0.19
Big Cobb	55	R	23260	240	150	11.86	173.11	0.00	2779	0	2779	0.08	0.33	0.17
Big Cobb	56	L	23860	250	250	15.84	360.00	-0.02	52	1395	-1342	0.00	NA	0.00
Big Cobb	57	L	24110	50	50	8.62	323.59	0.07	NA	NA	NA	NA	NA	NA
Big Cobb	58	R	24540	190	0	13.83	109.34	-0.12	4252	257	3996	NA	0.31	0.31
Big Cobb	59	R	24890	90	90	15.77	147.76	0.32	NA	NA	NA	NA	NA	NA
Big Cobb	60	R	25170	180	180	16.95	139.51	0.11	2452	0	2452	0.20	NA	0.20
Big Cobb	61	R	25480	290	210	15.72	195.64	-0.03	NA	NA	NA	NA	NA	NA

River	ID	Bank	Distance From Mouth	River Length along Bluff	Vegetated Length	Height	Average Aspect	Migration Rate (m/yr) negative #s indicate deposition	1938-2005 top area lost (m^2) Total	1938-2005 top area gained (m^2) Total	1938-2005 top area (m^2)	Traced rate (m/yr) Vegetated	Traced rate (m/yr) Un-Vegetated	Traced rate (m/yr)
Big Cobb	62	L	26050	90	20	13.85	52.63	0.00	1538	0	1538	0.31	0.24	0.26
Big Cobb	63	L	27440	170	170	11.13	121.22	0.04	NA	NA	NA	NA	NA	NA
Big Cobb	64	R	28050	120	120	10.68	360.00	0.19	855	0	855	0.11	NA	0.11
Big Cobb	65	L	28330	260	260	13.82	150.27	-0.06	1938	62	1876	0.11	NA	0.11
Big Cobb	66	L	29340	420	420	14.70	360.00	0.00	6882	0	6882	0.24	NA	0.24
Big Cobb	67	L	30020	130	130	11.93	325.24	-0.02	NA	NA	NA	NA	NA	NA
Big Cobb	68	L	30230	170	170	6.39	308.73	0.02	NA	NA	NA	NA	NA	NA
Big Cobb	69	L	30300	90	90	7.29	318.93	-0.04	520	0	520	0.09	NA	0.09
Big Cobb	70	R	30600	430	430	15.82	167.29	0.00	2254	825	1429	0.05	NA	0.05
Big Cobb	71	R	31310	240	240	12.34	217.11	-0.07	NA	NA	NA	NA	NA	NA
Big Cobb	72	L	31680	330	330	14.01	91.15	0.03	4508	0	4508	0.20	NA	0.20
Big Cobb	73	L	32270	150	150	14.92	15.00	0.11	2363	0	2363	0.24	NA	0.24
Big Cobb	74	L	32550	200	200	15.07	295.69	-0.59	NA	NA	NA	NA	NA	NA
Big Cobb	75	R	33100	180	180	9.31	94.59	-0.12	NA	NA	NA	NA	NA	NA
Big Cobb	76	R	33350	290	290	13.42	148.33	-0.12	2620	801	1818	0.09	NA	0.09
Big Cobb	77	R	33690	80	80	14.06	194.89	-0.11	194	245	-50	0.00	NA	0.00
Big Cobb	78	L	33950	210	210	8.64	15.00	-0.06	3314	0	3314	0.24	NA	0.24
Big Cobb	79	R	34330	30	30	11.53	214.71	-0.37	197	110	87	0.04	NA	0.04
Big Cobb	80	R	35500	200	0	10.91	248.03	-0.17	NA	NA	NA	NA	NA	NA
Big Cobb	81	R	36000	30	30	5.77	222.34	0.00	NA	NA	NA	NA	NA	NA
Big Cobb	82	L	40360	80	80	12.55	303.98	-0.09	0	594	-594	0.00	NA	0.00
Big Cobb	83	R	40650	270	270	11.34	108.93	-0.43	1736	0	1736	0.10	NA	0.10
Big Cobb	84	R	40970	50	50	11.86	156.42	0.03	NA	NA	NA	NA	NA	NA
Big Cobb	85	L	41450	250	250	10.85	23.17	1.12	317	810	-492	0.00	NA	0.00
Big Cobb	86	R	42210	130	130	10.75	124.38	-0.75	NA	NA	NA	NA	NA	NA
Big Cobb	87	R	42790	190	190	9.50	148.59	0.08	NA	NA	NA	NA	NA	NA
Big Cobb	88	L	43170	300	300	6.67	360.00	-0.11	NA	NA	NA	NA	NA	NA
Big Cobb	89	R	43560	60	60	7.44	98.15	0.08	NA	NA	NA	NA	NA	NA

River	ID	Bank	Distance From Mouth	River Length along Bluff	Vegetated Length	Height	Average Aspect	Migration Rate (m/yr) negative #s indicate deposition	1938-2005 top area lost (m^2) Total	1938-2005 top area gained (m^2) Total	1938-2005 top area (m^2)	Traced rate (m/yr) Vegetated	Traced rate (m/yr) Un-Vegetated	Traced rate (m/yr)
Big Cobb	90	R	43670	200	200	10.51	119.37	0.27	2738	0	2738	0.20	NA	0.20
Big Cobb	91	R	4396	290	290	10.78	207.75	0.01	96	9280	-9184	0.00	NA	0.00
Big Cobb	92	L	44550	400	400	9.26	360.00	NA	1139	4340	-3201	0.00	NA	0.00
Big Cobb	92	L	44650	120	120	9.26	360.00	NA	NA	NA	NA	NA	NA	NA
Big Cobb	93	R	45570	60	60	4.73	211.14	-0.15	NA	NA	NA	NA	NA	NA
Big Cobb	94	L	46300	360	360	7.92	360.00	-0.38	774	1946	-1173	0.00	NA	0.00
Big Cobb	95	R	50140	430	430	10.09	207.91	-0.07	0	7429	-7429	0.00	NA	0.00
Big Cobb	96	R	50850	200	100	9.69	121.12	-0.09	2738	0	2738	0.16	0.25	0.20
Big Cobb	97	R	51610	220	220	6.31	163.37	-0.29	NA	NA	NA	NA	NA	NA
Big Cobb	98	R	52980	30	30	4.59	55.16	0.21	63	36	27	0.01	NA	0.01
Big Cobb	99	R	54210	40	40	7.07	168.30	-0.31	NA	NA	NA	NA	NA	NA
Big Cobb	100	R	54460	90	90	7.96	207.17	-0.25	NA	NA	NA	NA	NA	NA
Big Cobb	101	R	54560	390	390	11.51	245.84	NA	NA	NA	NA	NA	NA	NA
Big Cobb	102	R	55000	90	90	9.83	360.00	NA	828	62	766	0.13	NA	0.13
Big Cobb	103	L	55530	130	130	6.55	112.34	NA	1696	0	1696	0.19	NA	0.19
Big Cobb	104	L	56110	320	320	9.27	94.80	NA	5272	0	5272	0.25	NA	0.25
Big Cobb	105	L	56510	190	190	10.54	360.00	NA	824	1071	-247	0.00	NA	0.00
Big Cobb	106	R	57180	130	130	4.89	142.37	NA	NA	NA	NA	NA	NA	NA
Big Cobb	107	NA	5733	NA	NA	5.19	138.04	NA	NA	NA	NA	NA	NA	NA
Big Cobb	108	R	57390	240	240	8.20	186.33	NA	NA	NA	NA	NA	NA	NA
Big Cobb	109	L	57850	680	680	9.91	175.77	NA	NA	NA	NA	NA	NA	NA
Big Cobb	110	R	58660	580	580	10.26	103.10	NA	NA	NA	NA	NA	NA	NA
Big Cobb	111	R	59280	550	550	7.29	200.32	NA	NA	NA	NA	NA	NA	NA
Big Cobb	112	L	59870	250	250	8.02	91.57	NA	NA	NA	NA	NA	NA	NA
Big Cobb	113	L	60490	70	70	4.86	329.24	NA	NA	NA	NA	NA	NA	NA
Big Cobb	114	R		40	40	6.32	158.89	NA	NA	NA	NA	NA	NA	NA
Big Cobb	115	L		50	50	3.82	297.28	NA	NA	NA	NA	NA	NA	NA
Big Cobb	116	R		50	50	4.70	126.28	NA	NA	NA	NA	NA	NA	NA

River	ID	Bank	Distance From Mouth	River Length along Bluff	Vegetated Length	Height	Average Aspect	Migration Rate (m/yr) negative #s indicate deposition	1938-2005 top area lost (m^2) Total	1938-2005 top area gained (m^2) Total	1938-2005 top area (m^2)	Traced rate (m/yr) Vegetated	Traced rate (m/yr) Un-Vegetated	Traced rate (m/yr)
Little Cobb	117	L	1450	390	390	6.55	15.00	-0.31	4615	0	4615	0.18	NA	0.18
Little Cobb	118	L	8050	50	0	7.99	39.39	-0.33	1241	0	1241	NA	0.37	0.37
Little Cobb	119	L	9320	90	90	9.62	96.42	0.16	NA	NA	NA	NA	NA	NA
Little Cobb	120	L	3170	80	80	9.47	237.44	NA	NA	NA	NA	NA	NA	NA
Little Cobb	121	L	9820	60	60	7.97	360.00	-0.16	NA	NA	NA	NA	NA	NA
Little Cobb	122	L	11190	80	80	7.22	329.23	-0.18	0	377	-377	0.00	NA	0.00
Little Cobb	123	L	13550	30	30	4.91	139.40	0.11	NA	NA	NA	NA	NA	NA

Appendix D: Experimental Results

Run 1:

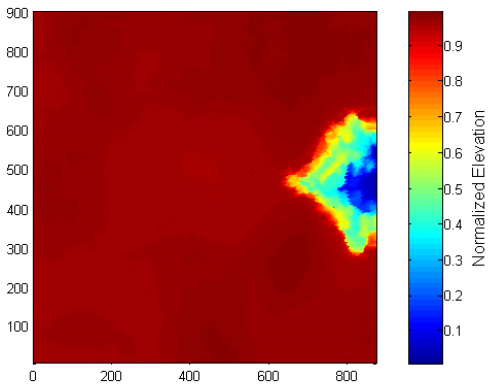

Scan 2: 15 min & 4.09cm^3 removed

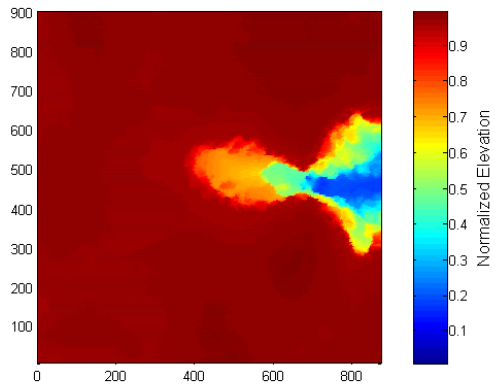

Scan 3: 30 min & 6.57 cm^3 removed

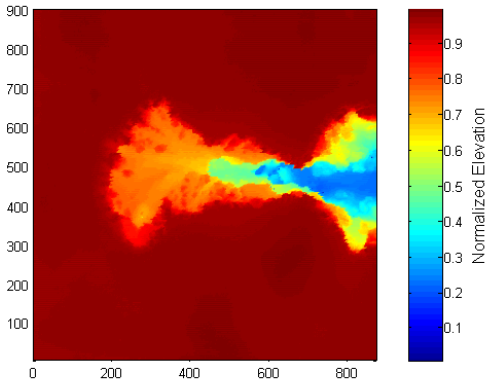

Scan 4: 45 min & 9.81 cm^3 removed

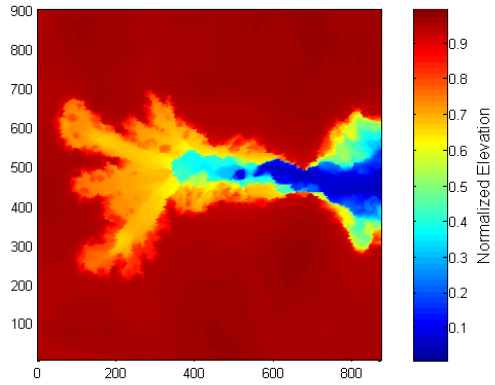

Scan 5: 60 min & 11.92 cm^3 removed

D_{50} = 12 μm

Total Volume = 190 L

Total Run Time = 60 minutes

Flow Rate = 52.58 ml/sec

Total Volume Removed: 11.92 cm^3

Run 1 Final Hypsometry

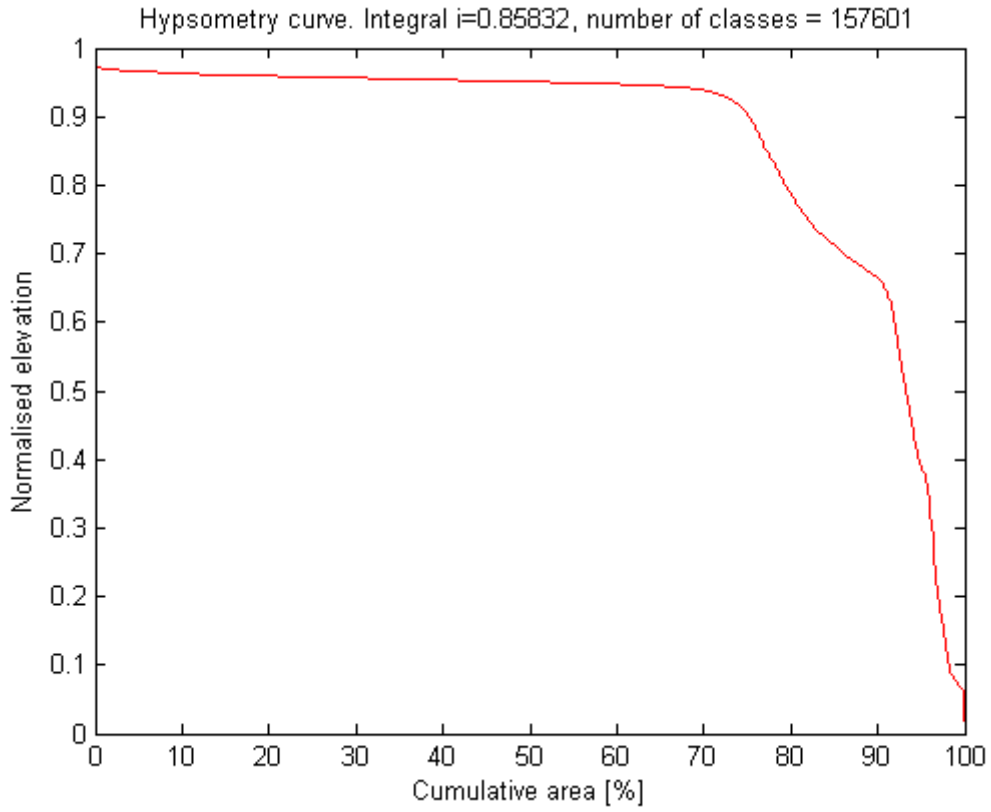

Run 2:

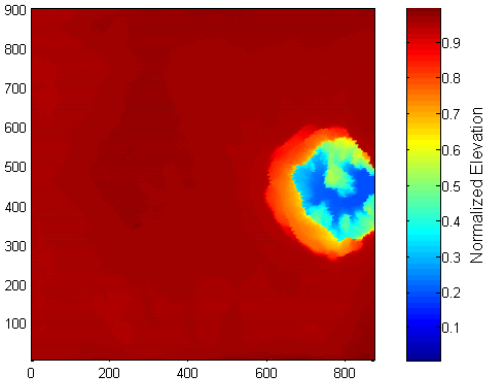

Scan 2: 8 min & 5.85 cm^3 removed

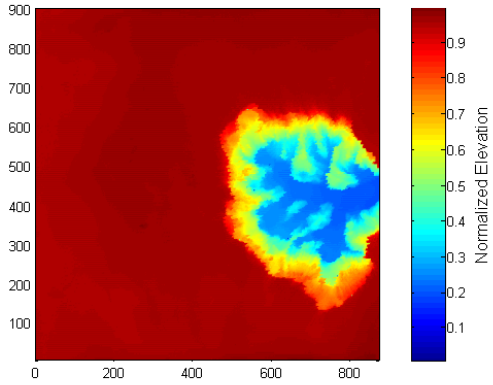

Scan 3: 16 min & 14.73 cm^3 removed

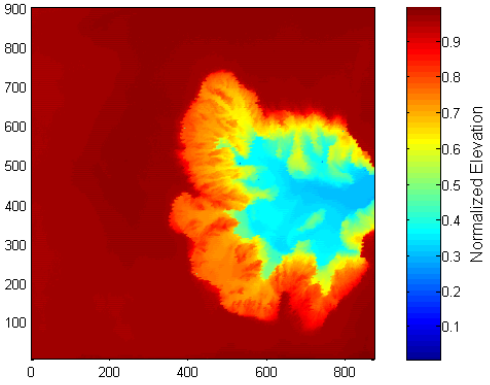

Scan 4: 24 min & 19.92 cm^3 removed

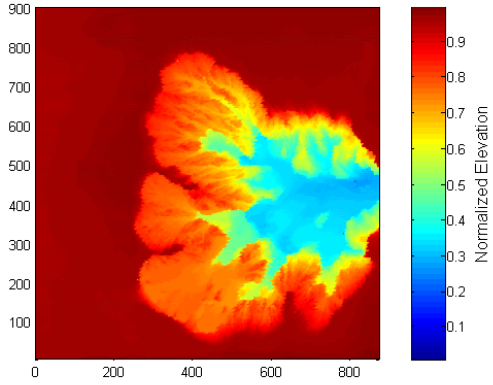

Scan 5: 32 min & 24.51 cm^3 removed

D_{50} = 12 µm

Total Volume = 190 L

Total Run Time = 32 minutes

Flow Rate = 98.58 ml/sec

Total Volume Removed: 24.51 cm^3

Run 2 Final Hypsometry

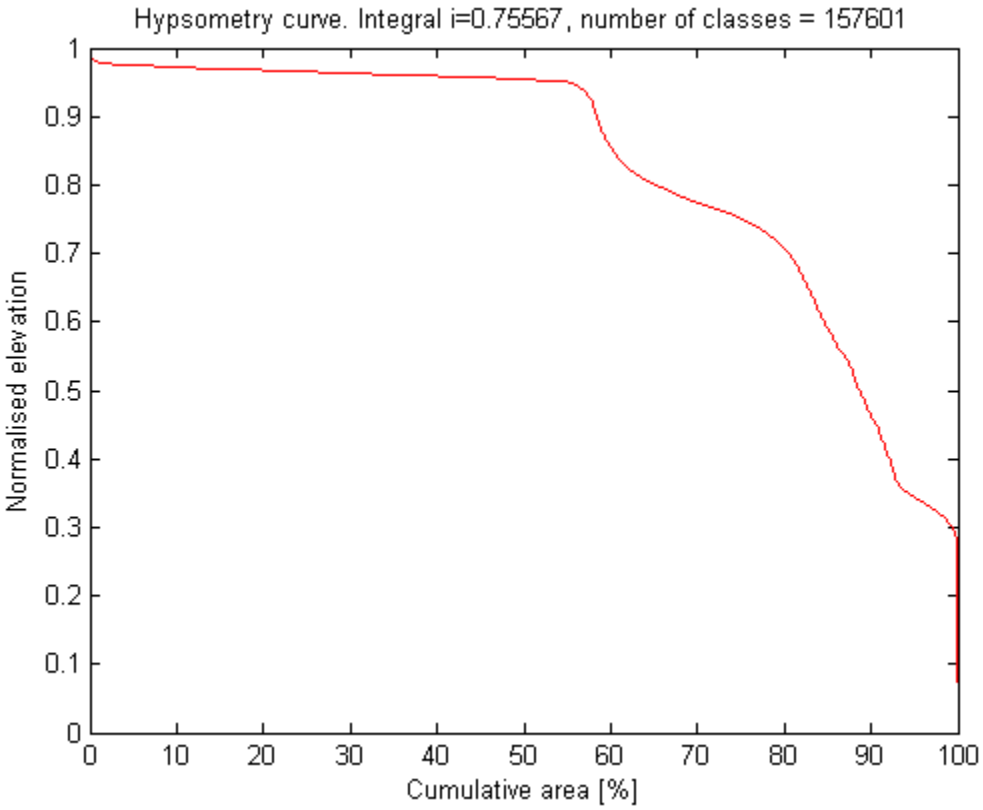

Run 3:

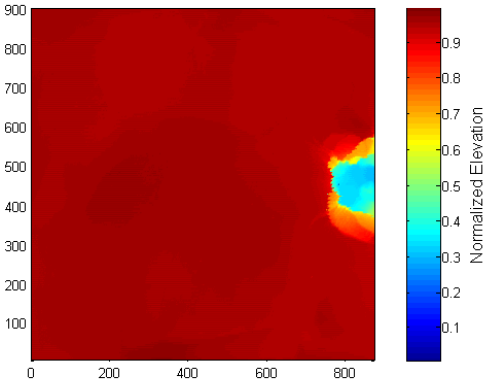

Scan 2: 4 min & 2.59 cm^3 removed

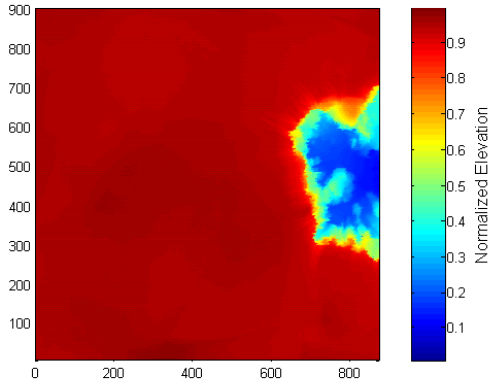

Scan 3: 8 min & 7.78 cm^3 removed

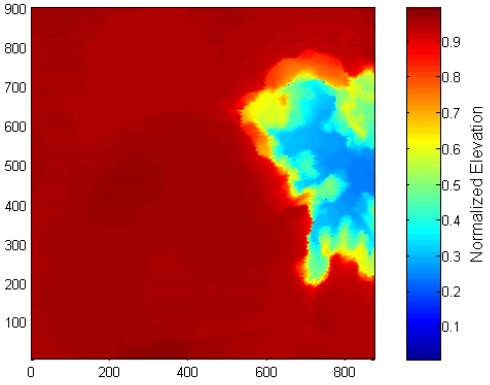

Scan 4: 12 min & 13.33 cm^3 removed

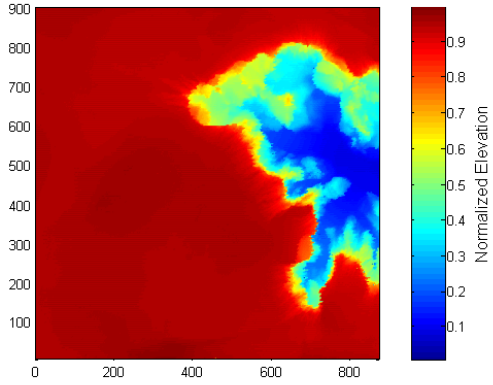

Scan 5: 16 min & 17.94 cm^3 removed

D_{50} = 12 µm

Total Volume = 190 L

Total Run Time = 16 minutes

Flow Rate = 197.16 ml/sec

Total Volume Removed: 17.94 cm^3

Run 3 Final Hypsometry

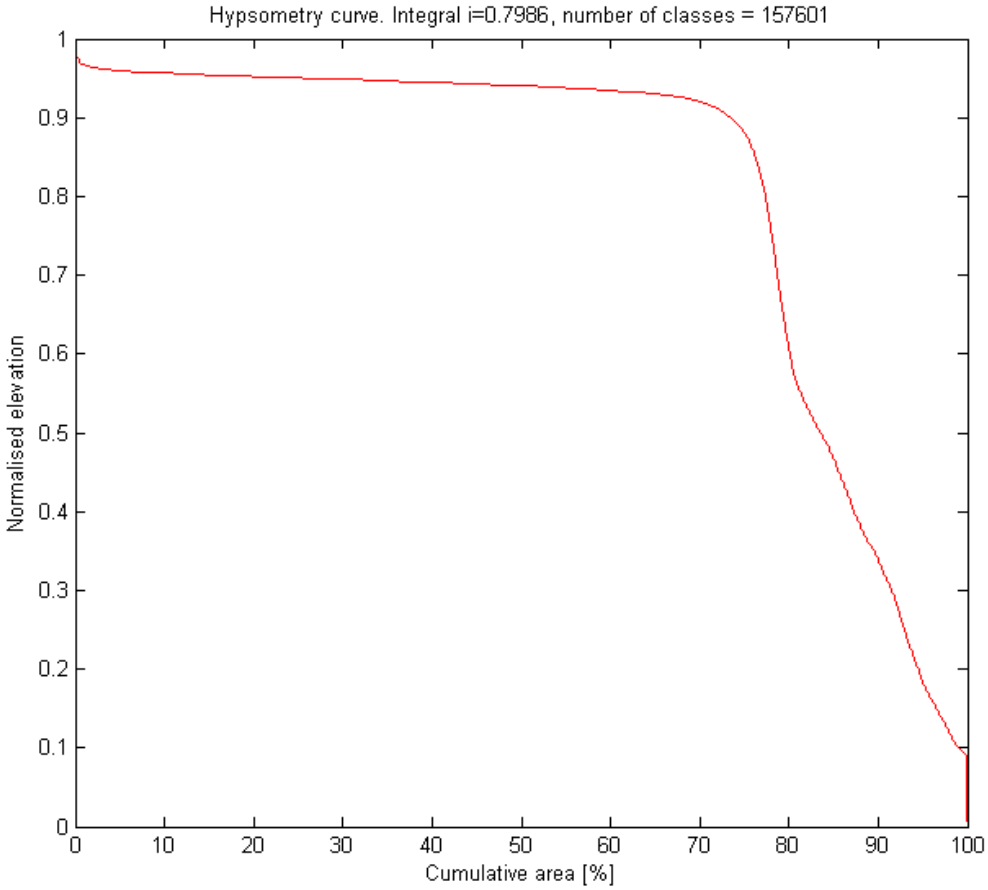

Run 4:

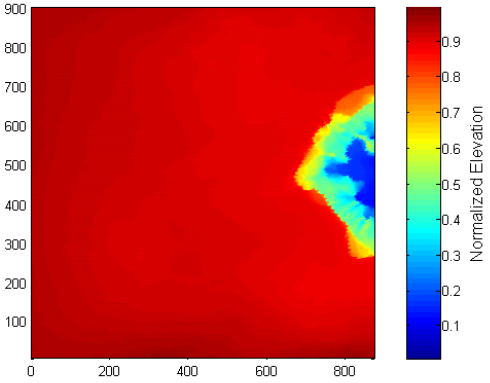

Scan 2: 6 min & 4.04 cm^3 removed

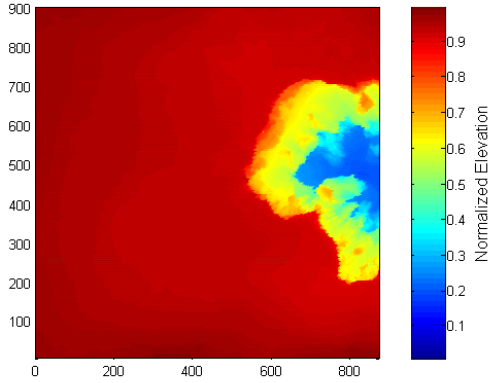

Scan 3: 12 min & 9.08 cm^3 removed

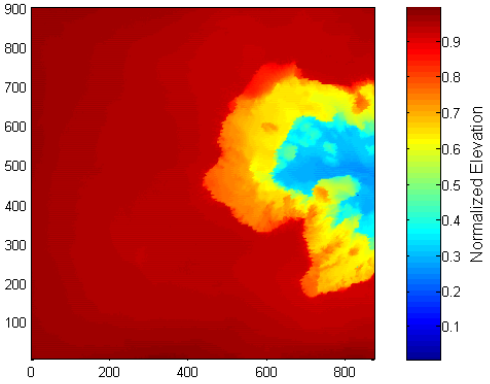

Scan 4: 18 min & 12.56 cm^3 removed

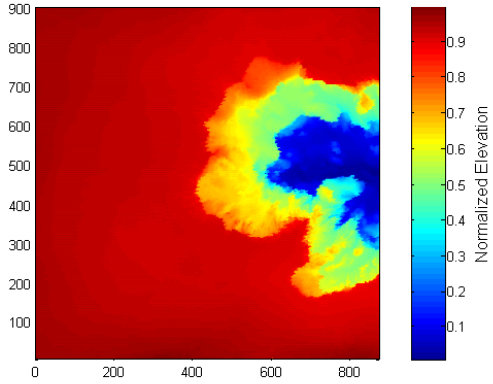

Scan 5: 21.25 min & 13.78 cm^3 removed

D_{50} = 12 µm

Total Volume = 190 L

Total Run Time = 21.25 minutes

Flow Rate = 148.45 ml/sec

Total Volume Removed: 13.78 cm^3

Run 4 Final Hypsometry

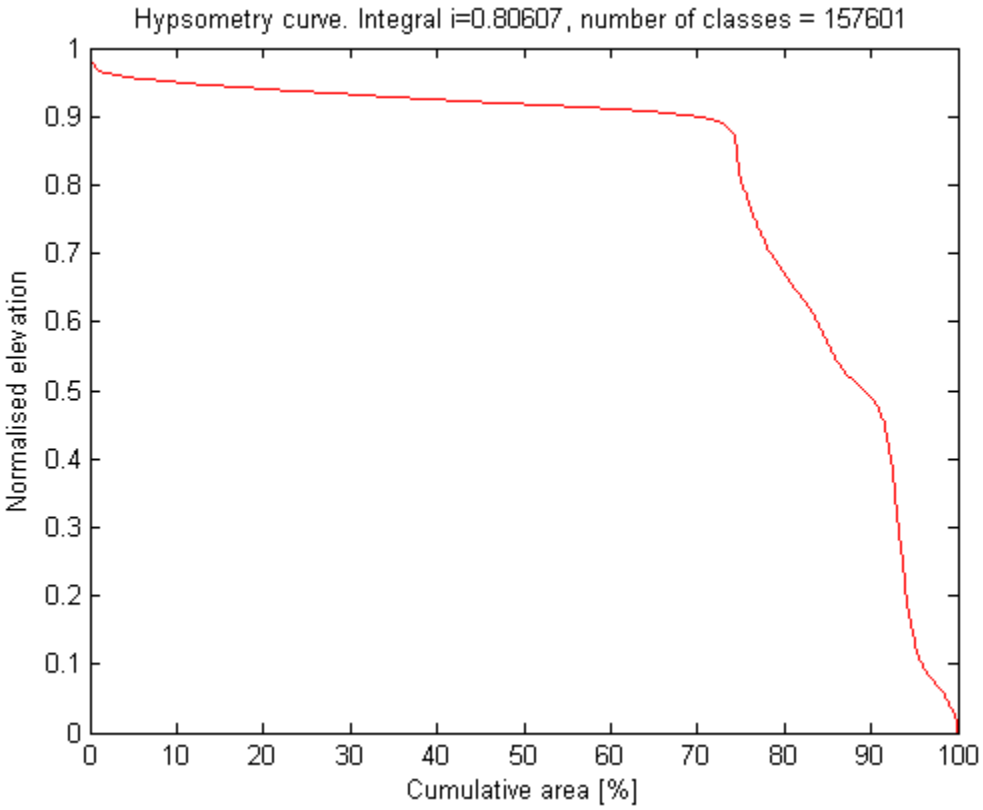

Run 5:

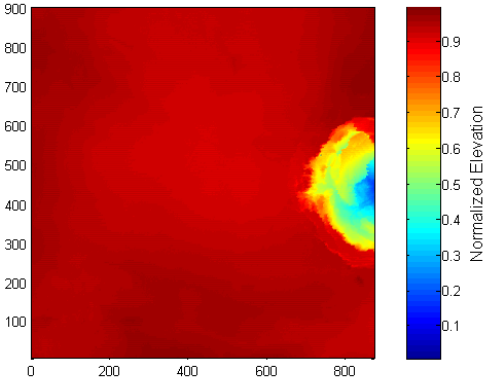

Scan 2: 4 min & 3.30 cm^3 removed

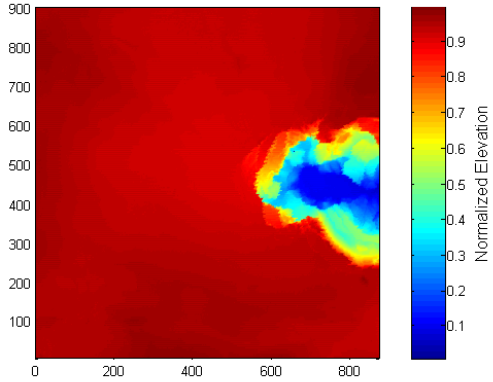

Scan 3: 8 min & 7.35 cm^3 removed

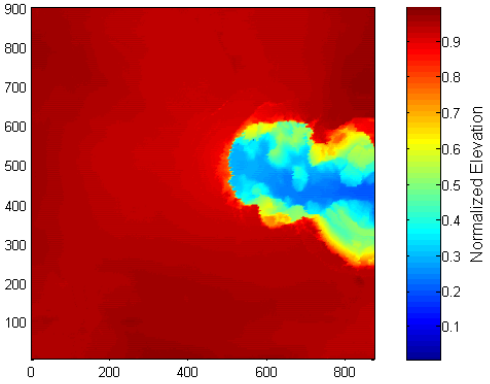

Scan 4: 11 min & 10.38 cm^3 removed

D_{50} = 12 µm

Total Volume = 190 L

Total Run Time = 11 minutes

Flow Rate = 286.77 ml/sec

Total Volume Removed: 10.38 cm^3

Run 5 Final Hypsometry

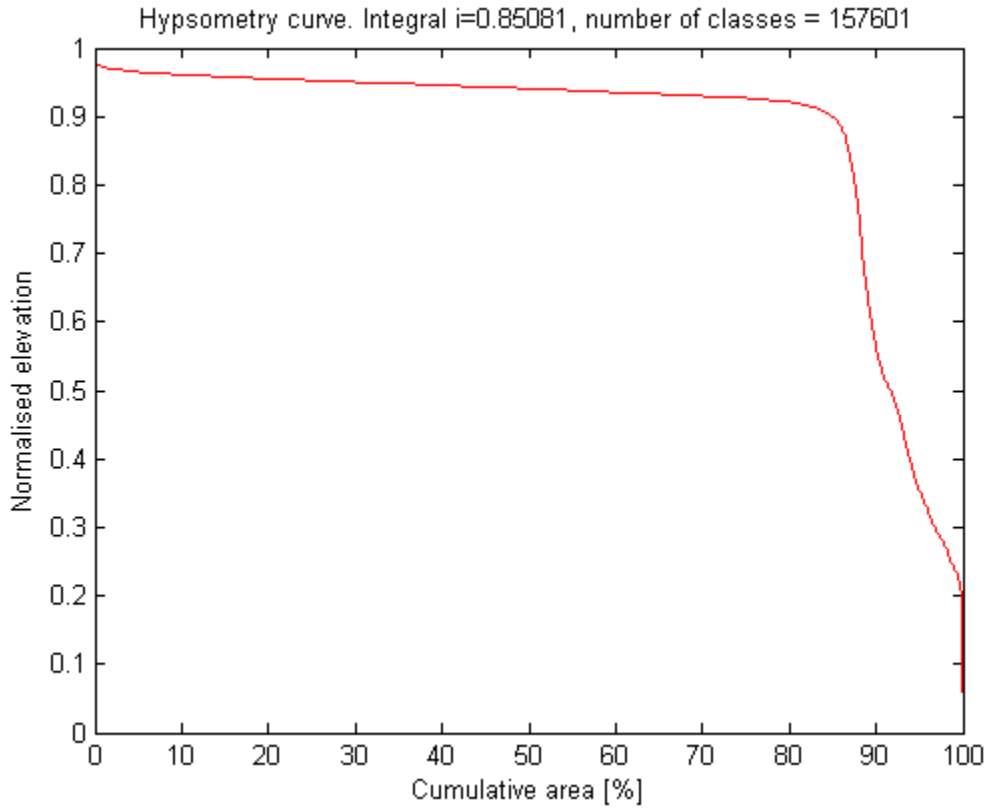

Run 6:

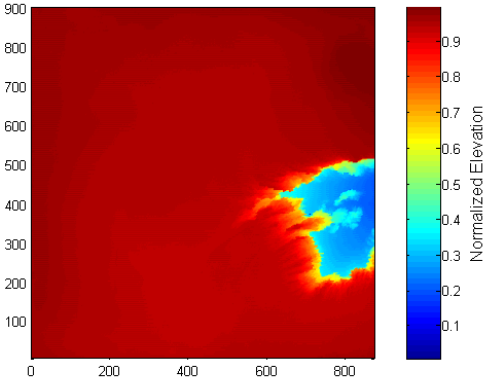

Scan 2: 30 min & 6.38cm^3 removed

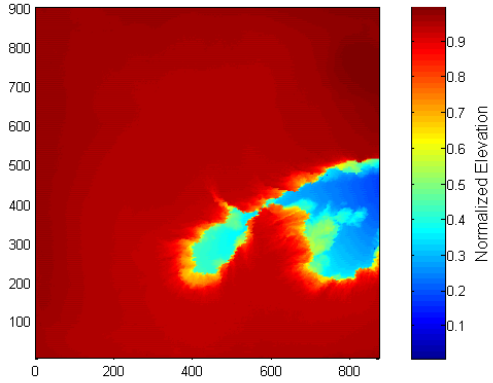

Scan 3: 60 min & 9.01 cm^3 removed

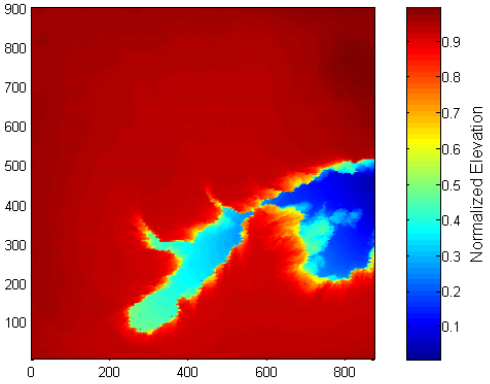

Scan 4: 90 min & 10.56 cm^3 removed

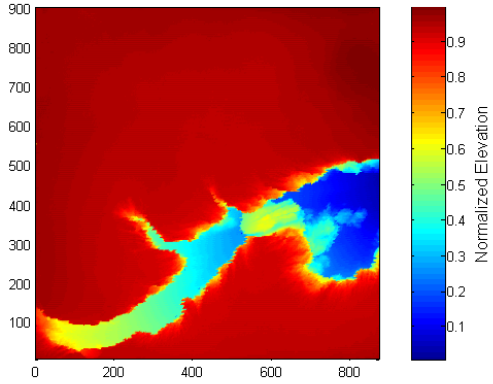

Scan 5: 120 min & 11.85 cm^3 removed

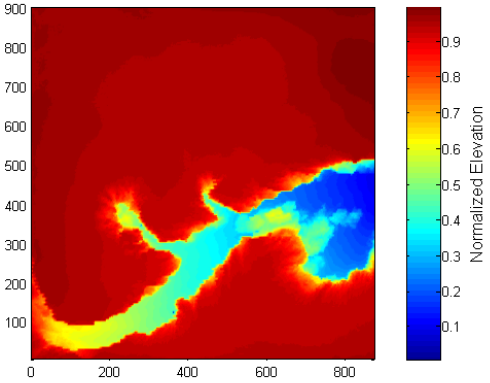

Scan 6: 150 min & 12.55 cm^3 removed

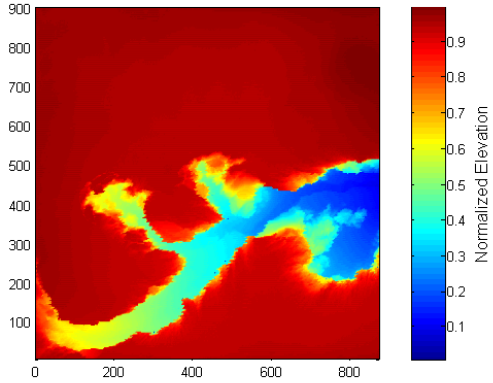

Scan 7: 360 min & 13.90 cm^3 removed

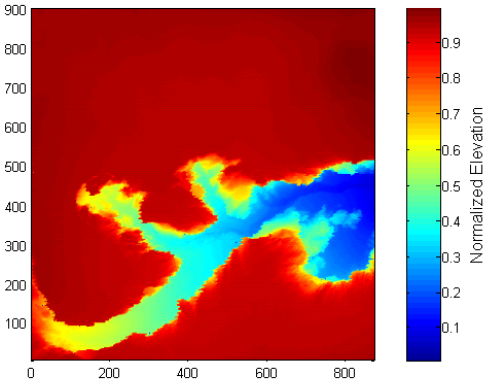

Scan 8: 738 min & 14.90 cm^3 removed

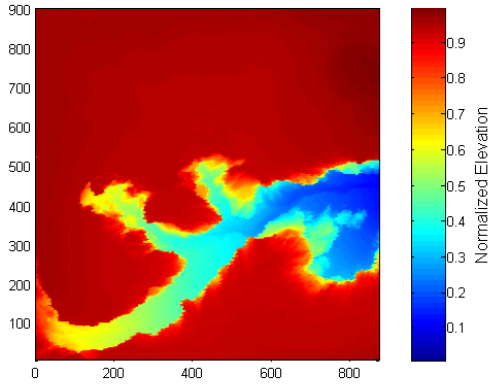

Scan 9: 872 min & 14.90 cm^3 removed

D_{50} = 12 µm

Total Volume = 190 L

Total Run Time = 872 minutes

Flow Rate = 3.62 ml/sec

Total Volume Removed: 14.90 cm^3

Run 6 Final Hypsometry

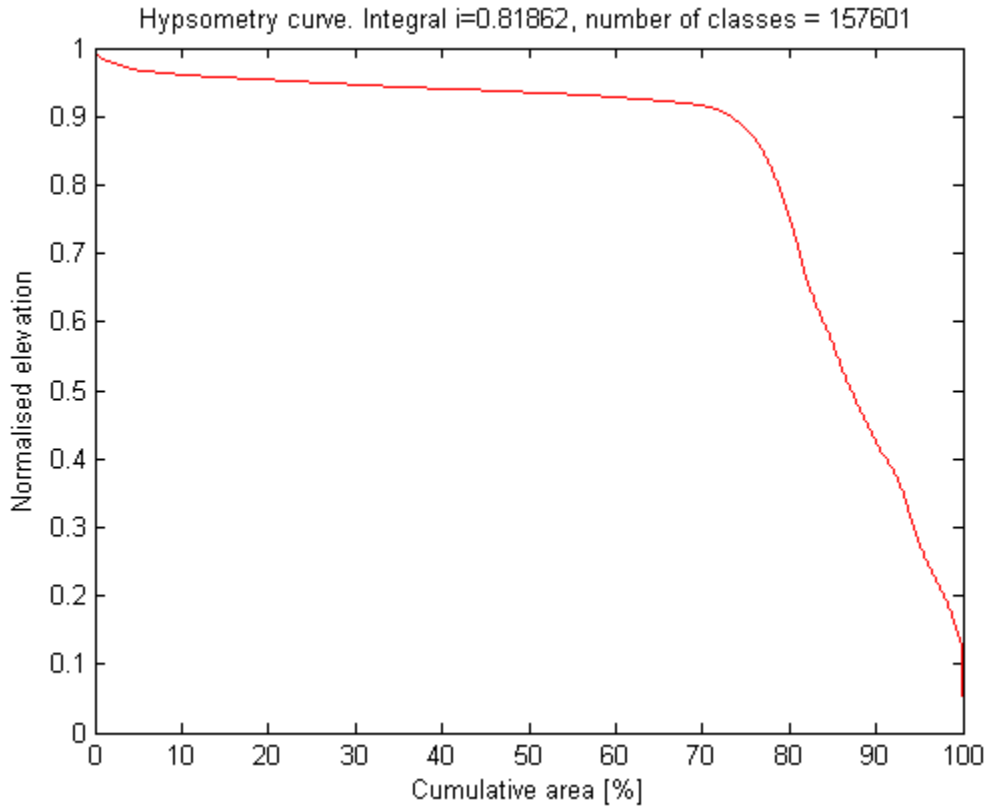

Run 7:

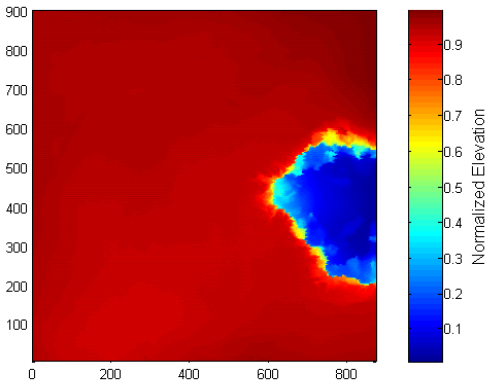

Scan 2: 10.13 min & 8.91 cm^3 removed

D_{50} = 12 μm

Total Volume = 190 L

Total Run Time = 10.13 minutes

Flow Rate = 311.40 ml/sec

Total Volume Removed: 8.91 cm^3

Run 7 Final Hypsometry

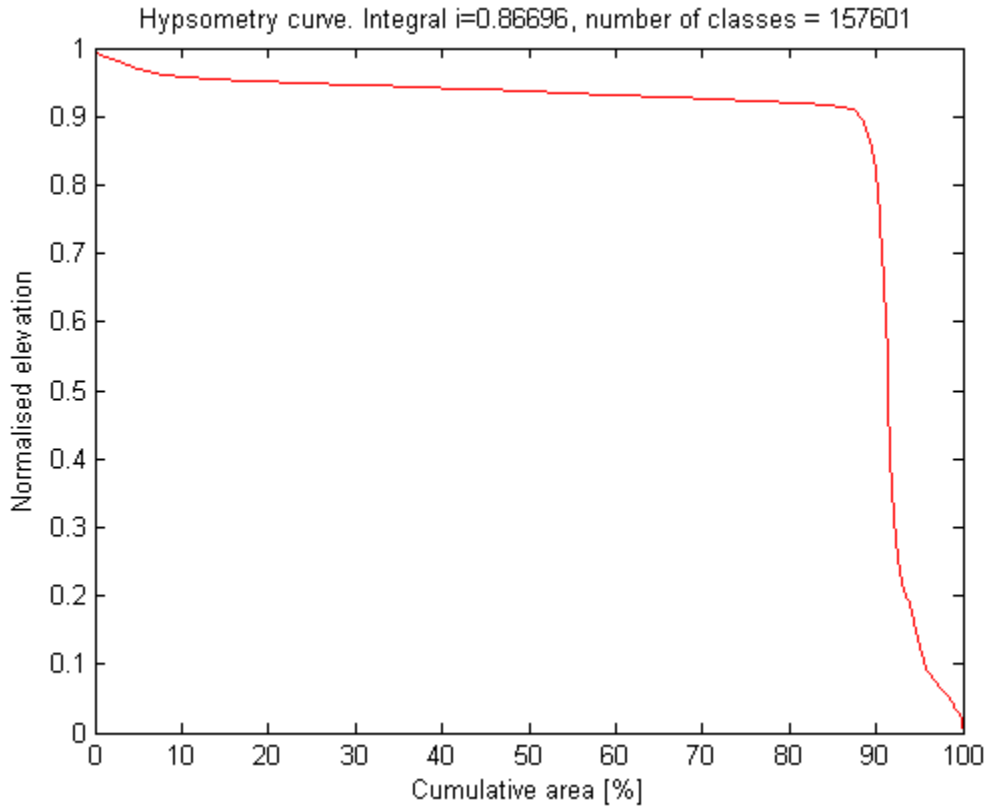

Run 8:

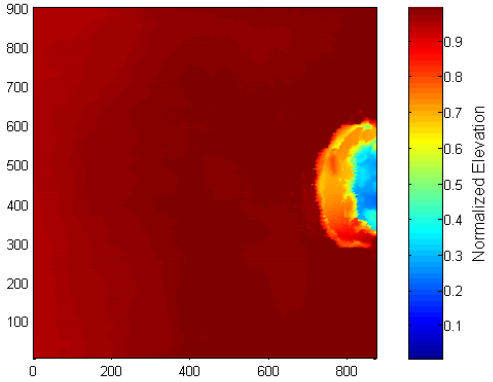

Scan 2: 6 min & 3.10 cm^3 removed

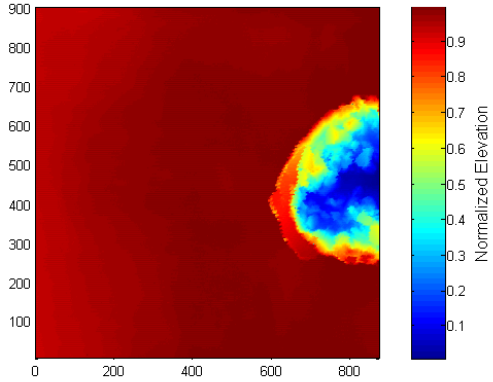

Scan 3: 12 min & 7.38 cm^3 removed

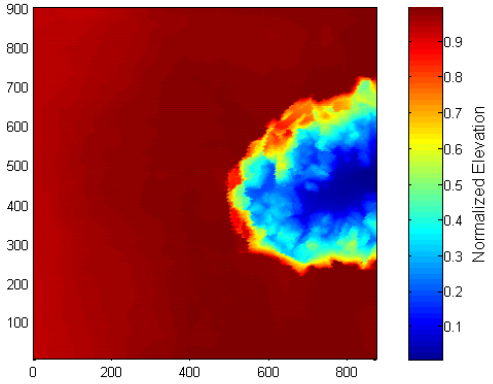

Scan 4: 21.5 min & 13.91 cm^3 removed

D_{50} = 12 µm

Total Volume = 190 L

Total Run Time = 21.5 minutes

Flow Rate = 146.72 ml/sec

Total Volume Removed: 13.91 cm^3

Run 8 Final Hypsometry

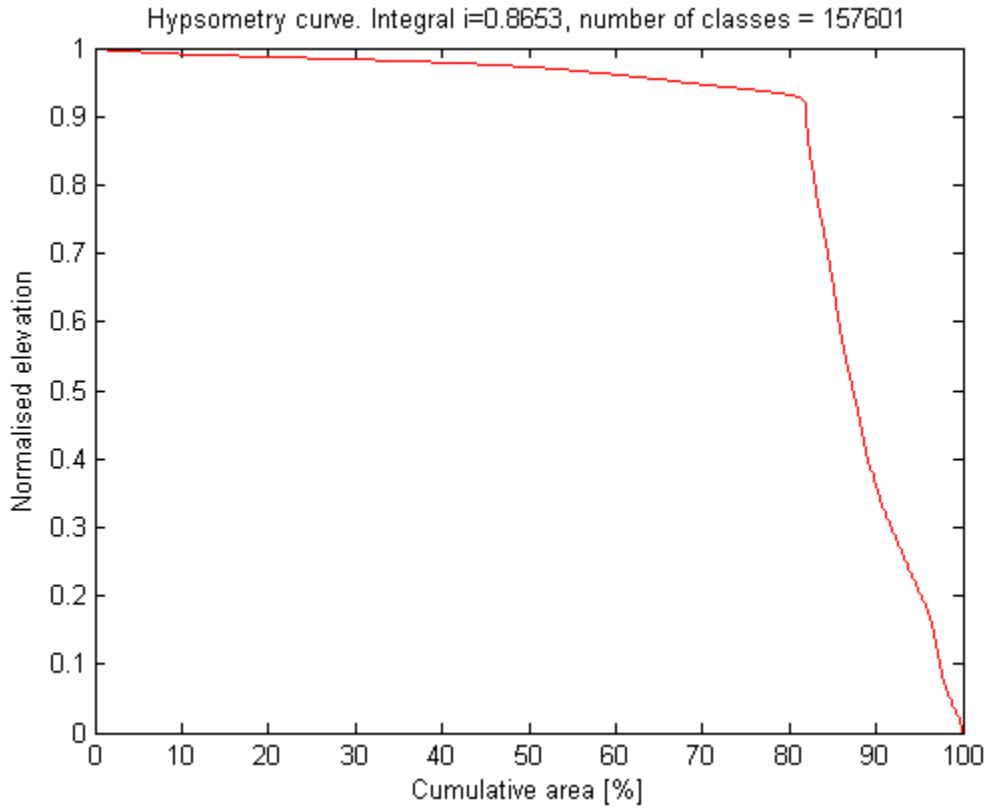

Run 9:

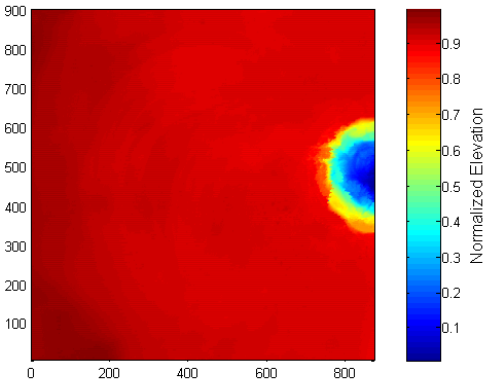

Scan 2: 3 min & 2.03 cm^3 removed

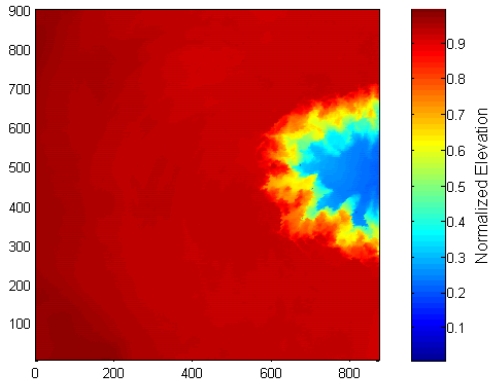

Scan 3: 6 min & 7.20 cm^3 removed

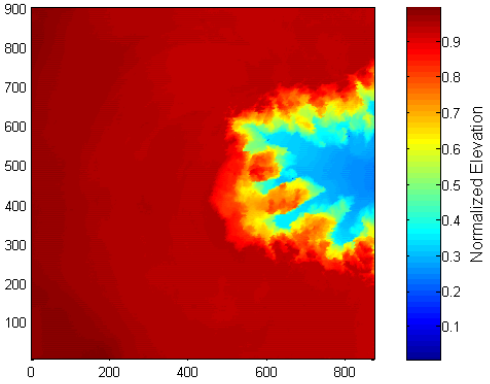

Scan 4: 9 min & 11.39 cm^3 removed

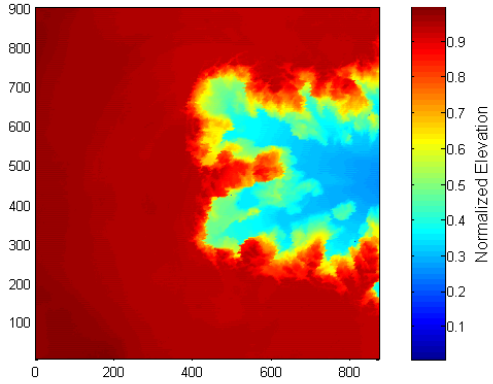

Scan 5: 15.5 min & 18.65 cm^3 removed

D_{50} = 12 µm

Total Volume = 190 L

Total Run Time = 15.5 minutes

Flow Rate = 203.52 ml/sec

Total Volume Removed: 18.65 cm^3

Run 9 Final Hypsometry

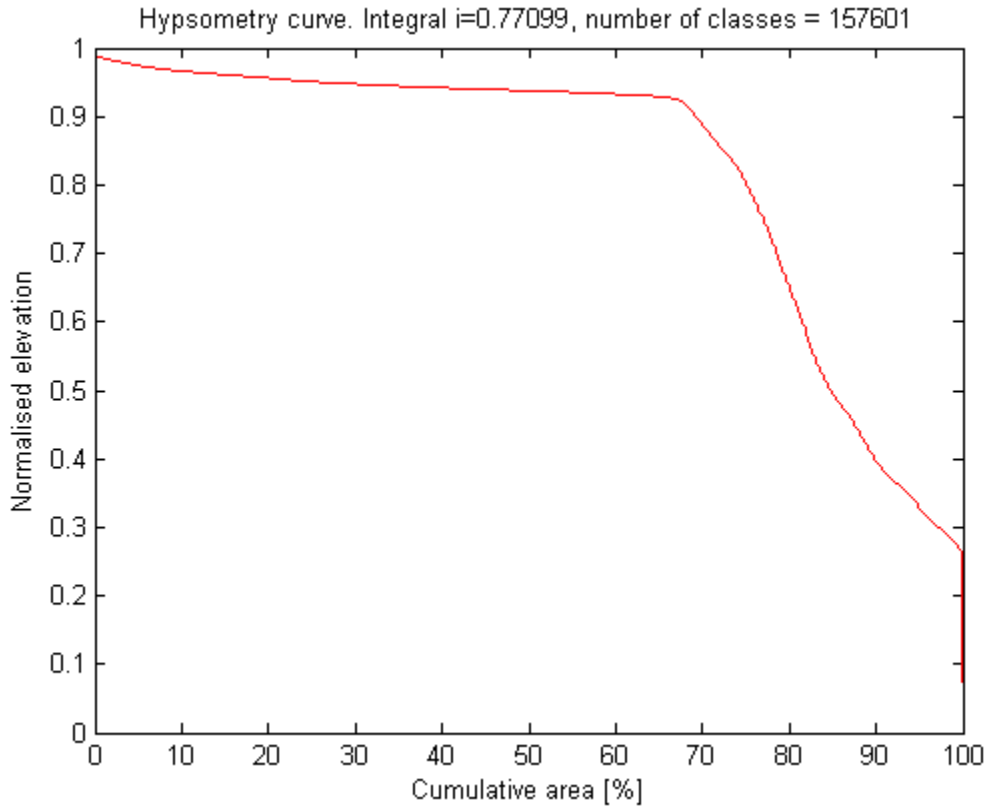

Run 10:

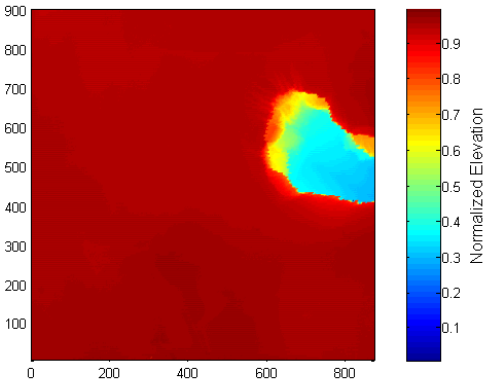

Scan 2: 15 min & 6.88 cm^3 removed

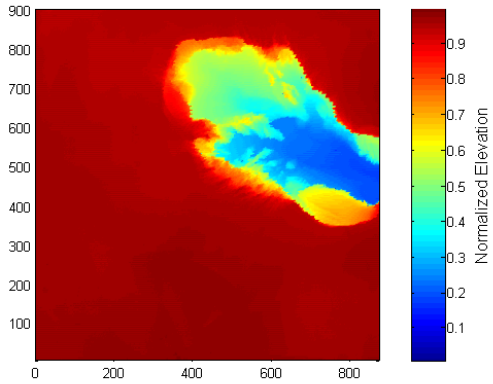

Scan 3: 30 min & 15.42 cm^3 removed

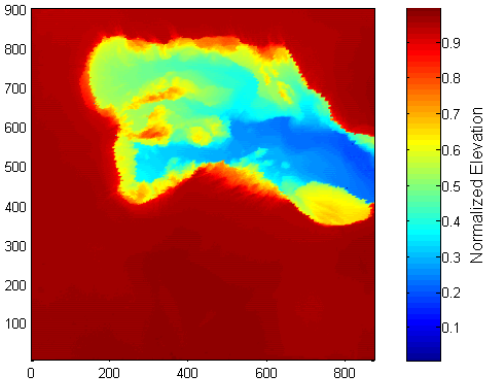

Scan 4: 44 min & 23.16 cm^3 removed

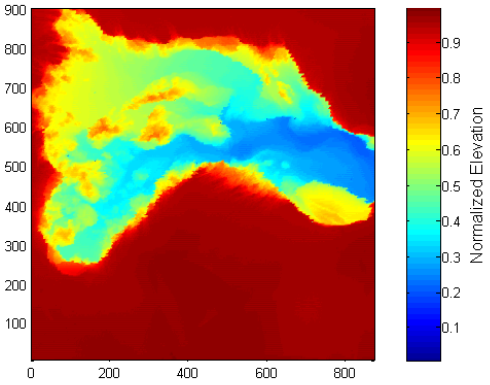

Scan 5: 59 min & 32.00 cm^3 removed

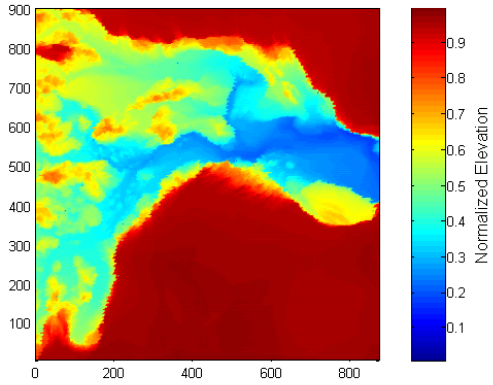

Scan 6: 74 min & 37.95 cm^3 removed

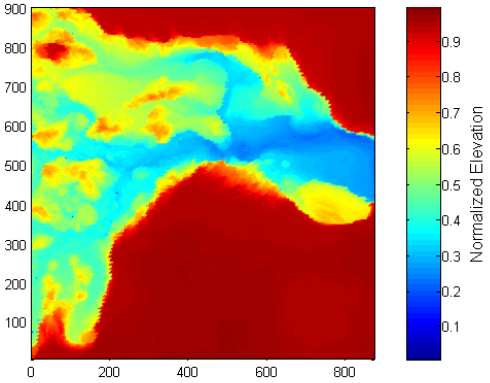

Scan 7: 91.5 min & 39.05 cm^3 removed

D_{50} = 12 µm

Total Volume = 380 L

Total Run Time = 91.5 minutes

1st 190L Flow Rate = 71.69 ml/sec

2nd 190L Flow Rate = 66.41 ml/sec

1st Half Total Volume Removed = 23.16 cm^3

Total Volume Removed: 39.05 cm^3

Run 10 1st Half Hypsometry

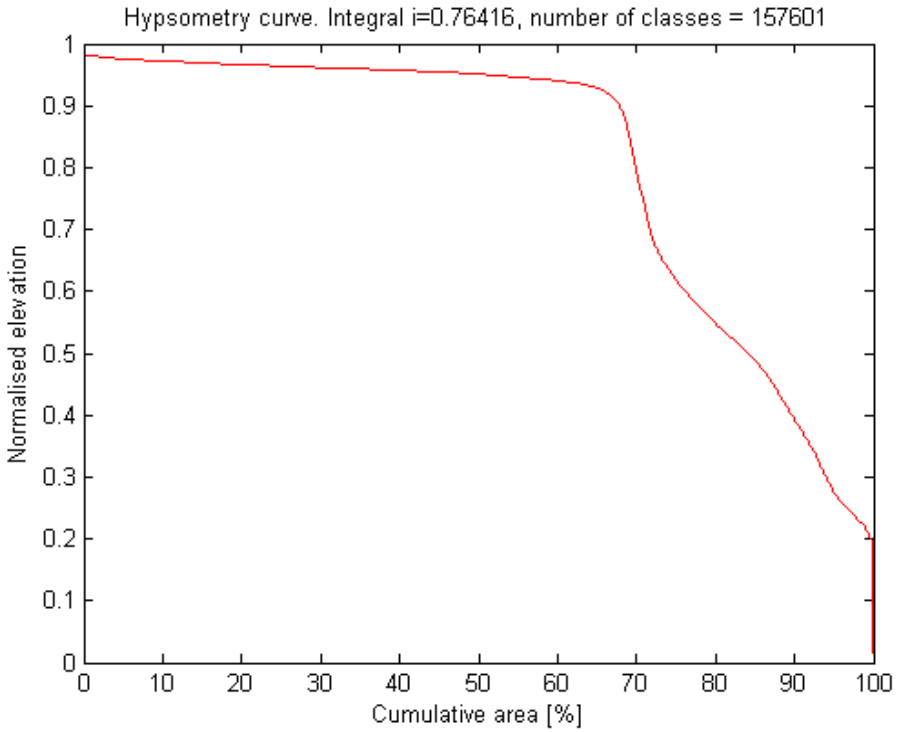

Run 10 Final Hypsometry

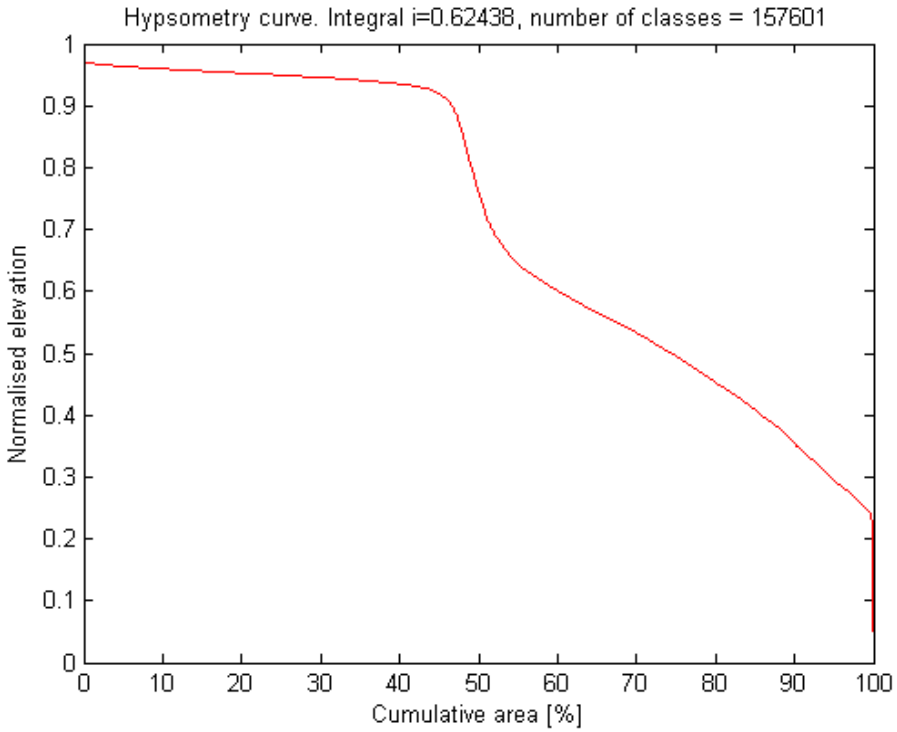

Run 11:

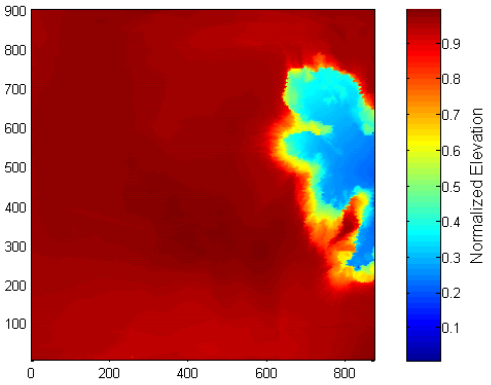

Scan 2: 15 min & 10.31cm^3 removed

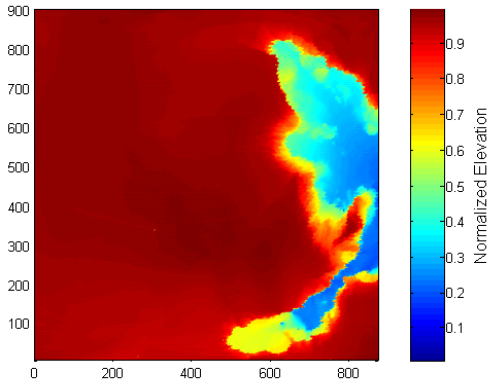

Scan 3: 30 min & 13.90 cm^3 removed

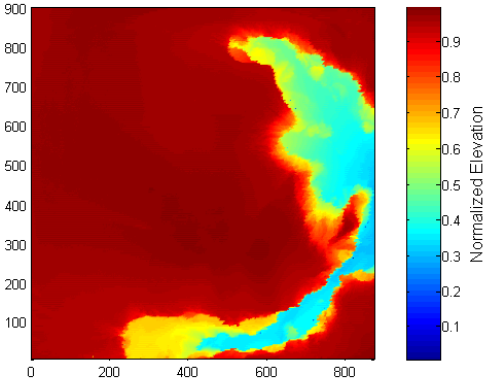

Scan 4: 43 min & 17.12 cm^3 removed

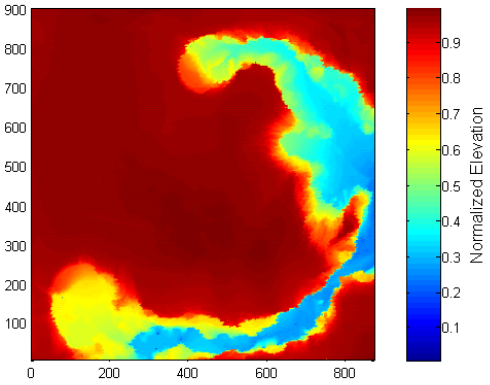

Scan 5: 51 min & 22.18 cm^3 removed

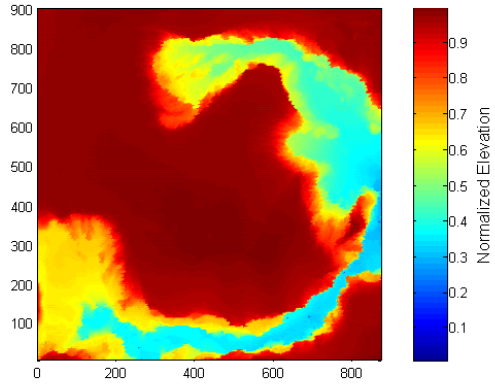

Scan 6: 59 min & 27.39 cm^3 removed

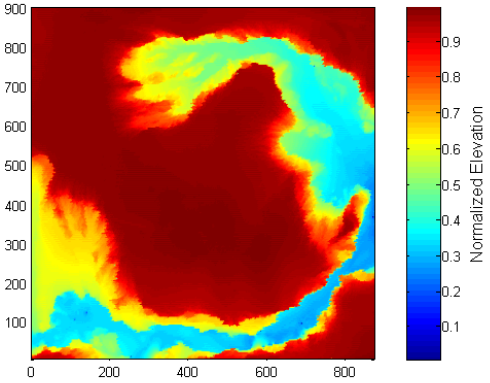

Scan 7: 65 min & 30.16 cm^3 removed

D_{50} = 12 µm

Total Volume = 380 L

Total Run Time = 65 minutes

1st 190L Flow Rate = 73.36 ml/sec

2nd 190L Flow Rate = 143.39 ml/sec

1st Half Total Volume Removed = 17.12 cm^3

Total Volume Removed: 30.16 cm^3

Run 11 1st Half Hypsometry

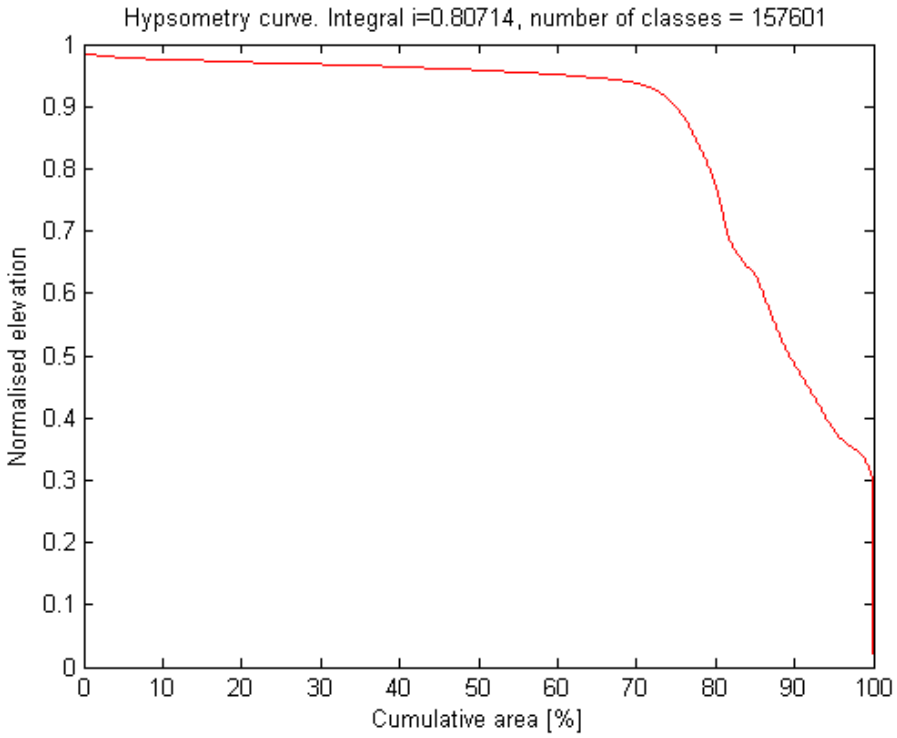

Run 11 Final Hypsometry

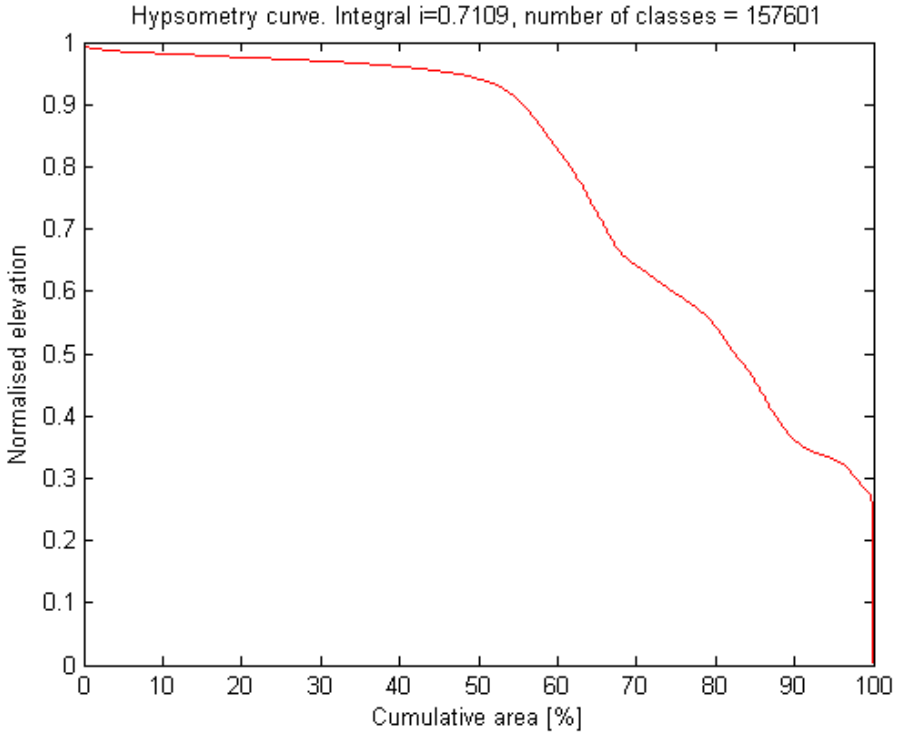

Run 12:

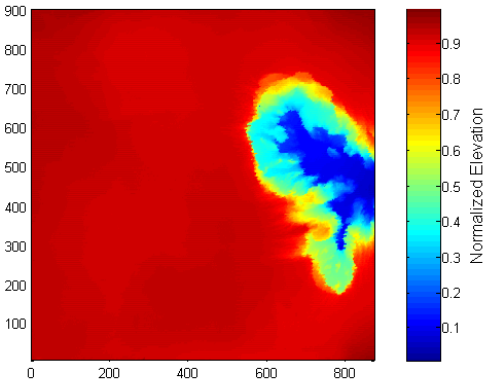

Scan 2: 15 min & 10.96cm^3 removed

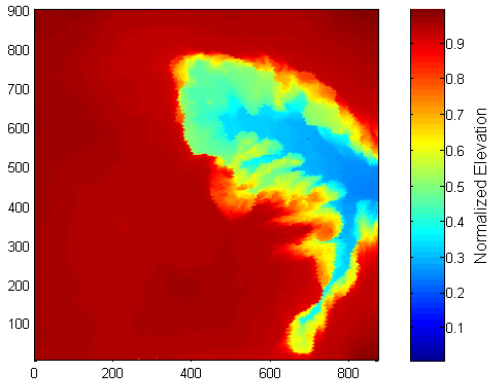

Scan 3: 30 min & 19.17 cm^3 removed

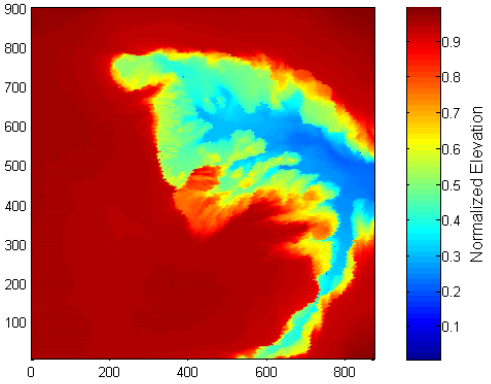

Scan 4: 41 min & 23.38 cm^3 removed

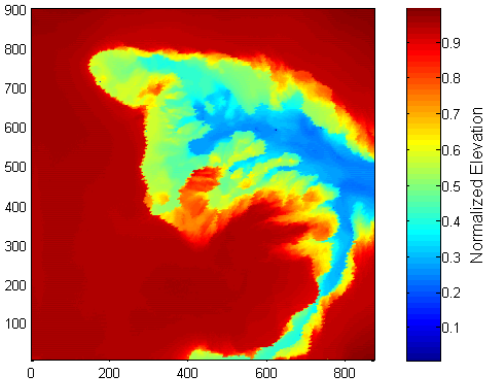

Scan 5: 45 min & 26.65 cm^3 removed

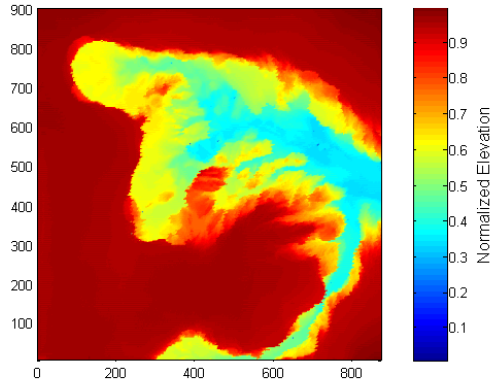

Scan 6: 49 min & 30.12 cm^3 removed

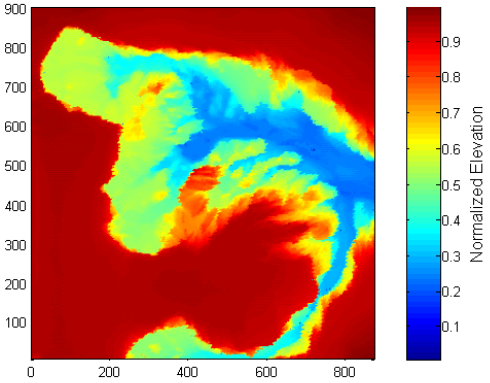

Scan 7: 53 min & 33.85 cm^3 removed

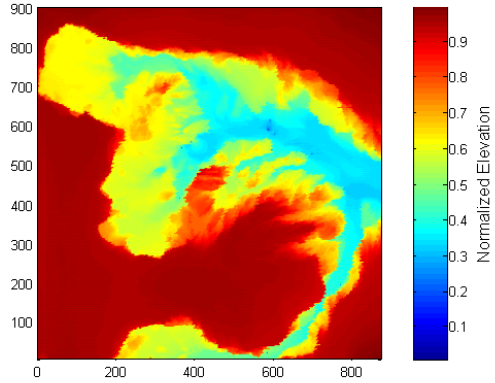

Scan 8: 54.5 min & 35.53 cm^3 removed

D_{50} = 12 µm

Total Volume = 380 L

Total Run Time = 54.5 minutes

1st 190L Flow Rate = 76.94 ml/sec

2nd 190L Flow Rate = 233.67 ml/sec

1st Half Total Volume Removed = 23.38 cm^3

Total Volume Removed: 35.53 cm^3

Run 12 1st Half Hypsometry

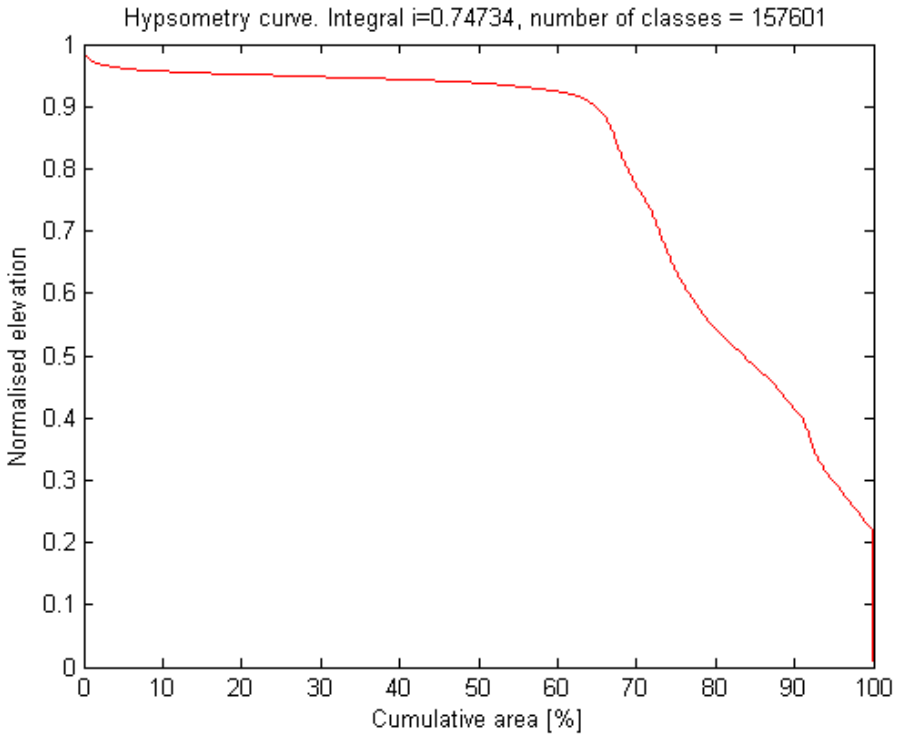

Run 12 Final Hypsometry

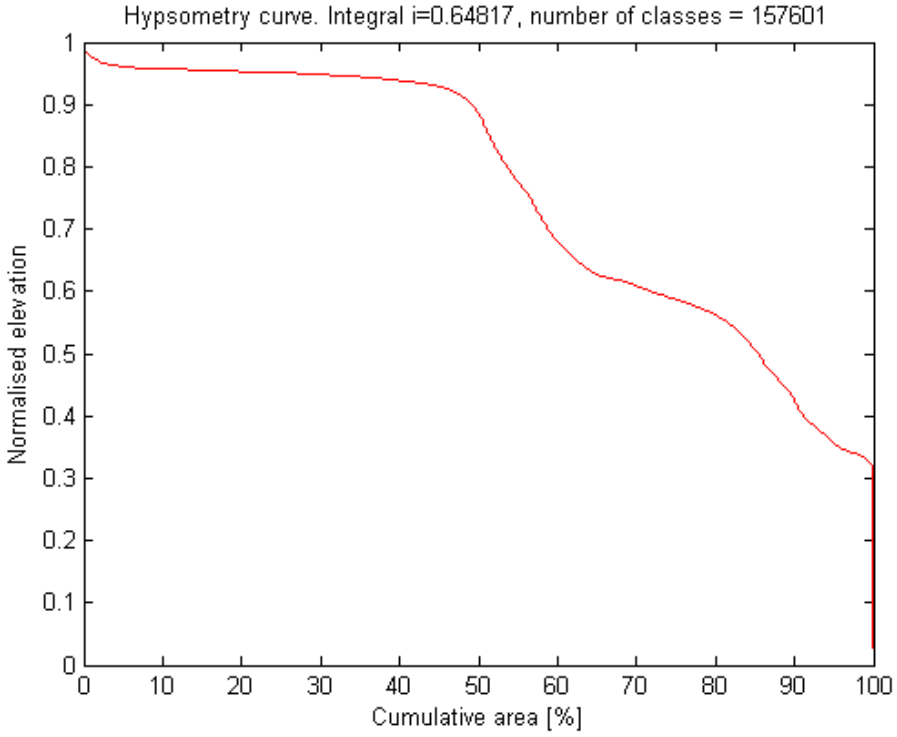

Run 13:

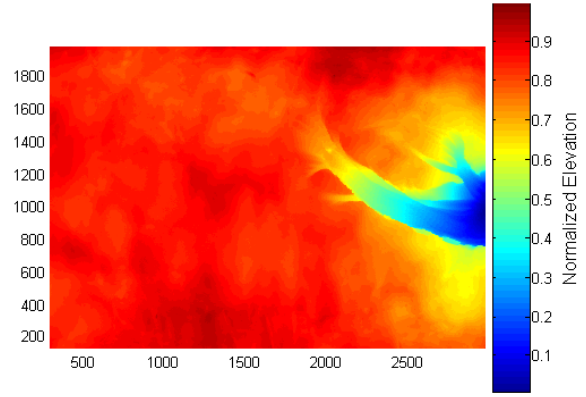

Scan 2: 6.5 min & 10.02 cm^3 removed

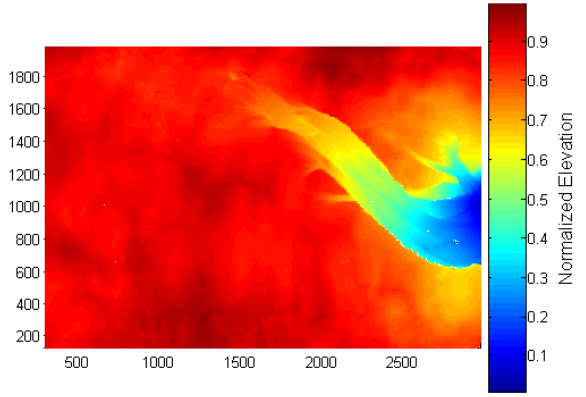

Scan 3: 25.25 min & 17.76 cm^3 removed

D_{50} = 96 µm

Total Volume = 190 L

Total Run Time = 25.25 minutes

Flow Rate = 124.93 ml/sec

Total Volume Removed: 17.76 cm^3

Run 14 Final Hypsometry

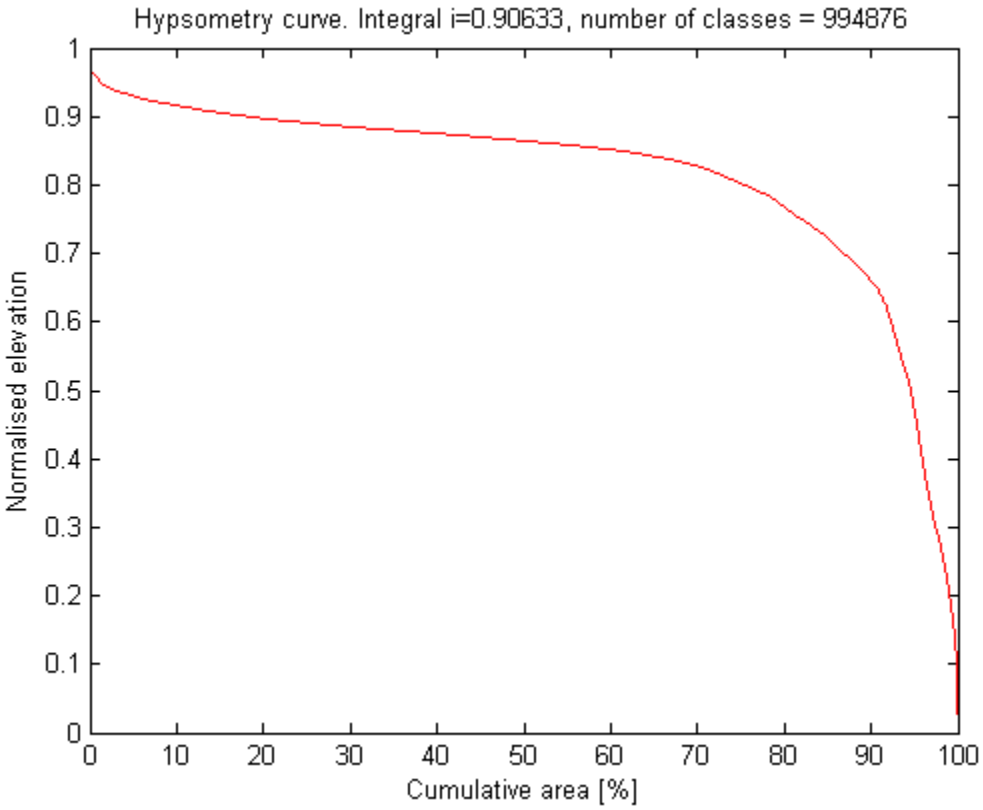

Run 14:

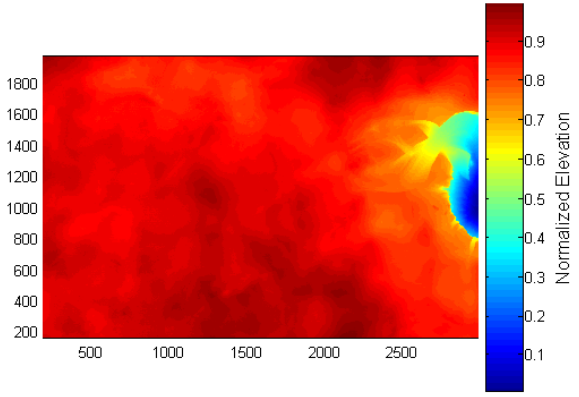

Scan 2: 10 min & 5.06 cm^3 removed

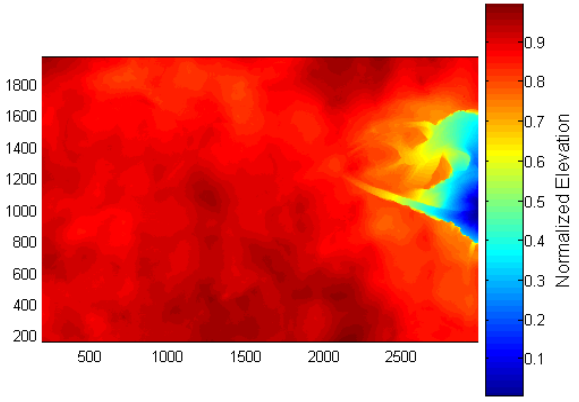

Scan 3: 20 min & 8.77 cm^3 removed

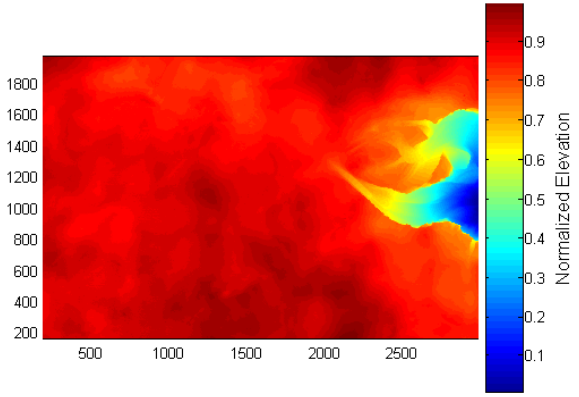

Scan 4: 30 min & 10.67 cm^3 removed

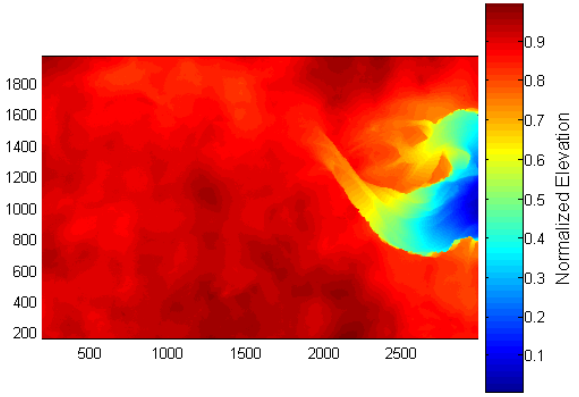

Scan 5: 56.5 min & 18.65 cm^3 removed

D_{50} = 96 µm

Total Volume = 190 L

Total Run Time = 56.5 minutes

Flow Rate = 55.83 ml/sec

Total Volume Removed: 18.65 cm^3

Run 14 Final Hypsometry

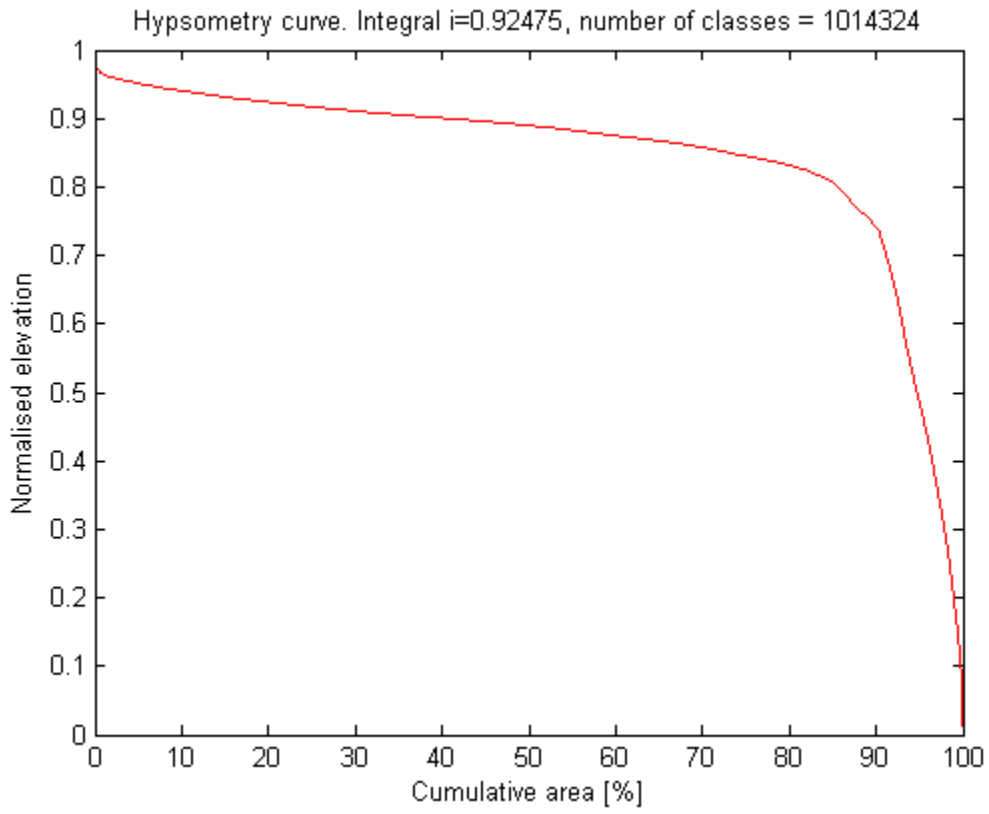

Run 15:

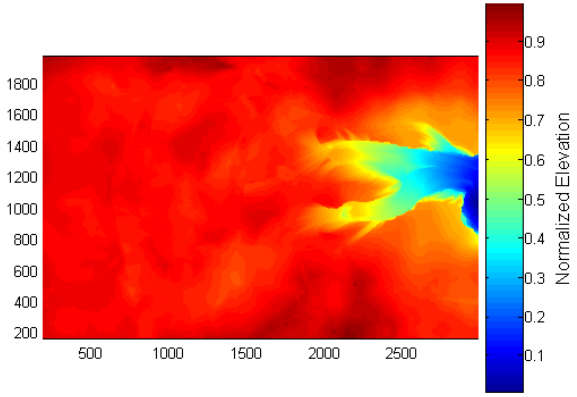

Scan 2: 6 min & 14.96 cm^3 removed

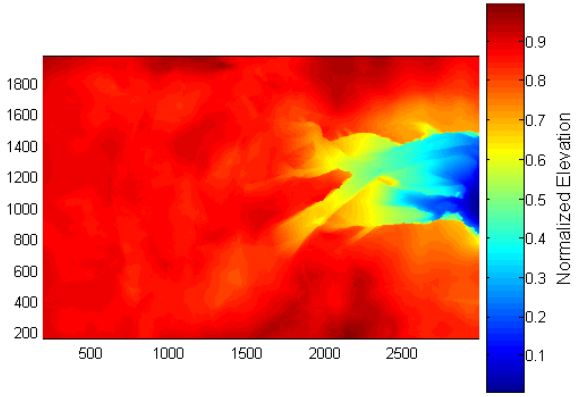

Scan 3: 13.5 min & 23.80 cm^3 removed

D_{50} = 96 µm

Total Volume = 190 L

Total Run Time = 13.5 minutes

Flow Rate = 233.67 ml/sec

Total Volume Removed: 23.80 cm^3

Run 15 Final Hypsometry

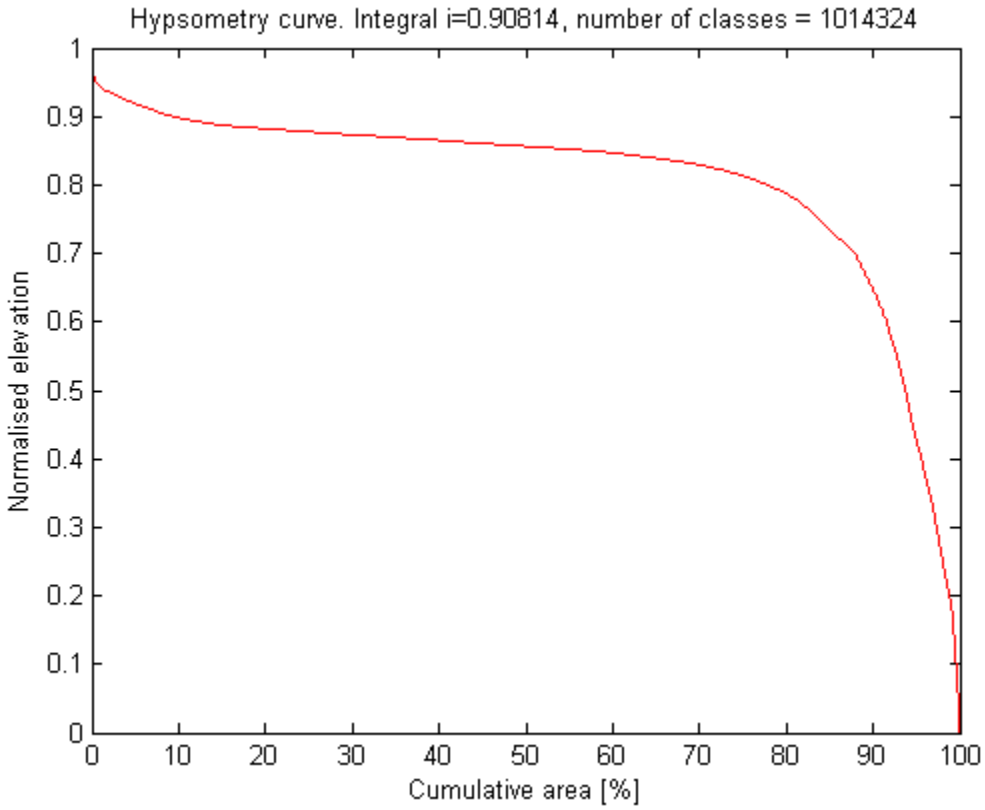

Run 16:

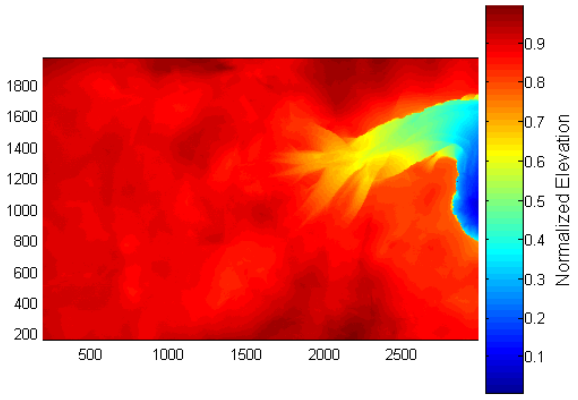

Scan 2: 12 min & 16.59 cm^3 removed

D_{50} = 96 µm

Total Volume = 190 L

Total Run Time = 12 minutes

Flow Rate = 262.88 ml/sec

Total Volume Removed: 16.59 cm^3

Run 16 Final Hypsometry

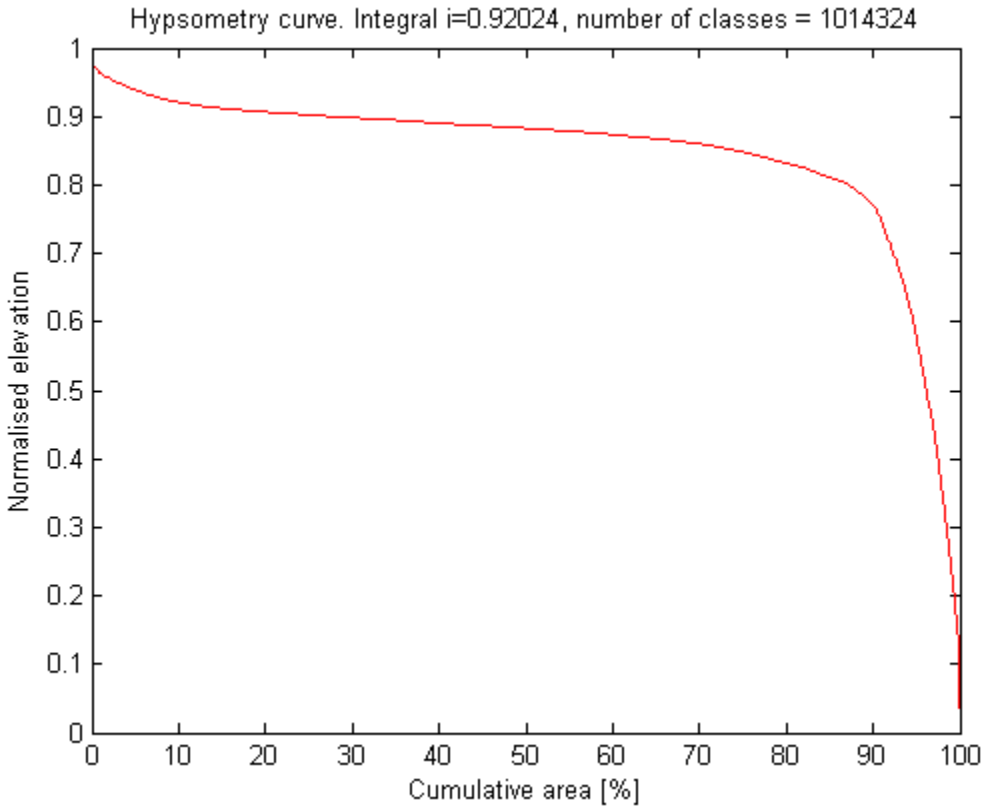

Run 17:

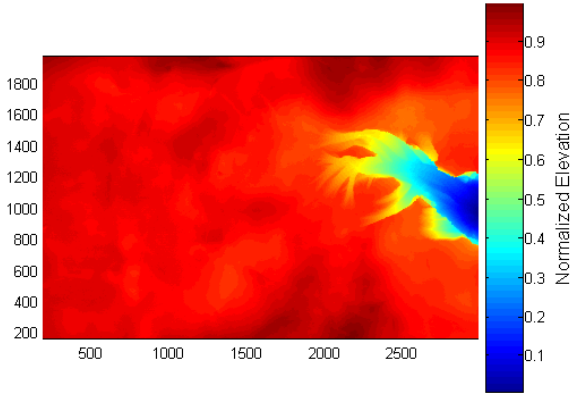

Scan 2: 7 min & 14.59 cm^3 removed

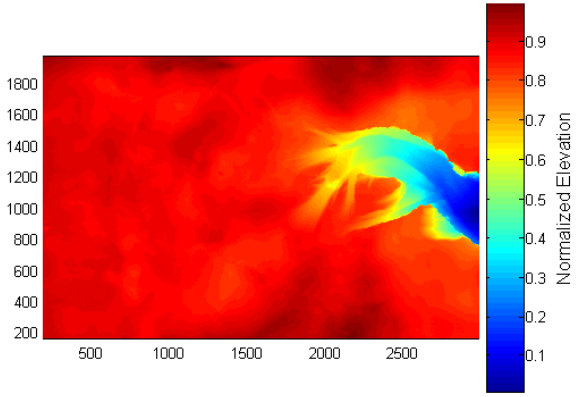

Scan 3: 14min & 20.07 cm^3 removed

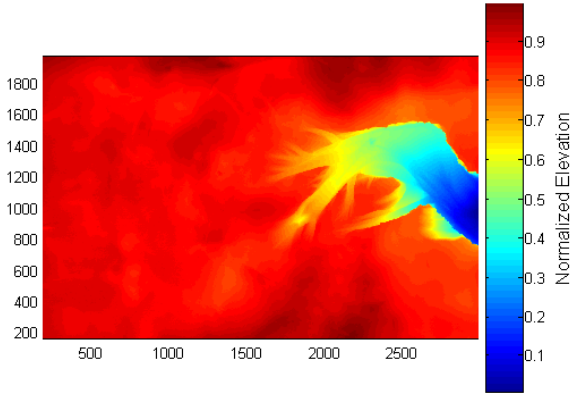

Scan 4: 20.25 min & 23.57 cm^3 removed

D_{50} = 96 µm

Total Volume = 190 L

Total Run Time = 20.25 minutes

Flow Rate = 155.78 ml/sec

Total Volume Removed: 23.57 cm^3

Run 17 Final Hypsometry

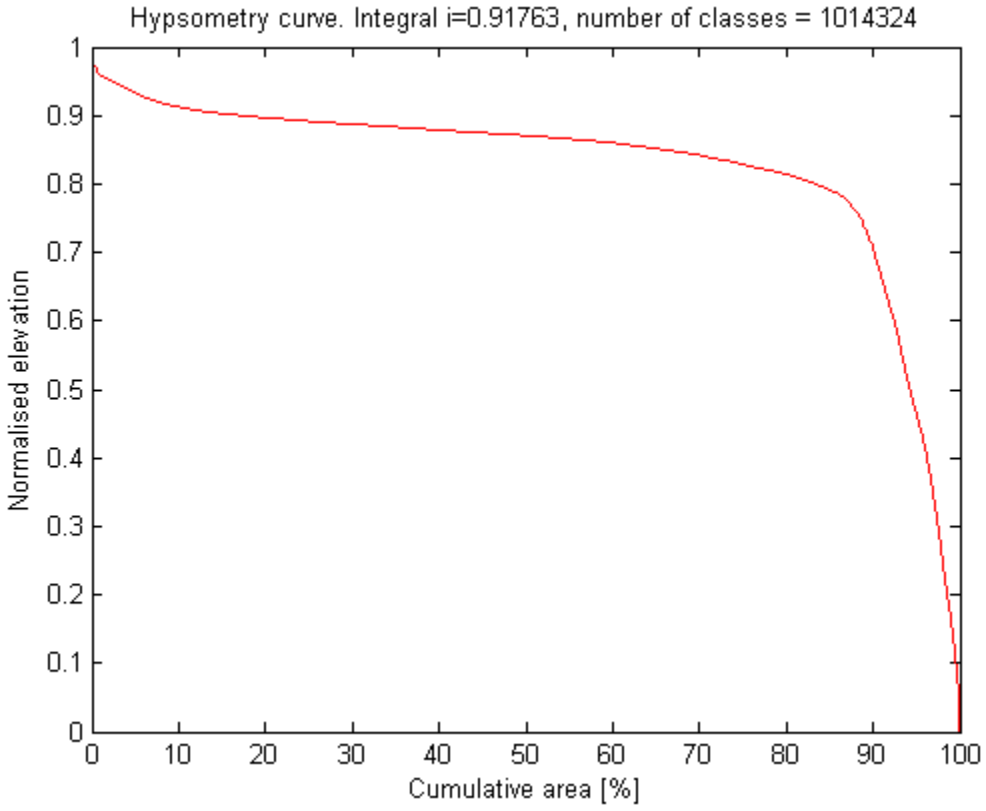

Run 18:

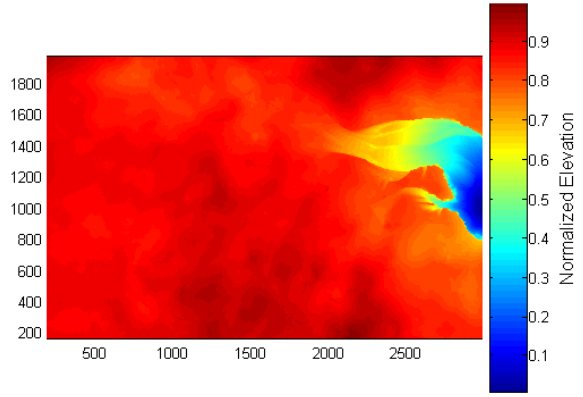

Scan 2: 15 min & 12.21 cm^3 removed

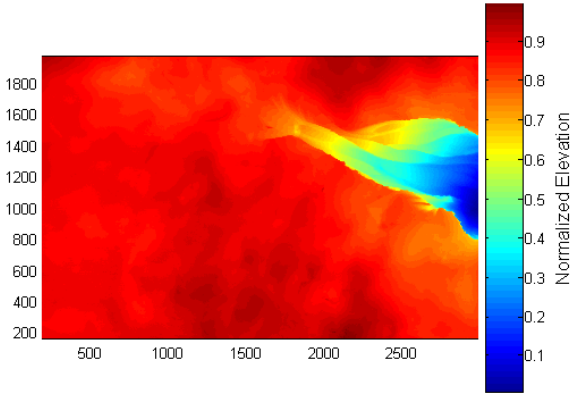

Scan 3: 39 min & 19.99 cm^3 removed

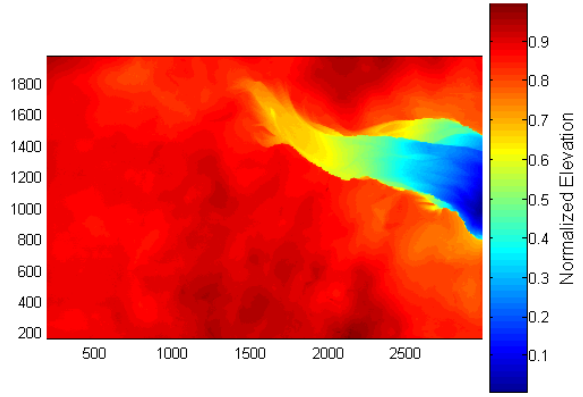

Scan 4: 45 min & 25.08 cm^3 removed

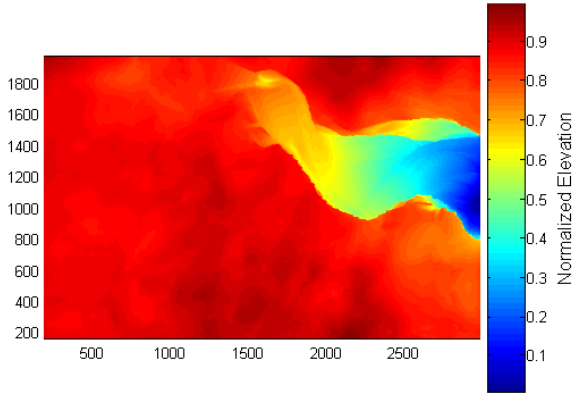

Scan 5: 56 min & 31.17 cm^3 remove

D_{50} = 96 μm

Total Volume = 380 L

Total Run Time = 56 minutes

1st 190L Flow Rate = 80.88 ml/sec

2nd 190L Flow Rate = 185.56 ml/sec

1st Half Total Volume Removed = 19.99 cm^3

Total Volume Removed: 31.17 cm^3

Run 18 1st Half Hypsometry

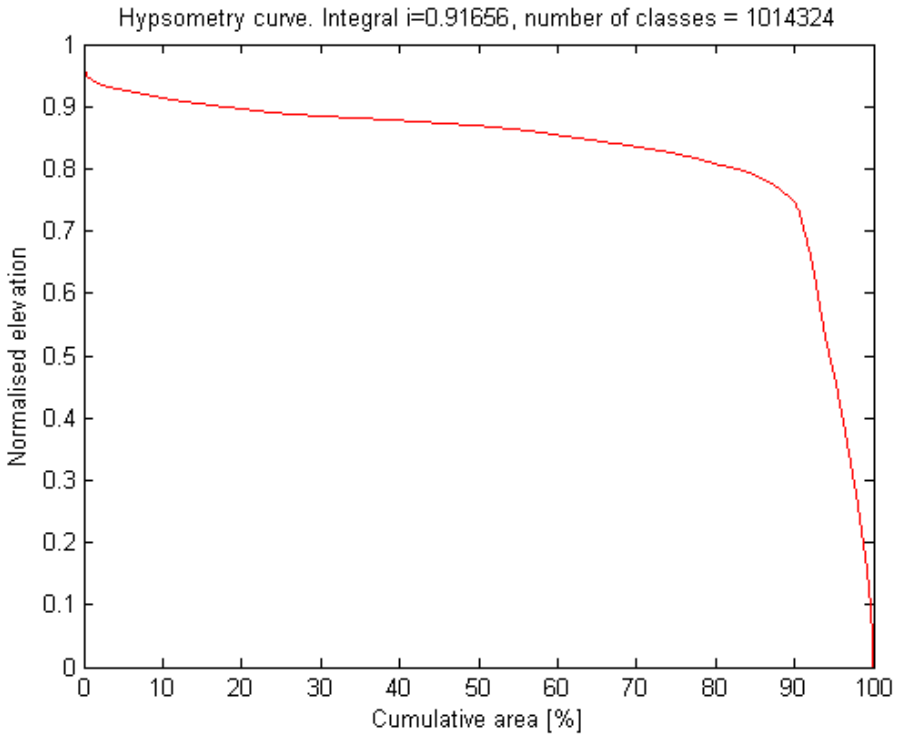

Run 18 Final Hypsometry

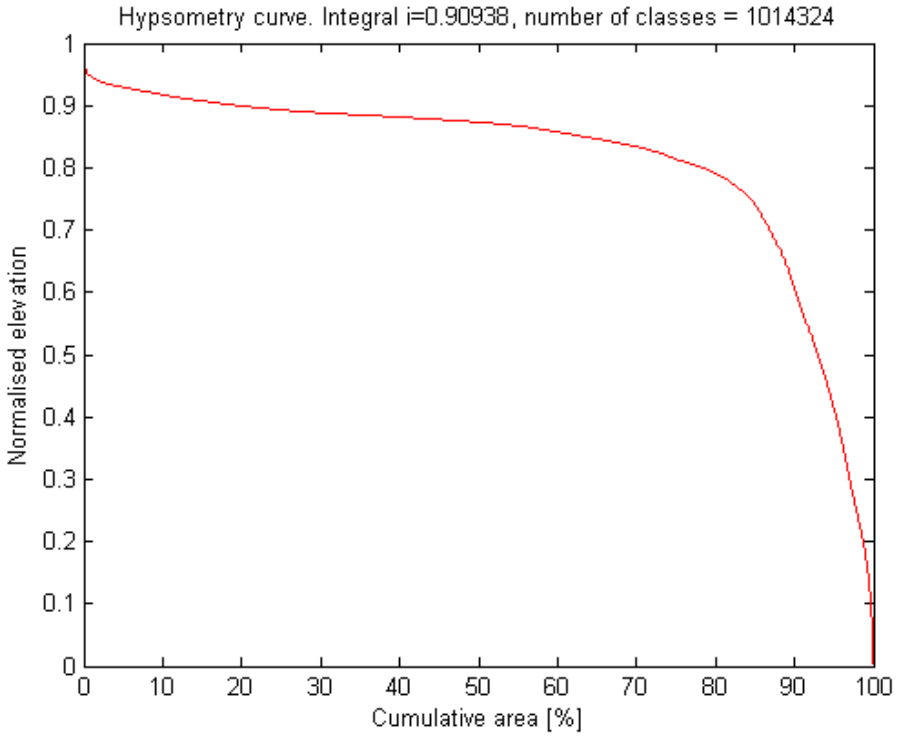

Run 19:

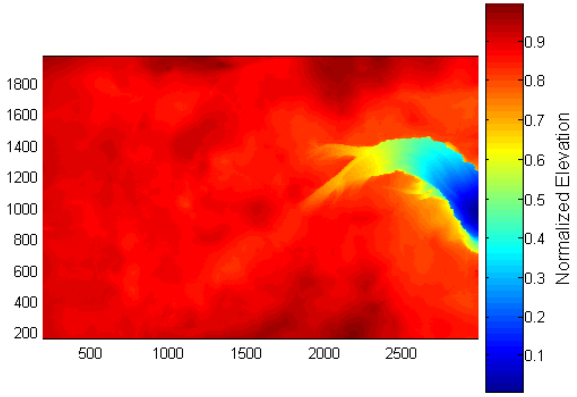

Scan 2: 26 min & 11.09 cm^3 removed

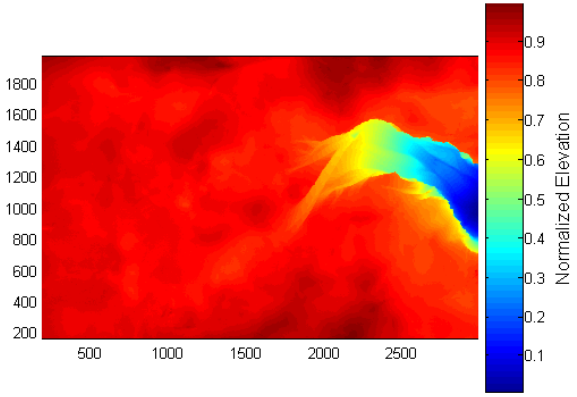

Scan 3: 57 min & 15.66 cm^3 removed

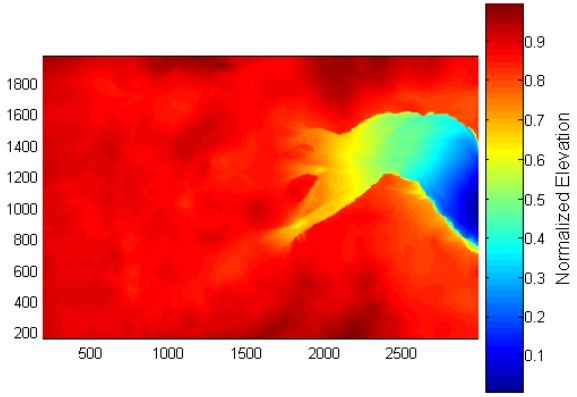

Scan 4: 64 min & 24.15 cm^3 removed

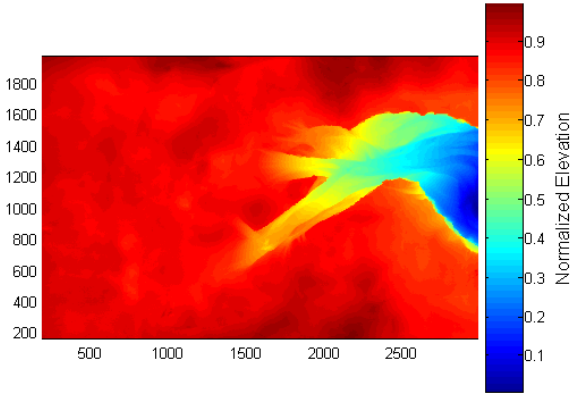

Scan 5: 71.5 min & 30.59 cm^3 removed

D_{50} = 96 μm

Total Volume = 380 L

Total Run Time = 71.5 minutes

1st 190L Flow Rate = 55.34 ml/sec

2nd 190L Flow Rate = 217.55 ml/sec

1st Half Total Volume Removed = 15.66 cm^3

Total Volume Removed: 30.59 cm^3

Run 19 1st Half Hypsometry

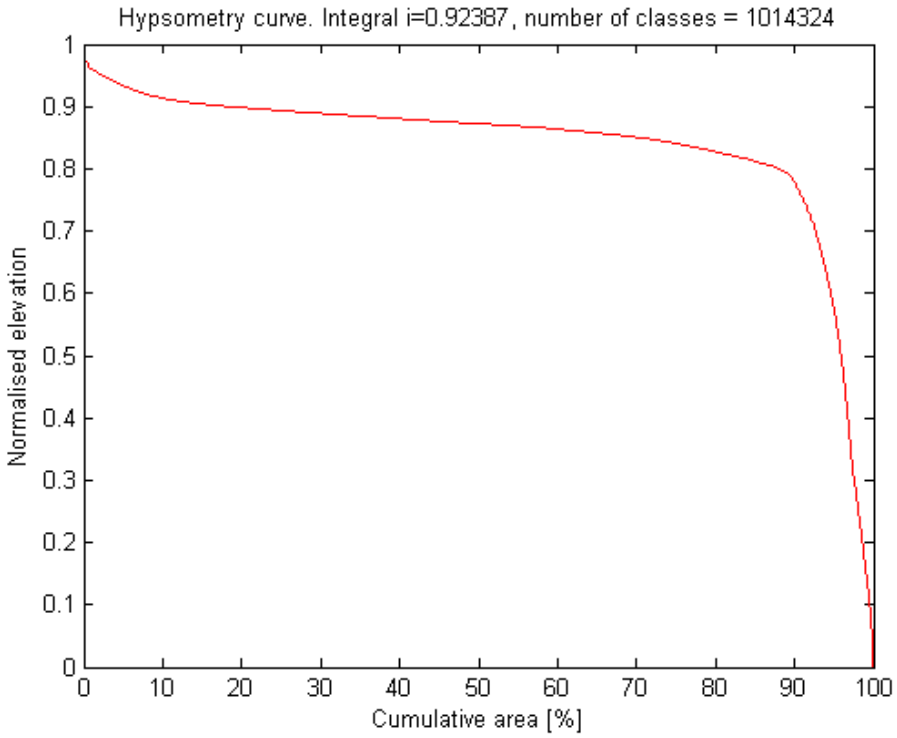

Run 19 Final Hypsometry

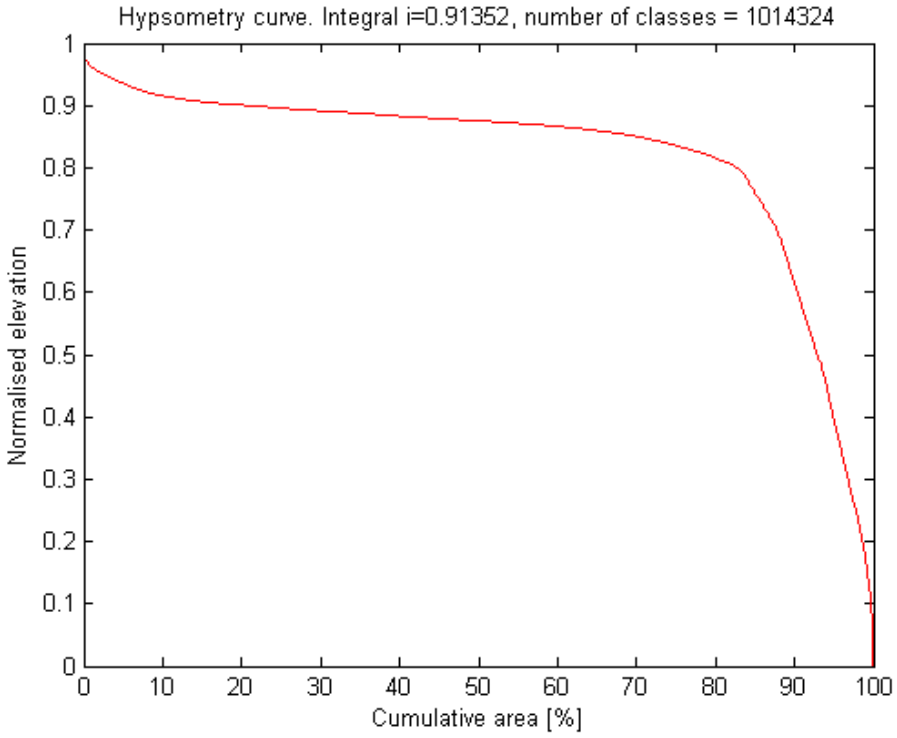

Run 20

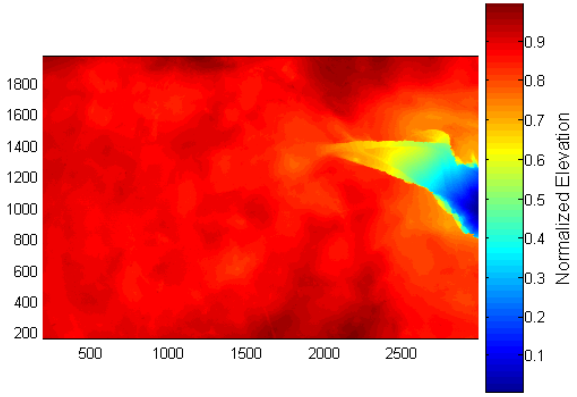

Scan 2: 25 min & 9.25 cm^3 removed

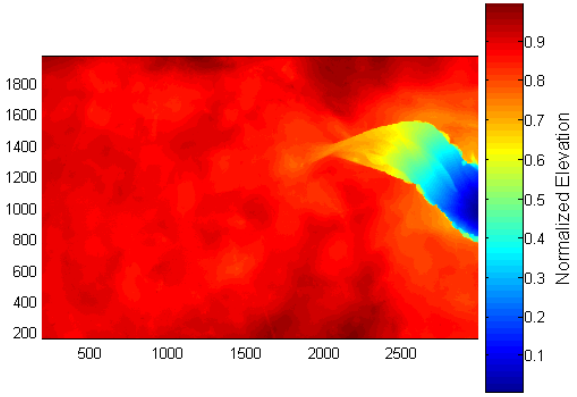

Scan 3: 50 min & 13.68 cm^3 removed

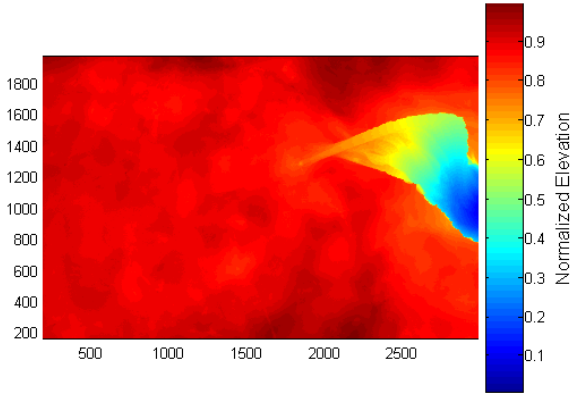

Scan 4: 75 min & 15.87 cm^3 removed

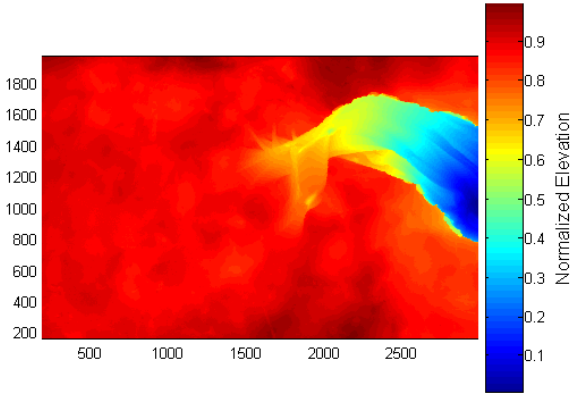

Scan 5: 89 min & 28.03 cm^3 remove

D_{50} = 96 μm

Total Volume = 380 L

Total Run Time = 42.06 minutes

1st 190L Flow Rate = 55.34 ml/sec

2nd 190L Flow Rate = 225.32 ml/sec

1st Half Total Volume Removed = 15.87 cm^3

Total Volume Removed: 28.03 cm^3

Run 20 1st Half Hypsometry

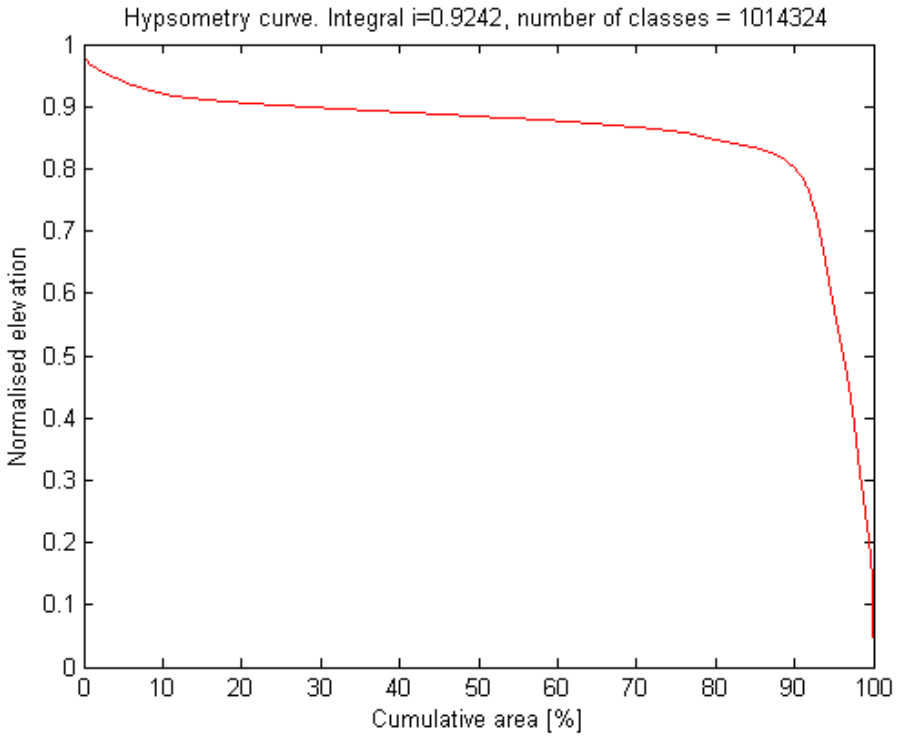

Run 20 Final Hypsometry

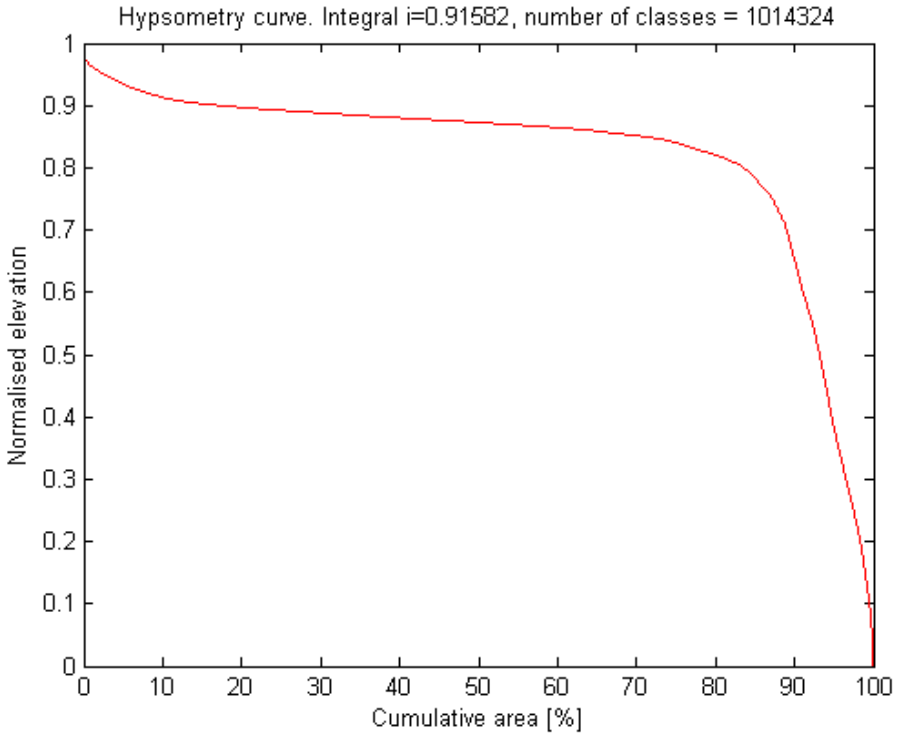

Appendix E: Large shift in source of fine sediment in the Upper Mississippi River

Authors: Patrick Belmont, Karen B. Gran, Shawn P. Schottler, Peter R. Wilcock, Stephanie S. Day, Carrie Jennings, J. Wesley Lauer, Enrica Viparelli, Jane K. Willenbring, Daniel R. Engstrom, Gary Parker

Published in: Environmental Science and Technology, 2011, V. 45, p. 8804–8810. dx.doi.org/10.1021/es2019109.

ABSTRACT

Although sediment is a natural constituent of rivers, excess loading to rivers and streams is a leading cause of impairment and biodiversity loss. Remedial actions require identification of the sources and mechanisms of sediment supply. This task is complicated by the scale and complexity of large watersheds as well as changes in climate and land use that alter the drivers of sediment supply. Previous studies in Lake Pepin, a natural lake on the Mississippi River, indicate that sediment supply to the lake has increased ten-fold over the past 150 years. Herein we combine geochemical fingerprinting and a suite of geomorphic change detection techniques with a sediment mass balance for a tributary watershed to demonstrate that, although the sediment loading remains very large, the dominant source of sediment has shifted from agricultural soil erosion to accelerated erosion of stream banks and bluffs, driven by increased river discharge. Such hydrologic amplification of natural erosion processes calls for a new approach to watershed sediment modeling that explicitly accounts for channel and floodplain dynamics that amplify or dampen landscape processes. Further, this finding illustrates a new challenge in remediating nonpoint sediment pollution and indicates that management efforts must expand from soil erosion to factors contributing to increased water runoff.

INTRODUCTION

Sediment and turbidity are leading causes of impairment in U.S. rivers and streams (1,2) and remedial action requires identification of the sources and mechanisms of sediment supply. Despite extraordinary efforts, sediment remains one of the most difficult nonpoint-source pollutants to quantify for several reasons (3-7). Erosion is typically episodic and highly localized. Erosion mechanisms are strongly nonlinear and their rates are contingent on multiple factors including climate, geology and land use history (8,9). Eroded sediment may exit the watershed quickly or be stored for very long periods (10,11). Finally, the accuracy of current methods for

estimating sediment yield from agricultural watersheds has been challenged (4,8,12) because most estimates are based on empirical models of soil erosion and require a scalar reduction factor to estimate sediment yield as a fraction of erosion. Few studies provide evidence to constrain this reduction factor and available observations indicate diverse and highly nonlinear scaling with drainage area (7).

Accurate identification of sediment sources and erosion rates are needed to understand and manage the landscape sediment routing system (13) and related biogeochemical processes (14). The reliability of sediment source estimates can be improved by using multiple, overlapping methods of measurement within the strong constraint of a mass balance, or sediment budget (15). A sediment budget is a useful tool for evaluating landscape change and sediment yield (10, 16-19). The scope and accuracy of sediment budgets depend strongly on the availability of information for earlier conditions in a watershed. For example, historical information such as photos, maps, and field studies have been used to provide reliable information on previous conditions in order to close a sediment budget over a time period long enough to average over stochastic temporal variability. This approach is strengthened by a suite of new research tools that allow precise dating of land surfaces, geochemical identification of sediment provenance, and high-resolution measurement of topography using airborne and terrestrial lidar (20,21).

The waters of the Upper Mississippi River (UMR) and its major tributaries have been listed as impaired for turbidity by the U.S. Environmental Protection Agency. Turbidity, eutrophication, and sedimentation have been identified as urgent problems for Lake Pepin, a natural lake on the Mississippi River of exceptional recreational and popular importance (Figure 1). Coring records examining the past 500 years indicate that sedimentation rates in Lake Pepin may have increased by as much as an order of magnitude over the past 150 years (22). Of the sediment delivered to Lake Pepin, past and present, 80% to 90% derives from the Minnesota River Basin (MRB), despite the fact that the MRB comprises only a third of the drainage area (22,23). The relatively high sediment yield of the MRB stems from a combination of Quaternary landscape history and human land and water management. Land cover in the basin has shifted from poorly drained tall-grass prairie and wetlands (24) to 78% row crop agriculture (25) over the 150 yr period of increased sedimentation, suggesting that the change in land use underlies the increase (26).

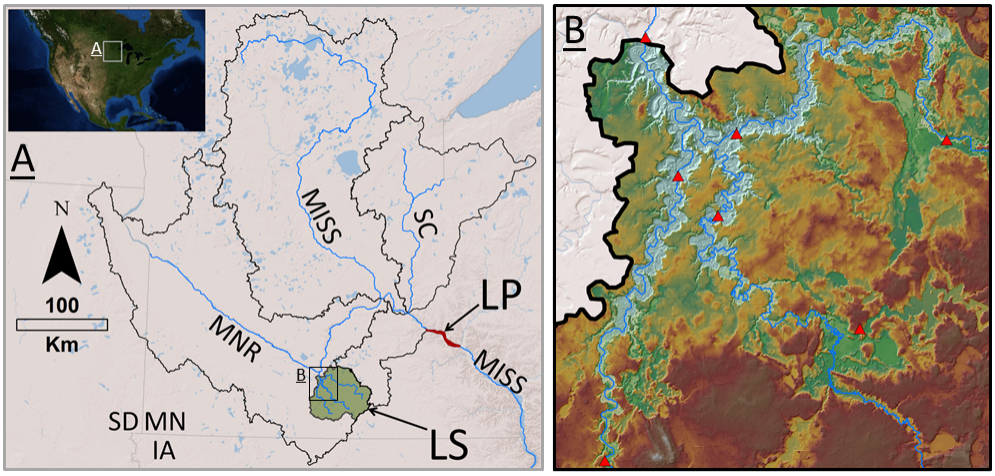

Figure 1: Inset A shows the Lake Pepin (LP) watershed within the upper Midwest, composed of the Minnesota (MNR), upper Mississippi (MISS) and St. Croix River (SC) watersheds. Inset B shows lidar topography data for the incised portion of the Le Sueur watershed (LS), including the locations of gaging stations on all three main branches.

The 2880 km^2 Le Sueur River watershed produces the highest sediment yield (73.5 Mg/km^2) of any Minnesota River tributary, accounting for as much as 30% of the Minnesota River sediment load (26). The Le Sueur landscape is naturally primed for rapid geomorphic change and large sediment supply. The geologic substrate is a 60 m thick package of semi-consolidated, but soft, fine-grained (67% silt and clay, 33% sand, <1% gravel and boulders) tills and glaciofluvial sands (27). Glacial Lake Agassiz drained catastrophically through the proto-Minnesota River 13,400 years ago, incising the Minnesota River valley up to 70 meters near the mouth of the Le Sueur (28,29). This incision was experienced by the Le Sueur as a drop in local base level causing a knickpoint, or a sharp increase in channel gradient, at the mouth of the Le Sueur. The knickpoint has propagated 40 km up the Le Sueur River network (30,31), leading to rapid vertical incision (~5 m/ka) producing valleys with steep river gradients (0.002 m/m), actively eroding bluffs, and ravines. We refer to this expanding, incised reach of the channel network as the knickzone, and the upstream propagating head of the knickzone where the slope discontinuity is observed as the knickpoint (Figure 2).

Prior to settlement, the landscape was dominated by tall-grass prairie and wetlands (24). Above the knickpoint the channel network was poorly connected with many areas that drained internally to wetlands and ponds within the watershed. Beginning in the 19th century, an expanding network of surface ditches and subsurface conduit has drained the wetlands and uplands, allowing development of agriculture (32). Beginning in the 1940s, changes in technology and markets led to consolidation of smaller farms into larger operations. These changes are perceived to have initially resulted in more intense and severe agricultural practices, which have more recently evolved into more careful and precise agricultural management (33). However, little quantitative information has been collected to constrain the magnitude of these effects on historical erosion and sediment delivery. Presently, row crops cover as much as 92% of the uplands in the basin (25).

The investment required to reduce sediment loading and other nonpoint-source water quality problems is enormous. As an indication, a substantial down payment was made in 2008 when Minnesotans passed a state constitutional amendment that will raise over $3.5 billion in tax revenue over 25 years for the purpose of protecting and restoring water, wildlife, and cultural

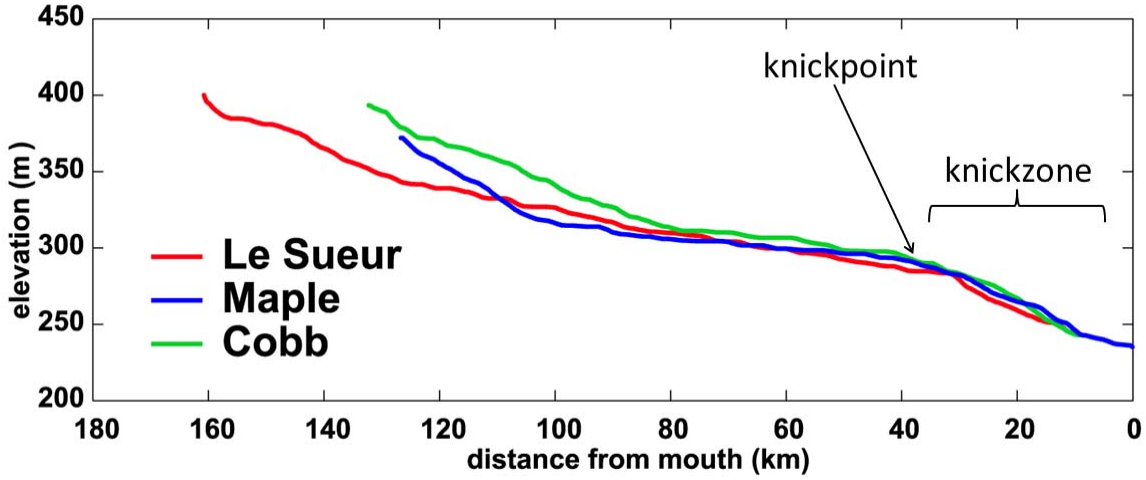

Figure 2: Longitudinal profiles of the Le Sueur River (red) and its two main tributaries, the Maple (blue) and Cobb (green) rivers. The locations of the knickpoint, approximately 40 km from the mouth in all three branches, as well as the knickzone, or reach of active incision, are indicated.

resources (34). Effective use of the portion of these funds dedicated to reducing sediment pollution will require accurate identification of sources and mechanisms of sediment supply. This issue is controversial, particularly in determining the role of historic and contemporary agricultural practice versus natural erosion processes (35). The stakes are high; management choices will have political, social, and financial implications, as well as environmental consequences.

In this study, we combine multiple, independent lines of evidence to evaluate sediment sources to the UMR. We use geochemical fingerprinting from Lake Pepin sediment cores to interpret erosional history at the landscape scale and to record shifts in the proportion of sediment derived from soil erosion vs. near-channel sources. For the purposes of this paper we use the term 'soil erosion' to refer to removal of sediment from the vast and relatively flat upland terrestrial surface via sheet wash, shallow gully erosion, and wind erosion. The term 'near-channel erosion' is used to refer to processes of channelized fluvial erosion including incision and undercutting of bluffs, banks, and ravines. We also use a sediment budget for the Le Sueur River, a primary contributor of sediment to the Minnesota River, to identify sediment source location and mechanism. We compare the sediment budget constrained for the time period 2000-2010 with the same averaged over the entire Holocene to provide context for the modern rates under current land use and environmental conditions. The sediment budgets are established for silt and clay (< 62 μm), which is the primary contributor to turbidity and deposition in Lake Pepin. Key to our approach is the use of multiple, redundant sources of information to constrain each component of the budget, including aerial lidar analyses, repeat terrestrial lidar scans, geochemical fingerprinting, radiocarbon and optically stimulated luminescence dating, air photo analyses, field surveys, and extensive water and sediment gaging. Details on methods and development of the sediment budgets are presented in Supplementary Information.

METHODS

Sediment Budgets.

The Holocene sediment budget was primarily constrained through analyses of high resolution (1 m) lidar topography data and dating of strath terraces. We hand-digitized polygons of the incised valley and ravines independently. The upper extent of the modern knickzone was defined by the location of discontinuities in log-log plots of local channel gradient versus contributing drainage

area for each of the three main tributaries using the Stream Profiler Tool (available for free download from www.geomorphtools.org). Over 600 strath terrace surfaces were mapped from aerial lidar and field surveys. Optically stimulated luminescence and Carbon-14 analyses of terrace alluvium confirmed the timing of initial incision and constrained rates of incision throughout the Holocene. To compute the mass of material in the incised valley and ravines we divided the valley polygons into 3 km sections and assumed a flat surface with an elevation consistent with surrounding topography. Volumes of sediment removed were converted into a mass using a bulk density of 1.8 g/cm^3 and 67% silt and clay and were divided by 13,400 years to obtain the long-term average rate of mass flux from the knickzone (29).

Each component of the 2000-2010 sediment budget was constrained using multiple lines of information. Annual sediment loads were computed by the Minnesota Pollution Control Agency for all seven gaging stations in the Le Sueur River basin using US Army Corps of Engineers FLUX program. Flow and sediment data were available for all years (2000-2010) for the gage at the mouth of the watershed. Average 2000-2010 loads were computed for each of the tributary gages based on available data (3-9 years depending on the tributary), with missing tributary data estimated relative to the gage at the mouth of the watershed (see Supplementary Information).

Bluff erosion rates were constrained over a decadal timescale from air photo analyses. A total of 451 bluffs were identified from air photos and their crests were manually digitized for multiple years between 1938 and 2005. Bluff toe retreat was independently estimated by measuring channel meander migration rate near the toe using the Planform Statistics Tool available online from the National Center for Earth-surface Dynamics Stream Restoration Toolbox (http://www.nced.umn.edu/content/tools-and-data). Additionally, bluff-related sediment sources were constrained by three years of repeat terrestrial laser scanning covering a wide range of hydrologic years including intermediate, dry, and wet years for 2008, 2009, and 2010, respectively. An Optech ILRIS-3$_6$D, ER Terrestrial Lidar Scanner from the Lidar Lab at Western State College of Colorado was used to scan 12 bluffs at resolutions varying from 1700 to 10,000 points per m^2. Polyworks metrology software (InnovMetric, Quebec City, Canada) was used to align scans, convert point cloud data to TINs, and digitally remove vegetation. An extensive error analysis was conducted to constrain error due to instrumentation, alignment, TIN creation, erroneous points, and assumptions made differencing scans from multiple years (36). Volumetric

bluff erosion rates were computed as the product of bluff height, length, and retreat rate and converted to mass flux using a bulk density of 1.8 g/cm^3 and 67% silt and clay.

Net local bank erosion rates were computed using the method of Lauer and Parker (37), which computes net, local sediment flux from bank erosion as a function of a measured meander migration rate and the difference in elevation between opposing channel banks. To perform this calculation we used the Planform Statistics Toolbox. Meander migration rates were measured from historic air photo analysis (1938-2005), discretizing the channel every 20 m, and bank elevations were extracted from 1 m aerial lidar (source: Blue Earth County Environmental Services) using a 10 m buffer on each bank. Bank contributions from channel widening were computed by digitizing banks from historic air photos (1937-2009), identified by vegetation line, for multiple years and over 14 reaches, each approximately 10 meander bends in length. Width change was converted to volumetric change by computing average depth from a basin- specific downstream hydraulic geometry relationship and assuming that depth remains constant as the channels widen at the observed rate. Volumetric bank erosion rates were converted to mass flux using a bulk density of 1.5 g/cm^3 and 50% silt and clay.

We used airborne lidar to map ravine locations throughout Blue Earth County and compared historical air photos from 1938 and 2005 to identify recent changes in ravine tip locations. Ravine loads were measured using auto-samplers to capture storm events for three monitoring seasons on up to four ravines. Loads were extrapolated to other ravines throughout the watershed based on incised area measured from aerial lidar. See Supporting Information for data and additional explanation of methods.

Geochemical Fingerprinting. We conducted sediment fingerprinting (38, 39) using naturally-occurring radiogenic tracers Beryllium-10 (^{10}Be) and Lead-210 (^{210}Pb), and Caesium-137 (^{137}Cs) measured in suspended sediment samples collected at multiple gages within the Le Sueur watershed as well as from Lake Pepin sediment cores. In brief, ^{10}Be and ^{210}Pb are produced in the atmosphere, delivered via rainfall and dry deposition, and are adsorbed to the outside of soil particles within the top 150 and 5 cm of the soil profile, respectively (40, 41). Thus, both tracers exhibit relatively high concentrations in sediment eroded from the soil surface and low concentrations in bluff material, which has experienced relatively little exposure to the atmosphere. Caesium-137 was delivered from atmospheric deposition primarily from nuclear

testing in the 1950s and 1960s (41, 42) and the concentration is also high in upland soils and low in near-channel (bluff, ravine, bank) sediment.

Because these tracers are radioactive and have very different half lives (1.4 million yr, 22.3 yr, and 30 yr for ^{10}Be, ^{210}Pb, and ^{137}Cs, respectively) their concentrations change during transport and storage in the channel-floodplain network (43-46). Specifically, ^{10}Be decay is negligible over the timescales in which channel transport and floodplain storage occur. However, some additional ^{10}Be is added to sediment during floodplain storage. In contrast, ^{210}Pb and ^{137}Cs decay over floodplain residence times (assumed to be 10^2-10^3 yr) and therefore the upland signature of these tracers is diluted to a degree that depends on the rate of channel floodplain exchange. In this way, ^{10}Be fingerprinting provides an upper constraint and ^{210}Pb and ^{137}Cs provide minimum constraints on the percentage of sediment derived from uplands. Determining a unique solution for sediment apportionment based on combined ^{10}Be, ^{210}Pb and ^{137}Cs data is not possible at this time for a number of reasons, including number of samples available, insufficient constraints on the variability of atmospheric delivery rates, and the lack of independent constraints on channel-floodplain exchange activity. Therefore, we compute source apportionment for suspended sediment samples based on ^{10}Be results using a two end-member unmixing model (bluffs: [^{10}Be] = 0.07 (± .01) x 10^8 atoms g^{-1}; uplands: [^{10}Be] = 2.0 (± .36) x 10^8 atoms g^{-1}). Suspended sediment samples were also analyzed for ^{210}Pb and ^{137}Cs by alpha and gamma spectroscopy. We collected a total of 28 suspended sediment samples from the Le Sueur River and tributaries during the 2009 field season. Sample activity for ^{210}Pb was corrected for direct deposition and sediment apportionment for both ^{210}Pb and ^{137}Cs were computed based on an extensive dataset from 30 reference lakes to constrain the upland tracer signature, described in detail by Schottler et al. (47). See Supporting Information for data and additional explanation of methods.

RESULTS AND DISCUSSION

The well-dated incision history and low-gradient post-glacial terrain of the Le Sueur watershed (29) allow us to establish an average sediment budget for the Holocene. We used aerial lidar combined with optically stimulated luminescence dating (48) to compute the volume of material excavated from the incised valley and ravines over the Holocene (Figure 3, top panel). Valley excavation produced 60,000 Mg/yr, with 80% from bluff erosion (Bl), bank erosion (Ba), and vertical channel incision (C) and 20% from ravine incision (R). A small amount of deposition

(Fp) within the incising valley, equivalent to 5000 Mg/yr, is recorded in strath terraces (29). Sediment evacuation modeling based on dated terraces suggests that sediment yield was relatively steady over the Holocene (48). Prior to Euro-American settlement in the early 19th century sediment supply from the poorly-drained, low-gradient, uplands of dense perennial grasses and wetlands was assumed negligible relative to that from the incising valley.

We developed a sediment budget for the period 2000-2010 (Figure 3, bottom panel), relying on estimated sediment loads at seven gaging stations, including one at the mouth of the watershed, and two on each of the three main branches, with one just upstream from their confluence and the other just above the knickpoint (red triangles in Figure 1). Bluff erosion (Bl) dominates the sediment budget, contributing 26,000 Mg/yr above the knickpoint and 107,000 Mg/yr within the knickzone, with erosion rates more than double the Holocene average. Ravines comprise only 0.3% of the watershed area, but contribute 5% of all sediment, including 1,000 Mg/yr above the knickpoint and 12,000 Mg/yr within the knickzone. Based on sediment fingerprinting results, agricultural uplands contribute 45,000 Mg/yr above the knickpoint and add an additional 23,000 Mg/yr within the knick zone. Based on air photo measurements of channel changes since 1938, net bank erosion (37) from meander migration (Ba_M) and channel widening (Ba_W) contribute 6,000 and 13,000 Mg/yr above the knickpoint, respectively, and 10,000 and 14,000 Mg/yr within the knickzone. Channel incision within the knickzone contributes an additional 4,000 Mg/yr.

Given the history of agricultural development in the watershed and the legacy of significant valley bottom deposition in areas with a similar history (10,11), the possibility that the modern sediment budget includes erosion of valley bottom legacy sediment must be carefully considered. Precisely constraining floodplain storage (legacy or otherwise) remains a difficult task in large watersheds. Yet, the importance of floodplain storage should not be understated in development of a watershed sediment budget (49). In this study, four separate observations, taken together, support the finding that historic and modern floodplain storage is neither large, nor changing considerably under current conditions. First and foremost, floodplain storage is expected to be small in incising systems. Within the knickzone, floodplains are relatively narrow (30) and continued, rapid vertical incision limits opportunity for vertical floodplain accretion. Second, we have observed floodplain inundation during multiple events and have mapped small pockets of deposition following a high flow event in September 2010. Specifically, we documented 0-20 cm of localized deposition, typically less than 10% silt and clay, though this grain size fractionation

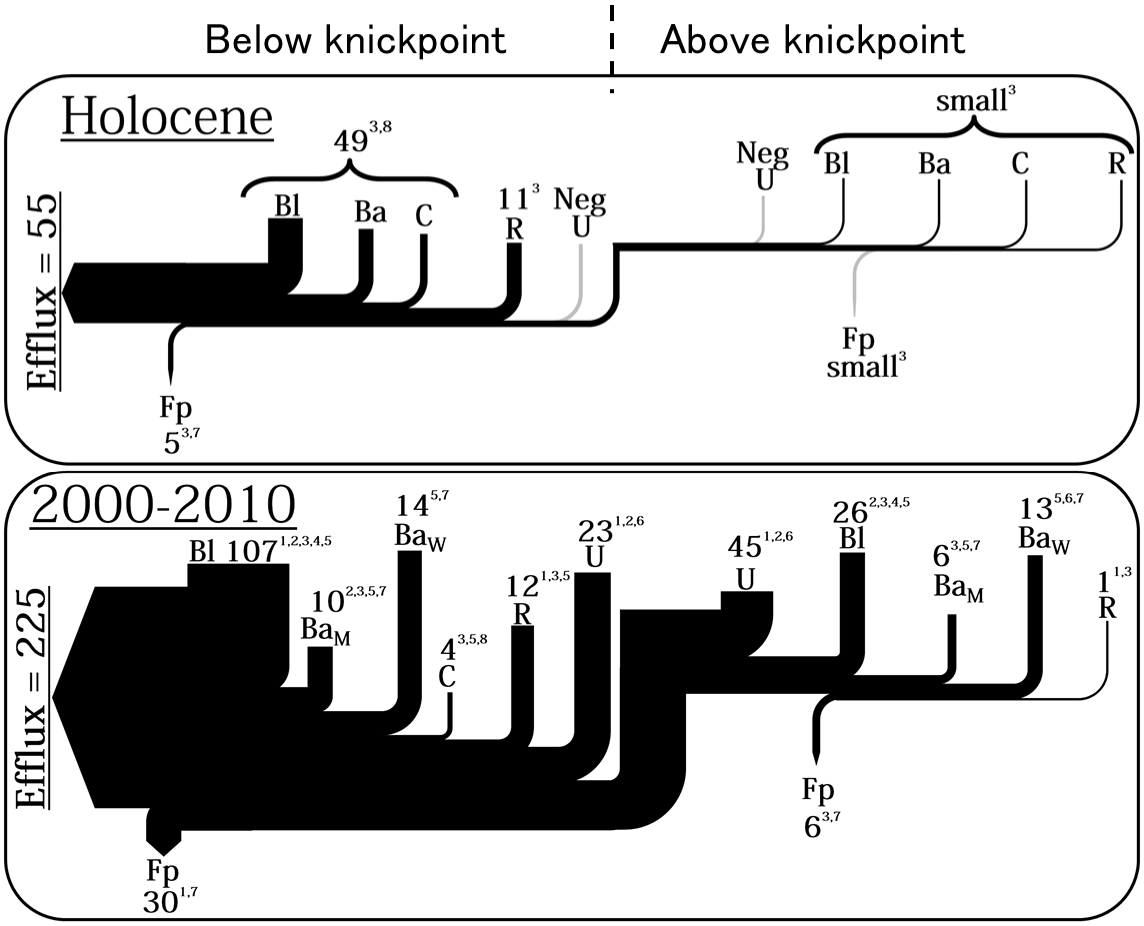

Figure 3: Fine sediment budgets (clay + silt) for the Le Sueur River, averaged over Holocene time and over 2000-2010. Values given in 10^3 Mg/yr. Sediment sources include Bluffs (Bl), Bank erosion resulting from channel migration (Ba_M) and widening (Ba_W), Channel incision (C), Ravines (R), and Uplands (U). Superscripts indicate methods used to constrain each flux (1: Gaging data, 2: Geochemical tracers, 3: Aerial lidar analysis, 4: Terrestrial lidar scans, 5: Air photo analysis, 6: Numerical modeling, 7: Field surveys, 8: OSL and ^{14}C dating).

may have been influenced by conditions specific to this event. In any case, our observations indicate that the channel is not unable to access floodplains, but also that floodplain storage is not a large number in any part of the channel network. Third, we do not observe large differences in height between eroding and depositing banks above the knickzone, which would otherwise indicate a larger amount of storage having occurred in the past and an ongoing process of net floodplain degradation. Lastly, some overbank deposition occurs behind large woody debris jams above the knickpoint. These debris jams are transient features that appear to form and degrade over annual to decadal timescales. Deposition behind the debris jams appears to be reasonably balanced by bank scour as the channel migrates around the jams. Assuming the frequency and magnitude of these woody debris jams has not changed significantly over recent decades, net sediment storage associated with them has also not changed. While floodplain storage is the least-well constrained number in our modern sediment budget these observations all suggest that floodplain storage is neither large, nor changing significantly from recent decades.

Significant year-to-year variability exists in sediment loading, which translates to variability in contributions from each of the sources. The suspended sediment load for the entire watershed during the driest year (2009) of our monitoring period was a mere 29,000 Mg in contrast to the wettest year (2010), which was 543,000 Mg. Years 2007 and 2008 exhibited intermediate flow, with annual watershed suspended sediment loads of 135,000 and 136,000 Mg, respectively. It was simply fortuitous that the years over which we intensively measured fluxes and erosion rates covered the full spectrum of hydrologic conditions.

Defining uncertainty in sediment budgets is a persistent problem. Budgets are typically assembled using a wide range of information of different types, each with their own uncertainty. These include sediment sources from topographic differencing, sediment flux measured at stream gages, and estimates of the proportion of sediment yield derived from terrestrial vs. near-channel sources. Because of the very different nature of these data (sediment supply averaged over large space and time scales, sediment concentration calculated from individual stream samples and extrapolated over time series of flow, and source proportions based on geochemical analyses of individual soil and sediment samples), a formal uncertainty analysis is difficult to define and interpret. Further, the strong constraint of mass balance and the plausible requirement that approximations hold across similar locations and time periods, add certainty to the combined

sediment budget that cannot be combined with the uncertainty of individual components in any obvious way.

Despite the lack of a formal uncertainty analysis, plausible conclusions can be drawn by invoking sediment mass conservation over multiple time and space scales. Values for each component of the sediment budget, drawn from a plausible range based on the uncertainty in each component, are subject to the collective constraint of mass conservation. For example, a sediment source may be judged to be minor if even exceptionally large values (within the measured range of uncertainty) do not produce a significant fraction of the overall mass balance. Further, the plausible range of uncertainty in any individual component may be constrained if exceptionally large or small values of that component require implausible combinations of other components in order to balance the budget. In the end, a weight-of-evidence approach, constrained by the use of multiple lines of evidence, is used to support conclusions regarding sediment sources, fluxes, and sinks. Here we have closed our budget for the 2000-2010 time period by applying a single parameter to adjust all predicted source fluxes as a fraction of their respective uncertainty (see Supporting Information). This approach provides an objective means to balance the budget in manner that is sensitive to the estimated uncertainty associated with each of the measurements.

Based on similar topographic history and land use, the sediment supply observed over the past decade on the Le Sueur is likely representative of other tributaries to the Minnesota River, which collectively account for the bulk of sediment contributed to the UMR and Lake Pepin (23). Sedimentation rates in Lake Pepin (Figure 4) have increased from an apparent 'background' rate of ~80,000 Mg/year prior to 1830 to as high as 850,000 Mg/yr between 1950 and 2008 (22).

We analyzed natural atmospheric fallout nuclides ^{210}Pb and ^{10}Be in Lake Pepin sediment cores as tracers that document the relative proportion of fine sediment derived from uplands versus near-channel sources over the past 500 years. Upland sources have high concentrations of both tracers, whereas bluffs and ravines have correspondingly low concentrations (40, 41; see Supporting Information). Both tracers show similar changes over time (Figure 4, red dots for ^{10}Be, orange Xs for ^{210}Pb). The low ^{10}Be concentration 500 years ago indicates very little upland soil erosion relative to bluff erosion. During the mid-20th century, a sharp increase in ^{10}Be concentrations indicates a pulse of soil erosion from agricultural fields. In the past three decades, both ^{10}Be and ^{210}Pb document a strong shift back toward near-channel sources, consistent with our 2000-2010

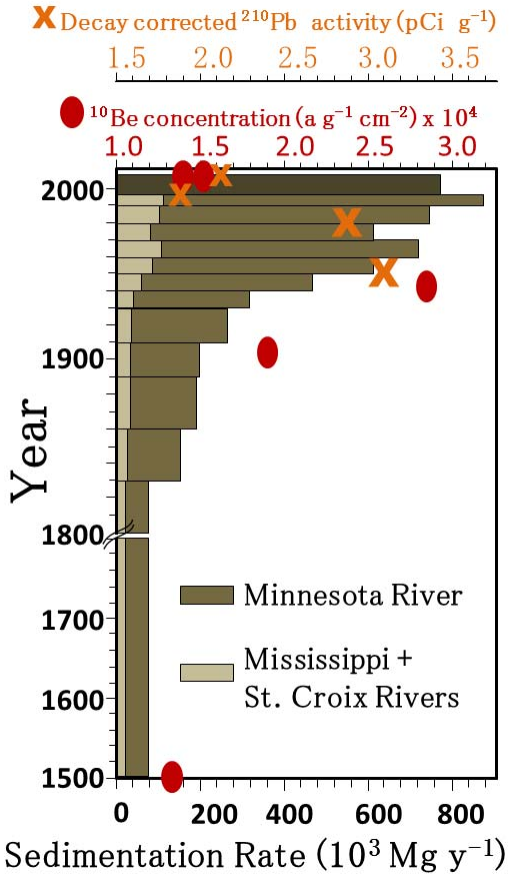

Figure 4: Depth profile of Lake Pepin sedimentary record showing sedimentation rate across the entire lake bottom (bottom axis) and concentrations of radionuclide sediment tracers (top axes). Upland soil erosion delivers sediment enriched in both tracers; bluffs and ravines deliver tracer-deficient sediment.

sediment budget in the Le Sueur watershed. Because ^{10}Be and ^{210}Pb have very different half-lives (^{210}Pb 22 years; ^{10}Be 1.4 million years), the decrease in both nuclide concentrations indicates a real decrease in field sources relative to bluffs and ravines, rather than recent activation of legacy field sediment stored in the valley bottom, which would be depleted in ^{210}Pb, but not ^{10}Be. Additionally, measured concentrations from source areas confirm that ^{10}Be concentration in upland soils remains high and therefore the decrease in ^{10}Be concentration is not related to prior erosion of nuclide-rich soil, which has been documented in parts of the Chesapeake Bay watershed (50). A ^{210}Pb apportionment model (47) indicates that the proportion of sediment derived from fields was high in the 1940s-1960s (3.2 pCi g^{-1} ~ 65% field source), remained relatively high through the 1980s (59% field), and then decreased by the mid-1990s (32% to 35% field).

Erosion rates of near-channel sources (particularly bluff and streambanks) are sensitive to changes in river discharge. Two recent hydrologic changes, both related to human activity, may be acting to increase discharge and amplify erosion of near-channel sources. First, climate records indicate that mean precipitation has increased in Minnesota, along with an increase in the frequency and magnitude of extreme events (51, 52). Climate models predict a continued upward trend in the 21st century across the mid-western U.S., primarily in the form of more frequent heavy rains (53). A second important driver is the extensive modification of the channel network with agricultural ditches (25% of the modern network) and subsurface tile drains, particularly over the past 30-40 years (54). These modifications have increased both the effective drainage area and the efficiency of drainage. Additionally, tile drains are likely increasing infiltration capacity and thereby reducing surface runoff, which would reduce fluvial soil erosion at the expense of increasing flow in the river, consistent with the apparent decrease in upland soil delivery and increase in near-channel erosion observed over the past few decades. However, at present we are unable to deconvolve the influence of tile drains from other land use and climatic factors that are also contributing to changes in hydrology.

The Lake Pepin sediment cores indicate that the rate of sedimentation in the past decade has remained large, even as the sediment supply has shifted from upland to near-channel sources (Figure 4). The Le Sueur 2000-2010 sediment budget (Figure 3, bottom panel) corroborates a dominant near-channel source of recent sediment supply. The combination of Holocene and modern sediment budgets and geochemical fingerprinting of Lake Pepin sediment cores provide

strong evidence that the dominant source of persistent large sediment loads has shifted from agricultural soil erosion to amplified near-channel erosion, driven by a combination of changing precipitation and a vastly altered drainage network.

Our results indicate that 70% of sediment contributed to the Le Sueur River during 2000-2010 is derived from the channel network (bluffs, banks, ravines, and channel incision), which comprises less than 1% of the landscape. This finding underscores the need for development of combined watershed erosion and sediment routing models that account for channel adjustments and changes in channel-floodplain storage in response to changes in flow and the amount and type of sediment supply. Such models are imperative for understanding sediment as a water quality metric, especially under non-stationary climate conditions, and for predicting the effectiveness of remedial actions. Such models will be strengthened by increasing availability of high resolution topography data that includes channel bathymetry, providing opportunities for development of 2D and 3D models of flow, erosion, and deposition. Incorporating theory for production and decay of radiogenic tracers associated with the sediment would provide a platform for hypothesis testing and model validation that would allow us to move beyond conventional empirical approaches for prediction of watershed sediment yield.

The research, management, and policy challenges posed by these findings are imposing: both the source and driving mechanism of elevated sediment loads are changing. Effective remediation must now accommodate both erosion and runoff controls. Land and water resource management must develop watershed-scale solutions to mitigate systemic hydrologic amplification of natural erosion processes.

ACKNOWLEDGEMENTS

This work was funded by the National Center for Earth-surface Dynamics NSF EAR 0120914, Minnesota Pollution Control Agency, and Minnesota Department of Agriculture. Additional support was provided by the Utah State University Agricultural Experiment Station (paper #8288), the University of Minnesota Limnological Research Center, and Minnesota Supercomputing Institute. Aerial lidar data provided by the Environmental Services Department of Blue Earth County, Minnesota. JKW thanks the Alexander von Humboldt foundation for a postdoctoral fellowship. We also thank Noah Finnegan, Caitlyn Echterling, Jenny Graves, Khalif

Maalim, Luam Azmera, Ashley Thomas, Bridget Wolfe, Mandy Kinnick, and James Ley for their assistance on the project.

ASSOCIATED CONTENT

Supporting Information. All supporting data used to constrain the Holocene and 2000-2010 sediment budgets, including synthesis of sediment excavation over Holocene time, a summary of modern sediment gaging data on main channels and ravines, air photo analysis of channel widening and channel migration, explanation of sediment fingerprinting sample processing and results, summary data for air photo and repeat terrestrial lidar analysis of bluff erosion are archived online in Supporting Information. Additional raw data and GIS shapefiles are available from the corresponding author upon request. This information is available free of charge via the Internet at http://pubs.acs.org/ .

REFERENCES

1. US Environmental Protection Agency. Water Quality Assessment and TMDL Information. 2011. http://iaspub.epa.gov/waters10/attains_nation_cy.control, accessed 6 March 2011.

2. Palmer, M.A. *et al.* Linkages between aquatic sediment biota and life above sediments as potential drivers of biodiversity and ecological processes. *BioScience.* 2000, 50, 1062-1075.

3. Walling, D.E. The sediment delivery problem. *Journal of Hydrology*. 1983, 65: 209–37.

4. Trimble, S.W., Crosson, P. U.S. Soil Erosion Rates –Myth and Reality. *Science*. 2000, 289, 248-250.

5. Langland, M. J., D. L. Moyer, and J. Blomquist Changes in streamflow, concentrations, and loads in selected nontidal basins in the Chesapeake Bay Watershed, 1985–2006, U.S. Geol. Surv. Open File Rep., 2007- 1372, 76 pp.

6. Smith, S.M.C., Belmont, P., Wilcock, P.R. Closing the gap between watershed modeling, sediment budgeting, and stream restoration. in Stream Restoration in Dynamic Systems: Scientific Approaches, Analyses, and Tools. Edited by Andrew Simon, Sean J. Bennett, Janine Castro, and Colin Thorne. AGU Monograph Series. in press.

7. Montgomery, D.R. Soil erosion and agricultural sustainability. *Proc. Nat. Acad. Sci.* 2007, 104, 13268-13272.

8. De Vente, J., Poesen, J., Arabkhedri, M., Verstraeten, G. The sediment delivery problem revisited. *Prog. Phys. Geog.* 2007, 31, 155-178.

9. Phillips, J.D. Evolutionary geomorphology: thresholds and nonlinearity in landform response to environmental change. *Hydrology and Earth System Sciences.* 2006, 10: 731-742.

10. Trimble, S.W. Decreased rates of alluvial sediment storage in the Coon Creek Basin, Wisconsin, 1975-93. *Science.* 1999, 285, 1244-1246.

11. Walter, R., and Merritts, D. Natural streams and the legacy of water-powered milling: *Science.* 2008, 319: 299-304.

12. Nearing, M.A. *et al.*, Measurements and Models of Soil Loss Rates. *Science.* 2000, 290: 1300b.

13. Allen, P.A. From landscapes into geological history. *Nature.* 2008, 451: 274-276.

14. Quinton J.N., Govers G., Van Oost K., Bardgett R.D. The impact of agricultural soil erosion on biogeochemical cycling. *Nat. Geosci.* 2010, 3: 311–314.

15. Reid, L.M., Dunne, T. *Rapid Evaluation of Sediment Budgets.* (Catena Verlag, Reiskirchen, Germany, 1996) 164 pp.

16. Gilbert, G.K. (1917) Hydraulic-mining debris in the Sierra Nevada, U.S. Geol. Survey Prof. Paper. 105: 154 pp..

17. Dietrich, W. E., and T. Dunne, Sediment budget for a small catchment in mountainous terrain, *Z. Geomorphol., Suppl.,* 1978, 29: 191-206.

18. Costa, J. E., Cleaves, E.T. The Piedmont landscape of Maryland: A new look at an old problem. *Earth Surface Processes and Landforms*, 1984, 9: 59-74.

19. Trimble, S.W. Man-induced soil erosion on the southern Piedmont. Ankeny, Iowa: Soil and Water Conservation Society. 2008

20. Snyder, N.P., Studying stream morphology with airborne laser elevation data, *Eos, Transactions, American Geophysical Union*, 2009, 90 (6): 45-46. doi:10.1029/2009EO060001.

21. Wheaton, J.M., Brasington, J., Darby, S.E. and Sear, D. Accounting for Uncertainty in DEMs from Repeat Topographic Surveys: Improved Sediment Budgets. *Earth Surface Processes and Landforms.* 2010, 35 (2): 136-156. DOI: 10.1002/esp.1886.

22. Engstrom, D.R., Almendinger, J.E., Wolin, J.A. Historical changes in sediment and phosphorus loading to the upper Mississippi River: mass-balance reconstructions from the sediments of Lake Pepin. *J. Paleolimnology.* 2009, 41, 563-588.

23. Kelley, D.W., Brachfeld, S.A., Nater, E.A., Wright, H.E. Jr. Historical changes in sediment and phosphorus loading to the upper Mississippi River: mass-balance reconstructions from the sediments of Lake Pepin. *J. Paleolimnology.* 2006, 35, 193-206.

24. Minnesota County Biological Survey (MCBS), Minnesota Department of Natural Resources. September 2007. *Native Plant Communities and Rare Species of The Minnesota River Valley Counties.* Minnesota Department of Natural Resources. http://www.mndnr.gov/eco/mcbs/index.html, accessed March 3, 2011.

25. Musser, K., S. Kudelka, and R. Moore. (2009) *Minnesota River Basin Trends Report.* 66 pp. http://mrbdc.wrc.mnsu.edu/mnbasin/trends/index.html, accessed March 10, 2011.

26. Wilcock, P. Synthesis Report for Minnesota River Sediment Colloquium. Report for MPCA (2009) http://www.lakepepinlegacyalliance.org/SedSynth_FinalDraft-formatted.pdf, accessed March 13, 2011.

27. Jennings, C.E. (2010) Open File Report 10-03, Minnesota Geological Survey, map, report and digital files. ftp://mgssun6.mngs.umn.edu/pub4/ofr10_03/

28. Clayton, L., Moran, S.R. Chronology of late-Wisconsinan glaciations in middle North America. *Quat. Sci. Rev.* 1982, 1: 55-82.

29. Gran, K.B. *et al.*, Management and restoration of fluvial systems with broad historical changes and human impacts. *GSA Sp. Paper.* 2009, 451: 119-130.

30. Belmont, P. Floodplain width adjustments in response to rapid base level fall and knickpoint migration. *Geomorphology*. 2011, 128: 92-102.

31. Gardner, T.W. Experimental study of knickpoint and longitudinal profile evolution in cohesive, homogenous material. *GSA Bull.* 1983, 94: 664-672.

32. Fry, P. A River runs through it: Cultures, economies and landscapes within the Minnesota River Basin to 1900. *Ph.D. Dissertation. University of Minnesota.* 1999, 288 pp.

33. Andersson, O., T.R. Crow, S.M. Lietz, and F. Sterns. Transformation of a landscape in the upper mid-west, USA: The history of the lower St. Croix river valley, 1830 to present. *Landscape and Urban Planning.* 1996, 35(4): 247-267.

34. Additional information available on Clean Water Funds at: http://www.pca.state.mn.us/

35. Star-Tribune, Seize momentum on water quality. Minneapolis-St. Paul Star Tribune Editorial, December 26, 2010.

36. Day, S.S., Gran, K.B., Belmont, P., Wawrzyniec, T. Change detection on bluffs using terrestrial laser scanning technology. Revision submitted to Earth Surface Processes and Landforms. in review.

37. Lauer, J.W., Parker, G. Modeling framework for sediment deposition, storage, and evacuation in the floodplain of a meandering river, Part I: Theory, *Water Resources Research.* 2008, 44, W04425.

38. Collins, A. L., Walling, D.E. Selecting fingerprint properties for discriminating potential suspended sediment sources in river basins. *J. Hydrol.* 2002, 261: 218–244.

39. Davis, C.M., Fox, J.F. Sediment Fingerprinting: Review of the method and future improvements for allocating nonpoint source pollution. *J. Env. Eng.* 2009, 135 (7): 490-504.

40. Willenbring, J.K., von Blanckenburg, F. Meteoric cosmogenic Beryllium-10 adsorbed to river sediment and soil: applications for Earth-surface dynamics. *Earth Science Reviews.* 2010, 98, 105-122.

41. Noller, J. S., Soweres, J. M., and Lettis, W. R. (eds.), Quaternary Geochronology: Methods and Applications, Washington, DC: American Geophysical Union, AGU Reference Shelf 2002, 4, 582 p.

42. Owens, P.N., Walling, D.E., He, Q. The behavior of bomb-derived Caesium-137 fallout in catchment soils. *J. Environ. Radioactivity.* 1996, 32 (3): 169-191.

43. Bonniwell, E.C., Matisoff, G., Whiting, P.J. Determining the times and distances of particle transit in a mountain stream using fallout radionuclides. *Geomorphology.* 1999, 27: 75-92.

44. Matisoff, G., Bonniwell, E.C., Whiting, P.J. Radionuclides as indicators of sediment transport in agricultural watersheds that drain to Lake Erie. *J. Environ. Qual.* 2002, 31: 62-72.

45. Lauer, J.W., Willenbring, J. Steady state reach-scale theory for radioactive tracer concentration in a simple channel/floodplain system. *Journal of Geophysical Research Earth Surface.* 2010, 115: F04018.

46. Viparelli, E., Lauer, J.W., Belmont, P., Parker, G. A Numerical Model to Develop Long-term Sediment Budgets Using Isotopic Sediment Fingerprints. Computers and Geosciences Special issue on Modeling for Environmental Change. in review.

47. Schottler, S.P., Engstrom, D.R., Blumentritt, D. Fingerprinting sources of sediment in large agricultural river systems. Report for MPCA. 2010. http://www.smm.org/static/science/pdf/scwrs-2010fingerprinting.pdf, accessed March 12, 2011.

48. Belmont, P., Gran, K.B, Jennings, C., Wittkop, C. Holocene Landscape Evolution and Erosional Processes in the Le Sueur River, Central Minnesota. Kirk Bryan Field Trip Guide for 2011 Geological Society of America Annual Meeting. 2011.

49. Walling, D.E., Owens, P.N., Leeks, G.J.L., The role of channel and floodplain storage in the suspended sediment budget of the River Ouse, Yorkshire, UK. *Geomorphology.* 1998, 22: 225-242.

50. Valette-Silver, J.N., Brown, L., Pavich, M., Klein, J., Middleton, R., Detection of erosion events using 10 Be profiles: example of the impact of agriculture on soil erosion in the Chesapeake Bay area USA. *Earth Planet. Sci. Lett.* 1986, 80, 82–90.

51. Novotny, E.V., Stefan, H.G. Stream flow in Minnesota: Indicator of climate change? *J. Hydrology.* 2007, 334, 319-333.

52. Min, S., Zhang, X., Zwiers, F.W., Hegerl, G.C. Human contribution to more-intense precipitation extremes. *Nature.* 2011, 470, 378-381.

53. USGCRP, *Global Climate Change Impacts in the United States.* Cambridge University Press New York, 2009.

54. Blann, K.L., Anderson, J.L., Sands, G.R., Vondracek, B. Effects of agricultural drainage on aquatic ecosystems: a review. *Critical Reviews in Environmental Science and Technology.* 2009, 39, 909-1001.

Appendix F: Geomorphic evolution of the Le Sueur River, Minnesota, USA, and implications for current sediment loading

Authors: Karen B. Gran, Patrick Belmont, Stephanie Day, Carrie Jennings, Andrea Johnson, Lesley Perg, Peter R. Wilcock

Published in: Geological Society of America Special Paper 451 , 2009,

ABSTRACT

There is clear evidence that the Minnesota River is the major sediment source for Lake Pepin and that the Le Sueur River is a major source to the Minnesota River. Turbidity levels are high enough to require management actions. We take advantage of the well-constrained Holocene history of the Le Sueur basin and use a combination of remote sensing, field, and stream gaging observations to constrain the contributions of different sediment sources to the Le Sueur River. Understanding the type, location, and magnitude of sediment sources is essential for unraveling the Holocene development of the basin as well as for guiding management decisions about investments to reduce sediment loads.

Rapid base level fall at the outlet of the Le Sueur River 11,500 yr BP triggered up to 70 m of channel incision at the mouth. Slope-area analyses of river longitudinal profiles show knickpoints have migrated 30-35 km upstream on all three major branches of the river, eroding $1.2 – 2.6 \times 10^9$ Mg of sediment from the lower valleys in the process. The knick zones separate the basin into an upper watershed, receiving sediment primarily from uplands and streambanks and a lower, incised zone, which receives additional sediment from high bluffs and ravines. Stream gages installed above and below knick zones show dramatic increases in sediment loading above that expected from increases in drainage area, indicating substantial inputs from bluffs and ravines.

INTRODUCTION

The Minnesota River drains 43,400 km^2 of south-central Minnesota (Figure 1), a landscape dominated by agricultural land use. The Minnesota River carries a high suspended sediment load, leading to the listing of multiple reaches as impaired for turbidity under section

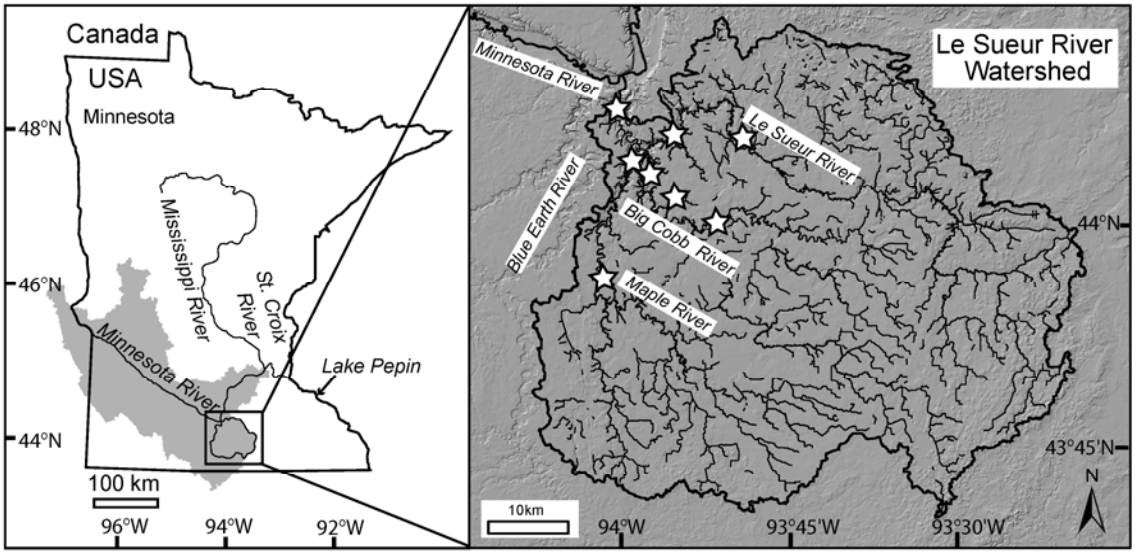

Figure 1: Location map showing Le Sueur River watershed in south-central Minnesota, USA. The shaded area on the state map indicates the extent of the Minnesota River basin. Stars on the inset watershed map on the right indicate locations of gaging stations.

303d of the Clean Water Act. Analyses of sediment cores in Lake Pepin, a naturally-dammed lake on the mainstem Mississippi River serving as the primary sediment sink for the Minnesota, St. Croix, and upper-Mississippi River systems, indicate that sediment loads into Lake Pepin have increased 10-fold since the onset of European settlement in the mid-1800s, from a background of ~75,000 Mg yr^{-1} to ~900,000 Mg yr^{-1} (Engstrom and Almendinger, 2000). Of this sediment load, the vast majority (85-90%) comes from the Minnesota River (Kelley and Nater, 2000).

To help restore clean water and improve ecosystem functionality in the Minnesota River and Lake Pepin, a large-scale effort is underway to lower sediment loading to the system. This involves targeting the dominant sources of sediment to the system, which are poorly constrained. Our research focuses on establishing an integrated sediment budget in one of the major tributaries of the Minnesota River, the Le Sueur River, in an effort to better define the source locations and transport processes for sediment entering the Minnesota River. Once source locations are well defined, best management practices can be targeted towards reducing the sediment load coming from these locations.

The first phase of our sediment budget involves bracketing the range of sediment volumes that have been eroded through time to compare current sediment loading with historic and Holocene-average rates. Recent changes in both land use and hydrology in the system may be exacerbating erosion in certain parts of the landscape, resulting in the observed increase in sediment loading to Lake Pepin in the past 170 years. The next phase involves setting bounds on the relative magnitude and proportion of sediment coming from each primary sediment source to determine which sources are currently important contributors of sediment to the Le Sueur River.

BACKGROUND

The Le Sueur River drains north and west to the Minnesota River in south-central Minnesota, USA (Figure 1). It covers 2,880 km^2 of primarily agricultural land use (87%), the vast majority of which are in row crops (> 90%) (Minnesota Pollution Control Agency (MPCA) et al., 2007). There are no major urban areas, although the municipality of Mankato is expanding into the northern portion of the watershed. There are three main branches to the Le Sueur River: the Maple River, the Big Cobb River, and the mainstem Le Sueur. The three branches come together within a span of 3 km, ~10 km upstream of the Le Sueur confluence with the Blue Earth River. The Blue Earth flows into the Minnesota River 5 kilometers downstream from the junction with the Le Sueur River.

Modern sediment gaging efforts indicate that ~24-30% of the total suspended solids (TSS) entering the Minnesota River come from the Le Sueur River, making it a primary contributor to the mainstem Minnesota and Lake Pepin (MPCA et al., 2007). This is a disproportionate sediment contribution relative to the Le Sueur watershed area, which comprises a mere 7% of the Minnesota River basin. From 2000 to 2006, TSS measured at the mouth of the Le Sueur River ranged from 0.9 – 5.8 x 10^5 Mg yr^{-1} (mean = 2.9 x 10^5 Mg yr^{-1}) (MPCA et al., 2007; MPCA pers. comm.) (Table 1). Annual flow-weighted mean concentrations of TSS from 2000 – 2006 ranged from 245 to 918 mg L^{-1} (mean = 420 mg L^{-1}) (MPCA et al., 2007; MPCA pers. comm.). Target values set by the MPCA in this region are 58-66 mg L^{-1} (MPCA,1993).

The lower reaches of the Le Sueur, Maple and Big Cobb Rivers are currently incising. Knickpoints are migrating upstream along major tributaries, leading to high relief in the in the lower, incised portion of the watershed. At the mouth of the Le Sueur, the channel is incised 70 m in a valley up to 800 m wide. High bluffs border many of the outer bends along the channel, and steep ravines snake into the uplands. This is in stark contrast to the low-gradient to flat uplands, which occupy most of the watershed area.

The basin is underlain by tills, glacial outwash, and ice-walled lake plains with a thin mantle of glaciolacustrine silts and clays covering 65% of the upland surface. The river is currently incising through the layered Pleistocene tills and the underlying Ordovician dolostone bedrock. Bedrock outcrops have been observed along the channel in patches within 15 km of the mouth.

The high relief in the lower Le Sueur River valley is the result of knickpoint migration through the basin. These knickpoints originated from a sharp drop in base level on the mainstem Minnesota River during the catastrophic draining of glacial Lake Agassiz. As the Laurentide ice sheet retreated from the mid-continent at the end of the last glaciation, meltwater from the wasting ice was impounded by a low moraine dam in western Minnesota and formed glacial Lake Agassiz. It eventually covered much of western Minnesota, eastern North Dakota, Manitoba, and western Ontario (Upham, 1890, 1895; Matsch 1972). The only outlet for much of this time was to the south through glacial River Warren, the valley now occupied by the Minnesota River. River Warren incised older tills, saprolite and in places exposed resistant rock in the valley floor (Matsch, 1983), creating a valley that was 45 m deep at its mouth and 70 m deep near Mankato, 300 km downstream.

The initial incision was around 11,500 radiocarbon years before present (rcbp) (Clayton and Moran, 1982; Matsch, 1983). The valley was occupied until about 10,900 rcbp. Two other

Table 1: TSS LOADS IN LE SUEUR RIVER, 2000-2006

	2000	2001	2002	2003	2004	2005	2006[§]	Mean
TSS* (Mg)	$5.8x10^5$	$4.2x10^5$	$1.1x10^5$	$8.6x10^4$	$4.1x10^5$	$2.7x10^5$	$1.5x10^{5§}$	$2.9x10^5$
FWMC[†] (mg/L)	918	355	318	245	475	356	270[§]	420

2000-2005 data come from MPCA et al. (2007).

*TSS = Total Suspended Solids

[†]FWMC = Flow-weighted mean concentration

[§]2006 data come from MPCA (pers. comm.), preliminary

outlets were used between 10,900 - 10,300 (Thorleifson, 1996) and 10,000 - 9,600 rcbp (Lowell et al., 2005) during which time the southern outlet was not used. River Warren was reoccupied after 9,600 rcbp and finally lost glacial lake discharge by 8,200 rcbp. Pre-existing tributaries like the Blue Earth and Le Sueur rivers were low-gradient streams of glacial meltwater origin that were stranded above the master stream when the initial incision occurred 11,500 rcbp. Knickpoint migration continues today, with bedrock waterfalls located within 5 to 10 km of the confluence on several major tributaries. In the Le Sueur River, the record of incision following glacial River Warren is manifest in over 400 terrace surfaces spread throughout the lower basin. Knickpoints are expressed as slope discontinuities evident on all three major branches of the river, and they have propagated approximately the same distance upstream on each branch.

The glaciolacustrine deposits blanketing much of the Le Sueur River watershed were deposited in glacial Lake Minnesota which drained shortly before the initial carving of the Minnesota River valley. These deposits are composed of highly erodible silts and clays. Given the fine-grained, erodible soils of the Le Sueur River watershed and the high relief in the basin, the watershed is primed to have high suspended sediment loads relative to other watersheds in the basin, and it is susceptible to erosion driven by changes to the landscape following the arrival of settlers of European descent in the mid-1800s.

The pre-settlement landscape of the Le Sueur River was dominated by prairie vegetation covering two-thirds of the basin, with hardwoods in the river valleys and the northeastern corner of the watershed. Wet prairie and open lakes occupied at least 15% (Marschner, 1930), and possibly as much as one-third of the watershed area (Minnesota Department of Natural Resources, 2007). Two major changes to the landscape have occurred in the last 200 years: conversion of original prairie to agriculture and alterations to the basin hydrology. Land cover in the basin is now primarily row crops (currently 87% cropland (MPCA et al., 2007)), with lakes and wetlands covering only 3% of the watershed area. Hydrologic alterations include draining wetlands, connecting previously closed basins to the drainage network, ditching small tributaries, and tiling agricultural fields to ensure rapid drainage of surface, vadose, and in some places, groundwater. The hydrologic alterations are both pervasive and dynamic. Nearly all farm fields have artificial drainage and the depth, density, and capacity of drainage have generally increased over time (Water Resources Center, 2000). Little documentation exists for these progressive hydrologic changes. Superimposed on these direct changes to the hydrologic system are indirect changes from climate change in the last ~50 years, including statewide increases in mean annual precipitation, number of days with precipitation, and number of intense rainfall events per year

(Novotny and Stefan, 2007). These changes are, in turn, superimposed on the template of the geomorphically evolving, incised channel network that was initiated by deep, rapid incision in the Minnesota River valley.

METHODS

This research effort focused on sediment loading to the Le Sueur River over multiple temporal and spatial scales, with the goal of identifying sources, fluxes, and sinks in the evolution of the drainage system and its response to human alteration. Most of the work on Holocene erosion volumes was done through analyses of digital topography, including high-resolution topography acquired through LiDAR (Light Detection and Ranging) in Blue Earth County. This dataset covers approximately 30% of the total watershed area, including all of the area below the major knickpoints. Holocene erosion volumes are compared with 2000-2006 sediment loads measured at stream gages as a comparison of current rates vs. background rates. Both of these erosion measures are compared with the signal of deposition at Lake Pepin over the past 400 years from Engstrom and Almendinger (2000).

Sediment sources to the Le Sueur River include upland-derived sediment, high bluffs, terraces, and ravines. Major sediment sources are shown in Figure 2. The primary sediment sources above the knick zone include upland-derived sediment and sediment eroded from streambanks due to lateral migration of channels. Normally, streambanks are not a net source of sediment, because the sediment eroded is balanced by deposition on floodplains. However, because the river is migrating into terraces and high bluffs, erosion from these features can lead to net sediment contributions to the channel from stream migration. Most of the terraces are located below the major knick zone, but there are smaller terraces throughout the basin, remnants of the passage of the upper knickpoint through the system. Through and below the major knick zones, ravines and bluffs become important sediment contributors. Information on total sediment flux was derived from paired gaging stations located above and below the knick zones on major tributaries. Analyses of historical air photos from 1938 to 2003 help constrain channel migration patterns and dynamics. These data combine to determine which sediment sources are significant components of the modern sediment budget.

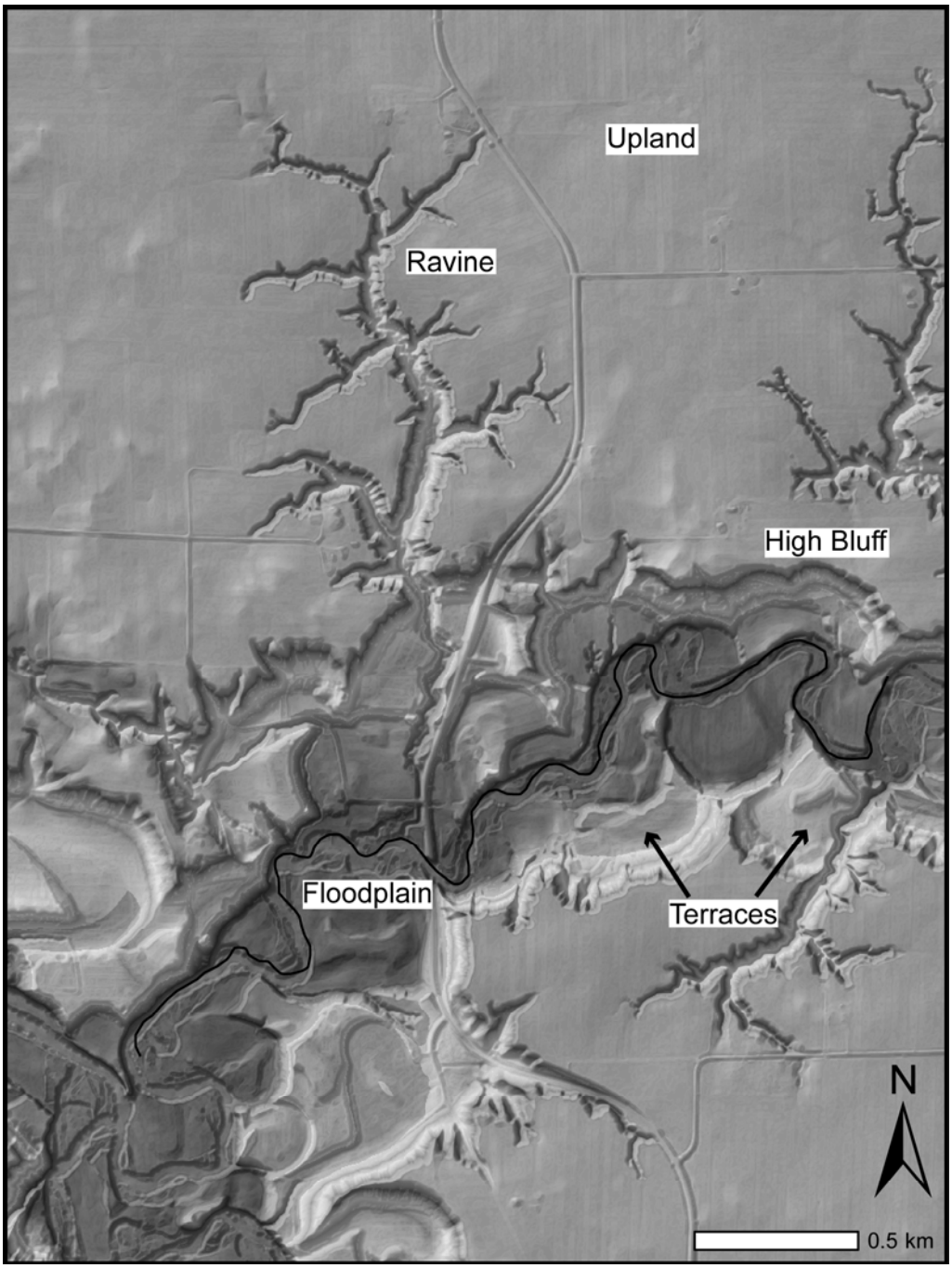

Figure 2: Primary sediment sources in the Le Sueur River watershed include uplands, ravines, high bluffs, and terraces. Shown here is a merged LiDAR DEM and slope map of lower Le Sueur River with different source areas labeled. Relief is approximately 70 meters from river valley to uplands.

LiDAR Analyses

We extracted river longitudinal profiles from 30-meter SRTM data obtained from the U.S. Geological Survey and analyzed the relationship between local channel gradient and contributing drainage area (see Wobus et al., 2006) along the entire river profile using the Stream Profiler utility (www.geomorphtools.org) with a 3-m contour, 1-km smoothing window, and an empirically derived reference concavity of 0.45 (Figure 3). Slope-area analyses were conducted on each of the three mainstem channels to find major slope discontinuities (see Figure 3B). In a graded system, the slope-area relationship should increase monotonically throughout the entire fluvial portion of the watershed. The sharp discontinuities evident in the slope-area plot highlight the locations of knickpoints.

We estimated the mass of sediment that has been excavated over the past 11,500 yr from the incised, lower reaches of all three branches of the Le Sueur River. To calculate the missing mass, we hand-digitized polygons delineating the incised portion of the river valleys using the 3-m resolution aerial LiDAR Digital Elevation Model (DEM) (Figure 4). Precision in this process was enhanced by overlaying the DEM with a semi-transparent hillshade and using a multi-band color scheme for the DEM, which we manipulated to most effectively depict small differences in the elevation range of interest. The valley walls are generally strikingly clear and easy to trace using this technique. Valley polygons were split into 3-km long reaches. We then converted each of those polygons to grids, attributing a paleosurface elevation value to each cell in the grid. The mass removed was determined by subtracting the current topography from the paleosurface.

To generate minimum and maximum estimates of the mass of excavated sediment we used two different paleosurface elevations. Our maximum estimate assumed that the watershed was initially a planar glacial lake bed with a paleosurface elevation of 327 m above sea level for all valley polygons, consistent with the average elevation of the surrounding, low-gradient uplands in this area. Our minimum estimate assumed a different paleosurface elevation for each 3-km valley reach consistent with the elevation of the highest terraces mapped in that reach. These elevations are the highest levels that we know were occupied by the river in the past 11,500 years.

Using the same approach, we hand-digitized all 95 ravines (considering only those with a planar area of incised valley > 0.5 km^2) and calculated the mass of material that has been excavated by ravines as a result of ravine incision and elongation only. The paleosurface

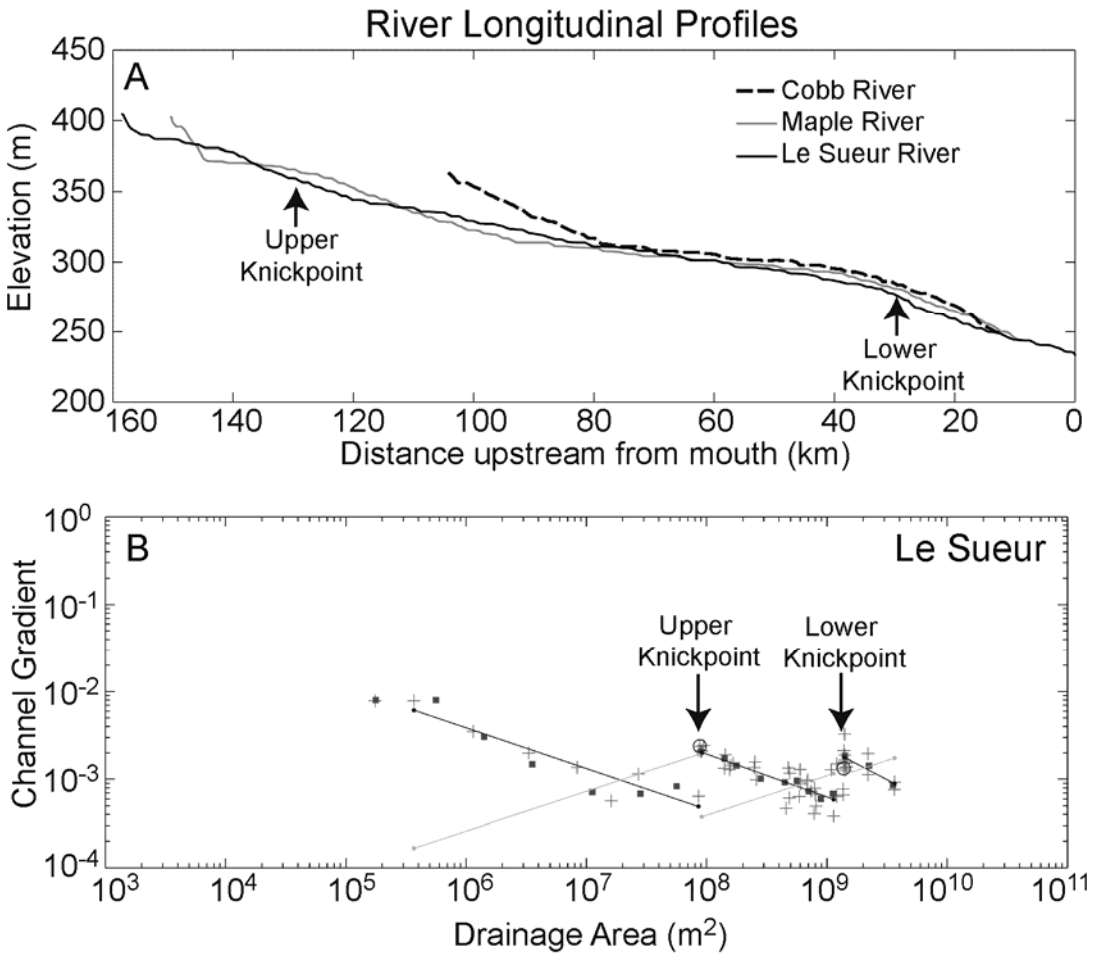

Figure 3: A) Longitudinal elevation profiles of the Le Sueur River and its two primary tributaries, the Cobb and Maple rivers, extracted from a 30-meter DEM. The locations of the two knickpoints delineated on the Le Sueur River branch using the slope-area analysis in B are shown. B) Analysis of local channel gradient and contributing drainage area of the Le Sueur River longitudinal profile, after smoothing with a 1-km moving window and sampling every 3-meter drop in elevation. The discontinuities in the slope-area relationship indicate the location of two knickpoints. Both data sets were extracted using the stream profiler tool available at geomorphtools.org.

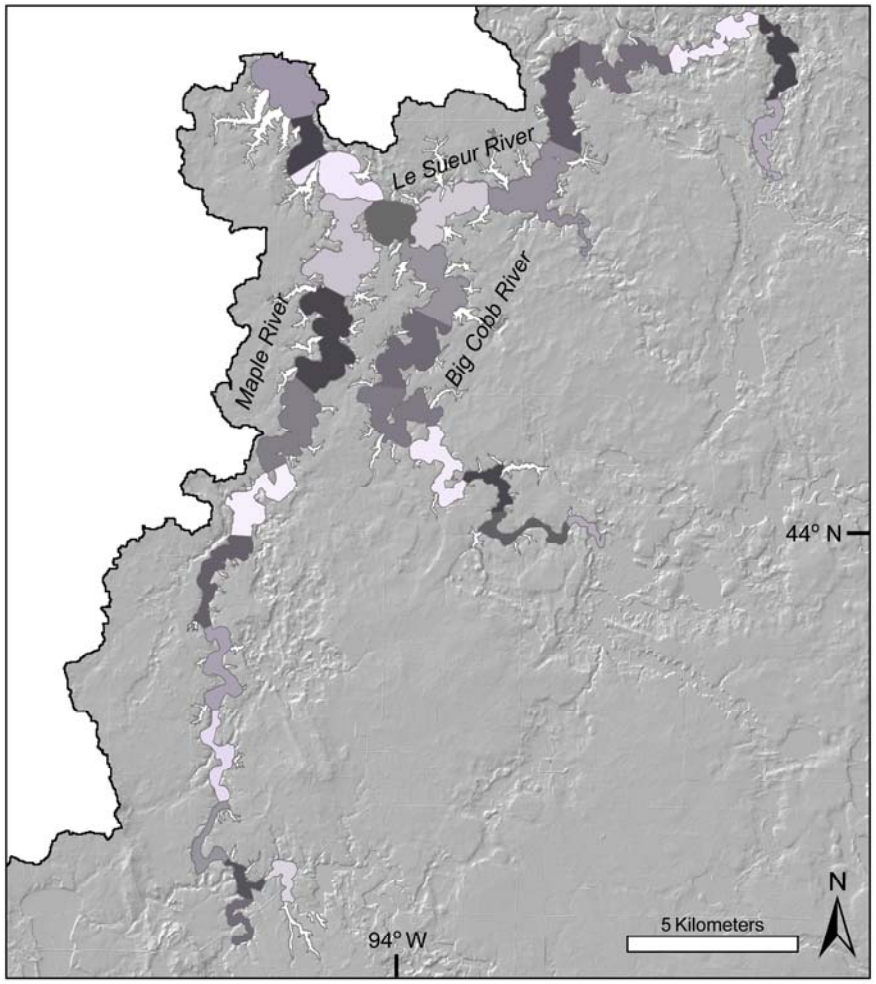

Figure 4: Valley and ravine polygons used to determine sediment mass excavated in the past 11,500 years, overlain on the LiDAR DEM.

elevation of each ravine was determined using the average of 10 upland surface elevations surrounding the ravine.

Volumes of sediment removed were converted into mass using a bulk density of 1.8 Mg m^{-3} (Thoma et al., 2005). To compare with TSS measurements, we assumed that only the silt and clay fractions (65% of the total mass) move downstream as suspended load. This mass could then be compared to the inorganic fraction of TSS from modern gaging efforts.

We mapped fluvial terrace surfaces from the 3-m aerial LiDAR DEM, using a semi-transparent hillshade to enhance visual precision (Figure 5). The criteria used to delineate terrace surfaces was visual observation of undissected, planar (< 1 m of relief) surfaces within the incised river valley that are > 2 m above the river water surface elevation from the LiDAR dataset. This relief criteria excluded floodplain surfaces where active deposition is still occurring.

Historic rates of channel migration

Aerial photographs from 1938 and 2003 were used to constrain short-term river migration rates. The 1938 photos were georeferenced in ArcGIS. At least seven stable control points were selected and matched in each photo, fit with a second-order polynomial function, and rectified after a total RMS error < 0.5 was achieved. Channel banks were digitized by hand in ArcGIS. In cases where vegetation obscured the channel edge, the bank was estimated assuming a width consistent with adjacent up/downstream reaches. To calculate channel migration rates, we used a planform statistics tool described in Lauer and Parker (2005) (available at http://www.nced.umn.edu/Stream_Restoration_Toolbox.html). This tool maps the center line of the channel based on the user-defined right and left banks. The program then compares the center line of the 1938 channel to the 2003 channel center line using a best-fit Bezier curve. Overall georeferencing error was +/- 4.5 m, although individual images varied around this average.

To estimate the potential net contribution of sediment eroded through lateral migration, bank heights were calculated along a profile line adjacent to the top of the banks in 2003. Bank elevations were averaged every 100 meters, and reach-average channel elevations subtracted to get bank heights. Since channels both erode and deposit on their floodplains, resulting in no net gain or loss of sediment, we removed areas with elevations at or below the floodplain elevation, leaving only banks in terraces and bluffs. This methodology gives a measure of the potential net flux of sediment into the channel from channel migration into these higher surfaces. Floodplain heights were measured off the LiDAR DEM at 25 different sites along the mainstem Le Sueur

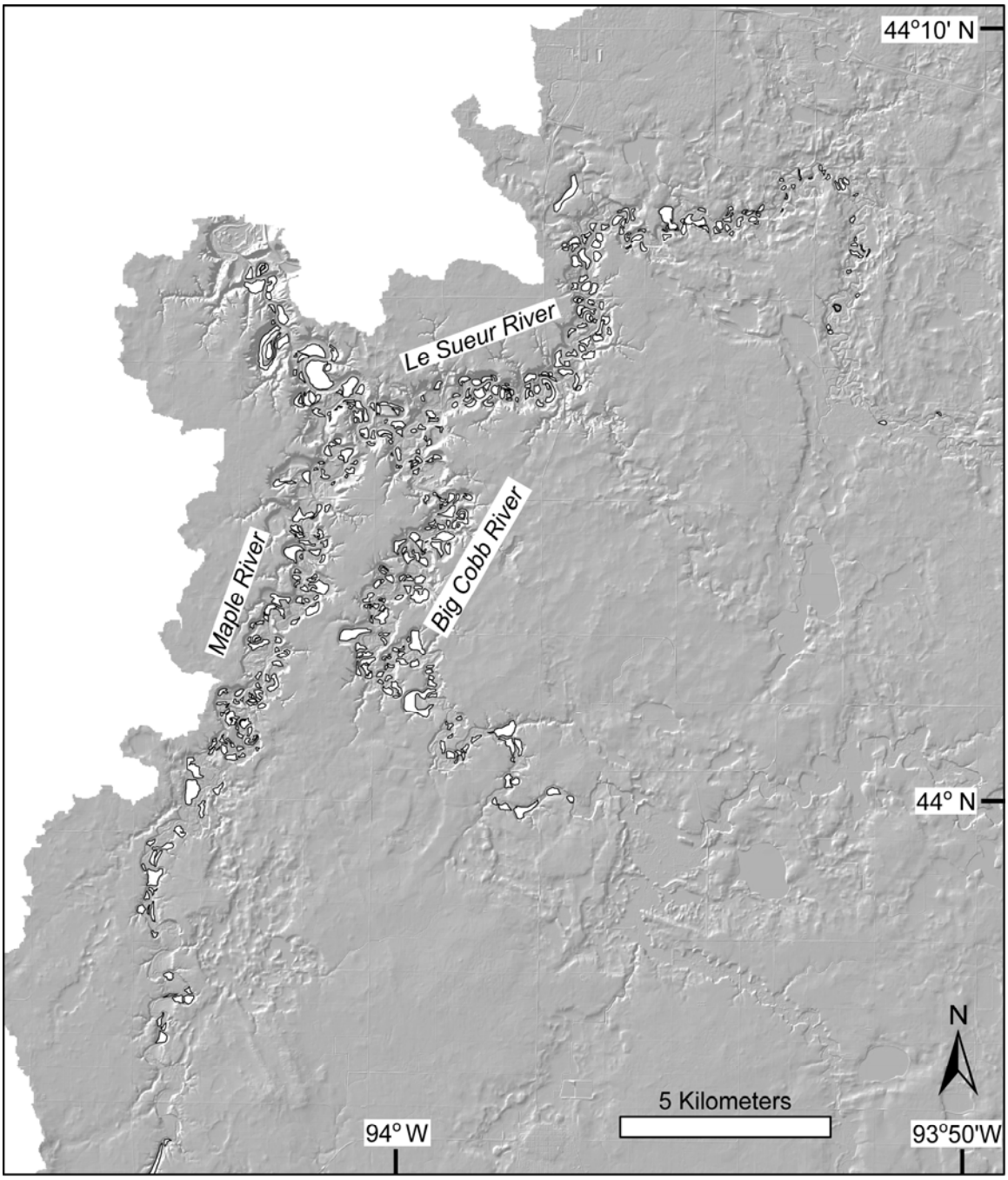

Figure 5: Terraces mapped in the lower Le Sueur River watershed, overlain on top of the LiDAR DEM. Only terraces > 2m above the channel were mapped, to exclude active floodplains.

River. The average floodplain height was 1.8 m +/- 0.5 m in the lower 25 km and 1.0 +/- 0.1 m from 25 - 75 km upstream. We measured volumes of sediment potentially entrained from terraces and bluffs along the lower 73.6 km of the mainstem Le Sueur River and then extrapolated to the rest of the mainstem Le Sueur, Maple, and Big Cobb Rivers, a total of 410 river km, to get a measure of the potential net volume of sediment that would be eroded into the channel from lateral migration into terraces and bluffs. These volumes were converted to mass using a bulk density of 1.8 Mg m^{-3}, and to potential suspended sediment load assuming a silt-clay content of 65% of the total sample.

Gaging Data

Modern sediment fluxes were calculated through continuous flow gaging at nine gaging stations located in the Le Sueur River watershed by the MPCA (Figure 1; Table 2). Approximately 30-40 grab samples were collected and processed by the MPCA throughout the year at each of these gaging stations and analyzed for TSS. Individual samples were converted into flow-weighted mean sediment concentrations by agency staff using the U.S. Army Corps of Engineers' FLUX program. Data from 2000 to 2005 were reported in MPCA et al. (2007). Data from 2006 come from the MPCA (pers. comm.) and include preliminary data from gages in their first year of operation.

To compare modern TSS loads with volumetric estimates of sediment removed over the Holocene, we removed the estimated organic fraction of the TSS. Samples were also analyzed for total suspended volatile solids (TSVS). Using TSVS as a proxy for organic content of TSS, estimates of organic content of TSS samples from the Le Sueur River in 1996 ranged from 16-34% (Water Resources Center, 2000). We adjusted the average TSS load from 2000-2006 by this amount to compare inorganic fractions only.

RESULTS

Until glacial River Warren incised and widened the ancestral Minnesota River valley, the Le Sueur River watershed contained a series of low-gradient, ice-marginal meltwater channels and a relatively flat glacial lake bed masking former channels. Most of the current river valley topography formed in the time since 11,500 yr BP. Terraces in the lower valley record the history of incision (Figure 5). On all three branches, knickpoints have migrated 30-35 river km

Table 2: GAGING STATIONS IN THE LE SUEUR RIVER WATERSHED

Station	Location	Years of Operation	Drainage Area (km^2)
LS1	Le Sueur R. at Red Jacket, BE County Rd. 66	1939-	2880
LS2	Le Sueur R., BE County Rd. 90	2006-	1210
LS3	Le Sueur R. at St. Clair, BE County Rd. 28	2007-	870
LC	Little Cobb R., BE County Rd.	1996-	336
BC	Big Cobb R., BE County Rd. 90	2006-	737
LM	Lower Maple R., BE County Rd. 35	2003-	878
UM	Upper Maple R., BE County Rd. 18	2006-	780
BD*	Beauford Ditch, MN Highway 22	1999-	18

*BD site was a former USGS gaging site in operation from 1959-1985

upstream from the confluence with the Blue Earth River (Figure 3), an average knickpoint migration rate of 3.0 – 3.5 m yr^{-1} over the past 11,500 years. A second knickpoint is seen between 120-140 river km upstream on all three branches, indicating an average upstream migration rate of 10.9 -12.6 m yr^{-1}. These exceptionally high migration rates speak to the poor strength of the underlying till and glaciolacustrine sediments at the surface. Elevation drop associated with the upper knickpoint appears to be relatively minor. Most of the relief in the basin is related to migration of the lower knickpoint.

The mass of sediment evacuated from incision since the initial base-level drop was used to determine an average yield per year (Table 3), broken down by sediment removed from the major river valley corridor versus sediment removed by ravines still present along the valley walls for each of the three major channels in the Le Sueur River watershed. Sediment removed from the valley was likely removed through a combination of lateral erosion into bluffs and streambanks, erosion by ravines no longer present because they have been consumed by lateral valley erosion, and vertical channel incision.

The amount of sediment excavated likely varied through time as the channel incised and the network expanded. Some studies of newly forming drainages have shown high rates of sediment evacuation early, diminishing through time (Parker, 1977; Hancock and Willgoose, 2002). Other studies have found the opposite, with lower rates of erosion initially, increasing until the drainage network was fully established (Hasbargen and Paola, 2000). The Le Sueur River is still very much in transition. It is in the early stages of channel incision and knickpoint migration, but the latter stages of drainage development, particularly following anthropogenic alterations to the drainage network. Other fluctuations in the sediment load likely occurred during the well-documented mid-Holocene dry period, ~5 to 8 ka BP (Grimm 1983; Webb et al. 1984; Baker et al., 1992; Webb et al., 1993; Geiss et al., 2003), which intermittently slowed sediment contributions from the Minnesota River to Lake Pepin (Kelley at al., 2006). Averaging over all the variability in the last 11,500 years, the average sediment export from the incised portion of the Le Sueur River valley and ravines is 1.1– 2.3 x 10^5 Mg yr^{-1}, equivalent to a suspended load (silt and clay fractions only) of 0.7– 1.5 x 10^5 Mg yr^{-1}. The average annual suspended sediment load was likely higher given the contribution of fine sand to the suspended load during peak flow events.

Modern sediment fluxes at the mouth of the Le Sueur River measured from 2000 to 2006 are listed in Table 1. The annual TSS flux for these seven years ranged from 0.86 – 5.8 x 10^5 Mg yr^{-1} with an average of 2.9 x 10^5 Mg yr^{-1}. The inorganic fraction (66-84% of TSS) was therefore

Table 3: MASS EXCAVATION FROM VALLEYS AND RAVINES

	Valley excavation (minimum estimate)		Valley excavation (maximum estimate)		Ravine excavation	
	mass (Mg)	flux* (Mg yr^{-1})	mass (Mg)	flux* (Mg yr^{-1})	mass (Mg)	flux* (Mg yr^{-1})
Maple	2.6×10^8	2.3×10^4	6.4×10^8	5.6×10^4	4.0×10^7	3.5×10^3
Cobb	1.6×10^8	1.4×10^4	4.3×10^8	3.7×10^4	4.2×10^7	3.7×10^3
Le Sueur	5.9×10^8	5.2×10^4	1.3×10^9	1.2×10^5	1.4×10^8	1.2×10^4
Total	1.0×10^9	8.8×10^4	2.4×10^9	2.1×10^5	2.2×10^8	1.9×10^4

*Fluxes are average rates over the past 11,500 years.

~1.9 – 2.4 x 10^5 Mg yr^{-1} on average from 2000 - 2006. These values are 1.3 to 3.4 times higher than the Holocene-average rate, considering only silt and clay fractions.

Spatial variations in sediment loading become apparent when we compare the 2006 results from gages positioned above and below the major knickpoints on two of the main branches (Table 4). On the Maple River, the drainage area increases very little from the upper gage to the lower gage (13% increase), but the TSS load increases by a factor of 2.8. From the gage on the Little Cobb River to the gage further downstream on the Big Cobb River, the drainage area increases by a factor of 2.2, but TSS increases by an order of magnitude. Processes on the uplands do not change markedly from the upper watershed to the lower watershed. The primary difference is that the lower watershed includes contributions from bluffs and ravines. If we assume upland sediment yields do not change appreciably from upstream to downstream, we can use the yield at the upper basin as a measure of upland erosion. These yields are 9.8 Mg km^{-2} on the Maple and 11.2 Mg km^{-2} on the Big Cobb. Applying these yields to the drainage areas at the lower gages, we end up with a mass of sediment that cannot be accounted for by upland erosion and get a measure of the potential importance of ravine and bluff erosion. On the Maple River, the excess sediment amounts to 14,000 Mg or 61% of the total sediment load. On the Big Cobb, the excess sediment is 25,000 Mg or 74% of the total sediment load. The role of bluff and ravine erosion to the total sediment budget in the Le Sueur River watershed is substantial and must be accounted for in the sediment budget.

To determine the relative importance of streambank erosion from lateral migration, we measured the potential volume of sediment that would be removed from lateral migration into high bluffs and terraces using average lateral migration rates from aerial photographs. Along the Le Sueur mainstem, channels moved an average of 0.2 m yr^{-1} between 1938 to 2003, with much of the movement concentrated on mobile bends. Given the current channel configuration and near bank elevations, this migration would lead to an average of 130 Mg river km^{-1} yr^{-1} of material entering the channel from lateral migration into terraces and high bluffs. If this rate is applied on all three mainstem rivers, the potential net sediment flux to the channel is ~ 4.4 x 10^4 Mg yr^{-1}, or 2.7 x 10^4 Mg yr^{-1} of silt and clay, should migration rates continue at the same pace.

DISCUSSION

The Le Sueur River currently has a very high suspended sediment load. TSS loads measured on the Le Sueur River are an order of magnitude higher than current standards set by

TABLE 4: TSS DATA FROM PAIRED GAGES IN 2006*

	Maple		Cobb	
	Upper	Lower	Upper	Lower
Drainage Area (km^2)	780	878	336	737
TSS† ($Mg\ yr^{-1}$)	$7.9x10^3$	$2.2x10^4$	$4.0x10^3$	$3.3x10^4$
TSS† yield ($Mg\ km^{-2}$)	9.9	25.4	11.8	45.4

*Data come from MPCA (pers. comm.), preliminary.

†TSS = Total Suspended Solids

the MPCA (MPCA et al., 2007). Sedimentation records from Lake Pepin indicate that deposition rates are an order of magnitude higher than pre-settlement deposition rates (Engstrom and Almendinger, 2000), and by extrapolation, we might assume the Le Sueur River had an order of magnitude increase in erosion rates over pre-settlement background rates as well. However, when comparing sediment volumes removed in the Le Sueur River, averaged over the past 11,500 yr, with gaging records from 2000-2006 at the mouth of the Le Sueur River, the increase appears more modest: an increase of 1.3 to 3.4 times over the Holocene-average background rate rather than a 10-fold increase.

The major modern sources of sediment to the mainstem channels include ravines eroding through incision, elongation, and mass wasting; bluffs eroding through mass wasting as a result of fluvial undercutting and sapping; upland erosion on agricultural fields (particularly in spring prior to closure of row crop canopy); and streambank erosion above and beyond the volume involved in floodplain exchange. The Le Sueur River has had two major changes to the landscape that have affected erosion from these sources: conversion of original prairie and forests to agriculture and alterations to the basin hydrology that have increased overall peak flows (Novotny and Stefan, 2007).

Clearing and continued use of land for agriculture likely only affected erosion from upland sources directly. Changes in basin hydrology and climate which led to higher discharges could increase erosion from streambanks and bluffs through channel widening and potentially higher rates of lateral channel migration. An increase in discharge in the large ravines could increase erosion significantly. These landscape features have high channel and side slopes and are particularly sensitive portions of the landscape. In many cases, drainage tile outlets empty directly into ravines, increasing peak flows dramatically. Observations from the field indicate that headcuts in ravines are highly active, particularly where ravine tips are eroding into glaciolacustrine sediments. Field observations during storm flows in ravines have found water running clear in low-intensity storms and very muddy in high-intensity storms, possibly indicating a threshold response in sediment flux from ravines once overland flow is generated.

Paired gages on the mainstem channels give us some insight into the relative importance of bluff and ravine erosion versus upland erosion. Gages installed on the upper and lower Maple River and on the Big Cobb and Little Cobb Rivers provide a basis for estimating sediment contributions from bluff and ravine erosion. The upper gage receives sediment primarily from upland fields, smaller tributaries and ditches, and streambank erosion into low terrace surfaces. The lower gage contains additional sediment derived from ravines and erosion of high bluffs.

The observed increase in TSS, above and beyond that expected from an increase in drainage area or discharge, indicates that bluffs and ravines are playing a significant role as sediment sources in the lower reaches. If the TSS yield from the watershed measured at the upper gage is applied to the increase in watershed area above the lower gage, the remaining TSS load provides an estimate of the contribution from ravines, banks, and bluffs. For the Maple and Cobb rivers in 2006, 61-74% of the sediment was potentially derived from these non-upland sources. Previous studies in the neighboring Blue Earth River have estimated that bank and bluff erosion alone account for 23-56% of TSS load (Thoma et al., 2005) and 31-44% (Sekely et al., 2002). On-going work by Schottler and Engstrom (pers. comm.) indicates that >75% of the suspended sediment at the mouth of the Le Sueur River was derived from non-field sources, including ravines, bluffs, terraces, and stored floodplain sediments.

Assessments of stream migration rates on the mainstem Le Sueur River coupled with bank and floodplain elevations indicate that stream migration on the three major branches of the Le Sueur River could potentially contribute 2.7×10^4 Mg yr^{-1} of suspended sediment as a net source to the channel not balanced by floodplain deposition. This volume is 11-14% of the average TSS load at the mouth of the Le Sueur River. Because the channel is incised and channel migration occurs into these high surfaces, not just into floodplains, a significant mass of sediment can be contributed to the channel above and beyond the amount deposited on the floodplain.

CONCLUSIONS

The Le Sueur River has a well-constrained geomorphic history that can be used to understand the current sediment dynamics of the system. A major knickpoint migrating through the Le Sueur River network divides the watershed into two main regions: above the knick zone where the watershed is dominated by low-gradient agricultural uplands composed of glaciolacustrine and till deposits, and below the knick zone where high bluffs and steep-sided ravines are added to the system. Gaging efforts indicate a significant rise in sediment load as rivers move through the lower reaches of the channel, below the knick zone, highlighting the importance of bluffs and ravines as sediment sources in the lower watershed. In addition, channel migration studies indicate that streambank erosion from channel migration may contribute a significant volume of sediment to the overall TSS load that is not lost to floodplain deposition due to the presence of high terraces and bluffs along the channel edge.

Sediment loads are high in the Le Sueur River, an order of magnitude higher than MPCA target values. Records from Lake Pepin indicate an order of magnitude increase in deposition, a rise which should be mirrored in the Le Sueur River, a major contributor of sediment to the Minnesota River and ultimately to Lake Pepin. However, calculations of sediment removed from the valley since base-level fall 11,500 yr BP indicate that modern sediment loads are only 1.3 to 3.4 times higher than the average load over the past 11,500 yr, even when grain size variations and organic content are accounted for. This Holocene-average rate assumes a linear progression of erosion through time, and the history of valley incision and erosion is more complicated than this. Efforts are on-going to determine terrace ages in the lower Le Sueur River valley to better constrain the history and evolution of incision and thus of sediment flux from the basin. Unraveling terrace histories will help resource management by better constraining pre-settlement sediment yields as well as shed light into the pattern and style of landscape evolution in an incising system.

ACKNOWLEDGEMENTS

This work was funded by the Minnesota Pollution Control Agency with funds from the Minnesota Clean Water Legacy Act. Additional support came from the STC program of the National Science Foundation via the National Center for Earth-surface Dynamics under the agreement Number EAR- 0120914. We thank the Minnesota Pollution Control Agency staff for providing us with preliminary 2006 gaging data. We appreciate the comments of two anonymous reviewers.

REFERENCES

Baker, R.G., Maher, L.J., Chumbley, C.A., and Van Zant, K.L., 1992, Patterns of Holocene environmental change in the Midwestern United States: Quaternary Research, v. 37, p. 379-389.

Clayton, L., and Moran, S.R., 1982, Chronology of late-Wisconsinan glaciation in middle North America: Quaternary Science Reviews, v. 1 p. 55 – 82.

Engstrom, D.R., and Almendinger, J.E., 2000, Historical changes in sediment and phosphorus loading to the Upper Mississippi River: Mass-balance reconstructions from the sediments of Lake Pepin: Final Research Report prepared for the Metropolitan Council Environmental Services, 28 p. + figures.

Geiss, C.E., Umbanhowar, C.E., Camil, P., and Banerjee, S.K., 2003, Sediment magnetic properties reveal Holocene climate change along the Minnesota prairie-forest ecotone: Journal of Paleolimnology, v. 30, p. 151-166.

Grimm, E., 1983, Chronology and dynamics of vegetation change in the prairie-woodland region of southern Minnesota, USA: New Phytology, v. 93, p. 311-350.

Hancock, G.R., and Willgoose, G.R., 2002, The use of a landscape simulator in the validation of the SIBERIA landscape evolution model: Transient landforms: Earth Surface Processes and Landforms, v. 27, p. 1321-1334.

Hasbargen, L.E., and Paola, C., 2000, Landscape instability in an experimental drainage basin: Geology, v. 28, n. 12, p. 1067-1070.

Kelley, D.W., Brachfeld, S.A., Nater, E.A., and Wright, H.E., Jr., 2006, Sources of sediment in Lake Pepin on the Upper Mississippi River in response to Holocene climatic changes: Journal of Paleolimnology, v. 35, p. 193-206.

Kelley, D.W., and Nater, E.A., 2000, Historical sediment flux from three watersheds into Lake Pepin, Minnesota, USA: Journal of Environmental Quality, v. 29, n. 2, p. 561-568.

Lauer, J.W., and Parker, G., 2005, Net transfer of sediment from floodplain to channel on three southern US rivers: Paper presented at ASCE World Water and Environmental Resources Congress, Anchorage, Alaska, May 15-19, 2005.

Lowell, T.V., Fisher, T.G., and Comer, G.C., 2005, Testing the Lake Agassiz meltwater trigger for the Younger Dryas: EOS Transactions of the AGU, Vol., 86, No. 40, p. 365 – 373.

Marschner, F.J., 1930, Interpretation of Francis J. Marschner's map of the original vegetation of Minnesota: Based on the notes of the Public Land Survey, 1847-1907.

Matsch, C.L. 1972, Quaternary Geology of Southwestern Minnesota, *in* Sims, P.K., G.B. Morey (eds.), Geology of Minnesota: A Centennial Volume: St. Paul, Minnesota Geological Survey, p. 548-560.

Matsch, C.L., 1983, River Warren, the southern outlet of Lake Agassiz, *in* Teller , J.T. and Clayton, L., eds., Glacial Lake Agassiz: Geological Association of Canada Special Paper 26, p. 232 – 244.

Minnesota Department of Natural Resources, 2007, Native Plant Communities and Rare Species of the Minnesota River Valley Counties: Minnesota County Biological Survey, Biological Report 89: St. Paul, Minnesota Department of Natural Resources.

Minnesota Pollution Control Agency, 1993, Selected water quality characteristics of minimally impacted streams from Minnesota's seven ecoregions. Addendum to descriptive characteristics of the seven ecoregions in Minnesota: St. Paul, MN.

Minnesota Pollution Control Agency, Minnesota Department of Agriculture, Minnesota State University, Mankato Water Resources Center, and Metropolitan Council Environmental Services, 2007, State of the Minnesota River: Summary of surface water quality monitoring 2000-2005. 20 p.

Novotny, E.V., and Stefan, H.G., 2007, Stream flow in Minnesota: Indicator of climate change: Journal of Hydrology, v. 334, p. 319-333.

Parker, R.S., 1977, Experimental study of drainage basin evolution and its hydrologic implications. [Ph.D. Thesis]: Fort Collins, Colorado State University, 331 p.

Sekely, A.C., Mulla, D.J., and Bauer, D.W., 2002, Streambank slumping and its contribution to the phosphorus and suspended sediment loads of the Blue Earth River, Minnesota: Journal of Soil and Water Conservation, v. 57, n. 5, p. 243-250.

Thorleifson, L.H., 1996, Review of Lake Agassiz history, *in* J.T. Teller, L.H. Thorleifson, G. Matile and W.C. Brisbin, 1996, Sedimentology, Geomorphology and History of the Central Lake Agassiz Basin - Field Trip Guidebook B2; Geological Association of Canada/Mineralogical Association of Canada Annual Meeting, Winnipeg, Manitoba, May 27 – 29, 1996.

Thoma, D.P., Gupta, S.C., Bauer, M.E., and Kirchoff, C.E., 2005, Airborne laser scanning for riverbank erosion assessment: Remote Sensing of the Environment, v. 95, p. 493-501.

Upham, W., 1890, Report of exploration of the glacial Lake Agassiz in Manitoba: Geological Survey of Canada. Annual Report 1888 – 89, part E, 156 p.

Upham, W., 1895, The Glacial Lake Agassiz: United States Geological Survey, Monograph 25, 658 p.

Water Resources Center, Minnesota State University, Mankato, 2000, Le Sueur River major watershed diagnostic report: Le Sueur River basin implementation framework, MPCA Clean Water Partnership Project #951-1-194-07, 162 p.

Webb, T., III, Cushing, E.J., and Wright, H.E., Jr., 1984, Holocene changes in the vegetation of the Midwest, *in* Wright, H.E., Jr. (ed.), Late-Quaternary environments of the United States, v. 2, The Holocene: Minneapolis, University of Minnesota Press, p. 142-165.

Webb, T., III, Ruddiman, W.F., Street-Perrott, F.A., Markgraf, V., Kutzbach, J.E., Bartlein, P.J., Wright, H.E., Jr., and Prell, W.L., 1993, Climatic changes during the past 18,000 years: regional syntheses, mechanisms, and causes, *in* Wright, H.E., Jr., et al., (eds.), Global climates since the Last Glacial Maximum: Minneapolis, University of Minnesota Press, p. 514-535.

Wobus, C., Whipple, K.X., Kirby, E., Snyder, N., Johnson, J., Spyropolou, K., Crosby, B., Sheehan, D., 2006. Tectonics from topography: procedures, promise, and pitfalls, *in* Willett, S.D., Hovius, N., Brandon, M.T., Fisher, D.M. (eds.), Penrose Conference Series. Tectonics, Climate and Landscape Evolution: Geological Society of America Special Paper, vol. 398, p. 55–74.